University College of Southeast Norway
Faculty of Technology

Master's Thesis
Study programme: FMH606
Spring 2016

Kwang{u Park

Optimization of partial CO_2 capture

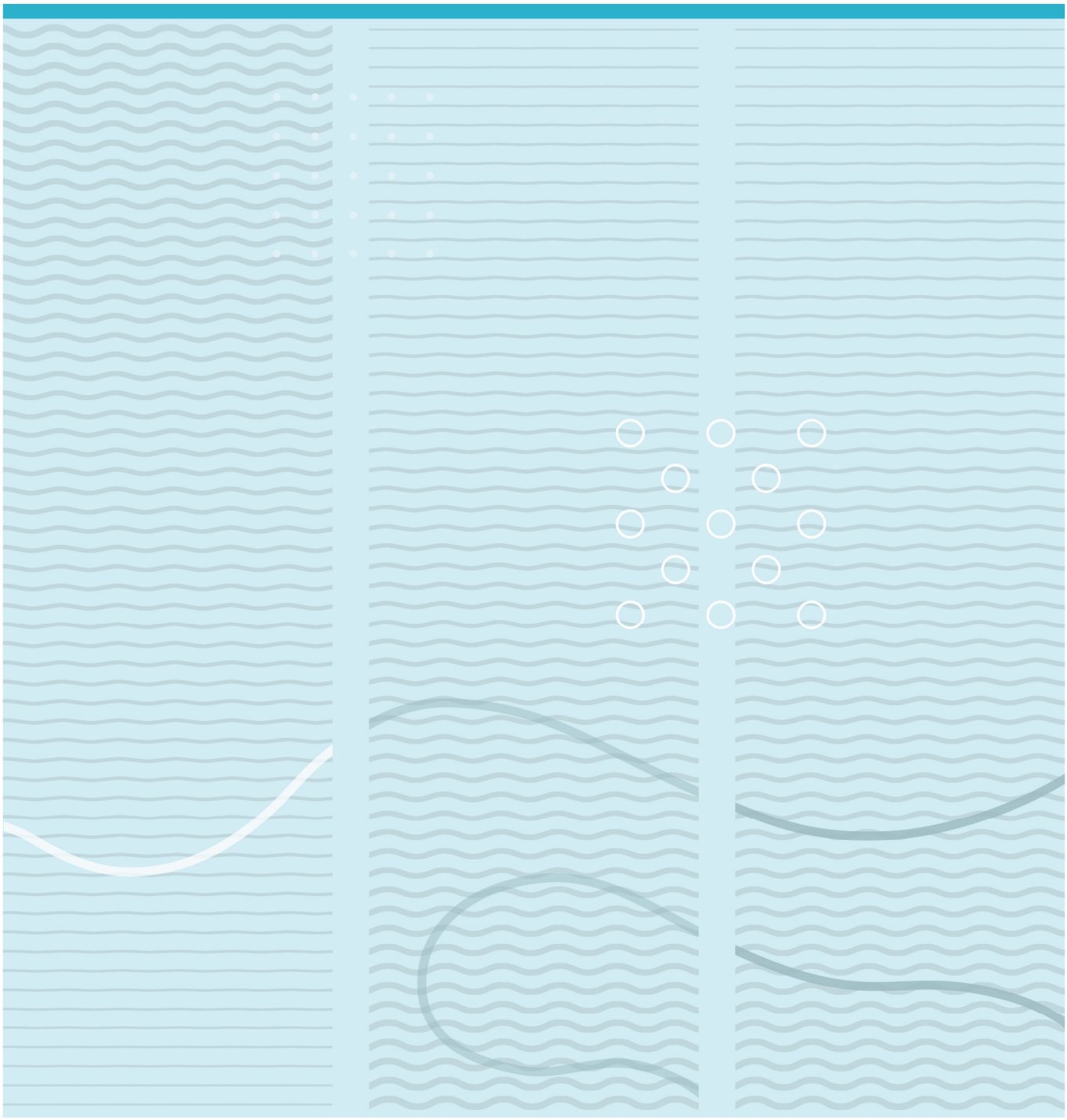

University College of Southeast Norway
Faculty of Technology
Institute of PEM
PO Box 235
NO-3603 Kongsberg, Norway

http://www.usn.no

Abstract

The cement industry accounts for about 5 % of the global anthropogenic CO_2 emissions. Traditional post-combustion CO_2 capture with monoethanolamine absorption is highly energy-intensive, which in turn leads to expensive capture cost.

To optimize the capture cost in a cement plant, this study focused on optimizing the post-combustion CO_2 capture process with Aspen HYSYS using waste heat only. Impact analysis was carried out based on the three process parameters: flue gas inflow ratio into the absorber, number of stages in the absorber column and the superficial gas velocity.

Despite the high investment, routing all of the flue gas into the absorber was calculated to be the most effective alternative in terms of capture cost because it gave the highest CO_2-capture rate. The capture rate showed little decrease even with fewer absorber stages. With the assumption that 1 m/packing is equivalent to a Murphree efficiency of 0,15, the number of absorber stages giving the minimum capture cost was five.

On the other hand, routing only part of the flue gas into the absorber column consistently resulted in lower capture rate. There were also limitations in reducing the absorber column stages to five, largely due to a sharp decrease in CO_2-capture rate with fewer column stages.

The effect of the gas velocity on capture cost was also studied. For Mellapak 250Y and 250X, the optimal gas velocity was found to be as low as 1,5 m/s mainly due to reduced pressure drops. In the case of Mellapak 2X, the minimum capture cost was obtained with the gas velocity of 2,0 m/s.

Of the three structured packings, Mellapak 2X yielded the minimum capture cost, with the value being 85 NOK/tonne CO_2. For Mellapak 250Y and 250X, they both showed the minimum capture cost of 86 NOK/tonne CO_2. The capture cost differences between these packings are not significant to determine the most cost-effective packing.

Contents

List of Figures and Tables

Figures

Tables

Preface

This thesis was written in the spring semester 2016 for submission to the Faculty of Technology at University College of Southeast Norway. Time surely has flown very fast after I first came to the college, and I enjoyed every minute of my life with my dear people around me sharing a lot of experiences together. By now I am proud of myself and the accomplishments I have achieved in the last two years. All the coursework, classes and all of the teaching staff I have met will be best remembered in my life.

First of all, I wish at the moment to express my thanks to God for giving me blessing, faith, peace of mind and self-confidence whenever I feel physically and mentally exhausted.

I would like to show my sincere gratitude to Lars Erik Øi, the supervisor of my thesis, for supporting me and giving constant encouragements during the progress of my thesis work. He has been always cooperative whenever I had trouble with the research work and gave me valuable advice and guidelines based on his research experiences.

I also would like to extend my appreciation to my co-supervisor, Nils Henrik Eldrup for sparing his precious time for giving meaningful guidance on cost estimation of the thesis.

I also cannot forget to express my cordial thanks to Prof. Carlos Pfeiffer for offering me an opportunity to be a teaching assistant in his class, as well as for his kind and valuable advice on my future career plans.

At this writing, I truly wish to dedicate my thesis to my parents, Jongook Park and Chunhee Lim. I am much obliged to them more than words can express for their constant support and unmeasurable love during the whole period of my life. I also realize the preciousness of my dear sister, Eunjung Park, and know how much she has meant to me. Though I am in a foreign land far away from home, I have never forgotten my family's favor and love.

Last but not least, I must be extremely grateful to my girlfriend, Sunny Seo, for all her endless support with patience, for standing by me in joy and sorrow at every moment, for cheering me on, for supporting and trusting me constantly.

Porsgrunn, June 2, 2016

Kwangsu Park

Nomenclature

Symbol	Unit	Description
a_g	[m^2/m^3]	packing geometric area
a_e	[m^2/m^3]	effective interfacial area
c_p	[kJ/kg·℃]	specific heat capacity
D_i	[m]	inner diameter
D_o	[m]	outer diameter
$h_{packing}$	[m/packing]	height per packing bed
v_g	[m/s]	superficial gas velocity
$v_{g,b}$	[m/s]	base superficial gas velocity (= 2,5 m/s)
C_h	[kJ/℃·s]	heat capacity rate of hot fluid (= $c_{p,h} * \dot{m}_h$)
C_c	[kJ/℃·s]	heat capacity rate of cold fluid (= $c_{p,h} * \dot{m}_c$)
P_f	[kW]	fan power
P_p	[kW]	pump power
N_{stage}	[-]	number of stages in absorber column
Δh	[m]	height difference
Δh_{Lean}	[m]	Lean amine inlet height of absorber column
Δh_{Rich}	[m]	Rich amine inlet height of desorber column
ΔP	[Pa]	differential pressure
$\Delta P_{packing}$	[Pa/m]	pressure drop per meter of packing bed
ΔT_{min}	[℃]	minimum temperature difference
η_a	[-]	adiabatic (isoentropic) efficiency
η_c	[-]	CO_2-capture efficiency
η_m	[-]	Murphree efficiency

Abbreviation	Unit	Description
CS		carbon steel
SS		stainless steel
CAPEX	[kNOK]	capital expenditure (= total installation cost)
OPEX	[kNOK/year]	operating expenditure (= total operating cost)
LMTD	[℃]	log mean temperature difference

1 Introduction

1.1 General overview of CO_2

Carbon dioxide has a chemical formula of CO_2 and was first identified in the 1750s by Joseph Black, a Scottish scientist[1]. It is colorless, incombustible, and at a low concentration almost scentless. CO_2 is classified as a trace gas and currently accounts for about 400 ppm by volume in the Earth atmosphere[2].

The carbon dioxide in the atmosphere is the primary source of carbon in living things, so it is among the vital gases to living creatures on Earth. Since late Precambrian age until just before industrialization, the atmospheric concentration of CO_2 was regulated by photosynthesis process in organisms and geological events[3]. In a carbon cycle, a broad range of plants and bacteria photosynthesize by using CO_2 and H_2O with the help of light energy and make oxygen as a product[4].

There are many natural sources of CO_2 such as volcanoes, carbonate rocks and hot springs. It is also found in seawater, rivers and lakes with a small fraction due to its solubility in water. Every aerobic organism produces CO_2 together with energy during metabolism[4]. CO_2 is also produced when organic materials are in the process of decaying or during the fermentation process of bread and beer[5]. Combustion of forest or fossil fuels such as coal, petroleum and natural gas leads to an anthropogenic production of CO_2 into the atmosphere.

CO_2 can be used as an industrial material for various purposes. One typical example is fire extinguishers, which are filled with non-flammable CO_2 gas under extreme pressure. In oil industries, CO_2 is used for enhancing oil recovery (EOR) by being injected into oil fields[2]. In the metalworking industry, CO_2 gas is supplied from the nozzle of the welding torch to shield the weld pool[4]. CO_2 is also added to drinking water and carbonated beverages including beer and sparkling wine to add effervescence.

Most importantly, CO_2 is considered as one of the important greenhouse gases contributing the global warming. Its atmospheric concentration has sharply risen after the industrial revolution owing to the increased use of carbon-containing fuels and farmland plowing, necessitating development of Carbon Capture and Storage (CCS) technology[6]. Many countries in the world have therefore been setting up environmental policies and international agreements to take measures against the increasing level of CO_2 emissions.

1.2 Background of CO_2 capture

Greenhouse gas is the key issue of environmental pollution and global warming. It is widely recognized that the global warming is indeed the serious environmental and ecological threat today. Capture of CO_2 has thus been under active discussion as one of the options for reducing greenhouse gas emissions.

Despite its relatively small atmospheric concentration, CO_2 is influential in the greenhouse effect and contributes to regulating the temperature of the Earth[1]. As well as other greenhouse gases, the current phenomena of global warming are also attributed to the increased concentration of CO_2 in the atmosphere. Research by Mahlia (2002) and Zhang et al. (2012) indicates that global warming is due to the anthropogenic sources of greenhouse gas emissions including CO_2. Industrial development and rapid increase of transportation facilities made CO_2 emissions reach a dangerous level, requiring an international solution.

From the era of Industrial Revolution, the global mean temperature has increased by between 0,6 ℃ and 1 ℃, while the global concentration of CO_2 has increased by above 40 %[6]. Its concentration was about 280 ppm in the middle of the 18th century, and recently in the first quarter of 2016 it measures about 402 ppm, which is regarded as the highest value over the last 20 million years[6]. This can be attributed to anthropogenic emission of CO_2 such as fossil fuel combustion, deforestation, cement production or livestock farming. In particular, carbon dioxide resulting from deforestation and the use of fossil fuel is considered as the main contributing factors[2]. Approximately 30 – 40 % of CO_2 emissions induced by human beings are dissolved into the sea or rivers and form carbonic acid, making detrimental impacts on the ocean[3, 5]. Today the concentration is growing at a rate of 2 ppm/year, and the increasing rate is predicted to rise even more in the near future[4]. If this trend continues without any measures, the atmospheric CO_2 level may reach twice that of the preindustrial period by the end of this century[4].

Efforts on limitations of CO_2 emission are therefore the priority for clean environmental management. The Kyoto Protocol (1997) and Copenhagen Accord (2009) were the last overall efforts of the United Framework Convention on Climate Change (UNFCCC), and the world's major industrialized nations decided to mitigate their greenhouse gases under these agreements[7]. The International Energy Agency modelling also indicated that the emissions of CO_2 will need to be slashed by half in 2050, compared to the current level to cope with the urgent environmental issues regarding climate change[8].

1.3 CO_2 emission from cement industry

Cement is considered an excellent construction material due to its good physical performance, low maintenance cost and customization. The manufacturing process, however, is highly energy-demanding. Research done by U.S. Energy Information Administration (EIA) in 2012 indicates that although the energy usage of cement industry only 0,25 % of total U.S. energy, the cement industry is the most energy-intensive among all manufacturing industries[9].

Cement manufacturing is also one of the major industries emitting a considerable amount of CO_2 on a global scale. Producing one tonne of cement involves around 900 kg of CO_2, which is estimated to take up 5 % of the global anthropogenic emissions[10, 11].

During the past decades, cement manufacturers have tried to lower the level of CO_2 emission through various means, including raw material substitution, fuel switching and reduction of clinker-to-cement ratio[12]. Since most of the modern cement plants are operated at maximum possible efficiencies, the deployment of CO_2 capture seems to be the sole realistic technology to curb greenhouse gas emissions[8].

During the manufacturing process of cement, CO_2 is produced as an inevitable by-product in both direct and indirect ways. Two primary sources of emissions are[8]:

1. Carbon dioxide originates directly from the burning of fossil fuels. The amount of this accounts for about 30 % of the total CO_2 emissions from a cement plant.
2. Decomposition of limestone by thermal energy produces CO_2 and calcium oxide[1]. Carbon dioxide emissions from this source account for about 60 % of the total CO_2 emissions from a cement plant.

Other sources of CO_2 include electricity consumption during fossil fuel burning, milling processes and transportation. However, the emissions from these sources are below 10 %[13].

The concentration of CO_2 in flue gases is often an important characteristic for the implementation of carbon capture technology[14]. As described above, the cement kiln has two main emission sources of CO_2 and therefore its CO_2 concentration of the flue gas is

[1] $CaCO_3(s) \rightarrow CaO(s) + CO_2(g)$

relatively high compared to other industries. While the CO_2 content in the flue gas reaches around 12 – 15 wt% in a coal-fired power plant and about 4 % in a gas-fired power plant, flue gases from cement plants contain between 14 – 33 wt% of CO_2[12]. On these grounds, employing CO_2 capture technology in cement industry is considered attractive and expected to yield a lower energy requirement. Table 1-1 summarizes the typical compositions of the flue gas from cement industry.

Table 1-1 Typical composition of flue gas stream in a cement plant [15]

Component	Concentration
CO_2	14 – 33 wt%
NO_2	5 – 10 % of NO_x
NO_x	< 200 – 3000 mg/Nm^3
SO_2	<10 – 3500 mg/Nm^3
O_2	8 – 14 vol%

The worldwide production of cement has risen from 1043 to 2840 Mt/year for the past 20 years[16]. During the period from 2000 to 2006, global emissions of CO_2 from cement industry increased by 54 %[17]. While the global emissions of CO_2 from a cement plant were 576 million tons in 1990, the emissions have been tripled in 2006, reaching 1,88 billion tons[18]. Table 1-2 indicates the amount of cement produced between 2008 and 2009 depending on different countries.

Table 1-2 Amount of cement production for different countries [19]

Country	Annual production of cement [Mt]
Brazil	51,9
China	1390
India	177
Japan	62,8
South Korea	53,9
Russia	53,6
Turkey	51,4
United States	87,6
Other countries	911,8
Total	2840

The cement demand worldwide is expected to grow by between 60 – 110 % in 2020, and the production of cement is anticipated to increase by 0,8 – 1,2 % per annum[18, 20]. If no countermeasures are taken against this trend, the global CO_2 emissions from cement industry are expected to reach 2,34 billion tons in 2050[21].

All these possible upcoming scenarios have urged cement industry and the governments to put time into drawing up solutions in order to implement various promising strategies and reduce climate impacts. To date, applications of separating CO_2 have been in operation primarily in the major industrial plants, including natural gas treatment facilities and ammonia production plants[22]. However, there have been no applications of capturing technology at cement plants to mitigate CO_2 emissions[8].

1.3.1 Norwegian cement industry and its future plan

The annual emissions of CO_2 in Norway add up to approximately 60 Mt, 25 % of which come from the industry sectors including cement plants[23]. Norcem, the only cement manufacturer in Norway, have two plants based at Brevik and Kjøpsvik respectively. Coal and biomass are often used in Norcem for the combustion process, achieving a combined production capacity of 1.415.000 tonnes of clinker annually[24]. CO_2 emissions from Norcem are known to account for 2,5 % of the national emissions. More than 60 % of the emissions from cement production relate to the process emissions[8].

Up to recently, CO_2 capture technology in Norway has focused primarily on emissions from offshore installations and gas power plants. Only a few feasibility studies have been conducted within regard to carbon capture in cement plants[8].

To make deep cuts in CO_2 emissions, Norcem installed a large-scale Mobile Test Unit (MTU) at Brevik in cooperation with Aker Solution in 2013[23]. This attempt is to study CO_2 absorption technology, as well as evaluating the realism of heat integration and its suitability for implementation. Since a CO_2 capture plant is energy-demanding in the regeneration process, high levels of capture cost have been considered as one big challenge.

Approximately 22 – 24 MW of waste heat can be made available from a cement kiln in Brevik, Norcem[8]. The waste heat in the flue gas comes from a cement kiln (i.e. preheater tower) and can be utilized by installing waste heat boilers downstream of the preheater. The temperature in the preheater outlet gas stream is around 350 – 450 ℃[25]. This high-temperature flue gas stream can be used to generate steam by using a waste heat boiler. The steam can then be used for solvent regeneration in an amine-based carbon capture plant. According to feasibility studies at Brevik, the steam energy from this source corresponds to about 40 % of the total energy duty in a traditional full-scale capture plant[8].

This naturally leads to the idea that alternative measures to reduce the energy use should be considered to economically optimize the CO_2 capture process. Since the capability of utilizing the waste heat has been of keen interest, possible opportunities for heat integration were already identified by Aker Solutions[8]. The performance of an amine–based solvent is also currently under active research, and the completion of the tests is expected to provide better estimates of the operational performance as well as the optimized post-combustion capture cost from cement industry.

1.4 CO_2 capture technology

Depending on the process specification or plant applications, CO_2 capture technology may be classified into three main approaches: pre-combustion, oxyfuel combustion and post-combustion.

1.4.1 Pre-combustion

Pre-combustion capture refers to removing CO_2 from fuels before combustion process. A chain of processes are involved as follows[26, 27].

i) Oxygen is separated by from the air by Air Separation Unit (ASU).

ii) Primary fuel (e.g. coal) is partially oxidized with air, oxygen or steam in a gasifier under high temperature and pressure. This produces the synthesis gas, the main components of which are CO and H_2.

iii) CO undergoes the reforming reaction with the steam in a water-gas shift (WGS) reactor and brings about H_2 and CO_2 as products. ($CO + H_2O \rightarrow CO_2 + H_2$)

iv) The CO_2 stream is separated from H_2 by the gasification process at a high pressure, and the CO_2 is transported through pipelines and stored.

v) The remaining H_2 serves as a carbon-free energy. After conditioning process, H_2 is fueled into the combustion chamber for power generation or heat recovery.

The initial gasification processes are elaborate, so the capital costs are often more expensive than conventional pulverized coal-fired power plants or post-combustion systems[27]. Nonetheless, high pressures and concentrations of CO_2 induced by the shift reactor (typically 15 – 60 vol% on a dry basis) make the CO_2 separation process more favorable[28]. Figure 1-1 illustrates the overall process of the pre-combustion system.

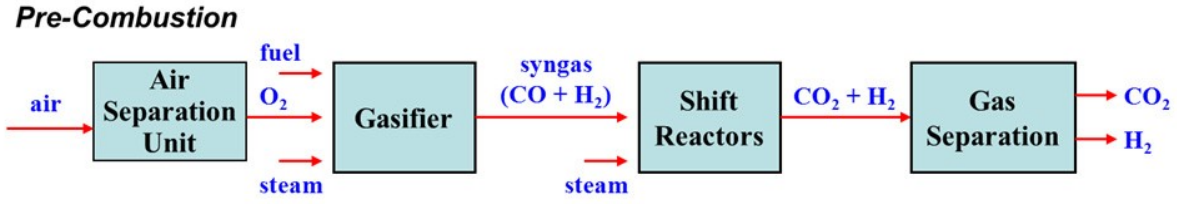

Figure 1-1 Schematic diagram of pre-combustion process [29]

1.4.2 Oxyfuel combustion

In contrast to the pre-combustion system where the ambient air is used, oxyfuel combustion systems apply a pure or enriched oxygen as an oxidizer[30]. Since no nitrogen is involved in the combustion of primary fuels, higher flame temperatures can be achieved with less consumption of fuel[2]. Moreover, because N_2 is removed from the air, NO_x production can be considerably reduced[31].

The following describes the major processes of oxyfuel combustion[32].

i) Nearly all of the nitrogen (N_2) is removed from the air by air separation unit (ASU) to make the stream oxygen-rich.

ii) The fuel is burned in the oxy-combustion boiler, producing primarily H_2O and CO_2. The volumetric concentration of CO_2 is greater than 80 %.

iii) The steam (water vapor) is removed by cooling and compressing processes (condensation). The remaining CO_2 is separated and compressed.

The main traditional problem in oxyfuel combustion is separating oxygen from the air. It is normally required that the O_2-rich gas has a purity of more than 95 %, which is energy demanding[3]. Besides, further treatment of the flue gases is often needed before sending CO_2 streams to the storage tank in order to remove secondary pollutants, e.g., SO_x, NO_x, N_2, etc. Putting it economically, current oxygen production techniques are known to be costly than other CO_2 capture technologies. The oxyfuel combustion is thus presently not considered to be competitive in the absence of any need to reduce CO_2 emissions[34]. A schematic drawing of the oxyfuel combustion system is illustrated in Figure 1-2.

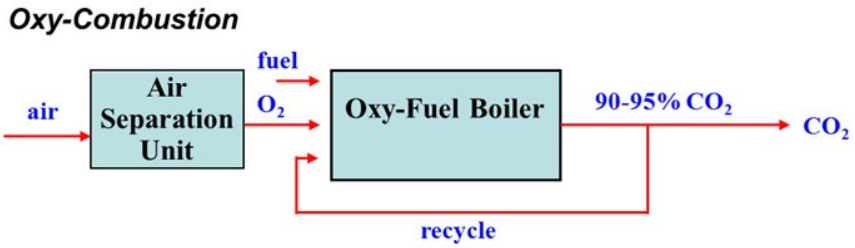

Figure 1-2 Schematic diagram of oxyfuel-combustion process [29]

[2] The mixture is usually diluted with the recycled flue gases to lower the temperature to some degree.

[3] For a coal-fired power station, nearly 15 % of the energy produced may be consumed for this process[33].

1.4.3 Post-combustion

In a post-combustion system, CO_2 is removed from the exhaust gas prior to its compression, transportation and storage. Two chief advantages of post-combustion system are[23]:

1. It is highly compatible and flexible because the capturing facilities can be easily retrofitted to the existing plant.
2. Because the capturing process occurs downstream the plant, no substantial effect is made on the core process of fuel-burning or product manufacturing.

Post-combustion system technologies include physical/chemical absorption, adsorption, membrane separation or cryogenic separation. Chemical absorption technology among these is the most well-known and matured method because it has been most commercially employed in process industry for the last decades[35]. Five major stages of the post-combustion system are summarized below[36].

i) Flue gas desulphurization (FGD) and De-NO_x process prior to CO_2 removal
ii) CO_2 absorption from exhaust gas in an absorber column by chemical solvent
iii) Regeneration of CO_2-rich solvent in desorber (stripper) in the presence of heat
iv) Compression & transportation of CO_2 through pipelines for storage or further use

Figure 1-3 illustrates the primary process of a post-combustion CO_2 capture.

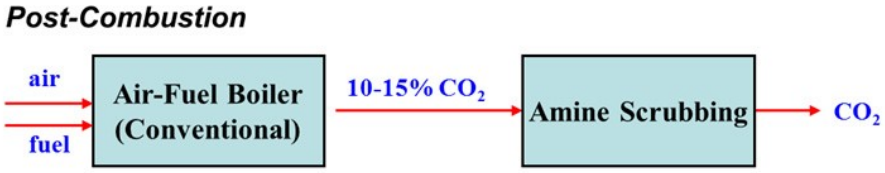

Figure 1-3 Schematic diagram of post-combustion process [29]

The chemical absorbent in the post-combustion system should ideally exhibit fast absorption kinetics, low heat-requirement for regeneration, resistance to degradation, high CO_2-loading capacity, low corrosiveness, low volatility, low price and a low toxicity[14]. The development of absorbent has therefore been under intensive research, and amine-based absorbents are currently known to be the benchmarking absorbent[37]. In particular, monoethanolamine

(MEA) is considered as a prototype for the amine-based capture of CO_2 because it has proven to be reliable in many post-combustion demonstration plants[38].

However, there also exist a few traditional drawbacks in amine absorption process as follows.

1. High energy requirement for solvent regeneration [14]
2. Low capacity of CO_2 loading (limited to 0,5 mol CO_2/mol MEA) [35]
3. High likelihood of equipment corrosion
4. Solvent degradation on account of SO_2, NO_2, and O_2 in exhaust gas
5. Large size of equipment (Resnik, 2004 and Haszeldine, 2009)

As mentioned above, one major challenge of amine absorption technology is its high energy demand during a CO_2-stripping process. The proportion of energy usage in the reboiler accounts for more than 80 % of the total operating cost[40]. In a traditional coal-fired power plant, the energy for stripping process of CO_2 ranges from 3,24 to 4,2 GJ per tonne of CO_2, which in turn reduces the electricity output up to 23 % (Bouillon et al., 2009; Knudsen et al., 2009). Another work done by Bohlin Svolsbru (2013) has shown that the specific heat consumption is between 3,67 and 3,69 MJ/kg CO_2 even with optimal operating ranges of Lean amine rate.

Due to expensive costs of low-pressure steam, high energy consumption of the post-combustion capture makes the costs of avoided CO_2 quite large. Research work done by Rochelle (2009) has shown that the overall cost of a CO_2 capture process is about 52 – 77 US$/tonne CO_2. Another techno-economic analysis on MEA-based CO_2 capture process reports that the operating cost takes up over 70 % of the total CO_2 capture cost[39].

The CO_2-capture cost of a post-combustion system is strongly associated with the absorber column design, absorbent characteristics and the process operating parameters[35]. Current studies have therefore focused on improving the absorbent with optimization of column design. Although many post-combustion studies have been carried out for power generation applications, relatively little research was conducted regarding cement manufacturing process[25]. So far a post-combustion capture with MEA scrubbing has been widely employed in relatively small cement plants with daily emissions of CO_2 up to 400 tonnes[41].

1.4.3.1 Amine absorption chemistry

Amine refers to a derivative of ammonia (NH_4), from which one or more hydrogen atoms are replaced by an aryl group. When only one of three hydrogen atoms of ammonia molecule is replaced, it is called primary amine, to which MEA belongs[42]. MEA with a weight fraction of around 30 % in aqueous solution is often used in the absorber column, where it reacts with CO_2 to form a carbamate solution[43]. One challenge is that the reaction mechanisms of CO_2 absorption into MEA are quite complicated[44]. Although there have been numerous research activities regarding the details of the reaction mechanism, there still exists controversy over the precise process of CO_2 absorption into MEA.

The chemical formula of MEA is denoted as $NH_2C_2H_2OH$, where C_2H_2OH is a substituent for a hydrogen atom in original ammonia molecules. The following reactions are typically presumed to occur when CO_2 forms chemical bonds with a primary amine (MEA) solution[37].

$$CO_2 + RNH_2 \rightarrow RH_2^+NCOO^- \quad (1)$$

$$RH_2 + NCOO^- + NRH_2 \rightarrow RH_2NCOO^-NRH_2^+ \quad (2)$$

$$CO_2 + 2NRH_2 \rightarrow RH_2NCOO^-NRH_2^+ \quad (3)$$

Chemical equation (3) results from adding (1) and (2) together, where it can be known that two MEA molecules absorb one molecule of CO_2[37]. If more details on chemical kinetics of the reaction are to be considered, transitional equations that describe intermediate reactions should be included in addition to equation (1) and (2). In a concise form, the overall process can also be expressed as below[37].

$$CO_2\ (gas) \rightarrow CO_2\ (absorbed) \quad (4)$$

Since Aspen HYSYS simulation stands upon equilibrium-related calculations, equation (4) is sufficient to calculate the absorption process[37]. Chemical dissolution of CO_2 into the amine is an exothermic process, so the temperature increases along the absorber height[45].

1.4.3.2 Column stage efficiency

The theoretical model of a column assumes that each stage perfectly achieves Vapor-Liquid Equilibrium (VLE). The real distillation column, however, does not operate perfectly because a part of the gas phase will not completely contact the liquid phase on the tray[46]. Therefore, the actual number of trays required in the column is greater than the number of theoretical stages[47]. This is because as mass transfer limitations prevent equilibrium from being completely achieved on each tray[48]. To estimate the actual number of trays, the number of theoretical stages must be multiplied by the overall stage efficiency, which is the efficiency of a column or a column section. As shown in Equation 1-1 the overall stage efficiency relates the number of ideal stages to the number of real stages, indicating the difference of a real column to a theoretical column[49].

$$E_o = \frac{E_{ideal}}{E_{real}} \qquad \text{Equation 1-1}$$

where

E_o = overall stage efficiency
E_{ideal} = theoretical (ideal) efficiency
E_{real} = real (actual) efficiency

For instance, when the overall stage efficiency is 50 %, the number of actual stages required are twice that of theoretical stages. The overall stage efficiency is applicable to separating sections of a column and typically ranges between 0,7 and 0,9 depending on the separating conditions or a defined column design[48].

In practice, the stage efficiency varies depending on each component, and more precise calculations require much more information on tray type, column geometry and physical properties of the operating fluids[48]. Another stage efficiency model, which is based on a single stage is also be used to consider a vapor-liquid contacting process on each stage independently. The most popular single-stage efficiency model is the Murphree stage efficiency based on either vapor or liquid phase. It is based on the assumption that the vapor leaving the tray achieves complete equilibrium with the liquid leaving the same tray[49]. Equation 1-2 shows how the Murphree stage efficiency is calculated[50].

$$E = \frac{Y_n - Y_{n+1}}{Y_n^* - Y_{n+1}} \qquad \text{Equation 1-2}$$

where

E = Murphree efficiency at stage n+1
Y_n = actual composition of vapor (liquid) leaving stage n
Y_{n+1} = actual composition of vapor (liquid) leaving stage n+1
Y_n^* = composition in equilibrium of vapor (liquid) leaving stage n

According to Equation 1-2 the Murphree stage efficiency can also be viewed as the ratio of the change of composition on an actual stage to the change of composition on an equilibrium stage[51]. A schematic drawing representing the compositions on different trays is shown in Figure 1-4.

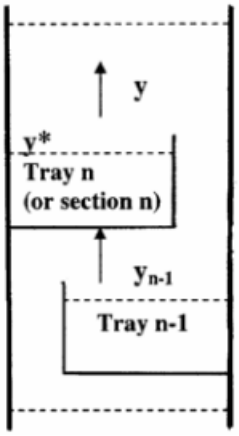

Figure 1-4 Schematic sketch illustrating the Murphree efficiency [37]

1.5 Process description in CO_2 capture plant

Figure 1-5 illustrates a typical post-combustion CO_2 capture process with the main pieces of equipment and flow directions. Detailed description for different types of process equipment are given in the following subchapters.

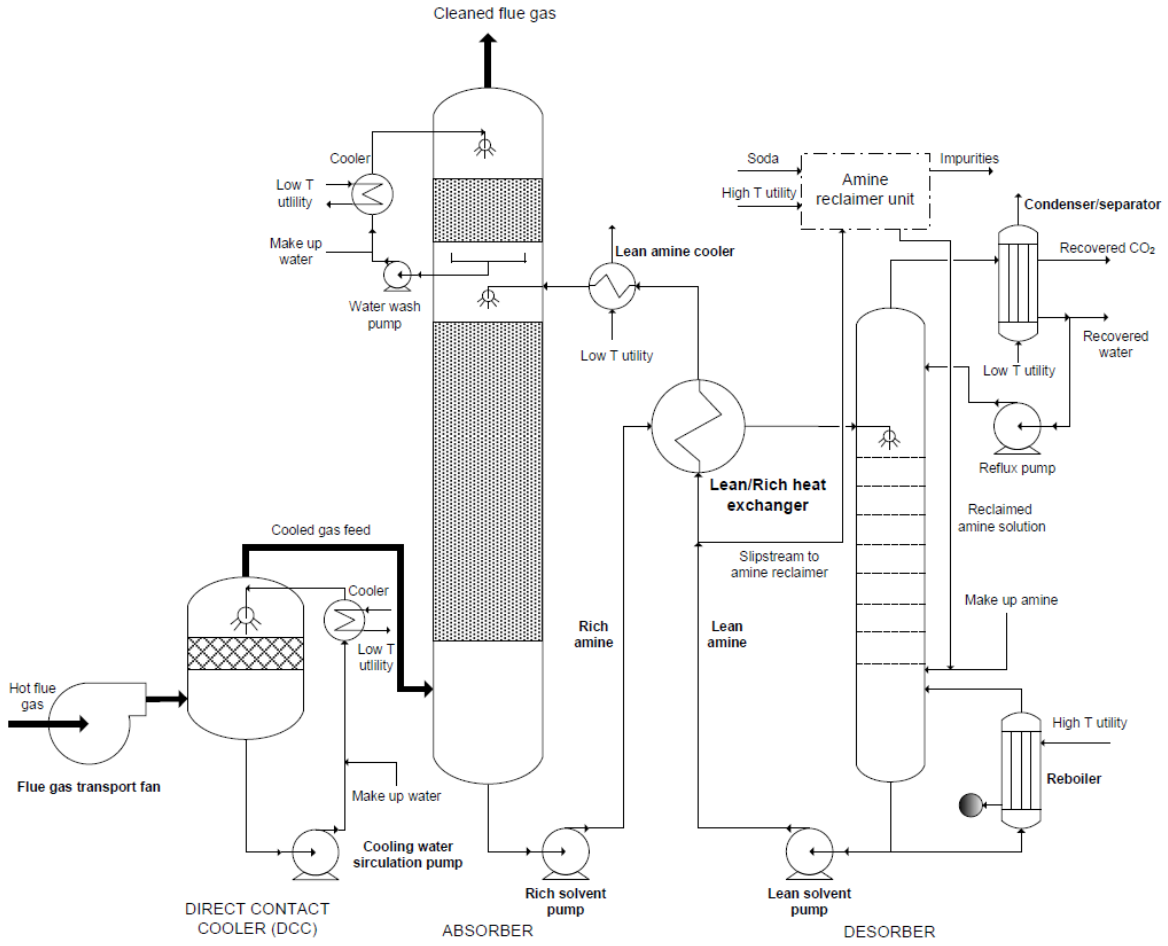

Figure 1-5 Schematic diagram of a typical post-combustion CO_2 capture plant [45]

1.5.1 Flue gas fan

The exhaust gases coming from a cement plant typically have an atmospheric pressure[45]. Because there are pressure drops in Direct contact cooler (DCC) and across the absorber column, a flue gas fan is installed before DCC to supply additional pressures to the flue gas. Aside from the CO_2-stripping process in desorber column, the Flue gas fan takes up a significant proportion of the entire energy use in traditional CO_2-capture plants. (Schach et al., 2010).

1.5.2 Direct contact cooler

The flue gas temperature coming into the capturing plant is about 70 – 90 ℃[45]. To ensure favorable conditions for CO_2-absorption, a direct contact cooler (DCC) is installed before the absorber column to cool the flue gas down to around 40 – 50 ℃[52]. The flue gas coming into DCC contacts with cooling water through the packings, which have large surface areas for efficient heat transfer. The cooling water circulating inside DCC also removes fine particulates of flue gases. During the process the cooling water is slightly heated, so it is cooled again by an external cold utility for continual use[45].

1.5.3 Absorber column

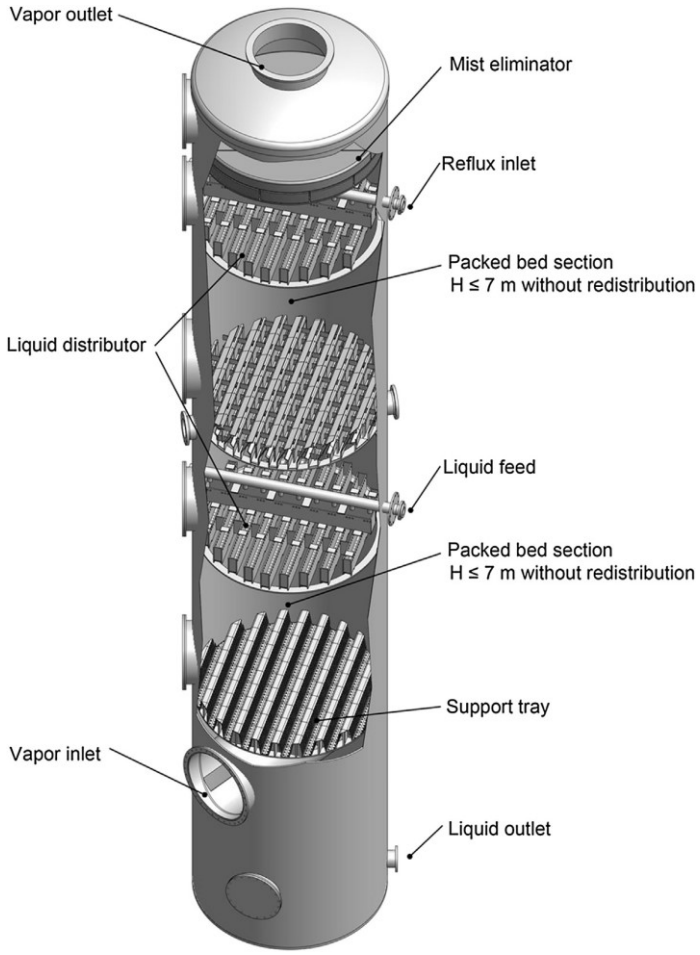

Figure 1-6 Schematic drawing of a typical absorber column [49]

Figure 1-6 illustrates a schematic sketch of typical column internals. Due to a large volume flow of flue gases, absorber column is generally the tallest unit in a capture plant, with its

total height reaching tens of meters[45]. Flue gases containing the CO_2 are routed into the bottom part of absorber column (i.e. 'Vapor inlet' in the figure). The gas flows upwards at a specified velocity through the packing beds and comes into contact with the liquid solvent flowing countercurrently. The liquid solvent chemically absorbs CO_2 molecules from flue gases and thereby mass transfer takes place along the column. The concentration of CO_2 steadily decreases until the flue gas reaches the top of absorber column, whereas the CO_2-loading of liquid solvent progressively increases until the absorbent exit the column bottom. Because the CO_2-absorption is an exothermic process, the temperature inside the column varies depending on the stage[45]. Typical operating temperature ranges from 40 to 60 ℃, while the pressure inside the absorber column is nearly equal to the atmospheric pressure[38].

1.5.3.1 Column packing

Packings are the core elements of absorber columns and act as vapor-liquid contacting devices by providing the large specific surface area[45]. While liquid solvents flowing inside the column wet the surface of packings, the vapor is led to pass through the wetted surface to bring about the mass transfer. Packings are broadly classified into random and structured packings. While the random packings are dumped into the column, the structured packings are arranged in an orderly way and stacked inside the column[46]. The structured packings are not only more capacitive than random packings (by 25 – 30 %) but also develop higher interfacial areas. The main reasons for this may be summarized as in the following[53]:

1. More amount of non-negligible droplets is generated than random packings (Alix and Raynal, 2009).
2. Structured packings produce fewer void fractions for a given geometric area.

Sulzer first introduced the sheet metal structured packing of in 1976 and named it 'Mellapak 250Y'. While the number '250' stands for a specific geometric area in unit of m^2/m^3, the symbol 'Y' indicates that an inclination angle of corrugation is 45°[49]. Figure 1-7 illustrates the structured packing element (Mellapak 250Y) composed of a number of corrugated metal sheets. To form a cylindrical shape, the sheets are often tightly packed against each other and surrounded by collars to curb bypassing of liquid and vapor along the column wall[49].

Figure 1-7 Structured packing (Mellapak 250Y) in one-piece form [49]

It is conventional to indicate the specific surface area and corrugation inclination angle by the name of packing type. Typically, the corrugation has an angle of 45° for 'Y-type' (e.g. Mellapak 250Y) and 30° for 'X-type' (e.g. Mellapak 2X). Specific geometric area of structured packings in industrial applications typically range from 50 to 750 m^2/m^3[49].

1.5.3.2 Liquid distributor

As a liquid feed flows down through the packing bundle, the liquid solvent gradually becomes less efficiently distributed over the packing, mainly due to interaction with the column walls[49]. This requires the liquid solution to be periodically collected and redistributed to minimize the maldistribution and solvent channeling. Liquid distributors are therefore installed to provide an even distribution of liquid solutions across the packing bed, optimizing the mass transfer of gas contaminant.

One important characteristic determining the distributor performance is the drip-point density, which is the ratio of the number of drip-points to the distributor area[49]. The drip point affects the absorption efficiency in the upper part of a packing bed, and is dependent on the geometric area of the packing[54].

Depending on the design specifications, distributors are either attached to the top of each packing bed or positioned above with the space of up to 0,2 m[49]. The height of liquid distributors is typically between 0,5 and 1 m, including a liquid collector[48]. Liquid collectors located between the packing beds mix the collect the liquid solvents and send them to another liquid distributor below through the ring channels.

1.5.3.3 Water wash section

The Lean amine coming downwards often suffers from liquid entrainment by flue gases flowing upwards, and therefore a water wash unit is installed in the upper part of the column[38]. Before the exhaust gas exits the absorber column into the atmosphere, it is scrubbed through the water wash section to remove amine components[45]. Since the temperature of water absorbent slightly increases due to warm temperatures of flue gases, the water is cooled down at regular intervals by external cold utility and circulates the loop by a pump. Additional water stream is often needed to make up for water losses out of absorber.

1.5.4 Rich pump

Rich amine solvent containing CO_2 is collected at the sump of absorber column. To overcome pressure drops inside the Lean/Rich heat exchanger and reach the desorber column, Rich amine is transported by Rich pump[45]. Additional duty should be considered if the Rich amine needs to overcome the height difference of desorber column.

1.5.5 Lean/Rich heat exchanger

Before the Rich amine stream enters the desorber column, it needs to be heated sufficiently to facilitate the CO_2-stripping process. The Lean amine stream out of desorber has relatively high temperatures, so it transfers heat energy to Rich amine feed inside the Lean/Rich heat exchanger. Since this process is a kind of heat integration, it contributes to saving the reboiler duty and therefore both the operating and capital cost of reboiler can be reduced[45].

Three critical process parameters of the Lean/Rich heat exchanger are: log mean temperature difference, overall heat transfer coefficient and the minimum approach temperature.

1.5.5.1 Log mean temperature difference (ΔT_{LMTD})

The log mean temperature difference, ΔT_{LMTD}, is a logarithmic average of temperature differences between the hot and cold streams at each end. It represents the driving force for heat transfer between the cold and hot streams. The larger the ΔT_{LMTD} is, the higher the heat transfer rate becomes between the fluids[55]. Under the condition of the constant heat transfer rate, a higher ΔT_{LMTD} will lead to a smaller heat transfer area, thereby reducing the equipment cost.

Calculation formula of ΔT_{LMTD} in a counterflow system is described in Appendix 2.

1.5.5.2 Overall heat transfer coefficient (U)

The overall heat transfer coefficient, U, represents the overall ability to transfer heat from one fluid to another through a series of convective or conductive barriers. It is dependent on the flow geometry, material property of heat exchanger and the fluid properties[56]. If both the heat exchanger duty (Q) and ΔT_{LMTD} are constant, the overall heat transfer coefficient is inversely proportional to the heat transfer area. Because the heat transfer area (A) is the basis for heat exchanger cost, determining the value of U correctly if of importance to enhance the reliability of cost estimation.

The relationship between U, Q, A and ΔT_{LMTD} is described in Appendix 2.

1.5.5.3 Minimum approach temperature (ΔT_{min})

The minimum approach temperature, ΔT_{min}, refers to the minimum temperature difference between the two fluids along the same position. If the two fluids contacting each other have the constant heat capacity, ΔT_{min} is also equal to the pinch temperature[48]. For this reason, setting the ΔT_{min} too low may result in decreased driving force of heat transfer.

As with ΔT_{LMTD}, ΔT_{min} is also a good measure of the heat transfer rate (or driving force) in heat exchangers. A trade-off of ΔT_{min} exists between the Lean/Rich heat exchanger and reboiler duty[45]. For instance, a lower ΔT_{min} will lead to increased Lean/Rich heat exchanger duty but at the same time the reduced reboiler duty.

The definition of ΔT_{min} for different flow conditions is given in Appendix 2.

1.5.6 Desorber column

The Rich amine flows into the upper part of the desorber and makes its way down to the bottom, where it is heated indirectly in Reboiler by steam at around 120 ℃[46]. The water content in Rich amine is vaporized into steam during this process and flows upwards along the column through a series of packing beds[23]. The steam contacts with the liquid Rich amine flowing downwards, it heats up the Rich stream and decreases the solubility of CO_2 in MEA. As a result, CO_2 is recovered gradually as a vapor phase and flow upwards to the top of

the column together with the remaining steam. The Rich amine solution therefore becomes leaner while flowing down through the desorber, and finally at the bottom of the column the Rich amine turns into Lean amine and is pumped back into the absorber for recycling.

The overhead products, which mainly consist of water and CO_2 in vapor phases, are cooled and condensed by condenser using cooling water. The CO_2-rich stream is sent to another series of processing units for dehydration, compression, and storage.

The desorption process is highly energy-demanding, and therefore the reboiler power accounts for a substantial part of energy consumption in the entire capturing process[12]. In general, the volume flow of Rich amine vapor into the desorber is much less than those of flue gases into the absorber, so the desorber size is much smaller than absorber columns[23].

1.5.7 Lean pump

Lean amine stream collected at the sump of desorber column is transported by Lean pump to the Lean/Rich heat exchanger. As with the Rich pump, the Lean pump duty is determined mainly by three parameters: pressure increase, Lean amine volume flow and the adiabatic efficiency. Additional duty should be considered if the Lean amine needs to overcome the height difference of absorber column.

1.5.8 Lean cooler

Because the Lean amine temperature out of Lean/Rich heat exchanger is too high to be directly routed into absorber column, the Lean amine should be cooled further by Lean cooler. Cooling water is often used in Lean cooler, and the Lean amine is cooled down to around 45 ℃ before entering the absorber column[45].

1.5.9 MEA reclaimer

Flue gases contain a small fraction of acid gases other than CO_2 such as salts, organic components, HF, NO_x, SO_x or dust[22]. The impurities accumulated over time react with amine solutions and produce effluents, particularly NH_3 and heat-stable salts[25]. Such processes lead to solvent degradation and reduced absorption performance of MEA, and therefore a reclaimer needs to be installed between the Lean pump and Lean/Rich heat

exchanger. The aqueous amines are vaporized by a hot utility and carried over to the absorber column for recycling, while the waste products such as heat-stable salt (HSS) and high-molecular organic substance remaining inside the unit are withdrawn into waste streams[45]. One previous study has experimentally found that the consumption of MEA ranges from 1,4 to 2,0 kg MEA/tonne CO_2 for a traditional CO_2-capture process in coal-fired power plants[57]. To remove particle- and carbon-containing byproducts, particulate filters also normally need to be installed in the solvent circuit[22].

Reclaimer is considered to be an essential unit especially when the sour gases are scrubbed with amine-based solvents due to amine characteristics[38]. It is however known to have little impact on total capital cost compared to other process equipment.

2 Project description

The main procedures of this thesis can be summarized as in the following[4]:

i) Base case simulation of post-combustion CO_2 capture process using steam only
ii) Alternative process simulation design using waste heat only
iii) Equipment dimensioning & Cost estimation
iv) Impact analysis of different process parameters on CO_2-capture cost
v) Determining the optimum process parameters yielding the minimum capture cost

The difference between the Base case and Alternatives is the source of heat energy for the CO_2-stripping process. As described in Chapter 1.4.3, traditional post-combustion CO_2 capture plants with steam are energy- and cost expensive, particularly in solvent-regeneration process at high temperatures. This thesis therefore focuses on optimization of a CO_2-capture process by integrating the waste heat potential of cement kilns[5]. Table 2-1 compares the Base case with Alternatives based on heat utility.

Table 2-1 Comparison overview of Base case and Alternatives

	Base case	Alternatives
Capture scale	Full-scale capture (η_c = 90 %)	Partial capture
Heat source	Low-pressure steam	Waste heat

CO_2-capture efficiency in Base case is set as 90 %, which is practically the maximum efficiency with commercial operating conditions in full-scale capture plants[8]. The amount of waste heat in this study is assumed to be 40 % of the reboiler duty in Base case.

For impact analysis of different process parameters on CO_2-capture cost, the Alternative is divided further based on three process parameters: flue gas rate, the number of stages in absorber column (N_{stage}) and the superficial gas velocity into the absorber column (v_g). Detailed descriptions on each parameter are given in the following subchapters.

[4] More details on the project description can be found in Appendix 1.

[5] CO_2 compression, transportation or storage are not encompassed in this thesis.

2.1 Parameter 1 – Flue gas rate

The first parameter to study is the flue gas rate. While the Base case has the full flow of the flue gas, the Alternative has four different flue gas rates. The term 'Full flow' in this study indicates that all of the flue gas from cement kilns is routed into the absorber column. The 'Partial flow' means that only a part of the flue gas is let into the absorber column, while the rest is routed into a bypass and released into the air without solvent scrubbing. Table 2-2 gives the comparison overview based on the flue gas rate.

Table 2-2 Comparison overview based on flue gas rate

Parameter	Base case	Alt. 1	Alt. 2	Alt. 3	Alt. 4
Flue gas rate	Full flow (100 %)	Full flow (100 %)	Partial flow (80 %)	Partial flow (60 %)	Partial flow (40 %)

Schematic diagrams of Base case and the four Alternatives are illustrated below from Figure 2-1 to Figure 2-5.

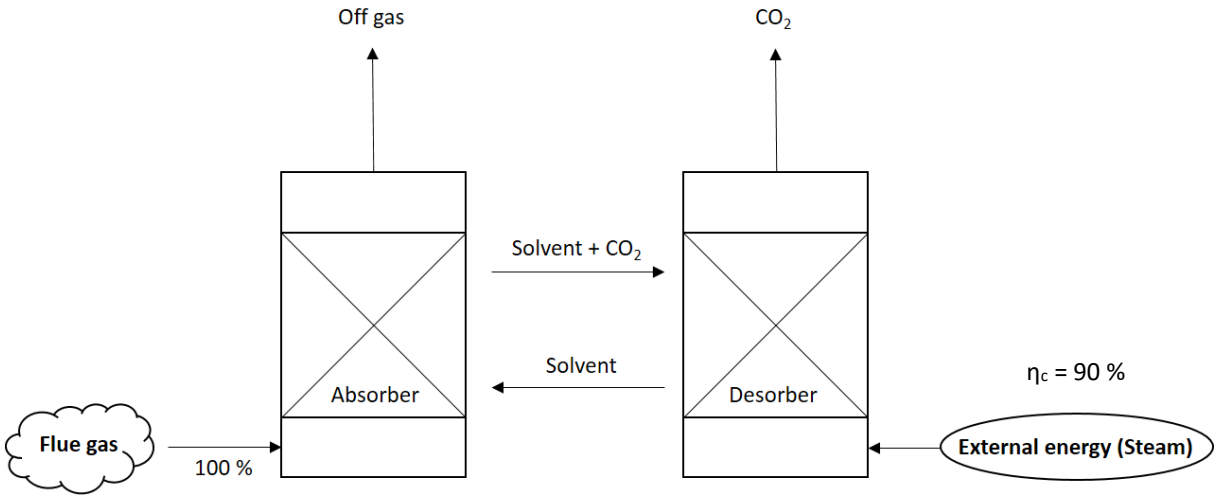

Figure 2-1 Schematic drawing of Base case

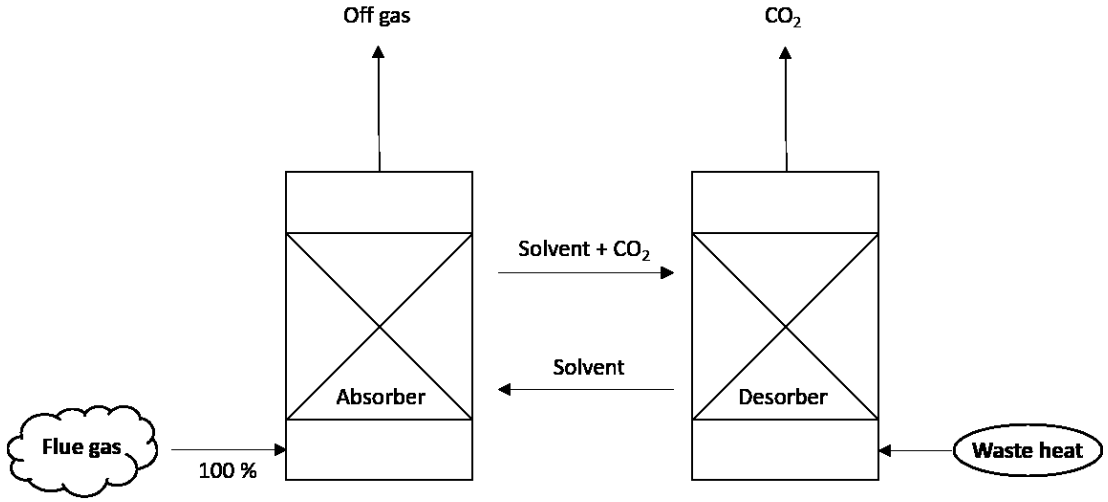

Figure 2-2 Schematic drawing of Alternative 1

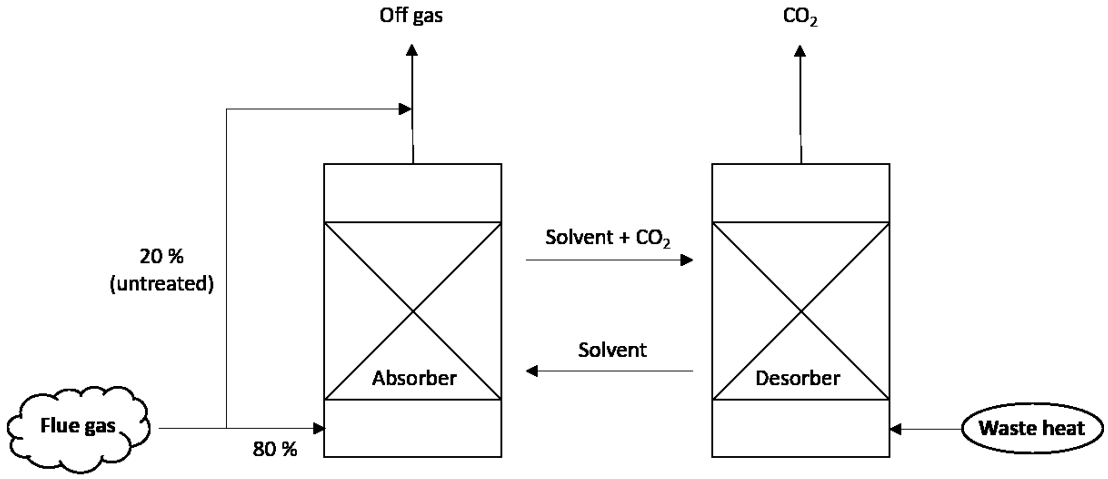

Figure 2-3 Schematic drawing of Alternative 2

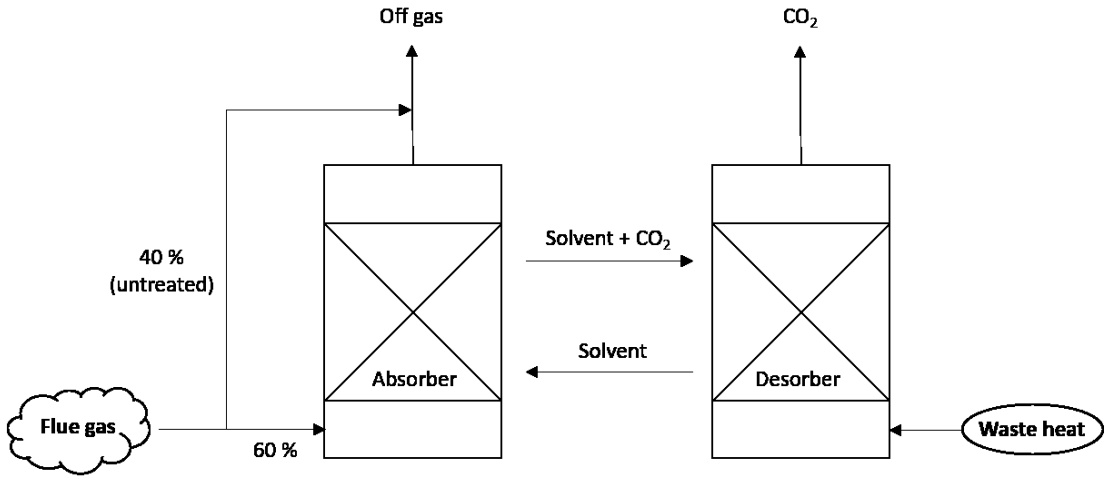

Figure 2-4 Schematic drawing of Alternative 3

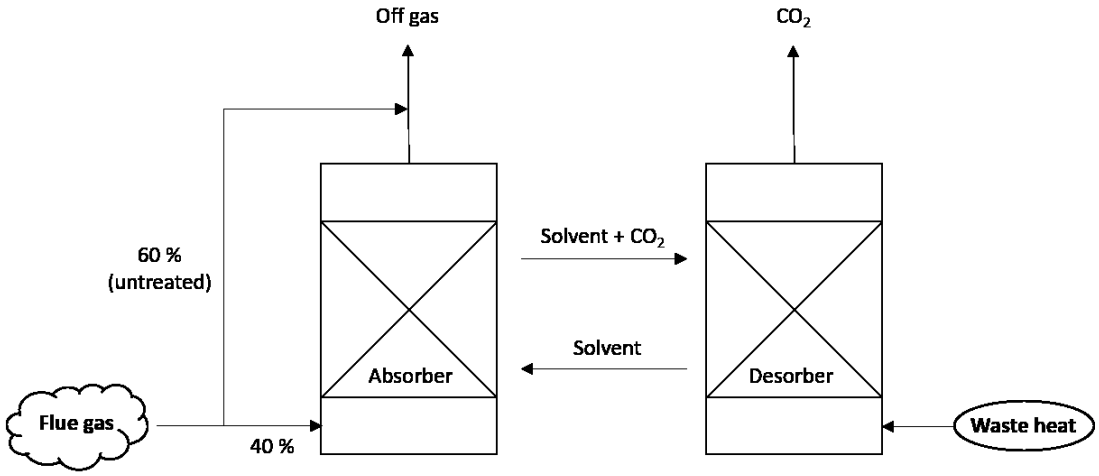

Figure 2-5 Schematic drawing of Alternative 4

2.2 Parameter 2 – Superficial gas velocity (v_g)

The first parameter to study is the superficial gas velocity into the absorber column. While the Base case has the gas velocity of 2,5 m/s, the Alternatives have four different gas velocities, i.e., 1,5 m/s, 2,0 m/s, 2,5 m/s and 3,0 m/s. Table 2-3 gives the comparison overview based on the flue gas rate and the gas velocity. The gas velocity of 2,5 m/s will be termed the 'Base gas velocity ($v_{g,b}$)' in this study.

Table 2-3 Comparison overview based on flue gas rate and v_g

Parameter	Base case	Alt. 1	Alt. 2	Alt. 3	Alt. 4
Flue gas rate	Full flow (100 %)	Full flow (100 %)	Partial flow (80 %)	Partial flow (60 %)	Partial flow (40 %)
Gas velocity (v_g)	2,5 m/s	1,5 – 3,0 m/s	1,5 – 3,0 m/s	1,5 – 3,0 m/s	1,5 – 3,0 m/s

2.3 Parameter 3 - Number of stages in absorber (N_{stage})

The third parameter to study is the number of stages in absorber column. While the Base case has fifteen stages in absorber column, the Alternatives have different numbers of stages ranging from five to fifteen. Table 2-4 gives the comparison overview based on the flue gas rate, gas velocity and the number of absorber stages.

Table 2-4 Comparison overview based on flue gas rate, v_g and N_{stage}

Parameter	Base case	Alt. 1	Alt. 2	Alt. 3	Alt. 4
Flue gas rate	Full flow (100 %)	Full flow (100 %)	Partial flow (80 %)	Partial flow (60 %)	Partial flow (40 %)
Gas velocity (v_g)	2,5 m/s	1,5 – 3,0 m/s	1,5 – 3,0 m/s	1,5 – 3,0 m/s	1,5 – 3,0 m/s
Number of stages (N_{stage})	15	5 – 15	5 – 15	5 – 15	5 – 15

The overall comparison of the Alternatives with Base case is summarized in Table 2-5.

Table 2-5 Overall comparison of the Alternatives with Base case

Base case (Reference model)	- Flue gas rate : full flow (100 %) - Gas velocity (v_g) : 2,5 m/s - CO_2-capture efficiency (η_c) : 90 % - Heat utility : low-pressure steam - Number of stages in absorber column (N_{stage}) : 15
Alternative 1	- Flue gas rate : full flow (100 %) - Gas velocity (v_g) : 1,5 – 3,0 m/s - Heat utility : waste heat - Number of stages in absorber column (N_{stage}) : 5 – 15
Alternative 2	- Flue gas rate : partial flow (80 %) - Gas velocity (v_g) : 1,5 – 3,0 m/s - Heat utility : waste heat - Number of stages in absorber column (N_{stage}) : 5 – 15
Alternative 3	- Flue gas rate : partial flow (60 %) - Gas velocity (v_g) : 1,5 – 3,0 m/s - Heat utility : waste heat - Number of stages in absorber column (N_{stage}) : 5 – 15
Alternative 4	- Flue gas rate : partial flow (40 %) - Gas velocity (v_g) : 1,5 – 3,0 m/s - Heat utility : waste heat - Number of stages in absorber column (N_{stage}) : 5 – 15

According to Table 2-5, the total number of cases to be studied in Alternatives (excl. Base case) is:

$$4 \text{ (flue gas rate)} * 4 \text{ (gas velocity)} * 11 \text{ (number of absorber stages)} = 176$$

On the basis of the Base case capture efficiency (i.e. 90 %), it is possible to roughly estimate the capture efficiency of the four Alternatives by using process parameters: the ratio of waste heat to Base case steam power, flue gas rate and the number of absorber stages. Table 2-6 shows the expected CO_2-capture efficiencies based on the rule-of-thumb calculation.

Table 2-6 Expected CO_2-capture efficiency for different Alternatives

	When $N_{stage} = 15$	When $N_{stage} < 15$
Base case	$\eta_c = 90\ \%$	–
Alt. 1	$\eta_c \approx 90\ \% \times \frac{40\ \text{(waste heat)}}{100\ \text{(steam)}} \times \frac{100\ \text{(full flow)}}{100\ \text{(full flow)}} = 36\ \%$	$\eta < 36\ \%$
Alt. 2	$\eta_c \approx 90\ \% \times \frac{40\ \text{(waste heat)}}{100\ \text{(steam)}} \times \frac{100\ \text{(full flow)}}{80\ \text{(partial flow)}} = 45\ \%$	$\eta < 45\ \%$
Alt. 3	$\eta_c \approx 90\ \% \times \frac{40\ \text{(waste heat)}}{100\ \text{(steam)}} \times \frac{100\ \text{(full flow)}}{60\ \text{(partial flow)}} = 60\ \%$	$\eta < 60\ \%$
Alt. 4	$\eta_c \approx 90\ \% \times \frac{40\ \text{(waste heat)}}{100\ \text{(steam)}} \times \frac{100\ \text{(full flow)}}{40\ \text{(partial flow)}} = 90\ \%$	$\eta < 90\ \%$

For each Alternative, it is expected that the maximum capture efficiency is obtained when the number of absorber stages is the maximum (i.e. N_{stage} of 15). For example, Alternative 1 is anticipated to have the maximum capture efficiency of 36 % when N_{stage} is 15. Fewer numbers of stages than fifteen are expected to have lower capture efficiency.

The efficiencies shown in Table 2-6 will be compared with the actual capture efficiencies obtained from HYSYS in later chapters. Detailed values of the process parameter (e.g. flue gas rate, equipment duties, operating temperature etc.) are also described in later chapters.

3 Process simulation

3.1 Aspen HYSYS as simulation tool

Aspen HYSYS is a comprehensive process simulation program developed by AspenTech[58]. It is used as a process modeling and optimization tool and carries out complex calculations regarding thermodynamic properties with built-in equilibrium models. Equipped with several specialty models including Amines Property Package, it is also able to model a sweetening process of sour systems with amines (e.g. MEA)[58].

A precise description of mass transfer between amine solvent and the flue gas is essential to obtain practical information on a realistic process. The chemical absorption of CO_2 is regulated by its equilibrium solubility into amine absorbent and the reaction kinetics[46]. Since the absorption of CO_2 into MEA is an exothermic process, the effects of heat on the overall performance are also need to be considered. Amines Property Package takes this effect into account and computes compositions of different components at equilibrium state based on a collection of experimental data. Aspen HYSYS employs the following models for calculating vapor liquid equilibrium (VLE) [46].

- Liquid phase: Kent-Eisenberg or Li-mater model
- Vapor phase: Peng-Robinson (PR)
- Enthalpy/Entropy: Curve-fitting

The Kent-Eisenberg model has often been used in previous studies for the equilibrium of liquid phase, and therefore the same one is to be used in this study[45, 46]. The Kent-Eisenberg model predicts phase equilibrium data for CO_2 in amine solutions by defining the chemical reaction equilibrium in liquid phases[59]. Amine Property Packings also features a Murphree efficiency model, which can specify an efficiency for each individual stage to consider deviations from the ideal equilibrium stage[46]. With the chosen amine solution, the correlation between heats of solution and component compositions is made.
Applications of Amine Property Package are however limited to CO_2, H_2S, COS and CS_2[45]. The simulation environment in this thesis considers CO_2 only as a sour gas, and therefore no effects of other sour gases on CO_2 are considered.
To date, most of the studies on CO_2 removal with Aspen HYSYS have been focused on natural gas only. On the other hand, little research have been done regarding CO_2 removal in the atmospheric exhaust gas coming from industrial process, including cement industry[37].

3.2 Simulation overview and assumption

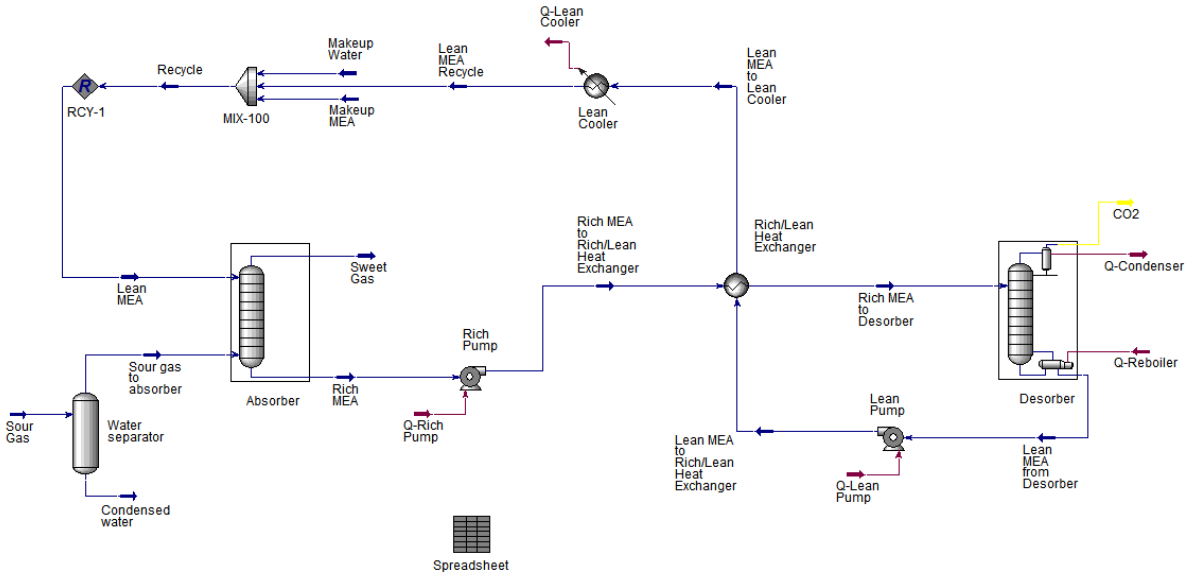

Figure 3-1 Process flow diagram (PFD) of Base case simulation in Aspen HYSYS

Figure 3-1 illustrates the typical process flow diagram (PFD) of CO_2 capture process, where each stream and equipment is denoted by its own name. An enlarged image of Figure 3-1 is available in Appendix 13.

The simulation design and configuration of Figure 3-1 was initially developed by Lars Erik Øi in his previous study[37]. As a continuation of the previous studies, the present thesis extends the use of this model with MEA aqueous solution for process optimization. The Base case and Alternatives of this study basically follows the same process as in Figure 3-1, whereas several process parameters are individually varied for impact analysis.

Amine Property Package is known to have limitations on MEA specifications. It is also recommended not to exceed an acid gas loading of 0,50 in order to facilitate the convergence procedure and in a realistic way to achieve the optimum plant operating conditions[46]. Table 3-1 summarizes the allowable range of the use of Amine Property Package.

Table 3-1 MEA specifications in Amine Property Package [60]

Specification	Unit	Required range
CO_2-loading	[mol CO_2/mol MEA]	< 1
MEA concentration	[wt%]	0 – 30
CO_2 partial pressure	[bar]	0 – 20
MEA temperature	[°C]	25 – 126

The limitation of MEA concentration to 30 wt% is in part due to corrosion problems[38]. All the simulations studied in this thesis meet the required specifications in Table 3-1.

The simulation scope of this thesis is assumed to contain the following equipment:

- Water separator (before absorber column)
- Absorber column
- Rich & Lean pump
- Lean/Rich heat exchanger
- Desorber column (incl. condenser and reboiler)
- Lean cooler
- Makeup water/MEA

The absorber column has specified Murphree efficiencies linearly ranging from 0,11 to 0,21 depending on the number of stages. Predetermined values of Murphree efficiency can be found in Appendix 3. For the Lean/Rich heat exchanger, the minimum approach temperature is set as 10 ℃ in all simulation cases to ensure sufficient driving force of heat transfer between the fluids. Although included in simulation environments, the effect of Water separator (before absorber column) on capture costs will not be considered in later chapters.

Other miscellaneous equipments will also be necessary for actual operation of CO_2-capture plants as listed below, but they are not included in simulations.

- Flue gas fan
- Direct contact cooler (DCC)
- Water wash unit (in absorber and desorber column)
- MEA reclaimer

Instead of including the Flue gas fan and DCC, the flue gas conditions are specified as 1,1 bar and 40 ℃. Additionally, the flue gases contain CO_2, N_2 and H_2O only in process simulations, though there are also other sour gases (e.g. O_2, NO_x, SO_x etc.) in practice. Water wash units (in absorber column) are not considered in simulation, but MEA losses out of absorber will be compensated by makeup flows of MEA and H_2O based on mass balance equations. Although the Flue gas fan and water wash units are not included in simulations, they will be considered later in equipment dimensioning and cost estimation chapters.

Because the MEA solution does not undergo thermal or chemical degradation in the simulation environment, MEA reclaimer units may also not be included.

3.3 Simulation specification

This chapter presents the simulation specifications applied to Base case and Alternatives. Some part of specification data were cited from previous studies by Braut Kallevik (2010) and Bohlin Svolsbru (2013) to reflect the actual process parameters in a real cement plant.

3.3.1 Base case

Table 3-2 shows the input and output parameters used in Base case simulation.

Table 3-2 Simulation specifications of Base case

Process parameter		Unit	Value
Input parameter	**Flue gas temperature**	[°C]	40
	Flue gas pressure	[bar]	1,1
	Flue gas rate	[kmol/h]	8974
	CO_2 content in flue gas	[mol%]	17,8
	H_2O content in flue gas	[mol%]	20,63
	Lean amine temperature	[°C]	45,02
	Lean amine pressure	[bar]	1,01
	Lean amine rate	[kg/h]	1583000
	MEA content in Lean amine	[wt%]	28,8
	CO_2 content in Lean amine	[wt%]	5,4
	Number of stages in absorber column (N_{stage})	[-]	15
	Murphree efficiency in absorber column	[-]	0,11 – 0,21
	Pressure increase across Rich pump	[bar]	1,1
	Rich amine temperature out of Lean/Rich HX	[°C]	106,8
	Number of stages in desorber column	[-]	10
	Murphree efficiency in desorber column	[-]	0,5
	Reflux ratio in desorber column	[-]	0,3
	Reboiler temperature	[°C]	120
	Reboiler pressure	[bar]	2
	Pressure increase across Lean pump	[bar]	2
Output parameter	**CO_2 content in flue gas (after water separator)**	[mol%]	19,5
	H_2O content in flue gas (after water separator)	[mol%]	6,72
	ΔT_{min} in Lean/Rich heat exchanger	[°C]	10,00
	CO_2-capture efficiency	[-]	90,00
	Energy demand	[MJ/kg CO_2]	3,89
	Reboiler power	[MW]	67,93

The simulation specifications are classified into input and output parameters. The input parameters refer to process parameters that can be given values directly in simulation environment and thus are controllable within the allowable range of Amine Property Package. On the other hand, the output parameters are process parameters calculated on the basis of the input parameters and thus cannot be directly adjusted. Therefore, it can be said that the output parameters are resultant figures, which can be controlled indirectly by adjusting the input parameters.

Specifications of makeup MEA and H_2O are not included in Table 3-2 since they do not have big effects on the overall simulation process. In the case of the parameters marked in bold in the table, they are kept constant in this study and therefore the value of these process parameters remain unchanged throughout all the simulations.

3.3.2 Alternatives

Simulation specifications of each Alternative are available in Appendix 15, where the parameters having the same value as in Table 3-2 are not included.

Overall procedures to configure simulation parameters of Alternatives from the base case can be found in Appendix 5.

3.4 Calculation formulas in simulation

This chapter presents some useful calculation formulas used in HYSYS simulations.

- **CO_2-capture efficiency**

$$\text{Capture efficiency [\%]} = \frac{\dot{n}_{co2,sour} - \dot{n}_{co2,sweet}}{\dot{n}_{co2,sour}} \qquad \text{Equation 3-1}$$

where

$\dot{n}_{co2,sour}$ = CO_2 molar flow into absorber [kmol/h]

$\dot{n}_{co2,sweet}$ = CO_2 molar flow out of absorber [kmol/h]

- **Energy demand (energy per unit mass of CO_2)**

$$\text{Energy demand [MJ/kg]} = \frac{Q_{reboiler}}{\dot{m}_{co2,condenser}} \qquad \text{Equation 3-2}$$

where

$\dot{m}_{co2,condenser}$ = CO_2 mass flow out of condenser [kg/s]

$Q_{reboiler}$ = reboiler power [MW]

- **CO_2-capture rate**

$$\text{Capture rate [tonne } CO_2\text{/year]} = \dot{m}_{co2,condenser} \times 8000 \left[\frac{h}{year}\right] \times \frac{1}{1000}\left[\frac{tonne}{kg}\right]$$

$$= 8 * \dot{m}_{co2,condenser} \qquad \text{Equation 3-3}$$

where

$\dot{m}_{co2,condenser}$ = CO_2 mass flow out of condenser [kg/h]

Calculation formulas of Rich & Lean pump power, LMTD in heat exchangers and the minimum approaching temperature (ΔT_{min}) can be found in Appendix 2.

3.5 Simulation result

This chapter presents the simulation results of the Base case and Alternatives with focus on four important process parameters: CO_2-capture efficiency, CO_2-capture rate, energy demand and Lean amine rate.

3.5.1 CO_2-capture efficiency

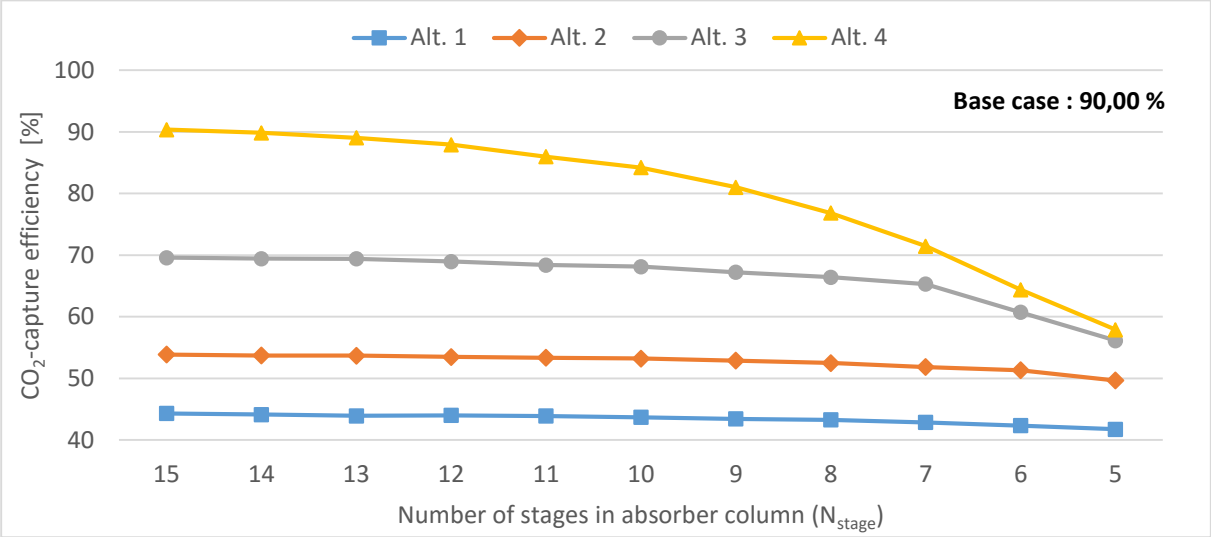

Figure 3-2 CO_2-capture efficiency versus N_{stage} for each Alternative

Figure 3-2 indicates the CO_2-capture efficiency changes for each Alternative according to N_{stage}. A close look at the figure suggests that the sensitivity of efficiency to N_{stage} differs between the Alternatives. While the capture efficiency of Alternative 1 is relatively little influenced by N_{stage}, the capture efficiency of Alternative 4 is quite sensitive to N_{stage} and thus displays noticeable drops with decreasing N_{stage}. Exact values corresponding to Figure 3-2 are arranged in Table 3-3.

Table 3-3 CO_2-capture efficiency versus N_{stage} for each Alternative (unit: %)

N_{stage}	15	14	13	12	11	10	9	8	7	6	5
Alt. 1	44,33	44,15	43,93	44,00	43,91	43,69	43,43	43,28	42,87	42,34	41,74
Alt. 2	53,87	53,71	53,69	53,48	53,36	53,22	52,88	52,51	51,86	51,33	49,68
Alt. 3	69,59	69,43	69,41	68,96	68,40	68,14	67,23	66,43	65,29	60,73	**56,13**
Alt. 4	90,37	**89,94**	**89,05**	**87,92**	**85,98**	**84,20**	**81,02**	**76,83**	**71,45**	**64,39**	**57,90**

(Base case: 90,00 %)

It is observed that the overall efficiencies in Table 3-3 are higher than previously anticipated in Table 2-6. Taking the Alternative 1 as an example, the maximum expected efficiency was 36 %, yet the actual efficiencies in Table 3-3 show greater values irrespective of N_{stage}. The same trend is also observed in Alternative 2, and except for the N_{stage} of five Alternative 3 also shows the higher efficiencies than the maximum expected efficiency. In the case of Alternative 4, only one case yields a better efficiency (i.e. N_{stage} of 15) than what was predicted in Table 2-6. Efficiencies lower than the maximum expected efficiency were marked in bold in Table 3-3.

Overall, the following facts can be deduced from the Table 3-3.

1. With a constant and limited amount of reboiler power (i.e. waste heat), higher flue gas rates tend to yield better capture efficiencies than expectation over the defined range of N_{stage}.
2. The less the flue gas is, the more sensitive the capture efficiency becomes to N_{stage}.

3.5.2 CO_2-capture rate

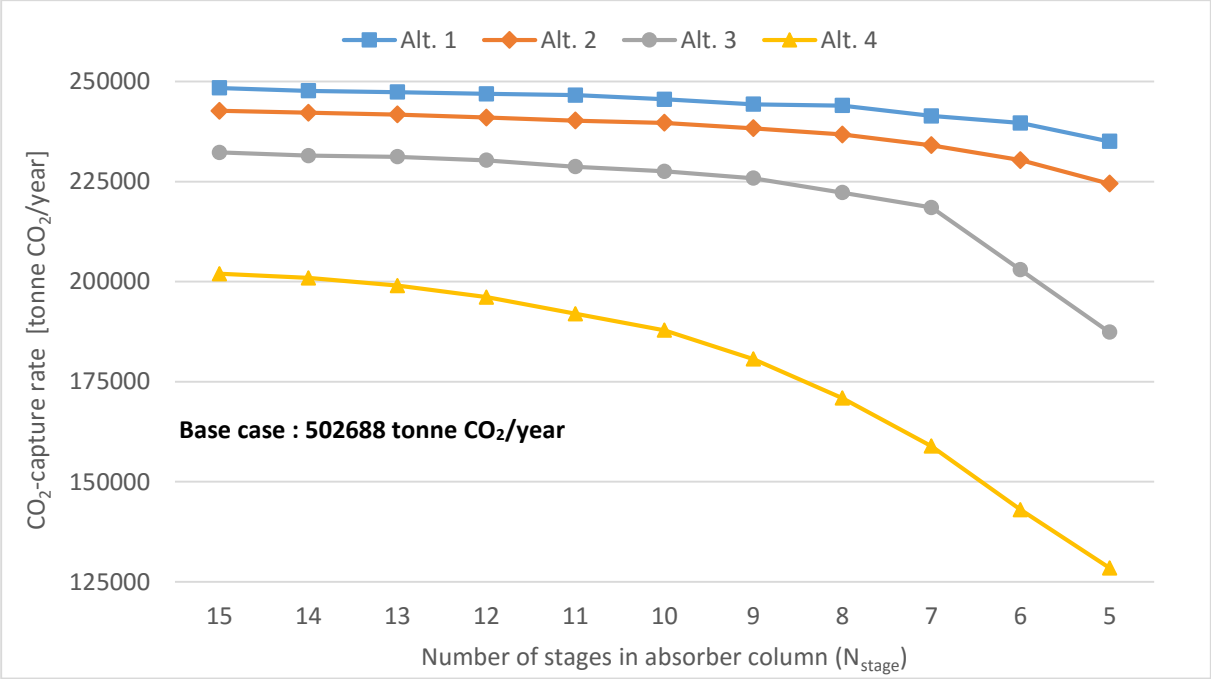

Figure 3-3 CO_2-capture rate versus N_{stage} for each Alternative

Figure 3-3 illustrates the CO_2-capture rate according to N_{stage} for each Alternative. It is clear that regardless of N_{stage}, the capture rate becomes greater with higher flue gas rates. This

suggests that with the constant reboiler power (i.e. waste heat), a higher flue gas rate leads to a more desirable condition for capturing CO_2.

It can also be found that the graphs in Figure 3-3 bear a strong resemblance to those of the capture efficiency in Figure 3-2. This is because the amount of CO_2 removed in absorber is directly related to the CO_2 mass flow out of desorber (i.e. capture rate). The position of each graph in Figure 3-2 becomes reversed in Figure 3-3, which is due to absolute differences in the flue gas rate. For example, although Alternative 1 has the lowest capture efficiencies in Figure 3-2 due to its high flue gas rate, its capture rate is the greatest in Figure 3-3.

Exact values corresponding to Figure 3-3 are arranged in Table 3-4.

Table 3-4 CO_2-capture rate versus N_{stage} for each Alternative (Unit: tonne CO_2/year)

N_{stage}	15	14	13	12	11	10	9	8	7	6	5
Alt. 1	248404	247688	247365	246906	246597	245571	244315	243981	241413	239651	235055
Alt. 2	242685	242196	241754	240977	240253	239671	238330	236766	234079	230370	224498
Alt. 3	232275	231489	231188	230299	228709	227543	225824	222219	218528	202951	187374
Alt. 4	201956	200927	199001	196141	191957	187844	180653	170900	158875	143012	128464

(Base case: 502688 tonne CO_2/year)

Taken together, the following facts can be deduced from Figure 3-3 and Table 3-4.

1. The more the flue gas rate is, the higher the capture rate becomes for all N_{stage}.
2. As is the capture efficiency, the capture rate becomes more sensitive to N_{stage} as the flue gas rate is reduced.

3.5.3 Energy demand

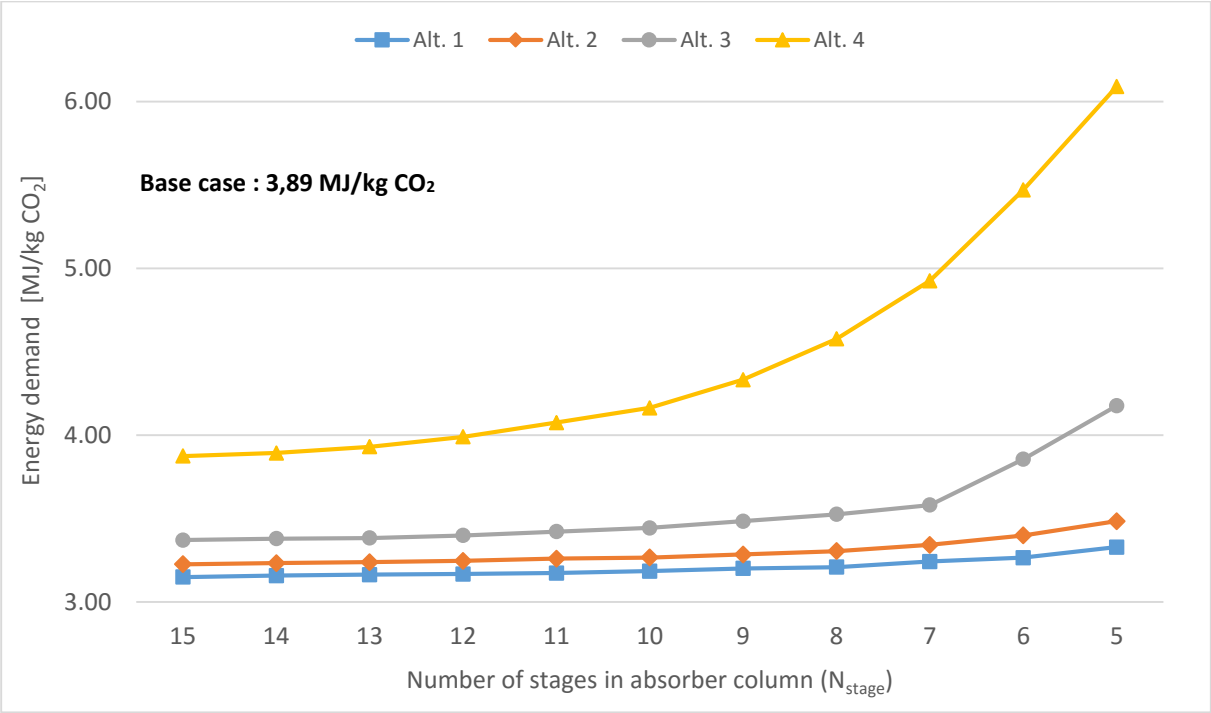

Figure 3-4 Energy demand versus N_{stage} for each Alternative

Figure 3-4 illustrates the changing aspects of energy demand for each Alternative according to N_{stage}. energy demand refers to the amount of heat energy needed to strip unit mass of CO_2 from the liquid solvent in regeneration process. In this sense, CO_2-capture processes with lower energy demand are generally more attractive from the viewpoint of cost- and energy optimization.

According to Equation 3-3, the energy demand is in inverse proportion to the CO_2 mass flow out of condenser (i.e. capture rate), while it is directly proportional to the reboiler duty. Since the reboiler power is constant as 27,17 MW (i.e. waste heat), it can be said that the energy demand is a function of the capture rate only. In this regard, the less the capture rate is, the higher the energy demand becomes. This is well reflected in Figure 3-4, where the shape of each graph is exactly turned upside down compared to those in Figure 3-3. For example, Alternative 1 has the highest capture rate in Figure 3-3, so its energy demand is the lowest in Figure 3-4. The same explanation may apply for the other three Alternatives.

Table 3-5 contains the detailed figures corresponding to Figure 3-4.

Table 3-5 Energy demand versus N_{stage} for each Alternative (Unit: MJ/kg CO_2)

N_{stage}	15	14	13	12	11	10	9	8	7	6	5
Alt. 1	3.16	3.17	3.16	3.18	3.17	3.19	3.20	3.21	3.24	3.27	3.33
Alt. 2	3.23	3.23	3.24	3.25	3.26	3.27	3.29	3.31	3.34	3.40	3.49
Alt. 3	3.37	3.38	3.38	3.40	3.42	3.44	3.49	3.53	3.58	3.86	**4.18**
Alt. 4	3.88	**3.90**	**3.93**	**3.99**	**4.08**	**4.16**	**4.33**	**4.58**	**4.93**	**5.47**	**6.09**

(Base case: 3,89 MJ/kg CO_2)

In Table 3-5, the energy demands higher than that of Base case (i.e. 3,89 MJ/kg CO_2) are marked in bold. It can be known that the overall energy demand of Alternative 4 is even higher than 3,89 MJ/kg CO_2 except at N_{stage} of 15. Alternative 3 also has one case with higher energy demand than 3,89 MJ/kg CO_2, but the energy demands of Alternative 1 and 2 are always below 3,89 MJ/kg CO_2. Comparing Table 3-5 and Table 3-3, it is clear that there is a good agreement between the two tables. In Table 3-3, capture efficiencies lower than the maximum expected value consistently show higher energy demand than 3,89 MJ/kg CO_2 in Table 3-5.

Overall, it can be deduced that:

1. Higher flue gas rates lead to the lower energy demand due to higher capture rates.
2. With lower flue gas rates, the energy demand also becomes more sensitive to N_{stage} because it is a function of the capture rate.
3. By comparing the obtained capture efficiencies with the maximum expected efficiency, it can be well predicted whether the energy demand will be higher than that of the Base case or not.

3.5.4 Lean amine rate

In simulation environment, Lean amine rate is an influential parameter regulating the reboiler duty. Provided that other operating variables remain unchanged, increasing the Lean amine rate will bring about a higher reboiler duty, and vice versa.

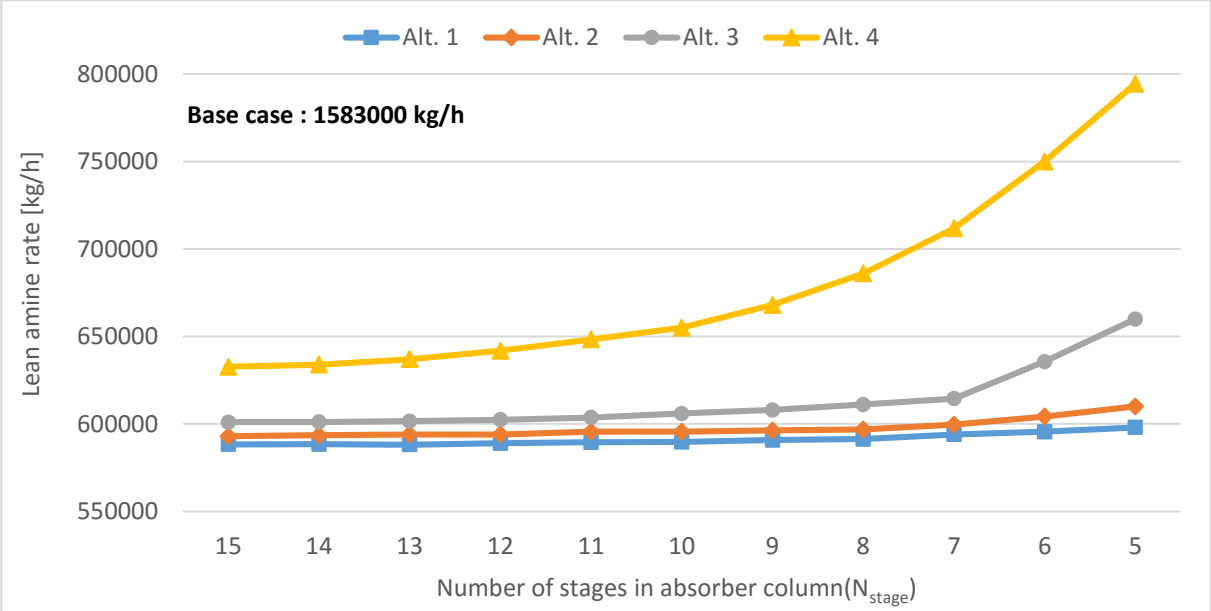

Figure 3-5 Lean amine rate versus N_{stage} for each Alternative

Figure 3-5 shows the changing trends of Lean amine rate along with N_{stage}. It is observed by and large that decreasing N_{stage} leads to higher lean amine rates. This is because the less number of stages reduces the possibility of CO_2 absorption into MEA. With the fewer number of stages, the absorption efficiency, in turn, deteriorates, and therefore the CO_2-loading of Rich amine is decreased. The decreased CO_2-loading of Rich amine into the desorber finally reduces the reboiler duty below 27,2 MW. This necessitates greater Lean amine rates in order to bring the reboiler power back to 27,2 MW.

It can be also seen from the figure that the changing aspects of Lean amine rate differ depending on the Alternative. When the flue gas is supplied at full capacity (i.e. Alternative 1), no big changes of Lean amine rate are observed over the defined range of N_{stage}. On the other hand, if the flue gas is provided at the smallest scale (i.e. Alternative 4), the Lean amine rate shows a strong tendency to increase with decreasing N_{stage}. This implies that the lower the flue gas rate is, the more the reboiler duty is affected by N_{stage}.

It can also be found that although the Alternative 4 has greatest Lean amine rates over the whole range of N_{stage}, its CO_2-capture rate is the lowest as previously shown in Figure 3-3.

Table 3-6 contains the detailed values of the Lean amine rate corresponding to Figure 3-5. It is apparent that the base case has by far the highest Lean amine rate, which is needed to achieve the CO_2-capture efficiency of 90 % with the full flue gas rate.

Table 3-6 Lean amine rate versus N_{stage} for each Alternative (Unit: kg/h)

N_{stage}	15	14	13	12	11	10	9	8	7	6	5
Alt. 1	588300	588400	588100	589000	589500	589700	590800	591300	594000	595500	598000
Alt. 2	593000	593500	594000	594000	595500	595500	596300	596800	599600	604200	610000
Alt. 3	601000	601100	601600	602400	603700	606000	608000	611100	614500	635600	660000
Alt. 4	632700	633900	637000	641800	648300	655000	668000	686000	711800	750000	794500

(Base case: 1583000 kg/h)

4 Equipment dimensioning

Based on process simulation results, this chapter describes the dimensioning procedure for different equipment together with relevant assumptions, specifications and the material selection. Equipment specifications determined in dimensioning process will be the basis of the cost estimation in later chapters.

4.1 Flue gas fan

Equation 4-1 shows that the fan power is directly proportional to the flue gas volume flow and pressure increase across the fan[61].

$$P_f = \frac{\dot{V} * (\Delta P)}{\eta_a} \qquad \text{Equation 4-1}$$

where

P_f = fan power [W]
$\dot{V}$ = flue gas volume flow [m^3/s]
ΔP = pressure increase [Pa]
η_a = adiabatic efficiency [-]

Both the flue gas and offgas out of absorber have the atmospheric pressure, and therefore the pressure increase across the Flue gas fan is assumed to be equal to the total pressure drop across the absorber column. Pressure drops of flue gases mainly take place in packing beds inside the absorber column. The pressure drop across the packing bed, in turn, is strongly influenced by the superficial gas velocity (v_g) and liquid load (Q_L)[51].

In this thesis, dry pressure drops will mainly be considered without taking account for the effects of liquid load. Thus, some degree of under-estimation on the actual pressure drop is expected. Nevertheless, the pressure drop data used in this chapter are assumed to be sufficiently enough for determining the optimum process parameters (e.g. gas velocity).

Three different structured packings to be studied are: Mellapak 250Y, Mellapak 250X and Mellapak 2X.

4.1.1 Pressure drop data of Mellapak 250Y

For the Mellapak 250Y, three experimental data of pressure drops versus v_g are plotted in Figure 4-1. The figure is based on the assumption that the liquid holdup is constant as 0,09 and the operating conditions are below the loading point[38].

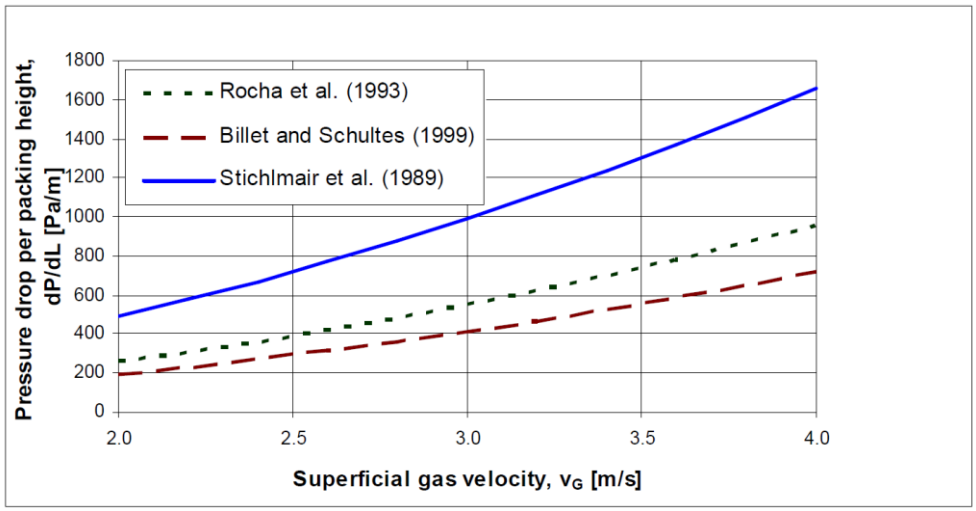

Figure 4-1 Pressure drops versus v_g for Mellapak 250Y [38]

Among the three graphs, 'Billet and Schultes (1999)' will be used in this study because it is known to be the closest to pressure drop data estimated by Sulzer Chemtech[38]. Based on this curve, Paneru (2014) determined the approximate pressure drop values for different superficial gas velocities by using data correlations as in Table 4-1.

Table 4-1 Pressure drop values (Mellapak 250Y) based on correlation [62]

Superficial gas velocity (v_g)	[m/s]	1,5	2,0	2,5	3,0
Pressure drop per meter of packing bed ($\Delta P_{packing}$)	[Pa/m]	111	192	293	414

4.1.2 Pressure drop data of Mellapak 250X

Figure 4-2 illustrates the dry pressure drop data for different Mellapak structured packings. For the Mellapak 250X, pressure drop data experimentally obtained by Tsai et al. (2011) will be used in this thesis[63].

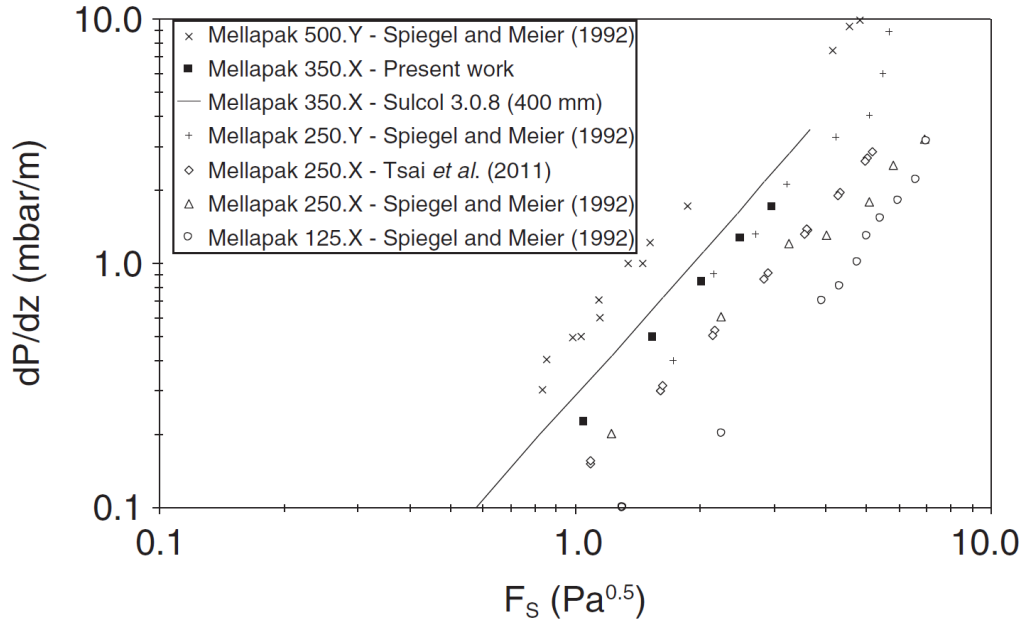

Figure 4-2 Dry pressure drops versus F-factor for Mellapak structured packings [53]

By applying the linear interpolation between the separate points in Figure 4-2, approximate pressure drop values for Mellapak 250X depending on the F-factor can be obtained as Table 4-2.

Table 4-2 Dry pressure drop values (Mellapak 250X) read off from Figure 4-2

Superficial gas velocity (v_g)	[m/s]	1,5	2,0	2,5	3,0
Flue gas density (ρ)	[kg/m^3]	1,30	1,30	1,30	1,30
F-factor[a] (F_s)	[Pa$^{0.5}$]	1,71	2,28	2,85	3,42
Pressure drop per meter of packing bed ($\Delta P_{packing}$)	[mbar/m]	0,32	0,57	0,87	1,27

[a] $F_s = v_g \cdot (\rho^{0.5})$

4.1.3 Pressure drop data of Mellapak 2X

Figure 4-3 shows the dry pressure drops of Mellapak 2X versus F-factor with two different graphs: one by experimental study and the other from simulation. Of the two graphs, the experimental data will be used in this study.

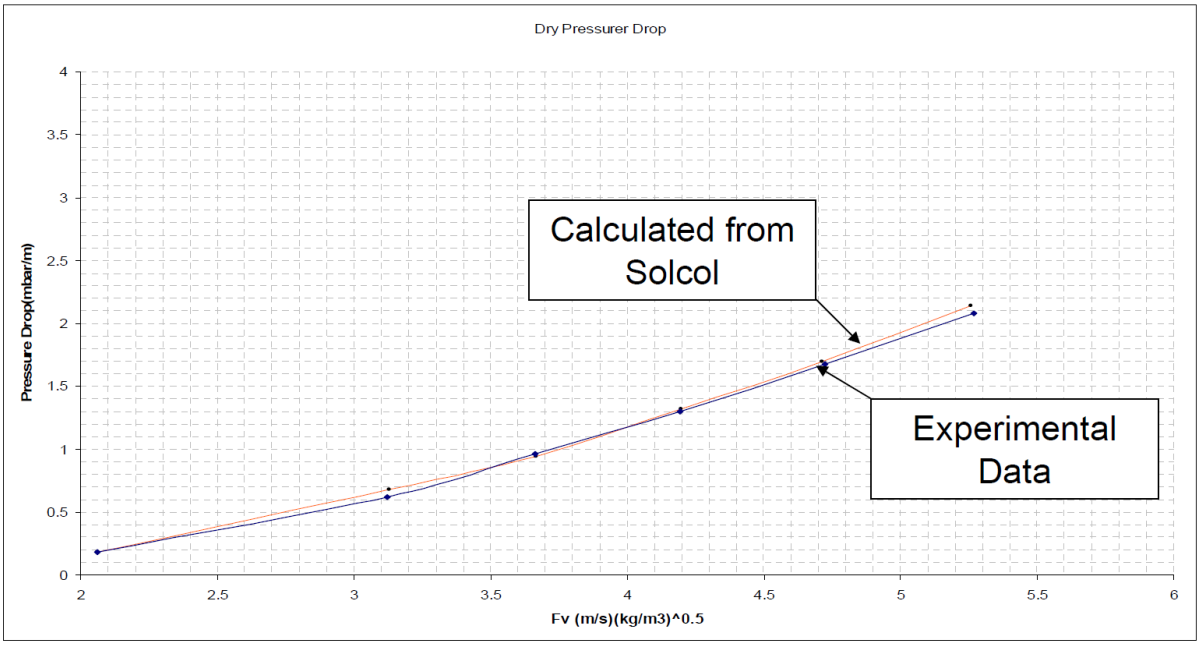

Figure 4-3 Dry pressure drops versus F-factor for Mellapak 2X [64]

Table 4-3 summarizes the pressure drop values that were read off from Figure 4-3 based on linear interpolation. For the gas velocity of 1,5 m/s, the linear extrapolation was used.

Table 4-3 Dry pressure drop values (Mellapak 2X) read off from Figure 4-3

Superficial gas velocity (v_g)	[m/s]	1,5	2,0	2,5	3,0
Flue gas density (ρ)	[kg/m^3]	1,30	1,30	1,30	1,30
F-factor (F_s)	[Pa$^{0.5}$]	1,71	2,28	2,85	3,42
Pressure drop per meter of packing bed ($\Delta P_{packing}$)	[mbar/m]	0,03	0,27	0,50	0,79

In practice, pressure drops also occur at the absorber inlet, absorber outlet as well as the water wash section, so the pressure drop from these sections should be considered as well. The overall pressure drop (including the inlet and the outlet) of the absorber column needs to be kept minimum and normally should not exceed 100 mbar[53].

The water wash section in this study is assumed to have two packing beds. Hence, the pressure drop across the unit is equivalent to $(2 * \Delta P_{packing}) * h_{packing}$, where $h_{packing}$ is the height per packing bed. Under the condition of the base velocity (i.e. v_g = 2,5 m/s), the $h_{packing}$ is assumed

to be 1 m/packing in this study. For other gas velocities than 2,5 m/s, however, the $h_{packing}$ will vary due to changes in column diameter and the effective interfacial area.

For the inlet and outlet of the absorber column, the pressure drop is respectively assumed to be equivalent to one packing bed (i.e. $P_{packing} * h_{packing}$). Table 4-4 summarizes the assumptions made on the pressure drop for each section.

Table 4-4 Assumed pressure drop in different sections of absorber column

Section	Pressure drop (ΔP)
Absorber column inlet (ΔP_{inlet})	$\Delta P_{packing} * h_{packing}$
Water wash unit (ΔP_{wash})	$2 * (\Delta P_{packing} * h_{packing})$
Absorber column outlet (ΔP_{outlet})	$\Delta P_{packing} * h_{packing}$

Therefore, the total pressure drop across the absorber column is expressed as Equation 4-2.

$$\Delta P_{total} = (\Delta P_{inlet}) + (\Delta P_{wash}) + (\Delta P_{outlet}) + (N_{stage} * \Delta P_{packing} * h_{packing})$$
$$= 4 * (\Delta P_{packing} * h_{packing}) + N_{stage} * (\Delta P_{packing} * h_{packing})$$
$$= (4 + N_{stage}) * (\Delta P_{packing} * h_{packing}) \qquad \text{Equation 4-2}$$

By substituting the term 'ΔP_{total}' into Equation 4-1, the new calculation formula of fan power can be obtained as Equation 4-3 below.

$$P_f = \frac{\dot{V} * [(N_{stage} + 4) * (\Delta P_{packing} * h_{packing})]}{\eta_a} \qquad \text{Equation 4-3}$$

where

P_f = fan power [W]
$\dot{V}$ = flue gas volume flow [m3/s]
$\Delta P_{packing}$ = pressure drop per meter of packing [Pa/m]
η_a = adiabatic efficiency [-]

Due to corrosivity of flue gases, stainless steel (SS316) is assumed as the Flue gas fan equipment material. Detailed calculation results for the Base case are given in Appendix 16.

4.2 Absorber column

4.2.1 Column shell

For the dimensioning of absorber column shells, the following assumptions apply.

- Column geometry : cylindrical
- Construction material : carbon steel [65]
- Column shell thickness : 0,01 m
- Total column height [m] = $3 * (N_{stage} * h_{packing})$
- Superficial gas velocity (v_g) : 1,5 – 3,0 m/s

Calculation formula of the absorber diameter can be found in Appendix 2. Details on the overall calculation results are available in Appendix 17.

4.2.2 Column packing

For the dimensioning of absorber column packings, the following assumptions apply.

- Equipment material : stainless steel (SS316)
- Height per packing bed ($h_{packing}$) : 1 m/packing when v_g = 2,5 m/s [66]
- Packing type : structured packing (Mellapak 250Y, Mellapak 250X and Mellapak 2X)
- Murphree efficiency : 0,11 – 0,21 (Linearly varied along the stages) [46]

One important factor influencing the absorption efficiency and the column design is the effective interfacial area of the packing[39]. Enhancing the interfacial area will decrease the volume of packing beds, leading to reduced packing costs[67]. Although the specific surface area (geometric area) of structured packings are constant, the effective interfacial area may vary depending on the liquid load[53]. The liquid load, in turn, is dependent on the Lean amine rate and column diameter. In this study, the following correlation will be used to estimate the effective interfacial area of the three structured packings[53].

$$\frac{a_e}{a_g} = 0{,}0075 * Q_L + 0{,}697 \quad (2 \leq Q_L \leq 40)$$

$$\frac{a_e}{a_g} = 1 \quad (Q_L > 40) \qquad \text{Equation 4-4}$$

where

a_e = effective interfacial area (wetted area) [m^2/m^3]
a_g = packing geometric area [m^2/m^3]
Q_L = solvent liquid load [$m^3/(m^2 \cdot h)$]

Equation 4-4 is a normalized function and has an uncertainty of ±10%, thus it can be efficiently used to predict the effective interfacial area[53]. The equation is based on the experimental data of structured packings having a geometric area of 250 m^2/m^3, but it is assumed that the equation is also applicable to Mellapak 2X[6].

It can be seen that when the liquid load is above a certain point, i.e., $Q_L > 40$ $m^3/(m^2 \cdot h)$, the effective interfacial area is considered to be equal to the packing geometric area (i.e. 250 m^2/m^3). This implies that when the liquid absorbent is supplied sufficiently, it is possible to fully take advantage of the packing geometric area.

The liquid flow is assumed to be homogeneous, so the effective interfacial area is constant all along the packing beds in absorber column.

Details on the overall calculation results are available in Appendix 17.

4.2.3 Water wash section

For the dimensioning of water wash sections, the following assumptions apply.

- Packing type : structured packing (SS316)
- Number of packing beds : 2 EA [65]
- Total packing height = $2 * h_{packing}$

The packing specifications in the water wash unit are the same as those of the column packings. Details on the overall calculation results can be found in Appendix 17.

[6] The geometric area of Mellapak 250Y and 250X is 250 m^2/m^3, whereas the geometric area of Mellapak 2X is 205 m^2/m^3[62].

4.2.4 Liquid distributor

For the dimensioning of liquid distributors, the following assumptions apply.

- Equipment material : stainless steel (SS316)
- Distributor shell thickness : 0,01 m (assumed) [65]
- Distributor volume : (Absorber area) ∗ (Distributor shell thickness)
- Number of units in absorber column : 2 EA [65]
- I-beam support volume = (I-beam sectional area) ∗ (Absorber inner diameter)
- Number of I-beam supports : 2 EA per unit of liquid distributor

I-beams are used to support the liquid distributor inside the absorber column, and the 'IPE 160' is used in this study. IPE is a French abbreviation for 'I-Profile Européennes (English: European I-Beam profile)' and serves as the standard for I-beam dimensions in European nations. Table 4-5 describes the basic dimensions of I-beam support, while Figure 4-4 illustrates the schematic drawing of a typical I-beam.

Table 4-5 Dimensions of I-beam (IPE 160) [68]

Height (H)	160 mm
Width (W)	82 mm
Web thickness (t_w)	5 mm
Flange thickness (t_f)	7,4 mm
Sectional area	0,00201 m^2

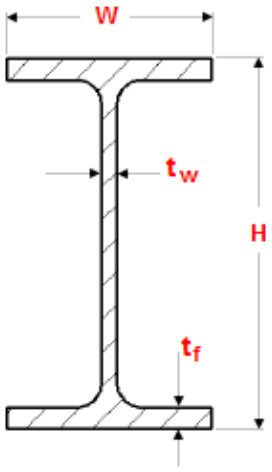

Figure 4-4 Schematic sketch of I-beam dimensions [69]

4.3 Rich pump

For the dimensioning of Rich pumps, the following assumptions apply.

- Equipment material : stainless steel (SS316)
- Adiabatic efficiency : 75 %
- Pressure increase : 1,1 bar
- (Actual duty) = (Duty obtained from HYSYS) + (Additional duty for overcoming Δh)
- Δh_{Rich} = 0,8 ∗ (Desorber column height) = 0,8 ∗ 20 m = 16 m

The Rich amine inlet is assumed to be as high as 80 % of the desorber column height. Since the height of desorber column is constant as 20 m, the height of Rich amine inlet is 16 m. In HYSYS simulations, however, the height difference is not taken into account in determining the pump duty, so manual calculations are needed to include an additional duty for overcoming the height difference. The actual duty is therefore the duty obtained in HYSYS plus the additional duty.

Calculation formula of pump power is described in Appendix 2. Details on the overall calculation result for each Alternative are available in Appendix 18.

4.4 Lean pump

For the dimensioning of Lean pumps, the following assumptions apply.

- Equipment material : stainless steel (SS316)
- Adiabatic efficiency : 75 %
- Pressure increase : 2 bar
- (Actual duty) = (Duty for overcoming Δh_{Lean})
- Δh_{Lean} = 0,8 ∗ (Absorber column height)

The Lean amine pressure out of desorber is set as 2 bar in simulation environment. Because the pressure drop across the Lean/Rich heat exchanger is assumed as 1 bar (as will be discussed in Chapter 4.6), the Lean amine pressure of 2 bar is considered to be sufficient to overcome pressure drops of the L/R heat exchanger. Nonetheless, for the sole purpose of activating (turning on) the Lean pump unit in simulation environment, a pressure increase of 2

bar was specified. Therefore, the specified pressure increase has no significance and the actual duty of Lean pump may be determined by considering the height difference only.

In the same way as Rich pump, the Lean amine inlet is assumed to be as high as 80 % of the absorber column. Calculation formula of pump power is described in Appendix 2. Details on the overall calculation result for each Alternative are available in Appendix 23.

4.5 Desorber column

For the dimensioning of desorber columns, the following assumptions apply.

- Column geometry : cylindrical
- Construction material : carbon steel [65]
- Column shell thickness : 0,01 m [65]
- Number of stages : 10
- Height per packing bed ($h_{packing}$) : 1m/packing [66]
- Total column height : 20 m
- Superficial gas velocity : 1,0 m/s [70]
- Murphree efficiency : 0,5 (constant for all stages) [66]
- Total volume flow of Rich amine into desorber ($\dot{V}_{Rich}$) $= \dot{V}_l + \dot{V}_g = \frac{\dot{m}_g}{\rho_g} + \frac{\dot{m}_l}{\rho_l}$

  where

  $\dot{V}_l$ = Rich volume flow in aqueous phase
  $\dot{V}_g$ = Rich volume flow in vapor phase
  $\dot{m}_l$ = Rich mass flow in aqueous phase
  $\dot{m}_g$ = Rich mass flow in vapor phase
  ρ_l = Rich density in aqueous phase
  ρ_g = Rich density in vapor phase

- Desorber area = $\frac{\dot{V}_{Rich}}{1\ m/s}$

For desorber columns, the specifications mentioned above are constant across all cases in this thesis. Assumptions previously made for the packing, liquid distributor and water wash sections in absorber column dimensioning will apply in the same way for desorber columns. Calculation formula of the desorber diameter is described in Appendix 2, while the calculation results of desorber for each Alternative can be found in Appendix 20.

4.6 Lean/Rich heat exchanger

For the dimensioning of Lean/Rich heat exchangers, the following assumptions apply.

- Equipment material : stainless steel (SS316) [65]
- Heat exchanger type : plate-and-frame [71]
- Overall heat transfer coefficient (U) = 1500 $W/m^2 \cdot K$ (assumed) [66]
- Maximum heat exchange area per one unit : 2000 m^2 [55]
- Pressure drop = 1 bar (Rich and Lean stream respectively) [71]

The idea of employing plate-and-frame type for Lean/Rich heat exchangers was recently explored by Laura A. Marcano (2015). She noted that[71]:

> The plate heat exchanger is considered to be the best option for the CO_2 capture process, since it is a more practical system, less energy consuming due to its low pressure drop and cheaper than the shell and tube heat exchanger. (p. 113)

Calculation formula of the heat transfer area is described in Appendix 2. Detailed calculation results for each Alternative are arranged in Appendix 7.

4.7 Lean cooler

For the dimensioning of Lean coolers, the following assumptions apply.

- Equipment material : stainless steel (SS316) [65]
- Heat exchanger type : shell-and-tube [65]
- Overall heat transfer coefficient (U) = 800 $W/m^2 \cdot K$ (assumed) [45]
- Cold utility : cooling water (T_{in} = 8 ℃, T_{out} = 23 ℃) [65]

Calculation formula of the Lean cooler heat transfer area is the same as Lean/Rich heat exchangers, which is described in Appendix 2. Detailed calculation results for each Alternative are arranged in Appendix 24.

4.8 Condenser

For the dimensioning of condensers, the following assumptions apply.

- Equipment material : stainless steel (SS316) [65]
- Heat exchanger type : shell-and-tube [65]
- Overall heat transfer coefficient (U) = 2000 W/m^2·K (assumed) [45]
- Cold utility : cooling water (T_{in} = 8 ℃, T_{out} = 23 ℃) [65]

Calculation formula of the condenser heat transfer area is the same as Lean/Rich heat exchangers, which is described in Appendix 2. Detailed calculation results for each Alternative are arranged in Appendix 21.

4.9 Reboiler

For the dimensioning of reboilers, the following assumptions are apply.

- Equipment material : stainless steel (SS316) [65]
- Heat exchanger type : Shell-and-tube [65]
- Overall heat transfer coefficient (U) = 2500 W/m^2·K (assumed) [45]
- Reboiler operating pressure : 2 bar
- Hot utility specifications : Low-pressure steam (2 bar, 130 ℃)

The specifications of cold and hot fluids in the reboiler are summarized in Table 4-6. While the Base case purchases the steam from external sources, Alternatives are totally self-sufficient in steam through the Waste heat boiler by cement kiln waste heat. Although the steam comes from different sources, its specifications are the same between the Base case and Alternatives.

Table 4-6 Specifications of cold and hot streams in Reboiler [53, 66]

	Cold stream (Lean amine)	Hot stream (H_2O)
Inlet temperature	116,4 ℃	130 ℃ (superheated steam)
Outlet temperature	120 ℃	120 ℃ (saturated water)

By taking advantage of heat of condensation of water, it is possible to substantially reduce the

mass flow. In Reboiler, the superheated steam transfers sensible heat to Lean amine while being cooled down to 120 ℃, and then it undergoes phase change to liquid because the boiling temperature of water is about 120 ℃ at 2 bar. The saturated steam, in turn, releases latent heat during condensation and leaves the Reboiler as saturated water at 120 ℃ and 2 bar.
Calculation formula of the condenser heat transfer area is the same as that of Lean/Rich heat exchanger, which is described in Appendix 2. Detailed calculation results for each Alternative are arranged in Appendix 22.

4.10 Waste heat boiler

For the dimensioning of Waste heat boilers, the following assumptions apply.

- Equipment material : stainless steel (SS316) [65]
- Heat exchanger type : shell-and-tube [65]
- Overall heat transfer coefficient, U = 50 $W/m^2 \cdot K$ [72]
- Operating pressure = 2 bar

The specifications of cold and hot fluids in Waste heat boilers are summarized in Table 4-7.

Table 4-7 Specifications of cold and hot streams in Waste heat boiler [25]

	Cold stream (H_2O)	Hot stream (Flue gas)
Inlet temperature	120 ℃ (Saturated water)	300 ℃
Outlet temperature	130 ℃ (Superheated steam)	150 ℃

Alternatives use the free waste heat coming from cement kilns by Waste heat boilers to make steam. Stainless steel is selected as equipment material because the flue gas contains corrosive components such as SO_x and NO_x. The operating pressure inside the boiler is specified to be the same as Reboiler, i.e., 2 bar.
As in the case of Reboiler, it is possible to substantially reduce the mass flow of saturated water coming into Waste heat boiler by using the heat of vaporization. When the saturated water at 120 ℃ and 2 bar comes from Reboiler into the waste heat boiler, it is thereupon vaporized at 120 ℃ by heat of flue gases. The saturated steam is heated further up to 130 ℃ (i.e. superheated steam) and then leaves the waste heat boiler to be used in Reboiler.

Calculation formula of the waste heat boiler heat transfer area is the same as Lean/Rich heat exchanger, which is described in Appendix 2. Detailed calculation results for each Alternative are arranged in Appendix 25.

4.11 Water pump

For the dimensioning of Water pumps, the following assumptions apply.

- Equipment material : carbon steel
- Pressure increase : 1 bar (assumed) [65]
- Adiabatic efficiency : 75 %

The Water pump transports the saturated water leaving the Reboiler to the Waste heat boiler. Carbon steel is selected as equipment material because the water is non-corrosive and the operating conditions are mild (i.e. around 120 ℃ and 2 bar).

Calculation formula of pump power due is decribed in Appendix 2. Details of the overall calculation results for each Alternative are shown in Appendix 26.

5 Cost estimation

Cost estimation of a process alternative is an essential procedure to determine the most cost-efficient CO_2-capture process with the optimum process parameters. It is on the basis of the equipment dimensioning and utilities involved. This study employs simplified methods with limited accuracy to estimate cost of process alternatives. However, cost results obtained in this thesis are sufficiently useful for order-of-magnitude estimates and reliable to compare different process alternatives regarding CO_2-capture cost[38].

Cost of a process plant project is broadly classified into two categories: capital expenditure (CAPEX) and operating expenditure (OPEX).

5.1 Capital expenditure (CAPEX)

Capital expenditure is a fixed and one-time expense incurred to purchase long-term physical assets (e.g. equipment facility, land, building etc.) or relevant services to make a plant project to be profitable[73]. In a nutshell, it is the total cost required to bring a plant project to a commercially operable status. The benefit from the capital expenditure tends to continue over long periods of time rather than diminishing in a short period[74].

The capital expenditure may be classified roughly into two types: equipment cost and installation cost.

5.1.1 Equipment cost estimation

Equipment cost refers to a purchasing cost of equipment[74]. The money a plant project spends on equipment is viewed as an investment that should be recovered as the equipment is utilized on the plant project. In order to obtain cost estimates of a piece of equipment, the historical equipment cost in a relevant plant needs to be known. One of the most precise estimate of the equipment cost of is to get a quote from suitable vendors with the current price information[75]. The cost information from this source is however usually not easily accessible. For this reason, estimating equipment cost is often implemented by utilizing the existing cost data of the same type of equipment purchased before.

5.1.1.1 Power law

Cost data are often illustrated as cost versus equipment capacity charts[48]. Power law (or exponential methods) in this sense is a simple and handy method for deriving a new equipment cost by correlating the cost data from one scale to another based on measure capacity[48, 73]. The measure capacity includes weight, area, volume and power etc. Equation 5-1 shows the basic principle of power law[48].

$$C_b = C_a \cdot \left(\frac{Q_b}{Q_a}\right)^M \qquad \text{Equation 5-1}$$

where

C_b = cost of new equipment with capacity of Q_b
C_a = cost of reference equipment with capacity of Q_a
Q_b = capacity of new equipment
Q_a = capacity of reference equipment
M = exponential factor

Equation 5-1 is often referred to as the '6/10ths Rule' because the average value of the exponential factor is about 0,6[76]. The exponential factor depends on the type of equipment, but it typically lies in the range of 0,5 – 0,85[75]. When no information on the exponential factor is available, a factor of 0,65 can give a good approximation[65]. Exponential factors for different equipment can be found in Appendix 30.

5.1.1.2 Cost index

Costs vary continuously over time due to changes in the value of money (e.g. inflation and deflation), technology development and the changes in labor resource and materials availability[74, 76]. The equipment cost estimated from the correlation table is therefore often out of date and might not be accurate. For this reason, it is needed to bring the cost from the past up to date based on the current year or the near future. Cost index (CI) refers to the ratio of cost today to cost in the past, so it is used to compare the cost level between two different periods[77]. With the known cost index in the past, the new cost corresponding to the present time can be determined. Various cost indexes were developed to keep up with the changing costs. Some popular cost indices are[48]:

- Chemical Engineering Indexes (CEPCI)

- Marshall and Swift Indexes
- Nelson-Farrar Cost Indexes

This study employs Chemical Engineering Index (CEPCI) because it is known to be primarily useful for a process plant design and construction[48]. CEPCI is a non-dimensional number and bases the index '100' on the period between 1957 – 1959[48]. There are four main components composing the CEPCI[48, 76].

- Equipment machinery and Supports Index (61 %)
- Erection and Labor Index (22 %)
- Buildings, Material and Labor Index (7 %)
- Engineering and Supervision Index (10 %)

The four indexes above are combined to yield a CEPCI Composite Index, and the percentage in the parenthesis indicates the proportion. This study uses the CEPCI Composite Index to update the cost level. Equation 5-2 shows the way in which the cost at the present time is calculated[76].

$$C_b = C_a \times \frac{CEPCI_b}{CEPCI_a} \qquad \text{Equation 5-2}$$

where

C_a = reference cost in year 'a'
C_b = new cost in year 'b'
$CEPCI_a$ = cost index in year 'a'
$CEPCI_b$ = cost index in year 'b'

CEPCI Composite Indices used in this study can be found in Appendix 4.

5.1.1.3 Currency exchange

If the base equipment cost is given in other currencies than Norwegian krone, the cost needs to be converted by using the exchange rate. Equation 5-3 shows the currency conversion formula, taking USD as an example.

$$C_{NOK} = C_{USD} \times K \qquad \text{Equation 5-3}$$

where

C_{NOK} = cost in Norwegian krone for a specific year [NOK]
C_{USD} = cost in US Dollars for a specific year [$]
K = currency exchange rate for a specific year [NOK/$]

Several currency exchange rates relevant to this study can be found in Appendix 4.

5.1.2 Installation cost estimation

Estimating installation cost is based on the major equipment costs, with the other costs being calculated as factors of the equipment cost[78]. This is called the 'Factorial method', the accuracy and reliability of which highly depends on the level of design stage and the availability of cost data. When detailed equipment specifications are acquired at later stages of the plant project, an installation cost can be estimated in a more accurate and rigorous way. Three well-known factorial methods are[75]:

- Lang factor method
- Hand factor method
- Detailed factor method

Of the three methods, this study employs the 'Detailed factor method' because it gives a more accurate estimate than the other two methods by considering each cost factor individually.

5.1.2.1 Detailed factor method

The detailed factor method evaluates all the cost factors individually in the direct and indirect cost with as many details as possible[75]. The installation factor of this method is broadly categorized into the following cost items[74]:

- Direct cost
- Engineering cost
- Administration cost
- Commissioning cost
- Contingency cost

The contribution of each of these items to the installation cost is calculated by multiplying the equipment cost by an appropriate factor. Determining the factor of each cost item are done by using historical cost data in of the corresponding industry[73]. The installation factor is calculated by adding up all the factors of the cost items described above.

Installation factors are in general based on a specific material, typically carbon steel. For other materials than carbon steel (CS), a material factor is multiplied by both the equipment and piping cost[75]. Material factors are in general not linearly proportional to the installation factor because the transportation cost, fabricator's cost or labor cost do not scale with the construction material of equipment (Chandel et al., 2016).

The calculation formula of installation cost is shown in Equation 5-4[74].

$$C_{install} = C_{equipment,CS} * [f_T + (F_M - 1) \cdot (f_E + f_P)] \qquad \text{Equation 5-4}$$

where

$C_{install}$ = installation cost by given material
$C_{equipment,CS}$ = equipment cost in carbon steel
f_T = installation factor in carbon steel
f_E = equipment factor (of Direct cost)
f_P = piping factor (of Direct cost)
F_M = material factor

Different cost factors in detail are available in Appendix 14. Overall results of installation cost calculation for each equipment are arranged from Appendix 16 to Appendix 26.

5.1.2.2 Location factor

Location factor is used to adjust the capital expenditure of a project plant built in one part of the world to that of an identical plant built in another part[79]. Therefore, it provides a way to assess cost differences relatively between the two geographical locations. Location factors include freights, duties, given costs, taxes, field indirect costs, project administration, and engineering and design[78]. On the basis of Rotterdam, where the location factor is 1, it varies

depending on countries or specific regions[7]. The location factor may also vary over time, and therefore for a different period it needs to be brought up to date by using the cost indices and exchange rates[79]. Typical location factors in Norway range from 1.02 to 1,70[75]. When location factors of other than 1 are used, they are multiplied by the total capital cost of a project plant. In this study, the location factor is assumed to be 1.

5.2 Operating expenditure (OPEX)

Operating expenditure refers to the expenses incurred to operate a piece of process equipment or facility, maintain the plant systems in optimal conditions or to administrate a project including utility expenses or labor salaries[76]. Unless the equipment has a required cost to operate or undergoes wear-out, the operating expenditure is usually incurred by all equipment[80]. In this thesis, operating expenditure is assumed to include the following components only.

- Utility (electricity, cooling water, steam) cost
- Maintenance cost

5.2.1 Maintenance cost

Aside from utilities, other miscellaneous operating costs such as labor wages or raw material expenditure are assumed to be included in the maintenance cost in this study. Depending on the project scale, annual maintenance cost may vary from about 1,5 % to more than 15 % of a project capital cost. Simple plants with relatively mild, non-corrosive conditions have the yearly maintenance cost ranging from 3 to 5 % of the capital cost[76]. In the case of complex plants with severe, corrosive conditions, the percentage of the maintenance often may exceed 10 %. Although the maintenance costs tends to increase with equipment or system age, the average value is often used in cost estimates[76]. This thesis assumes that the yearly maintenance cost is constant as 5 % of the total capital cost.

[7] As rules of thumb, every 1000 miles away from the closest main industrial plants adds 10 % to the location factor (Chandel et al., 2016).

5.3 Base cost data

This chapter introduces some base cost data used for the overall cost estimations in this study.

5.3.1 Equipment cost

Table 5-1 shows the base cost data used for estimating different equipment costs.

Table 5-1 Base data for equipment cost estimation

Equipment	Capacity measure	Base material	Base size	Base cost	Exponential factor (M)	Reference
Flue gas fan	[kW]	CS	50	12300 $	0,76	[73]
Column shell	[tonne]	CS	8	65600 $	0,89	[73]
Structured packing	[m^3]	SS316	1	7600 $	1	[80]
Lean/Rich HX[a]	[m^2]	SS316	356	57600 €	1	Appendix 33
Condenser[b]	[m^2]	SS316	995,7	223200 €	0,68	Appendix 32
Reboiler[b]						
Lean cooler[b]						
Waste Heat boiler[b]						
Rich pump	[kW]	CS	4	9840	0,55	[73]
Lean pump						
Water pump						

[a] Plate-and-frame type heat exchanger (PHE)

[b] Shell-and-tube type heat exchanger (SHTE)

5.3.2 Operating cost

Table 5-2 shows the base data used for estimating different operating costs.

Table 5-2 Base data for operating cost estimation [65]

Utility	Cost	Relevant equipment
Low-pressure steam	100 NOK/tonne	Reboiler (Base case only)
Electricity	0,5 NOK/kWh	Flue gas fan, Rich & Lean pump, Water pump
Cooling water	0,2 NOK/m^3	Lean cooler, condenser
Yearly maintenance	5 % of CAPEX	–

▪ **Unit conversion of steam cost into the yearly operating cost**

For equipments using low-pressure steam (i.e. reboiler in Base case), the yearly operating cost per unit kW (= kJ/s) of duty can be obtained as below.

$$\frac{1\ \text{kJ/s}}{2{,}15\left[\frac{\text{kJ}}{\text{kg}\cdot{}^{\circ}\text{C}}\right]\times(130-120)[{}^{\circ}\text{C}]+2202{,}1\left[\frac{\text{kJ}}{\text{kg}}\right]}\times 3600\left[\frac{\text{s}}{\text{h}}\right]\times 0{,}001\left[\frac{\text{tonne}}{\text{kg}}\right]$$

$$\times\ 100\left[\frac{\text{NOK}}{\text{tonne}}\right]\times 8000\left[\frac{\text{h}}{\text{year}}\right]\times 0{,}001\left[\frac{\text{kNOK}}{\text{NOK}}\right]\approx 1{,}295\ \text{kNOK/year}$$

where

2,15 kJ/(kg·℃) = average heat capacity of steam between 120 ℃ and 130 ℃ at 2 bar

2201,1 kJ/kg = heat of condensation of saturated steam at 120 ℃ and 2 bar

Therefore, for equipments using steam as utility, a proportional factor of 1,295 may be simply multiplied by its duty (kW) to directly convert into the yearly steam cost.

▪ **Unit conversion of electricity cost into the yearly operating cost**

For equipments using electricity (i.e. Flue gas fan, Rich & Lean pump, Water pump), the yearly operating cost per unit kW (= kJ/s) of duty can be obtained as below.

$$1\ \text{kW}\times\ 0{,}5\ \left[\frac{\text{NOK}}{\text{kWh}}\right]\times 8000\left[\frac{\text{h}}{\text{year}}\right]\times 0{,}001\left[\frac{\text{kNOK}}{\text{NOK}}\right]=4\ \text{kNOK/year}$$

Therefore, for equipments using electricity as utility, a proportional factor of 4 may be simply multiplied by its duty (kW) to directly convert into the yearly electricity cost.

▪ **Unit conversion of cooling water cost into the yearly operating cost**

For equipments using cooling water (i.e. Lean cooler, condenser), the yearly operating cost per unit kW (= kJ/s) of duty can be obtained as below.

$$\frac{1\left[\frac{\text{kJ}}{\text{s}}\right]}{4{,}19\left[\frac{\text{kJ}}{\text{kg}\cdot{}^{\circ}\text{C}}\right]\times(23-8)[{}^{\circ}\text{C}]}\div 998{,}7\left[\frac{\text{kg}}{\text{m}^3}\right]\times 3600\left[\frac{\text{s}}{\text{h}}\right]\times 0{,}2\left[\frac{\text{NOK}}{\text{m}^3}\right]\times 8000\left[\frac{\text{h}}{\text{year}}\right]$$

$$\times\, 0{,}001\left[\frac{\text{kNOK}}{\text{NOK}}\right]\approx 0{,}09177\ \text{kNOK/year}$$

where

4,19 kJ/(kg·℃) = average heat capacity of water between 8 ℃ and 23 ℃

998,7 kg/m^3 = average density of water between 8 ℃ and 23 ℃

Therefore, for equipments using cooling water as utility, a proportional factor of 0,09177 may be simply multiplied by its duty (kW) to directly convert into the yearly cooling water cost.

5.4 Cost estimation assumptions

This chapter describes assumptions made on some equipment regarding cost estimation.

5.4.1 Packing

For structured packings in absorber and desorber column, the following assumptions apply.

- Direct Cost factor includes Equipment and Erection factors only.
- Engineering Cost factor includes Engineering Process and Engineering Mechanical factors only.
- Administration Cost factors are not counted.

- Commissioning and Contingency factors are included.

5.4.2 Liquid distributor

For liquid distributors in the absorber and desorber column, the following assumptions apply.

- Equipment cost of the liquid distributor (incl. I-beam supports) is correlated by using the absorber shell equipment cost per unit volume [kNOK/m^3].
- The liquid distributor equipment cost (SS316) calculated is added to the absorber shell equipment cost (CS), which is in turn used to determine the installation factor of the absorber column shell.

5.4.3 Water wash unit

For water wash units in absorber and desorber column, the following assumptions apply.

- The water wash unit has two packing beds, the type of which is the same as those of the main part of columns.
- The total height of absorber column is assumed to be high enough to contain the water wash unit inside. Therefore, the skirt of water wash section may not be counted separately. This means that the equipment cost of water wash units may be determined by packing costs only[65].

5.4.4 Lean/Rich heat exchanger

For plate-and-frame heat exchangers (PHE), this study uses the existing cost data previously obtained from Aspen In-Plant Cost Estimator by Nils H. Eldrup[65]. The cost data is assumed to give reasonable estimations for plate heat exchanger (i.e. Lean/Rich heat exchanger) costs. Details on PHE cost data is available in Appendix 32.

5.4.5 Reboiler, Condenser, Lean cooler, Waste heat boiler

As with the PHEs, this study uses the existing cost data from the same source for all the shell-and-tube heat exchangers (STHE)[65]. The cost data is assumed to give reasonable cost estimations for shell-and-tube heat exchangers such as Reboiler, Condenser, Lean cooler and Waste heat boiler. Details STHE cost data is available in Appendix 33.

6 Project economics

This chapter describes basic concepts for assessing the economic feasibility of a plant project. Evaluating project economics is a vitally important step because a CO_2-capture plant project must be economically profitable and viable to sustain the capturing process operation. In other words, the costs of investment must be less than the income generated through capturing CO_2. Project economics is mainly determined by the effects of process design and operating parameters on economic performance. Therefore, it is also concerned with the process- and cost optimization[74].

In the following subchapter, brief explanations are given for several important concepts: cash flow, rate of return, discount factor and net present value.

6.1 Cash flow

To determine the economic performance of a process plant, the cash flow throughout the whole lifecycle of the project needs to be considered. Cash flow refers to the net amount of money transferred into or out of a business, and therefore it represents the operating activities of a business[81]. Because cash is the fuel driving a business or an investment, cash flow is considered to be the most important financial barometer of a plant project[82]. In this thesis, cash flow is assumed to simply mean the net transfer of money per annum. Equation 6-1 shows the calculation formula of cash flow in a simple form, where the unit of each term is kNOK/year.

$$(\text{Cash flow}) = (\text{Sum of income}) - (\text{Sum of expenditure}) \qquad \text{Equation 6-1}$$

In this thesis, the following assumptions apply to determining the cash flow.

- Capital investment (land purchasing, equipment investment, working capital etc.) begins at the beginning of year '0' and takes one year.
- The plant is put into operation from the beginning of year '1'.
- At the beginning of year '1', the income and operating cost take place simultaneously. Both the income and operating cost are constant and calculated annually (i.e. in the beginning of each year) throughout the project lifetime.

According to the assumptions above, the cash flow in year ‘0’ is negative because no income is made during this period. The cash flow turns positive from year ‘1’ onwards, so the cumulative cash flow increases with time until the end of the project.

6.2 Rate of return

In finance, the term ‘return’ is the gain or loss of an investment and often expressed as a percentage of the investment cost[77]. ‘Rate of return’, in this sense, refers to a profit on investments over a specific period of time. The rate of return is usually calculated annually and measured as a proportion of the original investment[74]. The reason that the money retrieved immediately has a higher value than that in the future is due to the rate of return. In this thesis, the annual rate of return is assumed as 7,5 %.

6.3 Discount factor

The cash flow takes place continuously over a long period of time, so the time value of money should be taken into account[77]. The value of money invested in banks can be maintained over time due to the compound interest occurring at regular intervals. However, the value of money not invested in banks will decrease with time. This indicates that cash flows in the future must be discounted at a specified rate of compound interest. Discount factors are used for this purpose, which are determined by the rate of return and the year number. Equation 6-2 shows the calculation formula of the discount factor[82].

$$D_n = \frac{1}{(1+r)^n} \qquad \text{Equation 6-2}$$

where

D_n = discount factor in year ‘n’
r = rate of return
n = year number

The project lifetime in this thesis is assumed to be 25 years. By adding up all the discount factors from the beginning to the end of the project (i.e. from year ‘0’ to year ‘25’), the sum of discount factors of the present study is calculated as below.

$$(\text{Sum of discount factor}) = \sum_{k=0}^{n} \frac{1}{(1+r)^k} = \sum_{k=0}^{25} \frac{1}{(1+\frac{7{,}5}{100})^k} \approx 11{,}15$$

6.4 Net present value

A projected cash flow of the upcoming period has less value than the cash flow of the present time. By discounting a projected cash flow at the rate of return, the present value of the cash flow can be obtained, namely, Net present value (NPV)[75]. Equation 6-3 shows that the net present value is a function of the cash flow, rate of return and the year number[48].

$$NPV_n = C \times D_n = \frac{C}{(1+r)^n} \qquad \text{Equation 6-3}$$

where

NPV_n = net present value in year 'n'
D_n = discount factor in year 'n'
C = cash flow
r = rate of return
n = year number

The cumulative value from the beginning up to a certain period is referred to as the 'Accumulated Net Present Value', which represents the net wealth that has been created or spent in a project plant[79]. Equation 6-4 shows the calculation formula of the accumulated NPV.

$$(\text{Accumulated NPV}) = \sum_{k=0}^{n} (NPV_k) = \sum_{k=0}^{n} \frac{C}{(1+r)^k} \qquad \text{Equation 6-4}$$

The accumulated NPV is often the major measurement used for analyzing the profitability of a plant project[77]. In order for a plant project to be economically feasible, the accumulated NPV must be a positive value. The higher the accumulated NPV is, the more attractive a project plan becomes. In the same way, a project with low positive accumulated NPV or negative accumulated NPV has low profitability.

6.5 CO_2-capture cost

CO_2-capture cost of a project plant is a decisive criterion in determining the degree of process- and cost optimization. The higher the capture cost is, the more the expenditure on removing a unit mass of CO_2 is needed. For this reason, to achieve the most attractive process alternative, the capture cost should be minimized by optimizing the operating parameters and process design. Equation 6-5 describes the calculation formula of the capture cost in this study. Derivation procedure of the equation is available in Appendix 31.

$$D = \frac{\frac{A}{11{,}15} + B}{C} \qquad \text{Equation 6-5}$$

where

A = CAPEX [kNOK]
B = OPEX [kNOK/year]
C = CO_2-capture rate [tonne CO_2/year]
D = CO_2-capture cost [kNOK/tonne CO_2]

7 Result and discussion

This chapter presents the cost estimation results with relevant discussions for the Base case and Alternatives. Before proceeding, the following should be noted.

- Alternatives are assumed to use the waste heat only, the amount of which is constant as 27,17 MW. Therefore, the reboiler has the same installation cost throughout all Alternatives.
- The reboiler power (i.e. 27,17 MW) of Alternatives is supplied by Waste heat boiler, so the duty of Waste heat boiler is equal to that of reboiler. Since the reboiler power is constant, the Waste heat boiler duty also remains unchanged. As a result, the installation cost of Waste heat boiler is also constant across all Alternatives.
- Due to the constant reboiler power, the mass flow of saturated water out of reboiler is also the same. Therefore, the installation and operating cost of Water pump are also unchanged throughout all Alternatives.

Table 7-1 summarizes the equipments mentioned above together with the costs involved. Since the specifications of Reboiler, Waste heat boiler and Water pump are constant throughout all Alternatives, further discussions on these equipments will not be dealt with in the following subchapters.

Table 7-1 Equipment with constant capacity and cost in Alternatives

Equipment	Duty	Installation cost	Operating cost	Reference
Reboiler	≈ 27 MW	≈ 16 MNOK	–	Appendix 22
Waste heat boiler	≈ 27 MW	≈ 58 MNOK	–	Appendix 25
Water Pump	≈ 1 KW	≈ 0,8 MNOK	7 KNOK/year	Appendix 26

As previously described in Table 2-2, each Alternative has its own flue gas rate. Therefore, impact analysis of the remaining two variables (i.e. N_{stage} and v_g) will be carried out for each Alternative. The discussion in the beginning starts with studying the effects of N_{stage} under the base velocity (i.e. v_g = 2,5 m/s), and thereafter the effects of the v_g variation (i.e. v_g of 1,5 m/s, 2,0 m/s and 3,0 m/s) will be studied in the following subchapters.

All the cost results and discussions are based on Mellapak 250Y. For the Mellapak 250X and 2X, only their capture cost data are available in Appendix 9 and Appendix 10 respectively.

7.1 Base case

7.1.1 Installation cost comparison

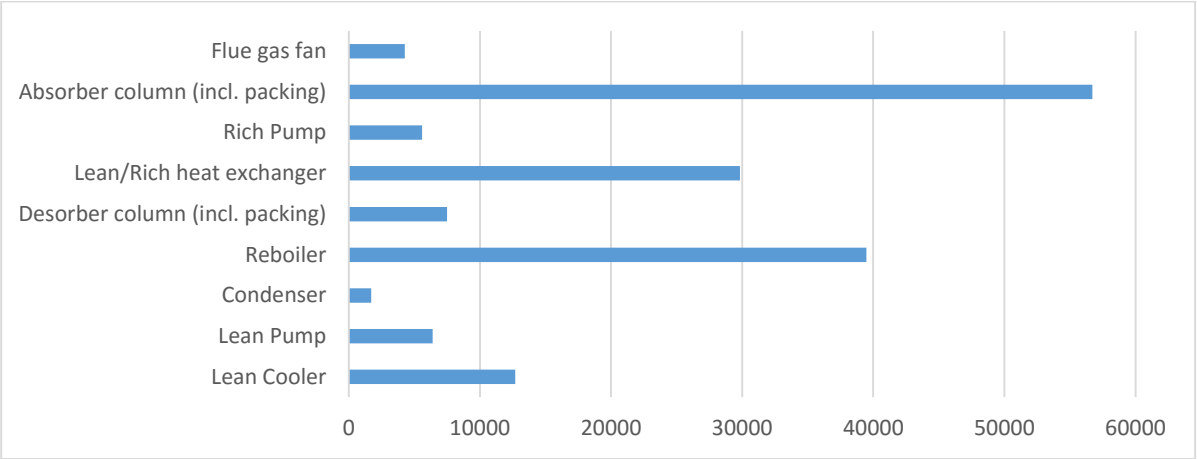

Figure 7-1 Installation cost comparison between equipments in Base case [unit: kNOK]

Figure 7-1 gives the overview of the Base case installation cost according to different equipments. Because the base case utilizes the steam only as an energy source, either Waste heat boiler or Water pump is not included in the figure. It is evident that the Absorber column takes up the biggest portion of CAPEX, followed by Reboiler and Lean/Rich heat exchanger. Detailed cost data of Figure 7-1 are arranged in Table 7-2.

Table 7-2 Installation cost comparison between different equipments in Base case

Equipment	Unit	Installation cost	Relative percentage
Flue gas fan	[kNOK]	4278	2.6%
Absorber column (incl. packing)	[kNOK]	56720	34.5%
Rich pump	[kNOK]	5596	3.4%
Lean/Rich heat exchanger	[kNOK]	29840	18.2%
Desorber column (incl. packing)	[kNOK]	7501	4.6%
Reboiler	[kNOK]	39473	24.0%
Condenser	[kNOK]	1708	1.0%
Lean pump	[kNOK]	6404	3.9%
Lean cooler	[kNOK]	12683	7.7%
CAPEX	**[kNOK]**	**164202**	**100.0%**

Table 7-2 indicates that approximately one third of the CAPEX is spent in constructing the absorber column, so the idea of reducing the size of absorber column naturally comes across as attractive. Impact analysis of the absorber column dimension on CO_2-capture cost will be addressed for each Alternative from Chapter 7.2.

7.1.2 Operating cost comparison

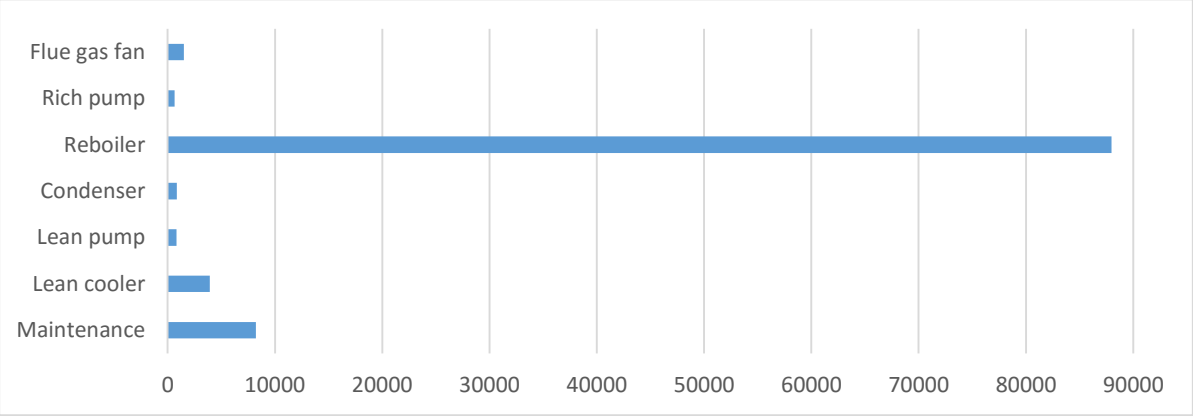

Figure 7-2 Operating cost comparison between equipments in Base case [unit: kNOK/year]

Figure 7-2 illustrates the operating cost of different equipments in Base case. As explained before, the Water pump operating cost is excluded from Base case. Apparently, the Reboiler accounts for by far the largest proportion of the OPEX, whereas the operating cost of other equipments is relatively marginal. Detailed cost data of Figure 7-2 are arranged in Table 7-3.

Table 7-3 Operating cost comparison between different equipments in Base case

Equipment	Unit	Operating cost	Utility	Relative percentage
Flue gas fan	[kNOK/year]	1510	Electricity	1.5%
Rich Pump	[kNOK/year]	639	Electricity	0.6%
Reboiler	[kNOK/year]	87981	Steam	84.7%
Condenser	[kNOK/year]	839	Cooling water	0.8%
Lean Pump	[kNOK/year]	817	Electricity	0.8%
Lean Cooler	[kNOK/year]	3916	Cooling water	3.8%
Maintenance	[kNOK/year]	9633	–	7.9%
OPEX	**[kNOK/year]**	**103913**		**100.0%**

Table 7-3 shows that as much as over 80 % of the OPEX is spent for the Reboiler. This is largely due to the high energy demand of CO_2-stripping process from the absorbent, as well as the expensive cost of steam. As explained in earlier chapters, high energy consumption in Reboiler has steadily been considered as the major shortcoming of a traditional CO_2-capture process with MEA absorption[27]. From Chapter 7.2, the use of alternative energy (i.e. free waste heat) instead of steam is assumed for all Alternatives.

7.1.3 CO_2-capture cost calculation

The CO_2-capture rate of Base case is 502688 tonne CO_2/year, as previously shown in Figure 3-3. By using Equation 6-5, the CO_2-capture cost of Base case can now be obtained as below.

$$(\mathrm{CO_2\text{-capture cost}}) = \frac{\frac{164202}{11{,}15} + 103913}{502688} \approx 0{,}236\ \mathrm{kNOK/tonne\ CO_2}$$

As will be discussed later, the capture cost obtained above is much higher than that of Alternatives because the Base case uses the steam only. From the following chapter, the capture cost discussions will be focused on Alternatives in line with impact analysis of different process parameters.

7.2 Alternative 1

7.2.1 Impact analysis of N_{stage} on costs (v_g = 2,5 m/s)

In this chapter, the effects of N_{stage} on CAPEX, OPEX and the capture cost are discussed under the condition of the base velocity (i.e. $v_g = v_{g,b} = 2{,}5$ m/s).

7.2.1.1 Impact of N_{stage} on installation cost (v_g = 2,5 m/s)

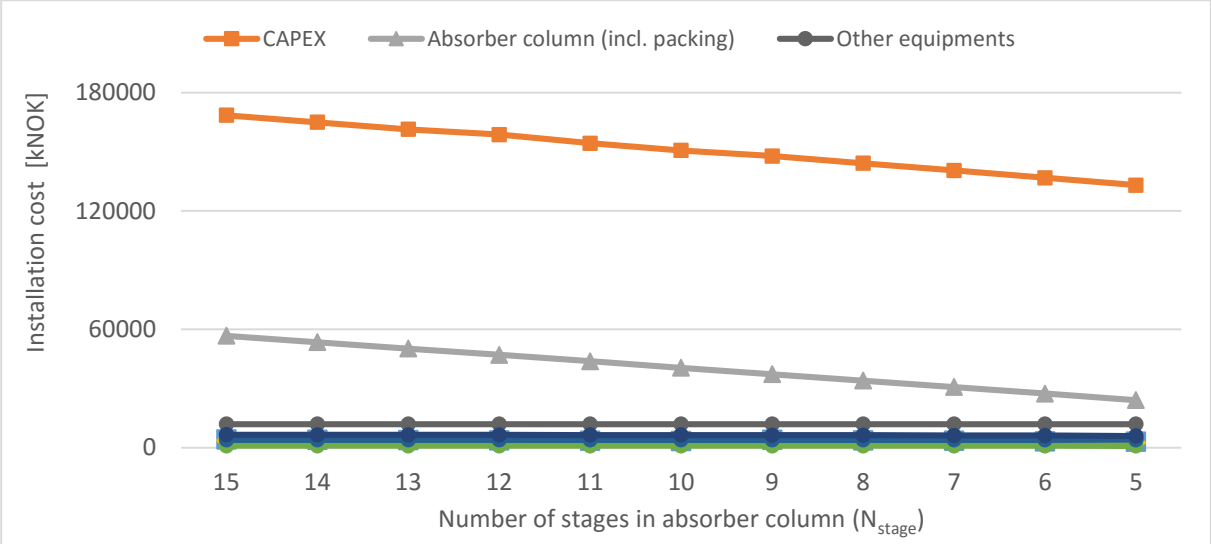

Figure 7-3 Installation cost versus N_{stage} in Alternative 1 (v_g = 2,5 m/s)

Figure 7-3 shows the installation cost changes for each equipment according to decreasing N_{stage}. As expected, the cost of absorber column declines steadily with decreasing N_{stage} owing to the reduced number of packing beds and smaller absorber shell size. The other equipment, on the other hand, shows little change in installation cost along with the N_{stage}. The decreasing trend of CAPEX, therefore, exhibits nearly the same aspect as that of absorber column, and the CAPEX reaches the minimum at N_{stage} of five[8]. This can be also identified from the fact that the cost change of absorber column from N_{stage} of fifteen to five is of the same order of magnitude as that of CAPEX, i.e., around -30000 kNOK. For other equipments showing no visible installation cost changes in Figure 7-3, an enlarged image is available in Appendix 27.

[8] In this thesis, the term 'CAPEX' means the total installation cost (i.e. the sum of installation costs of all equipment).

7.2.1.2 Impact of N_{stage} on operating cost (v_g = 2,5 m/s)

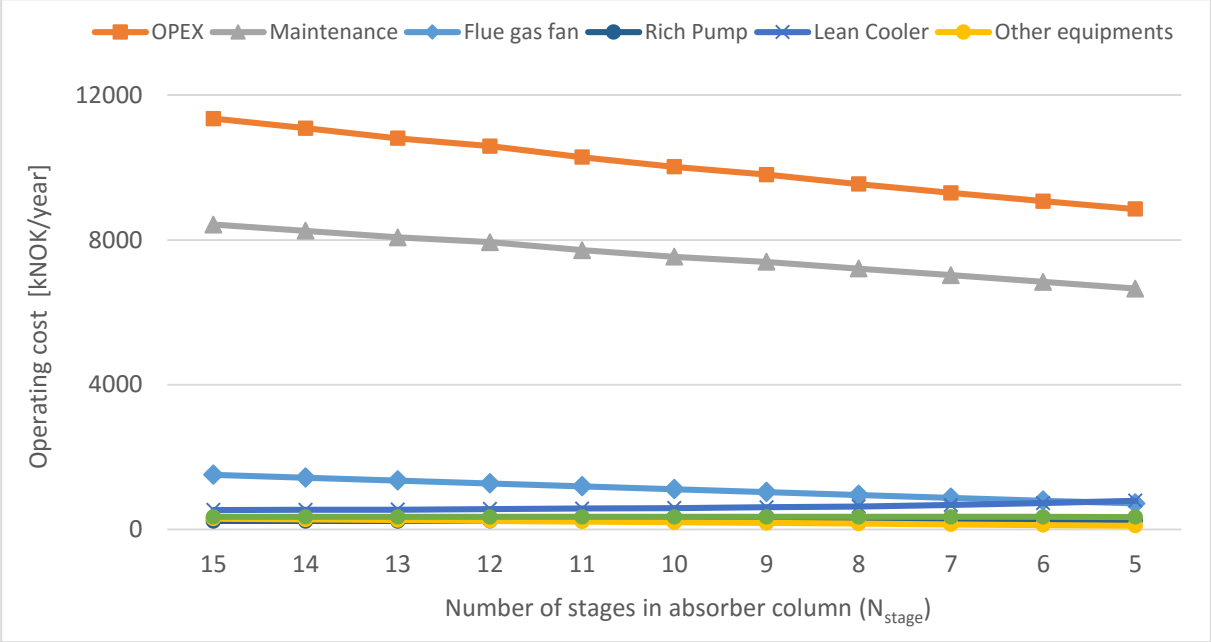

Figure 7-4 Operating cost versus N_{stage} in Alternative 1 (v_g = 2,5 m/s)

Figure 7-4 illustrates the yearly operating cost changes for different equipments according to N_{stage}. Because the CAPEX decreases steadily along with N_{stage} as shown in Figure 7-3, the yearly maintenance cost, which is 5 % of the total CAPEX, also exhibits the same changing aspects. For other miscellaneous equipments, they display no visible operating cost changes except for the Flue gas fan and Lean Cooler. Although the operating cost of Flue gas fan shows a tendency to decline, its effect is more or less offset by the increasing trend of Lean Cooler operating cost. Consequently, the OPEX changes have the similar order of magnitude as those of maintenance cost (i.e. around -2000 kNOK/year), so it can be said that the changing trend of OPEX is dominated by the maintenance cost changes[9].
For other equipments showing no visible operating cost changes in Figure 7-4, an enlarged image is available in Appendix 28.

For the changing aspects of Flue gas fan and Lean cooler operating costs, additional explanations are given below.

[9] In this thesis, the term 'OPEX' means the total operating cost (i.e. the sum of operating costs of all equipment, plus the yearly maintenance cost).

▪ **Operating cost changes of Flue gas fan**

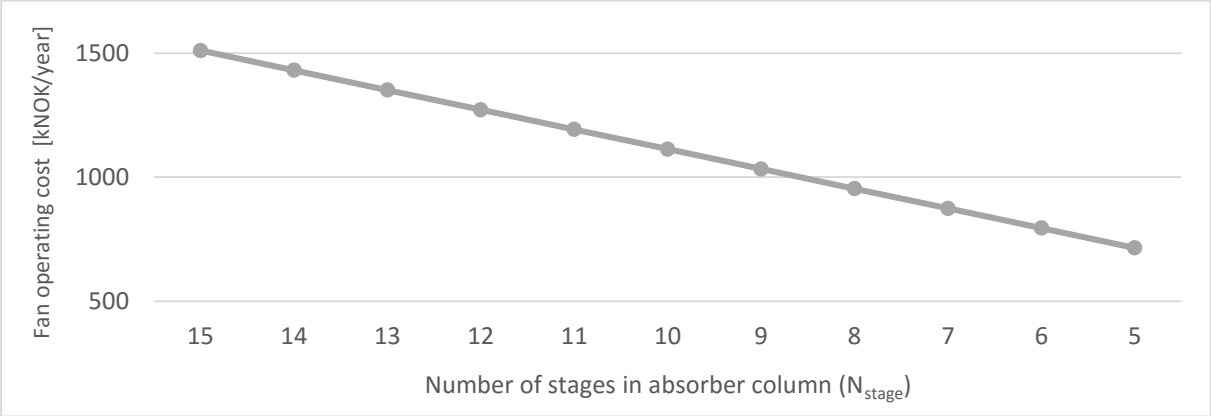

Figure 7-5 Flue gas fan operating cost versus N_{stage} in Alternative 1 (v_g = 2,5 m/s)

Figure 7-5 illustrates that the yearly operating cost of Flue gas fan declines purely linearly with decreasing N_{stage}. This is because the total pressure drop across the absorber column is in direct proportion to N_{stage}, as described earlier in Equation 4-3. The pressure drop, in turn, is equivalent to a pressure increase across the Flue gas fan, so the fewer number of absorber stages consequentially leads to less electricity consumption in Flue gas fan.

▪ **Operating cost changes of Lean cooler**

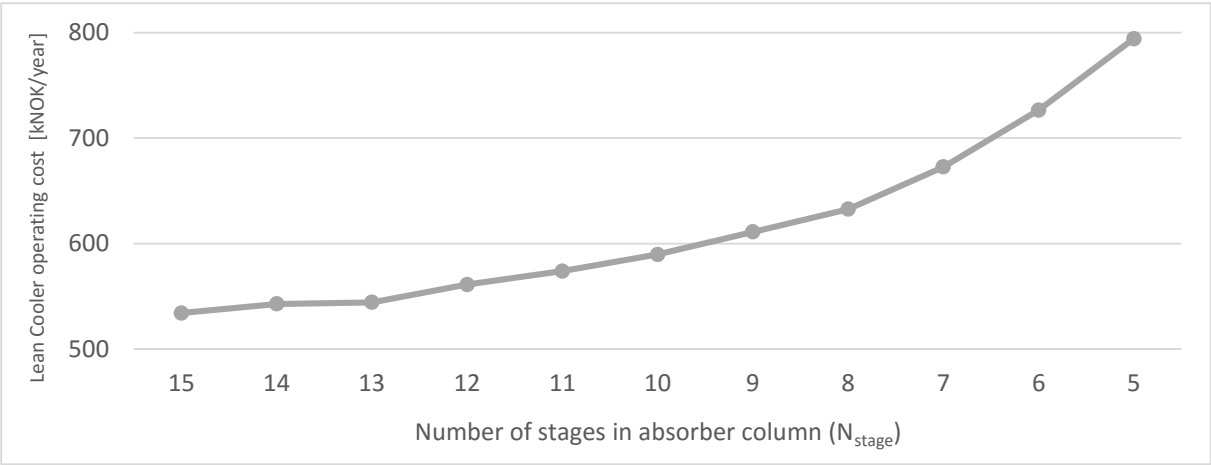

Figure 7-6 Lean cooler operating cost versus N_{stage} in Alternative 1 (v_g = 2,5 m/s)

Figure 7-6 shows an increasing tendency of the Lean Cooler operating cost with decreasing N_{stage}. The principal reasons for this trend can be elucidated as follows.

1. With decreasing N_{stage}, the CO_2-absorption efficiency in absorber column deteriorates because of the smaller packing volumes. As a result, CO_2-loading of Rich amine out of absorber also decreases, leading to less reboiler duties than 27,17 MW. This necessitates greater Lean amine rates in order to bring the

reboiler power back to 27,17 MW. The increased mass flow of Lean amine, in turn, causes the Lean Cooler duty to rise.

2. Decreasing N_{stage} also leads to the increased Lean amine temperature out of Lean/Rich heat exchanger. Since the Lean amine temperature out of Lean Cooler is constant as 45 ℃, higher Lean amine temperatures before Lean Cooler will lead to greater cooling duties. Figure 7-7 plots the Lean amine temperature (before Lean Cooler) versus N_{stage}.

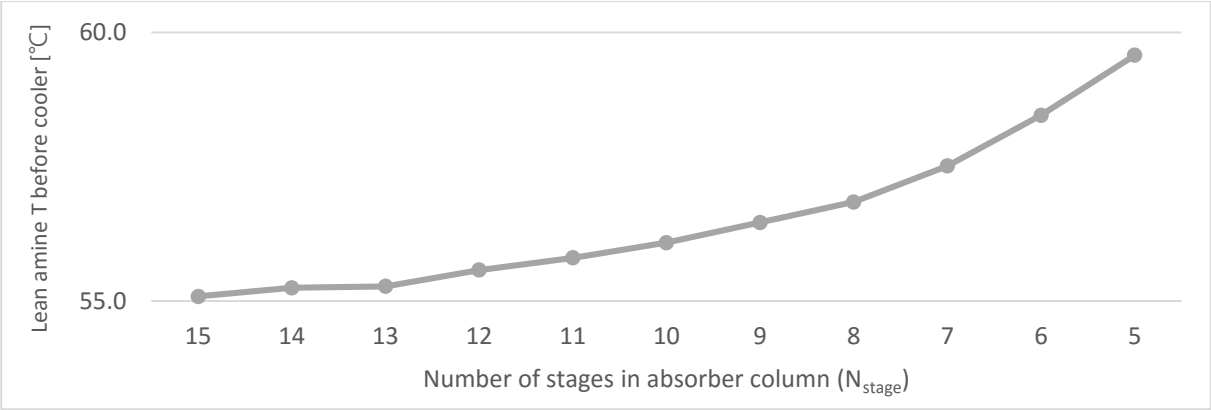

Figure 7-7 Lean amine temperature (before Lean cooler) versus N_{stage} in Alternative 1

In summary, due to higher mass flows of Lean amine and increased Lean amine temperatures out of Lean/Rich heat exchanger, the Lean Cooler duty finally keep increasing with decreasing N_{stage}.

7.2.1.3 Impact of N_{stage} on CO_2-capture cost (v_g = 2,5 m/s)

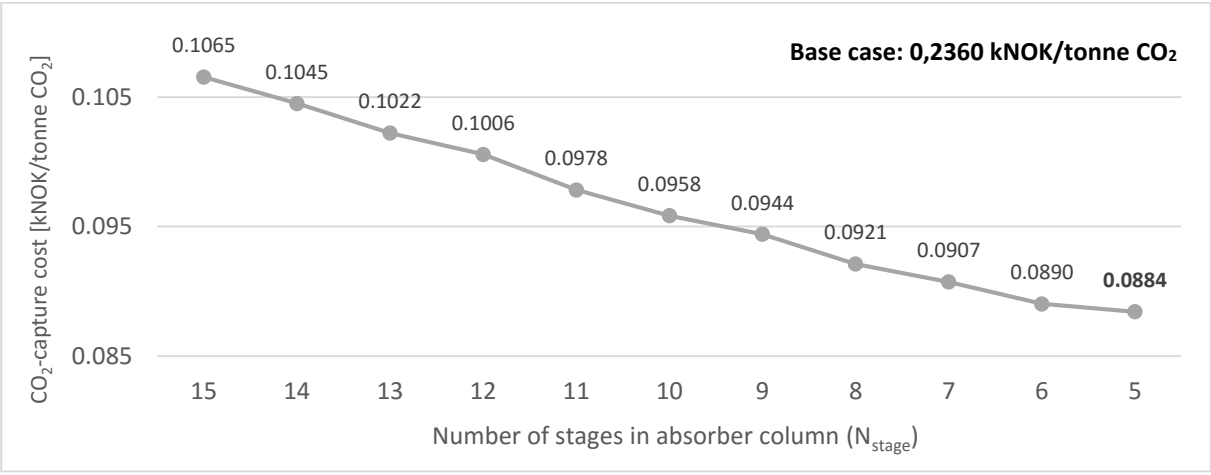

Figure 7-8 CO_2-capture cost versus N_{stage} in Alternative 1 (v_g = 2,5 m/s)

Figure 7-8 shows the changing aspects of CO_2-capture cost according to N_{stage}. The corresponding values above each circle point have been rounded off to four decimal places for

accuracy. It is obvious that the capture cost previously obtained as 0,2360 kNOK/tonne CO_2 in Base case can be reduced to 0,1065 kNOK/tonne CO_2 by simply replacing steam with the waste heat (without changing N_{stage} or v_g).

As mentioned in Equation 6-5, the capture cost is determined by the CAPEX, OPEX and CO_2-capture rate. Figure 7-3 and Figure 7-4 show that both the CAPEX and OPEX go down consistently with decreasing N_{stage}. The capture rate also displays a tendency to decline until N_{stage} of five (Figure 3-3), yet its degree of changes are insignificant compared with those of CAPEX and OPEX. In other words, the decreasing rate of CAPEX and OPEX along with N_{stage} overwhelms that of capture rate. For this reason, the CO_2-capture cost eventually keeps decreasing across the entire range of N_{stage}, with the minimum value being obtained as 0,0884 kNOK/tonne CO_2 at N_{stage} of five.

Consequently, it can be said that in Alternative 1, the number of absorber stages can be reduced down to the minimum (i.e. $N_{stage} = 5$) within the defined range of N_{stage}.

7.2.2 Impact analysis of v_g variation on cost change

In this chapter, the effect of v_g variation (i.e. 1,5 m/s, 2,0 m/s and 3,0 m/s) on the CAPEX, OPEX and CO_2-capture cost changes are discussed.

7.2.2.1 Impact of v_g variation on installation cost change

It should be noted that in this study, the variation in v_g affects the installation cost of the following equipment only.

1. Absorber column; column dimension (diameter, height) is dependent on v_g.
2. Lean pump; changes of column dimension, in turn, affect the Lean amine inlet height as well as the Lean pump duty.
3. Flue gas fan; fan power is dependent on column pressure drops. The pressure drop, in turn, is influenced by both v_g and the column (i.e. packing bed) height.

In other words, Δ(CAPEX) = Δ(absorber column installation cost) + Δ(Flue gas fan installation cost) + Δ(Lean pump installation cost).

▪ **Installation cost change of absorber column (incl. packing)**

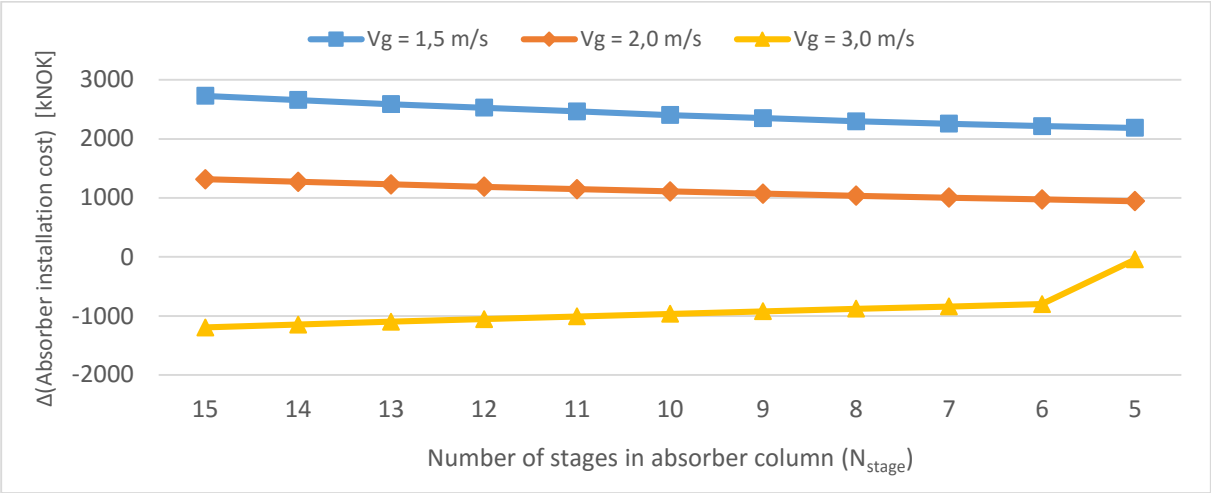

Figure 7-9 Δ(Absorber column installation cost) due to variation of v_g in Alternative 1

Figure 7-9 shows the installation cost changes of absorber column (incl. packing) due to variation in v_g. It can be seen that the two lower velocities than 2,5 m/s lead to higher installation costs, whereas the higher velocity (i.e. v_g = 3,0 m/s) makes the cost less expensive. Taking v_g of 3,0 m/s as an example, two factors influencing the installation cost of absorber column can be summarized as follows.

i) A higher v_g leads to a smaller inner diameter of the column, which in turn reduces the column sectional area (thickness part)[10]. However, the higher v_g also increases the column height, which is in direct proportion to v_g. This height increase is more influential in determining the column weight, so the installation cost of absorber shell consequently increases. (cost-increasing factor)

ii) Smaller absorber areas lead to a higher liquid load of Lean amine, which in turn increases the effective interfacial area of structured packings. This makes the volume of packing beds decreased, as well as the packing cost. (cost-decreasing factor)

The cost-decreasing factor ii) is dominant over the cost-increasing factor i), so the installation cost of absorber column is finally reduced when v_g is higher than the base gas velocity (i.e. 2,5 m/s). For the lower v_g than 2,5 m/s, the factors described above apply in the opposite way.

[10] (Absorber column sectional area) $= \frac{\pi}{4}(D_o^2 - D_i^2) = \frac{\pi}{4} * [(D_i + 0{,}02)^2 - D_i^2] = \frac{\pi}{4} * (0{,}04D_i + 0{,}02^2)$

▪ **Installation cost change of Flue gas fan**

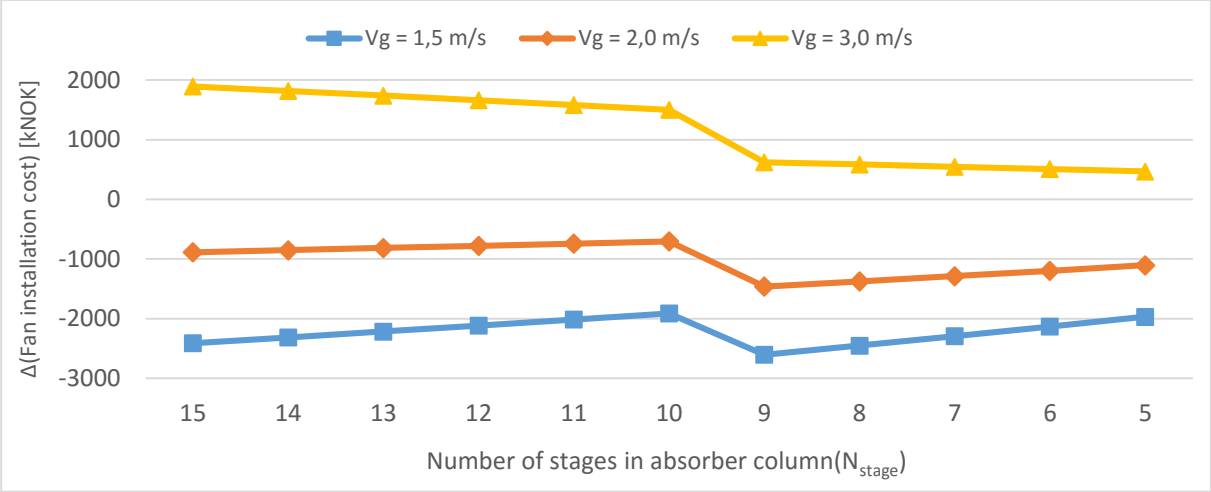

Figure 7-10 Δ(Flue gas fan installation cost) due to variation of v_g in Alternative 1

Figure 7-10 shows the installation cost changes of the Flue gas fan due to variation in v_g. It is clear that v_g of lower than 2,5 m/s saves the cost, reaching the most reductions at v_g of 1,5 m/s. In contrast, a higher gas velocity makes the cost more expensive. Two main reasons for these trends may be given as in the following:

1. As previously shown in Figure 4-1, the unit pressure drop per meter of packing bed becomes greater as v_g increases.
2. A higher v_g leads to a smaller column diameter. To maintain the total volume of packing beds, the height of packing beds increases, which in turn makes the column height increase. Consequently, the total pressure drop across the absorber column increases even more.

Because the pressure increase across the Flue gas fan is equivalent to pressure drops in absorber column, higher v_g leads to greater fan duty. Higher duties, in turn, make the installation cost of Flue gas fan more expensive and vice versa.

▪ **Installation cost change of Lean pump**

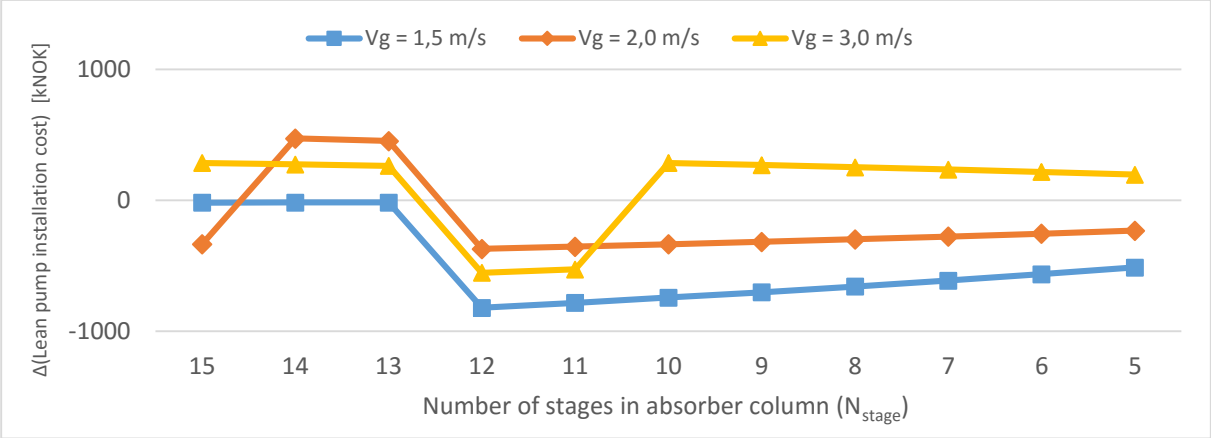

Figure 7-11 Δ(Lean pump installation cost) due to variation of v_g in Alternative 1

Figure 7-11 shows the installation cost changes of the Lean pump due to variation in v_g. When the v_g becomes higher than the base gas velocity, the Lean pump duty increases because of the increased absorber height to maintain the packing volume. In the same way, lower v_g makes the absorber height decreases, achieving the most cost reduction at v_g of 1,5 m/s. Some fluctuations observed from N_{stage} of 15 to 11 stem from sudden changes in installation factors, which vary depending on each specified cost range.

It can be also seen that the gaps between the three graphs become progressively narrower. This is because as the number of absorber stages decreases, the effect of v_g changes on the absorber column height becomes less.

▪ **Net changes of CAPEX**

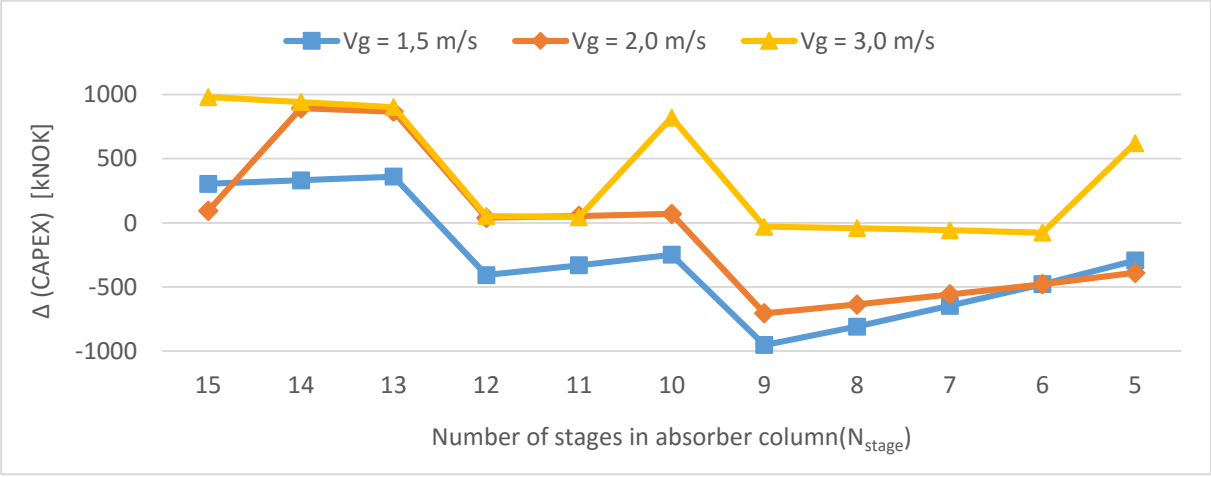

Figure 7-12 Δ(CAPEX) due to variation of v_g in Alternative 1

Adding up the data in Figure 7-9, Figure 7-10 and Figure 7-11 together according to each N_{stage}, the net changes of CAPEX can be obtained as shown in Figure 7-12. Several

fluctuations are observed along the N_{stage} due to the changes of installation factors; even so, the overall trend in Figure 7-12 indicates that the lower the v_g is, the more the CAPEX is reduced (and vice versa).

Detailed values corresponding to Figure 7-12 are summarized in Table 7-4.

Table 7-4 Δ(CAPEX) due to variation of v_g in Alternative 1 (unit: kNOK)

	N_{stage}										
v_g	15	14	13	12	11	10	9	8	7	6	5
3,0 m/s	745	715	685	-155	-153	634	589	-222	-228	-234	477
2,0 m/s	123	922	894	65	78	93	112	-630	-553	-473	-385
1,5 m/s	85	121	158	-601	-515	-424	-322	-978	-806	-626	-430

Taken as a whole, it can be said that the gas velocity of 1,5 m/s is the most optimum choice regarding CAPEX because it results in meaningful cost reductions for the most of N_{stage}. By contrast, the v_g of 3,0 m/s does not give significant reduction in CAPEX.

7.2.2.2 Impact of v_g variation on operating cost change

For similar reasons as given before, it should be noted that the net changes of OPEX are determined by Lean pump, Flue gas fan and the maintenance cost. In other words: Δ(OPEX) = Δ(Flue gas fan operating cost) + Δ(Lean pump operating cost) + Δ(Yearly maintenance cost). The term 'Δ(Yearly maintenance cost)', which is also equal to 0,05 ∗ Δ(CAPEX), may be ignored because its value is relatively marginal.

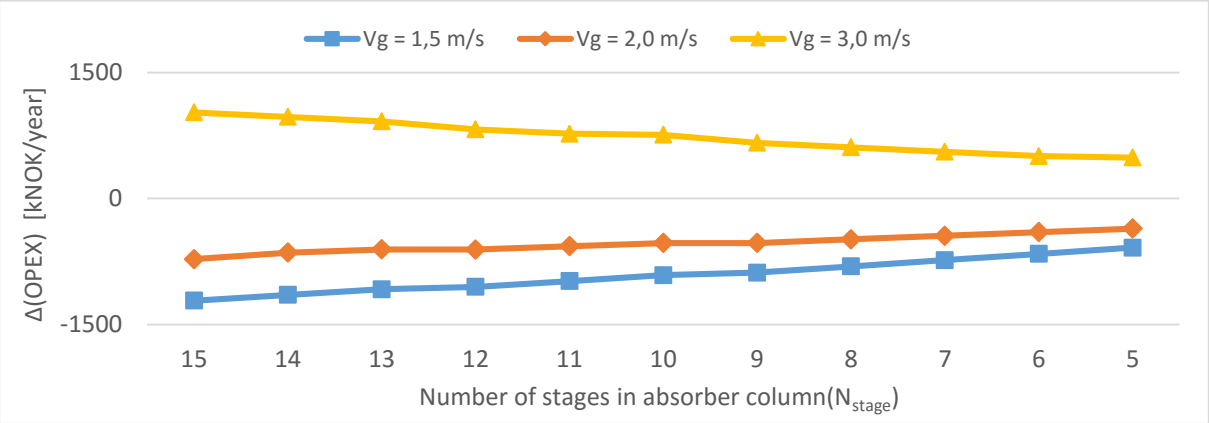

Figure 7-13 Δ(OPEX) due to variation of v_g in Alternative 1

Figure 7-13 shows the net changes of OPEX due to variation in v_g. The figure clearly indicates that a higher v_g leads to greater operating costs, whereas lower v_g makes the operating cost less expensive. After all, the graphs in Figure 7-13 display the similar trends as seen in Figure 7-10 or Figure 7-11. This is because for the Flue gas fan and Lean Pump, their duty (kW) serves as the basis of both the installation and operating cost. Accordingly, the same explanations given along with Figure 7-10 and Figure 7-11 may also apply for the trends in Figure 7-13.

Detailed values corresponding to Figure 7-13 are summarized in Table 7-5, where the v_g of 1,5 m/s results in the most reduction of operating costs.

Table 7-5 Δ(OPEX) due to variation of v_g in Alternative 1 (unit: kNOK/year)

	N_{stage}										
v_g	15	14	13	12	11	10	9	8	7	6	5
3,0 m/s	897	850	803	715	669	662	614	528	481	435	425
2,0 m/s	-722	-643	-606	-608	-569	-529	-489	-487	-444	-401	-358
1,5 m/s	-1300	-1229	-1157	-1125	-1050	-976	-901	-863	-785	-706	-626

7.2.2.3 Impact of v_g variation on CO_2-capture cost change

It was already shown in Equation 6-5 that the CO_2-capture cost can is determined by CAPEX, OPEX and the CO_2-capture rate. The term 'CO_2-capture rate' in Equation 6-5 depends only on the flue gas rate and N_{stage}, which are configured in HYSYS simulation. In other words, the capture rate obtained in HYSYS environment varies depending on N_{stage} and the flue gas rate only, so its value is independent of v_g. Therefore, the change of capture cost, i.e., Δ(capture cost), is determined by changes in CAPEX and OPEX only. Equation 7-1 expresses the capture cost changes in a mathematical form.

$$\Delta(\mathrm{CO_2\text{-capture cost}}) = \frac{\frac{\Delta(\mathrm{CAPEX})}{11{,}15} + \Delta(\mathrm{OPEX})}{(\mathrm{CO_2\text{-capture rate}})} \qquad \text{Equation 7-1}$$

In Equation 7-1, the values of Δ(CAPEX), Δ (OPEX) and (CO_2-capture rate) correspond to the figures in Table 7-4, Table 7-5 and Table 3-4 (first row; Alternative 1) respectively.

Putting all values of the three tables into Equation 7-1, the overall results of Δ(CO_2-capture cost) can be obtained as Table 7-6.

Table 7-6 Δ(capture cost) due to variation of v_g in Alternative 1 (unit: kNOK/tonne CO_2)

	N_{stage}										
v_g	15	14	13	12	11	10	9	8	7	6	5
3,0 m/s	0.004	0.004	0.003	0.003	0.003	0.003	0.003	0.002	0.002	0.002	0.002
2,0 m/s	-0.003	-0.002	-0.002	-0.002	-0.002	-0.002	-0.002	-0.002	-0.002	-0.002	-0.002
1,5 m/s	-0.005	-0.005	-0.005	-0.005	-0.004	-0.004	-0.004	-0.004	-0.004	-0.003	-0.003

Table 7-6 clearly indicates that the increase of v_g from the base velocity (i.e. 2,5 m/s) to 3,0 m/s brings out no improvement in regard to the capture cost, whereas the two lower v_g reduce the capture cost for all N_{stage}. The v_g of 1,5 m/s consequently gives the most optimization. The major reason for this result is attributed to the dominant influence of Δ(OPEX) on Δ(CO_2-capture cost). The numerator of Equation 7-1 shows that the coefficient of Δ(OPEX) is 11,15 times greater that of Δ(CAPEX). This indicates that the OPEX changes due to variation in v_g is 11,15 times more influential than CAPEX changes. Referring to Table 7-4 and Table 7-5, it is obvious that the order of magnitude of $\frac{\Delta(\text{CAPEX})}{11,15}$ is relatively negligible compared to that of Δ(OPEX). For this reason, despite some fluctuations of Δ(CAPEX) in Figure 7-12, their effects become unimportant relative to Δ(OPEX). Accordingly, the overall values of Δ(CO_2-capture cost) in Table 7-6 follow almost the same aspects as Δ(OPEX), i.e., Table 7-5.

The numbers in Table 7-6 indicate the capture cost changes only, so they need to be added to the initial capture cost data, which was previously given in Figure 7-8. Calculation results are summarized in Table 7-7, where the values are rounded to four decimal places. Figures in bold indicate the initial capture costs previously obtained with the base velocity.

Table 7-7 Overall CO_2-capture cost in Alternative 1 (unit: kNOK/tonne CO_2)

	N_{stage}										
v_g	15	14	13	12	11	10	9	8	7	6	5
3,0 m/s	0.1110	0.1088	0.1063	0.1039	0.1010	0.0992	0.0971	0.0946	0.0930	0.0911	0.0907
2,5 m/s	**0.1065**	**0.1045**	**0.1022**	**0.1006**	**0.0978**	**0.0958**	**0.0944**	**0.0921**	**0.0907**	**0.0890**	**0.0884**
2,0 m/s	0.1037	0.1022	0.1001	0.0981	0.0956	0.0937	0.0920	0.0899	0.0887	0.0872	0.0868
1,5 m/s	0.1018	0.1000	0.0980	0.0962	0.0937	0.0920	0.0905	0.0885	0.0874	0.0861	0.0858

(Base case: 0,2360 kNOK/tonne CO_2)

Figure 7-14 gives a visual illustration of Table 7-7 according to v_g and N_{stage}.

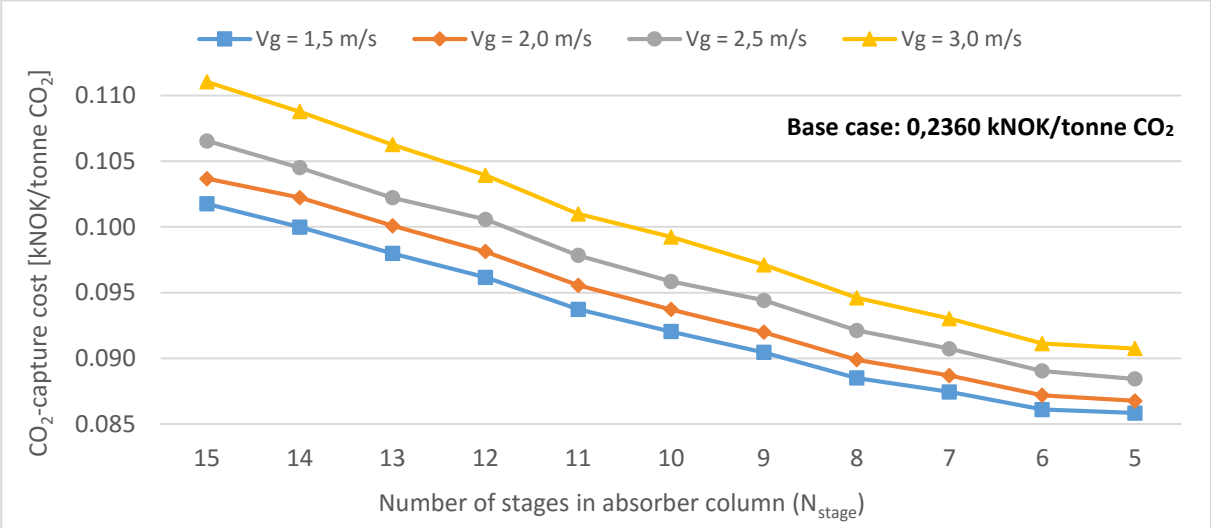

Figure 7-14 Overall CO_2-capture cost according to v_g and N_{stage} in Alternative 1

According to Figure 7-14, the following facts can be identified in Alternative 1.

1. CO_2-capture cost can be further optimized with the two lower gas velocities irrespective of N_{stage}, reaching the most optimization with v_g of 1,5 m/s. By contrast, a higher gas velocity than 2,5 m/s yields no improvement.
2. Regardless of v_g, the minimum capture cost is found at N_{stage} of five.

Consequently, the original capture cost, which was obtained earlier as 0,0884 kNOK/tonne CO_2 in Figure 7-8, can be further optimized by switching to v_g of 1,5 m/s, while maintaining the N_{stage} as five. The corresponding value with these operating parameters is read off as 0,0858 kNOK/tonne CO_2 in Table 7-7.

7.3 Alternative 2

7.3.1 Impact analysis of N_{stage} on costs (v_g = 2,5 m/s)

7.3.1.1 Impact of N_{stage} on installation cost (v_g = 2,5 m/s)

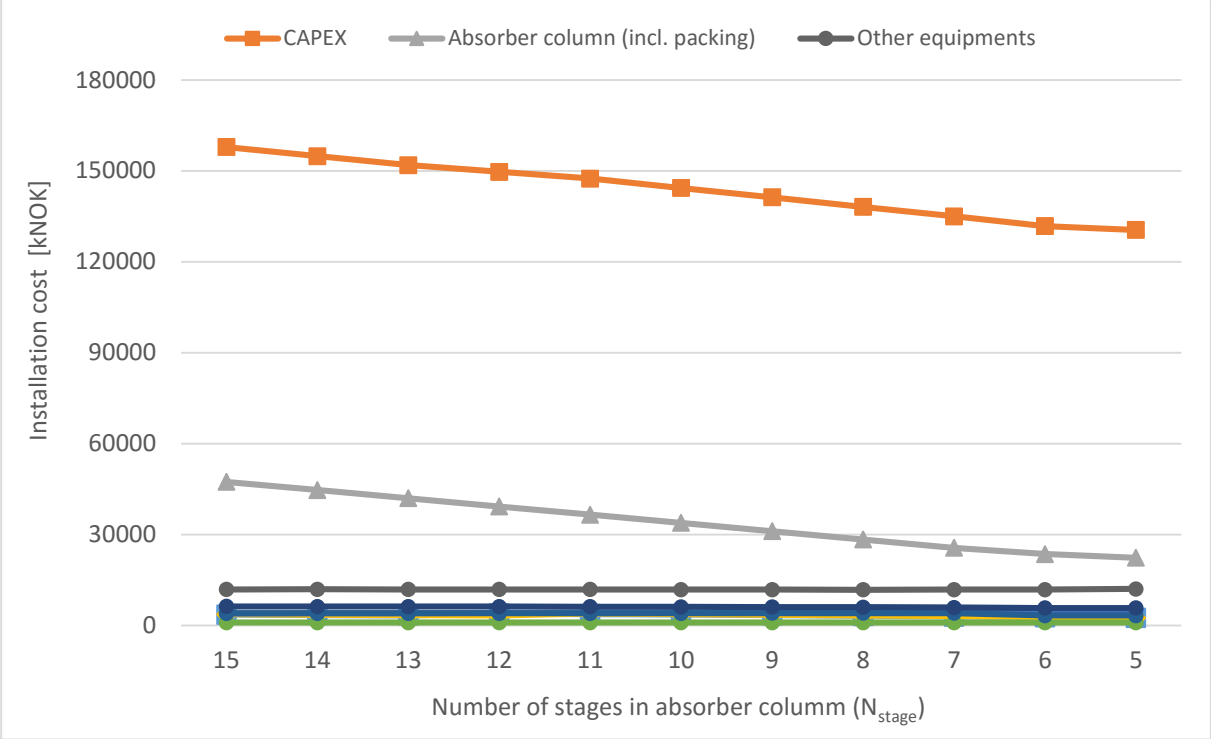

Figure 7-15 Installation cost versus N_{stage} in Alternative 2 (v_g = 2,5 m/s)

Figure 7-15 shows the installation cost changes for different equipments according to N_{stage}. A close look at the figure suggests that the installation cost of absorber column is lower than those in Figure 7-3. This is because in Alternative 2 the flue gas rate is reduced to 80 %, which makes the absorber column smaller.

As with the Alternative 1, the absorber cost declines with decreasing N_{stage}, whereas the installation cost of the other equipments show no visible changes. Hence, it can be said that the decreasing trend of the CAPEX is primarily attributed to the absorber column. This can be also identified from the fact that the installation cost change of absorber from N_{stage} of fifteen to five has the same order of magnitude as that of CAPEX (i.e. around -30000 kNOK).

For other miscellaneous equipments exhibiting little visible change of installation cost in Figure 7-15, an enlarged image of is available for reference in Appendix 27.

7.3.1.2 Impact of N_{stage} on operating cost (v_g = 2,5 m/s)

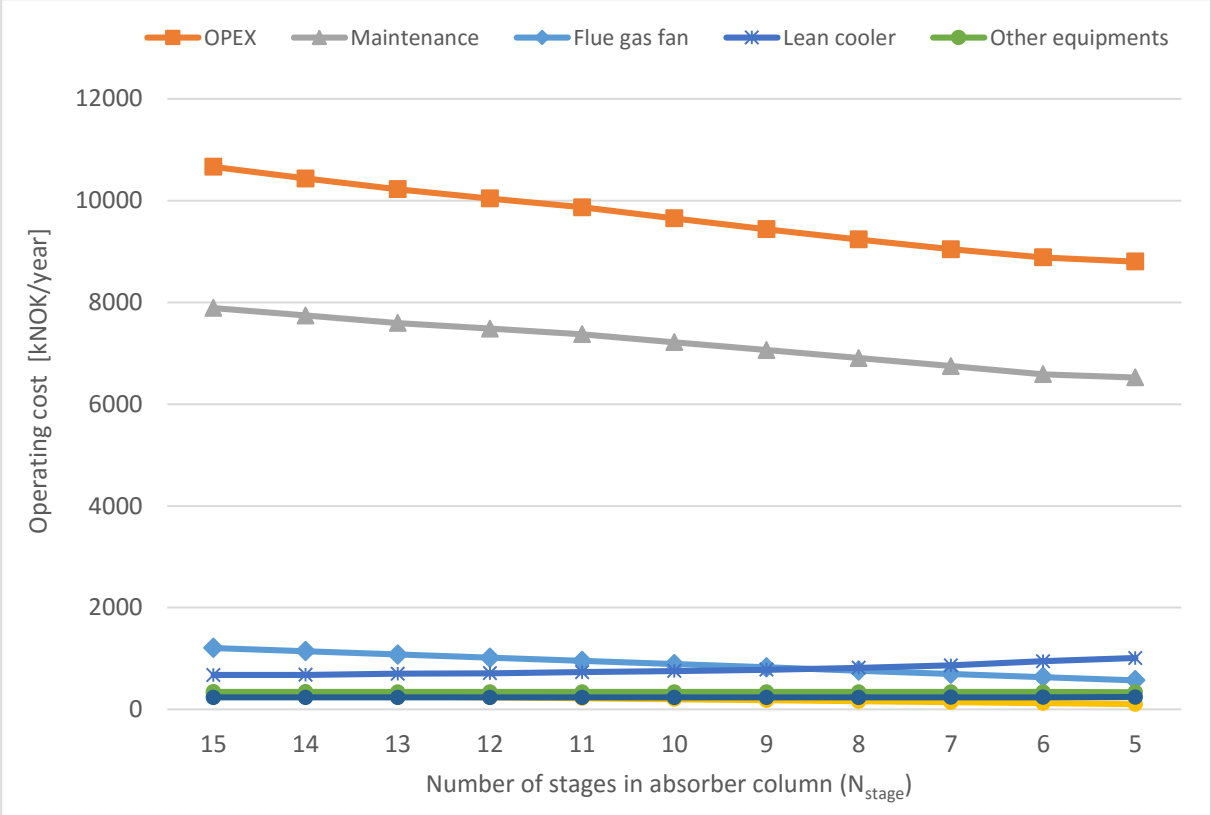

Figure 7-16 Operating cost versus N_{stage} in Alternative 2 (v_g = 2,5 m/s)

Figure 7-16 illustrates the operating cost changes for different equipments according to N_{stage}. Since the CAPEX decreases steadily as shown in Figure 7-15, the yearly maintenance cost also declines continuously. Other miscellaneous equipments, however, display no visible operating cost changes except for the Flue gas fan and Lean cooler. The operating cost of Flue gas fan shows a tendency to decline, yet its effect is more or less offset by the increasing trend of Lean cooler operating cost[11]. Consequently, as is the case of Alternative 1, the changing trend of the OPEX of Alternative 2 is largely attributable to the decreasing tendency of the yearly maintenance cost.

For other miscellaneous equipments displaying no visible operating cost changes in Figure 7-16, an enlarged image is available in Appendix 28 for reference.

[11] For these changing trends, the same explanations given earlier in Alternative 1 (Chapter 7.2.1.1) may apply.

7.3.1.3 Impact of N_{stage} on CO_2-capture cost (v_g = 2,5 m/s)

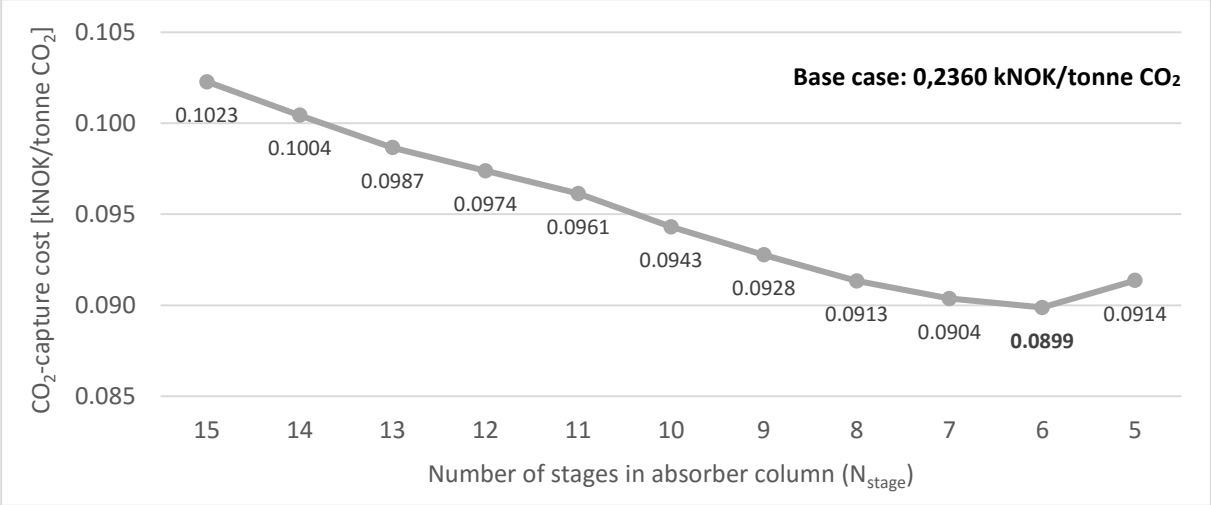

Figure 7-17 CO_2-capture cost versus N_{stage} in Alternative 2 (v_g = 2,5 m/s)

Figure 7-17 shows the CO_2-capture cost changes according to N_{stage} in Alternative 2, where the corresponding number above each circle point has been rounded off to four decimal places. For the same reason as explained in Alternative 1, the capture cost continuously decreases until N_{stage} reaches six. In the case of N_{stage} of five, however, the capture cost starts to rebound. This is because the decreasing rate of the CO_2-capture rate increases rapidly from N_{stage} of six, as demonstrated in Figure 3-3. In other words, the decreasing rate of capture rate is no longer overwhelmed by those of CAPEX and OPEX from N_{stage} of five. Therefore, the minimum capture cost is determined to be 0,0899 kNOK/tonne CO_2 at N_{stage} of six.

7.3.2 Impact analysis of v_g variation on cost change

7.3.2.1 Impact of v_g variation on installation cost change

- **Installation cost change of absorber column (incl. packing)**

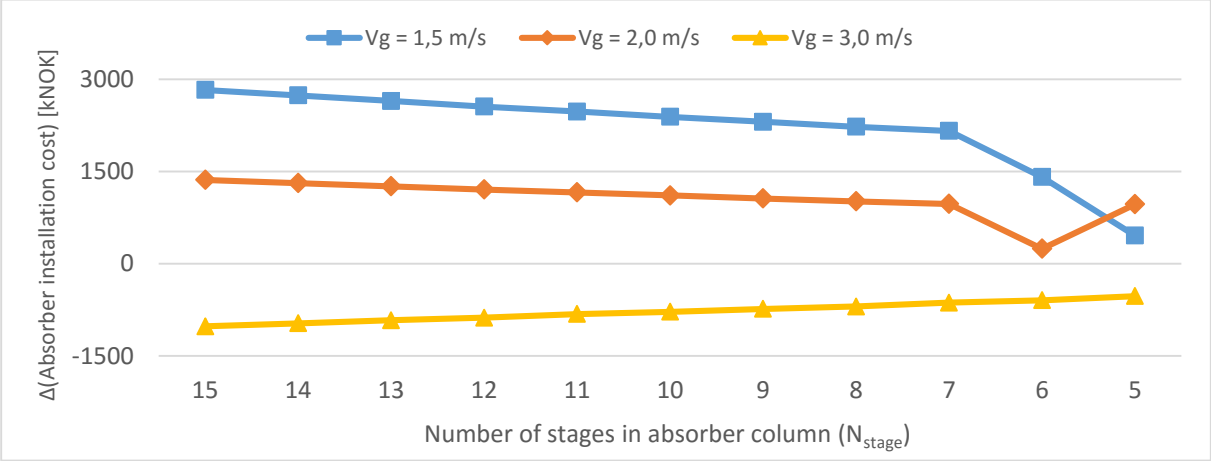

Figure 7-18 Δ(Absorber column installation cost) due to variation of v_g in Alternative 2

Figure 7-18 shows the installation cost changes of absorber column resulting from variation in v_g. As with the Alternative 1, the two lower v_g than 2,5 m/s result in more expensive cost, whereas a higher velocity (i.e. v_g = 3,0 m/s) leads to the reduced cost of absorber column. Therefore, the three cost-affecting factors previously described with Figure 7-9 may apply in the same way for the explanations of these trend.

- **Installation cost change of Flue gas fan**

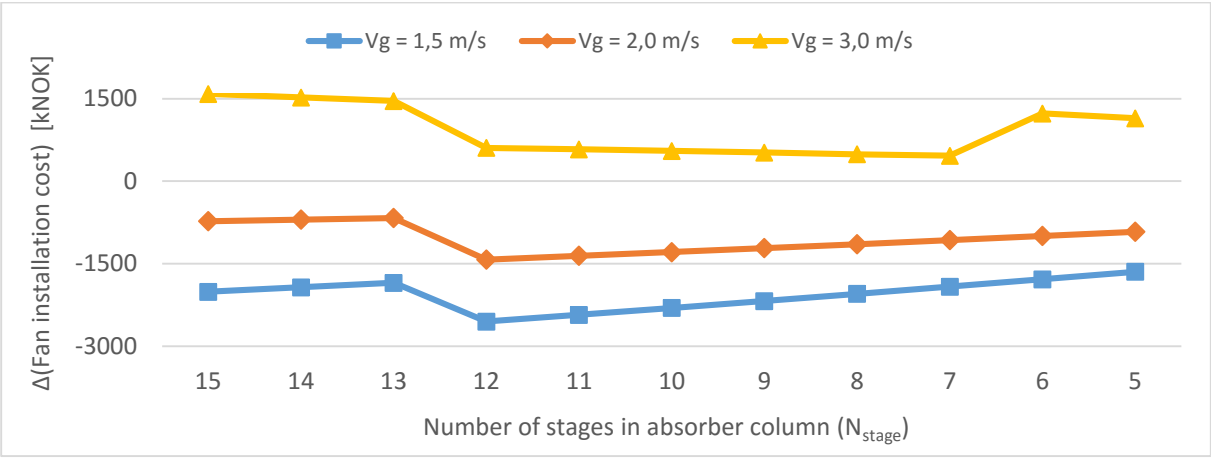

Figure 7-19 Δ(Flue gas fan installation cost) due to variation of v_g in Alternative 2

Figure 7-19 shows the installation cost changes of Flue gas fan cost due to variation in v_g. As in the case of Alternative 1, the two v_g lower than 2,5 m/s lead to reduced costs whereas a

higher gas velocity than 2,5 m/s makes the cost more expensive. Since the graphs in the figure exhibit the same aspects as observed previously, the same explanations as previously given with Figure 7-10 may apply.

- **Installation cost changes in Lean Pump**

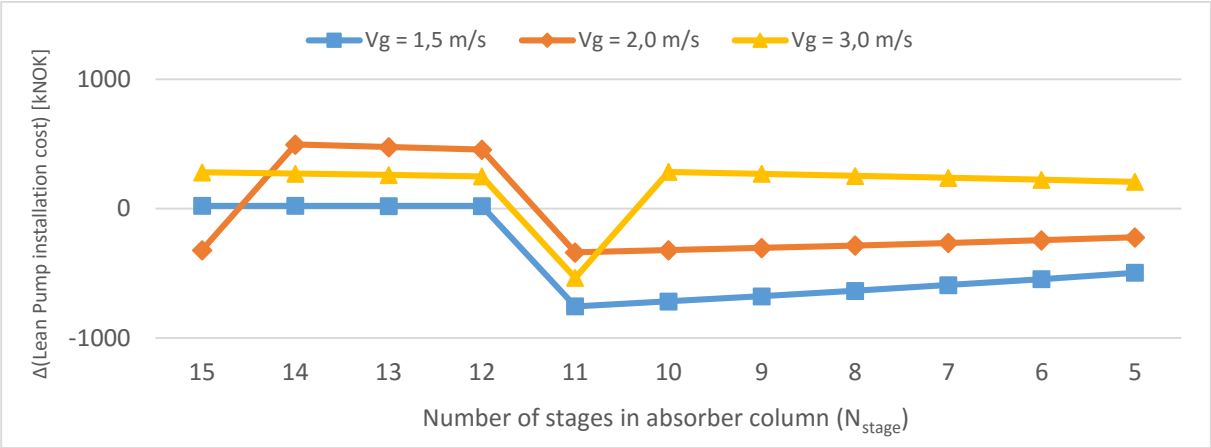

Figure 7-20 Δ(Lean Pump installation cost) due to variation of v_g in Alternative 2

Figure 7-20 shows the installation cost changes of Lean pump cost due to variation in v_g. Except for some fluctuations between N_{stage} of 15 and 11, which are due to change in installation factors, the graphs display the same trend as previously shown in Figure 7-11. Therefore, the same explanations given with Figure 7-11 may apply.

- **Net change of CAPEX**

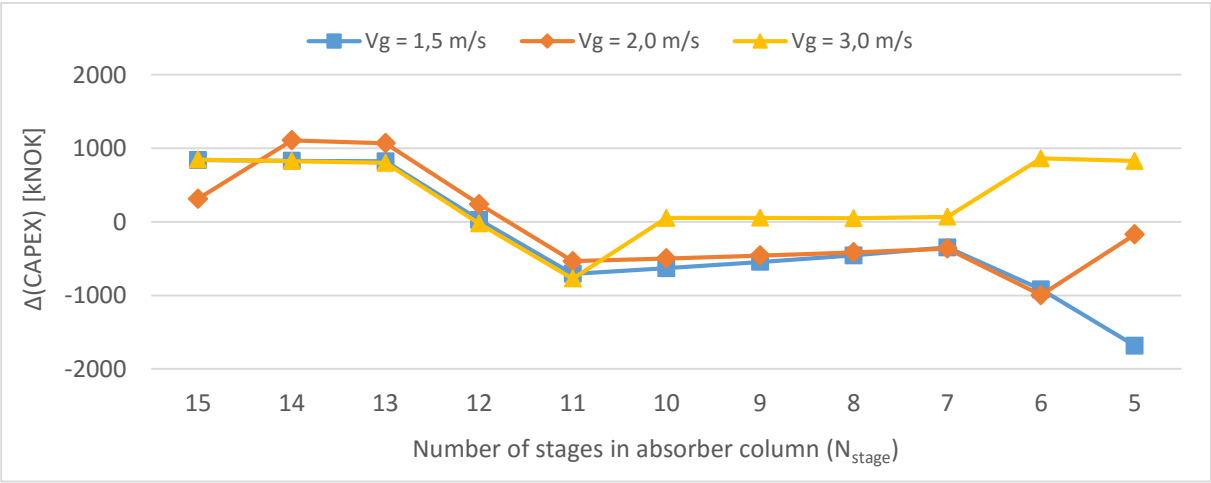

Figure 7-21 Δ(CAPEX) due to variation of v_g in Alternative 2

Adding up the data in Figure 7-18, Figure 7-19 and Figure 7-20 together, the net changes of CAPEX can be obtained as shown in Figure 7-21. For N_{stage} of less than 11, the v_g of 1,5 m/s

seems to be a better option than any other. Nevertheless, there is little distinction between the three graphs, making it difficult to generalize about the optimum v_g. The main reasons for this phenomenon can be explained as follows.

1. Comparing Figure 7-18, Figure 7-19 and Figure 7-20, the points where the installation factor shifts differ from each equipment. This makes the Δ(CAPEX) look less distinct over the entire range of N_{stage}.
2. Each equipment (i.e. Absorber column, Flue gas fan and Lean pump) has different orders of magnitude of the installation cost, so the scale of installation cost change is also different depending on the equipment.

Detailed values corresponding to Figure 7-21 are summarized in Table 7-8.

Table 7-8 Δ(CAPEX) due to variation of v_g in Alternative 2 (unit: kNOK)

	N_{stage}										
v_g	15	14	13	12	11	10	9	8	7	6	5
3,0 m/s	846	825	801	-24	-773	53	55	48	67	861	827
2,0 m/s	315	1109	1069	239	-535	-499	-458	-415	-364	-998	-172
1,5 m/s	841	831	823	27	-707	-632	-547	-456	-348	-919	-1684

7.3.2.2 Impact of v_g variation on operating cost change

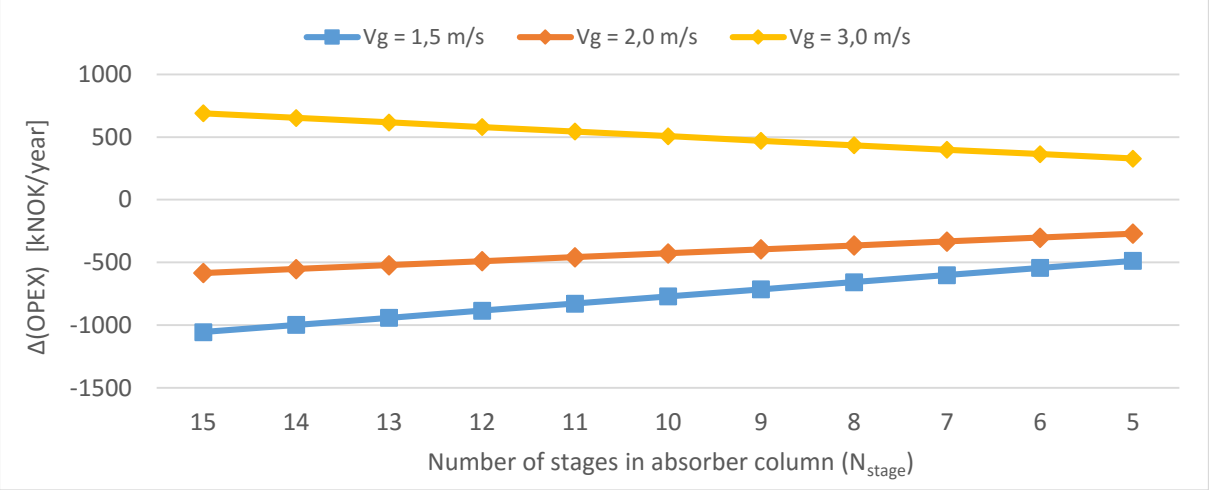

Figure 7-22 Δ(OPEX) due to variation of v_g in Alternative 2

Figure 7-22 shows the changes in operating cost due variation in v_g. As seen in Figure 7-19 and Figure 7-20, a higher v_g leads to greater operating costs and vice versa. The same

explanations previously given with Figure 7-10 and Figure 7-11 may also apply for the trends in Figure 7-22. Detailed values corresponding to Figure 7-22 are summarized in Table 7-9.

Table 7-9 Δ(OPEX) due to variation of v_g in Alternative 2 (unit: kNOK/year)

	N_{stage}										
v_g	15	14	13	12	11	10	9	8	7	6	5
3,0 m/s	827	785	742	659	581	580	539	497	457	457	416
2,0 m/s	-567	-496	-467	-477	-485	-451	-418	-385	-351	-351	-279
1,5 m/s	-954	-901	-848	-834	-817	-759	-701	-643	-584	-559	-543

7.3.2.3 Impact of v_g variation on CO_2-capture cost change

For calculation of capture cost changes, the same procedures as performed in Chapter 7.2.2.3 may apply. The values of Δ(CAPEX), Δ(OPEX) and (CO_2-capture rate) in Equation 7-1 correspond to the figures in Table 7-8, Table 7-9 and Table 3-4 (second row; Alternative 2) respectively. Putting all values of the three tables into Equation 7-1, the overall calculation results of Δ(CO_2-capture cost) are obtained as Table 7-10 below. Due to the dominant influence of Δ(OPEX) as explained in Chapter 7.2.2.3, the overall figures in Table 7-10 show nearly the same aspects as those of Δ(OPEX), i.e., Table 7-9.

Table 7-10 Δ(capture cost) due to variation of v_g in Alternative 2 (unit: kNOK/tonne CO_2)

	N_{stage}										
v_g	15	14	13	12	11	10	9	8	7	6	5
3,0 m/s	0.004	0.004	0.003	0.003	0.002	0.002	0.002	0.002	0.002	0.002	0.002
2,0 m/s	-0.002	-0.002	-0.002	-0.002	-0.002	-0.002	-0.002	-0.002	-0.002	-0.002	-0.001
1,5 m/s	-0.004	-0.003	-0.003	-0.003	-0.004	-0.003	-0.003	-0.003	-0.003	-0.003	-0.003

By adding up the values in Table 7-10 to the original capture cost data (i.e. Figure 7-17), the overall capture cost according to v_g and N_{stage} can be obtained as Table 7-11, where the numbers are rounded to four decimal places. Figures in bold indicate the initial capture costs shown previously in Figure 7-17 with the base velocity.

Table 7-11 Overall CO_2-capture cost in Alternative 2 (unit: kNOK/tonne CO_2)

	N_{stage}										
v_g	15	14	13	12	11	10	9	8	7	6	5
3,0 m/s	0.1060	0.1040	0.1020	0.1001	0.0982	0.0967	0.0950	0.0934	0.0923	0.0922	0.0935
2,5 m/s	**0.1023**	**0.1004**	**0.0986**	**0.0974**	**0.0961**	**0.0943**	**0.0927**	**0.0913**	**0.0903**	**0.0898**	**0.0913**
2,0 m/s	0.1000	0.0988	0.0971	0.0955	0.0939	0.0922	0.0908	0.0895	0.0887	0.0879	0.0900
1,5 m/s	0.0986	0.0970	0.0954	0.0939	0.0924	0.0909	0.0896	0.0884	0.0877	0.0871	0.0882

(Base case: 0,2360 kNOK/tonne CO_2)

Figure 7-23 gives a visual illustration of Table 7-11 depending on v_g and N_{stage}.

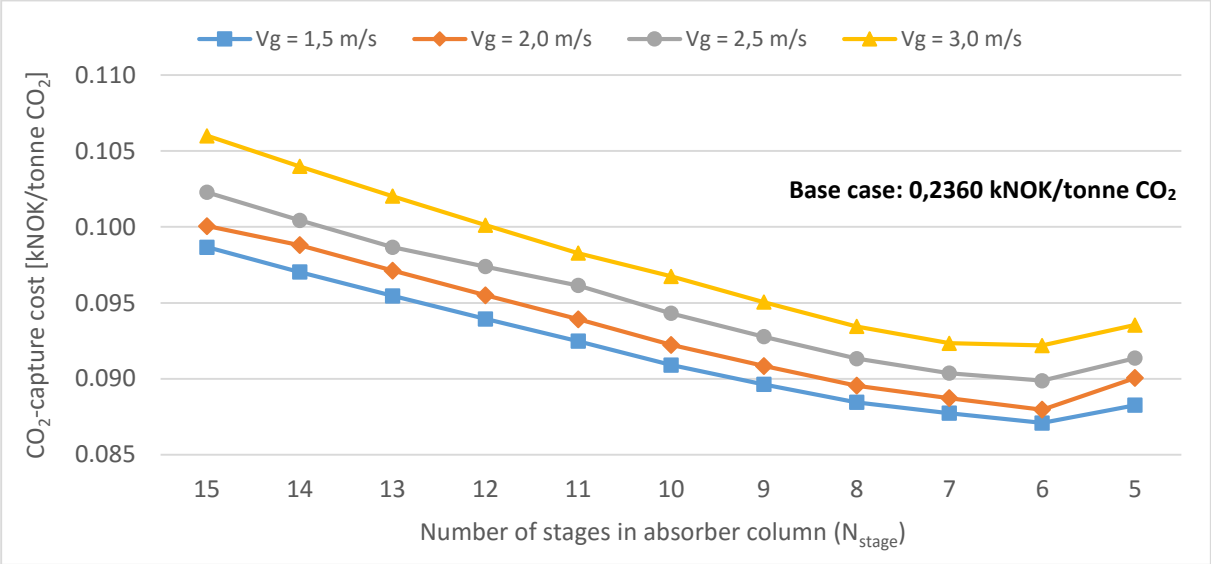

Figure 7-23 Overall CO_2-capture cost according to v_g and N_{stage} in Alternative 2

According to Figure 7-23, the following facts can be identified.

1. As in the case of Alternative 1, the lower the v_g is, the more optimized the CO_2-capture cost becomes for all the N_{stage}. The optimum v_g is therefore 1,5 m/s.
2. Regardless of v_g, the capture cost marks the minimum at N_{stage} of 6, where it starts to increase again. The optimum N_{stage} is therefore determined as six.

Consequently, the initial capture cost obtained earlier in Figure 7-17 can be further optimized by switching to v_g of 1,5 m/s, while keeping the N_{stage} as 6. The corresponding value with these operating parameters is read off as 0,0871 kNOK/tonne CO_2 in Table 7-11. Compared with the minimum capture cost obtained in Alternative 1 from Figure 7-14 (i.e. 0,0858 kNOK/tonne CO_2), it can be known that the Alternative 2 is overall less attractive regarding cost-benefit than Alternative 1.

7.4 Alternative 3

7.4.1 Impact analysis of N_{stage} on costs (v_g = 2,5 m/s)

7.4.1.1 Impact of N_{stage} on installation cost (v_g = 2,5 m/s)

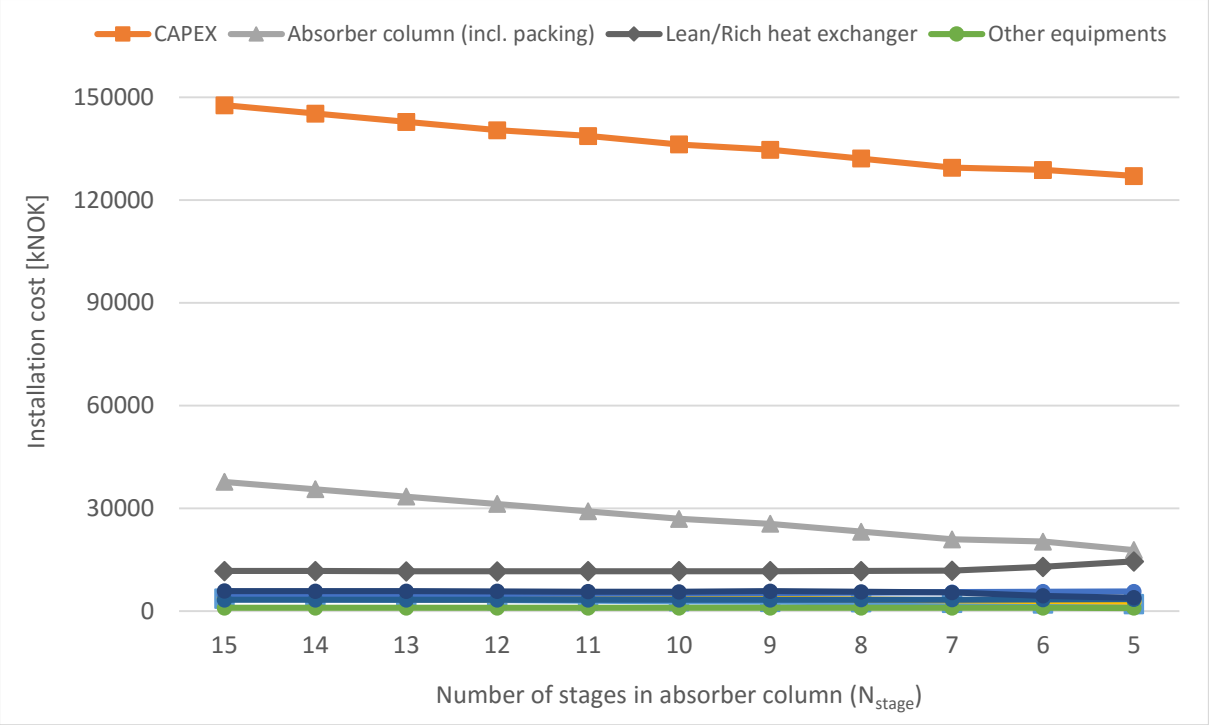

Figure 7-24 Installation cost versus N_{stage} in Alternative 3 (v_g = 2,5 m/s)

Figure 7-24 shows the installation cost changes for different equipments according to N_{stage}. As expected, the installation cost of absorber column displays steady decreases, whereas the installation cost of the other equipments shows no significant changes. Hence, it can be said that the installation cost changes of absorber column are the main contributing factor of CAPEX changes along with N_{stage}[12].

For other miscellaneous equipments exhibiting little visible change of the installation cost in Figure 7-24, an enlarged image is available in Appendix 27.

[12] Although the Lean/Rich heat exchanger cost begins to show slight rises from N_{stage} of six, which is primarily due to sharp increases in Lean amine rate, these effects are more or less offset by Desorber column and Lean pump installation cost changes. A clear view of Figure 7-24 is available in Appendix 27.

7.4.1.2 Impact of N_{stage} on operating cost (v_g = 2,5 m/s)

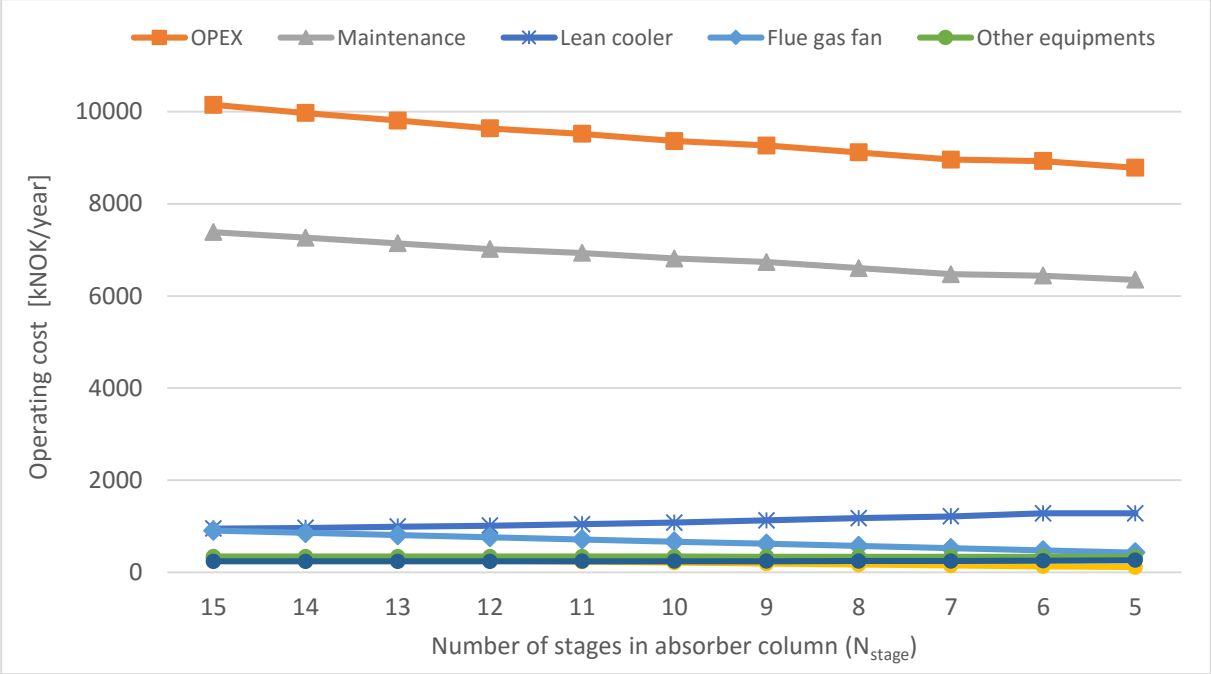

Figure 7-25 Operating cost versus N_{stage} in Alternative 3 (v_g = 2,5 m/s)

Figure 7-25 illustrates the operating cost changes for different equipments according to N_{stage}. The graphs in the figure all follow the same trends as observed in the two previous Alternatives (i.e. Figure 7-4 and Figure 7-16), so the same explanations given earlier may apply. Again, the changing trends of the OPEX along with N_{stage} is largely attributed to the decreasing tendency of the yearly maintenance cost.

For other miscellaneous equipments displaying no visible operating cost changes in Figure 7-25, an enlarged image is available in Appendix 28.

7.4.1.3 Impact of N_{stage} on CO_2-capture cost (v_g = 2,5 m/s)

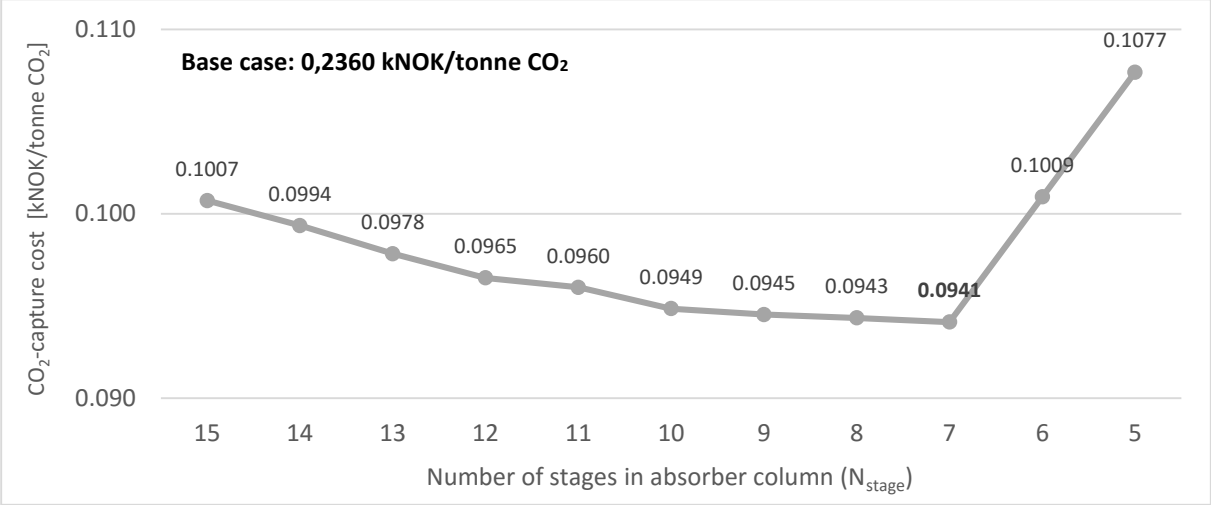

Figure 7-26 CO_2-capture cost versus N_{stage} in Alternative 3 (v_g = 2,5 m/s)

Figure 7-26 shows the CO_2-capture cost of Alternative 3, where the corresponding number above each circle point has been rounded off to four decimal places. For the same reason as explained before, the capture cost in the figure continuously decreases until N_{stage} reaches seven. Beyond this point, however, the capture cost begins to grow again because the decreasing rate of capture rate starts to outdo those of CAPEX and OPEX. Consequently, the minimum capture cost is found to be 0,0941 kNOK/tonne CO_2 at N_{stage} of seven.

The meaningful difference from the Alternative 2 is that while the Alternative 2 has the minimum capture cost at N_{stage} of six (as shown in Figure 7-17), Alternative 3 has the minimum cost at one stage earlier, i.e., at N_{stage} of seven,.

7.4.2 Impact analysis of v_g variation on cost change

7.4.2.1 Impact of v_g variation on installation cost change

- **Installation cost change of absorber column (incl. packing)**

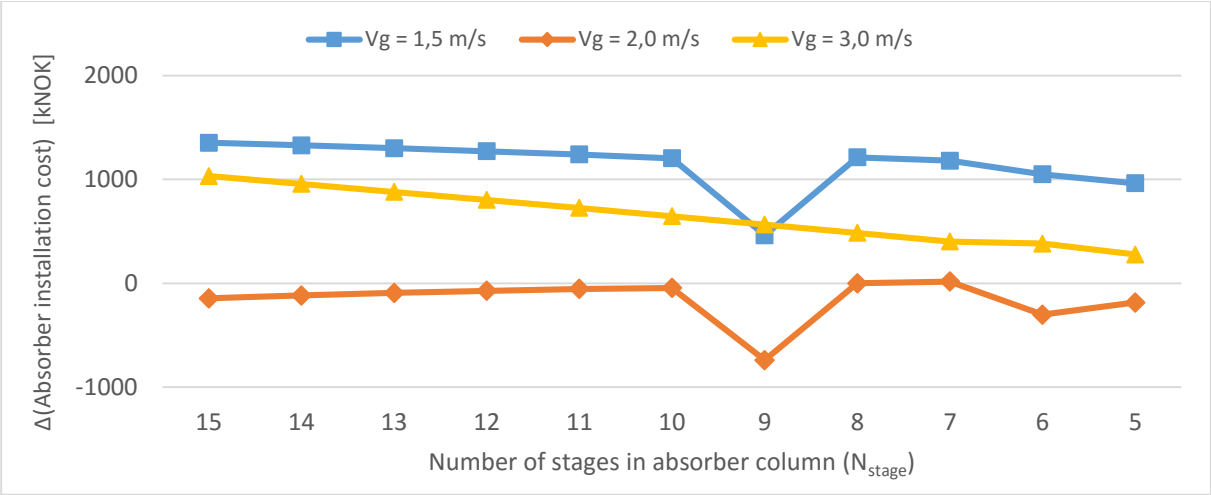

Figure 7-27 Δ(Absorber column installation cost) due to variation of v_g in Alternative 3

Figure 7-27 shows the installation cost changes of absorber column due to variation in v_g. It has been previously shown that the v_g of 3,0 m/s leads to the lowest absorber cost, as illustrated in Figure 7-9 and Figure 7-18. Figure 7-27, on the other hand, indicates that the v_g of 2,0 m/s reduces the cost more rather than 3,0 m/s over the entire range of N_{stage}. This is because the interfacial effective area (a_e) is not further increased from v_g of 2,5 m/s to 3,0 m/s, leading to no cost reduction in packings.

Figure 7-28 shows the Lean amine liquid load of Alternative 3. As described in Equation 4-4, the interfacial effective area reaches the maximum (i.e. $a_e/a_g = 1$) when the liquid load exceeds a certain limit, namely, 40 $m^3/(m^2 \cdot h)$. Under the condition of v_g = 2,5 m/s, the Lean amine liquid load of Alternative 3 already exceeds 40 $m^3/m^2 \cdot h$ for all N_{stage}. The same trend is also observed at v_g of 3,0 m/s. Two main reasons for this can be summarized as follows.

1. Higher gas velocities lead to smaller diameters of absorber column.
2. With decreasing N_{stage}, the Lean amine rate tends to increase. (Figure 3-5)

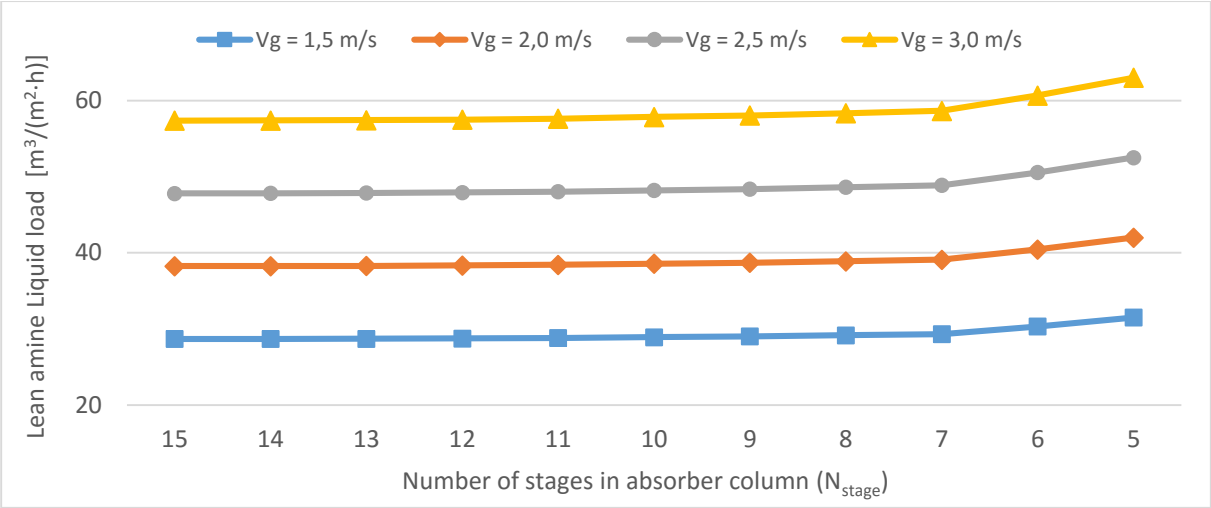

Figure 7-28 Lean amine liquid load (Q_L) according to v_g and N_{stage} in Alternative 3

Since the total volume of packing beds remains unchanged, the cost of packings remains also constant. Figure 7-29 visually represents the installation cost changes of absorber packings, where no changes (either increase or decrease) is observed at v_g of 3,0 m/s. When it comes to the two lower gas velocities than 2,5 m/s, the cost of packings increases due to reduced interfacial area.

Meanwhile, it can also be found that the packing cost increases at v_g of 2,0 m/s is relatively small than when v_g is 1,5 m/s. This is because when v_g is 2,0 m/s, the liquid load already approaches nearly 40 $m^3/(m^2 \cdot h)$ for most of the N_{stage}, as shown in Figure 7-28. Therefore, even though the v_g is reduced from 2,5 m/s to 2,0 m/s, the increase of packing bed size is relatively insignificant and so does the packing cost.

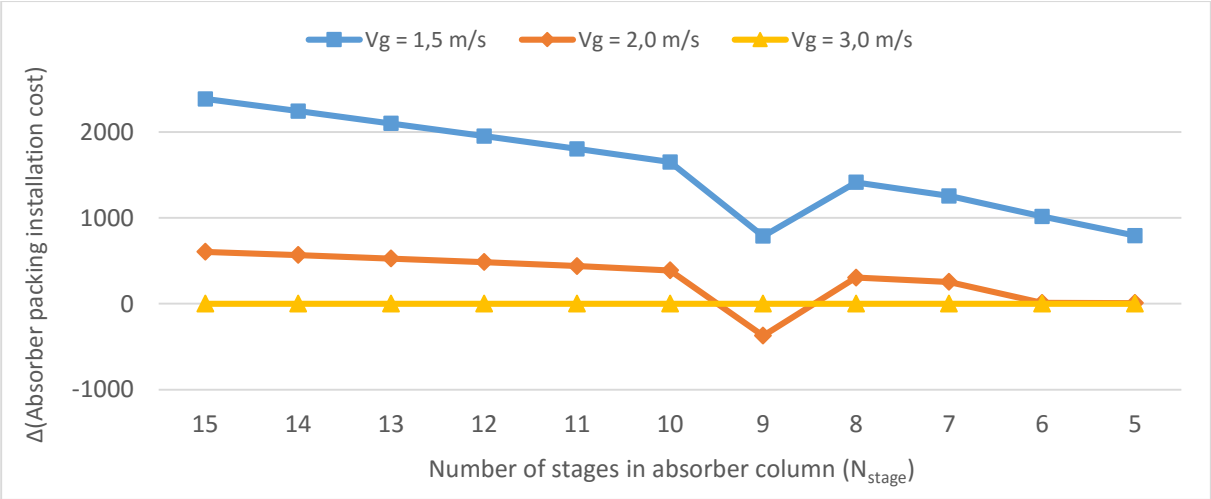

Figure 7-29 Δ(Absorber packing installation cost) due to variation of v_g in Alternative 3

Figure 7-30 shows the installation cost changes of absorber shell due to variation in v_g. Apparently, the gas velocities lower than 2,5 m/s make the absorber shell cost less expensive, whereas the v_g of 3,0 m/s increases the shell cost. Since no cost change in packings was observed at v_g of 3,0 m/s, it can be said that when v_g is 3,0 the installation cost change of absorber shell is equal to that of the absorber column.

Comparing Figure 7-29 and Figure 7-30, it can be seen that at v_g of 1,5 m/s, the cost increase of absorber packing is much higher than the cost reduction of absorber shell for most of the N_{stage}. For this reason, with v_g of 1,5 m/s, the installation cost of absorber column becomes more expensive than when v_g is 3,0 m/s. In the case of v_g of 2,0 m/s, the cost reduction of absorber shell is overall higher than the cost increase of absorber packing. After all, the installation cost of absorber column becomes most expensive with v_g of 1,5 m/s, whereas the v_g of 2,0 m/s makes the absorber column cost least expensive.

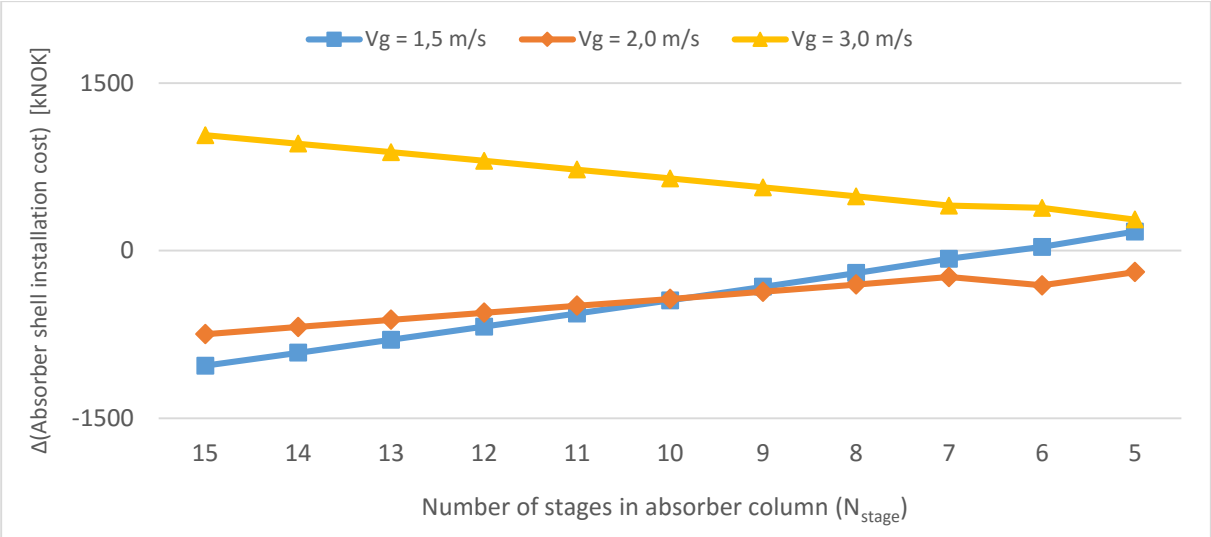

Figure 7-30 Δ(Absorber shell installation cost) due to variation of v_g in Alternative 3

▪ **Installation cost changes of Flue gas fan**

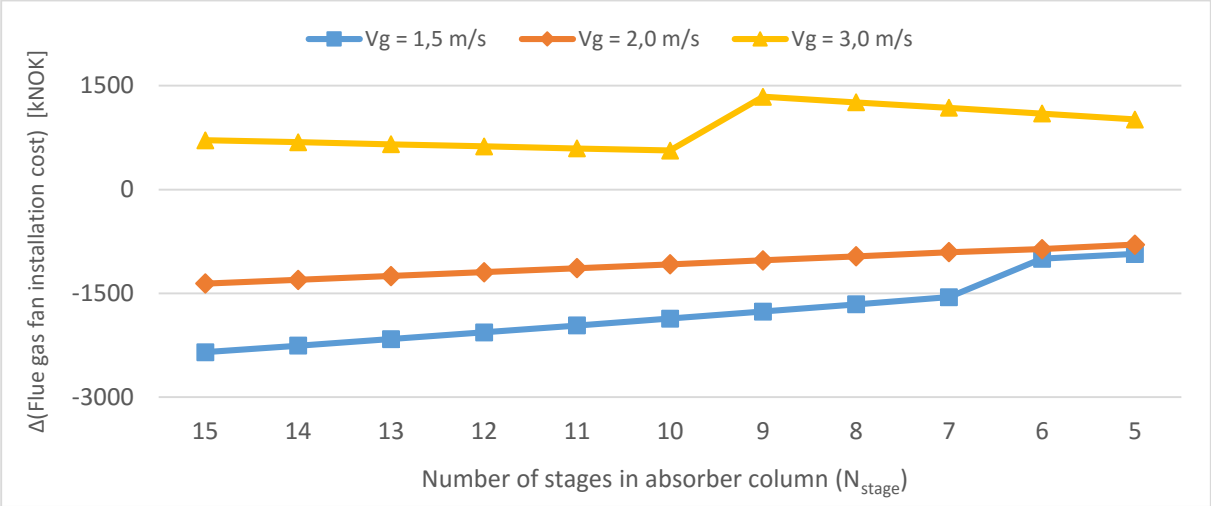

Figure 7-31 Δ(Flue gas fan installation cost) due to variation of v_g in Alternative 3

Figure 7-31 shows the installation cost changes of Flue gas fan due to variation in v_g. As with the previous Alternatives, the two gas velocities lower than 2,5 m/s lead to reduced cost whereas a higher gas velocity makes the cost more expensive. The overall graphs in the figure exhibit the same aspects as observed previously, so the same explanation given with Figure 7-10 may apply.

▪ **Installation cost changes of Lean Pump**

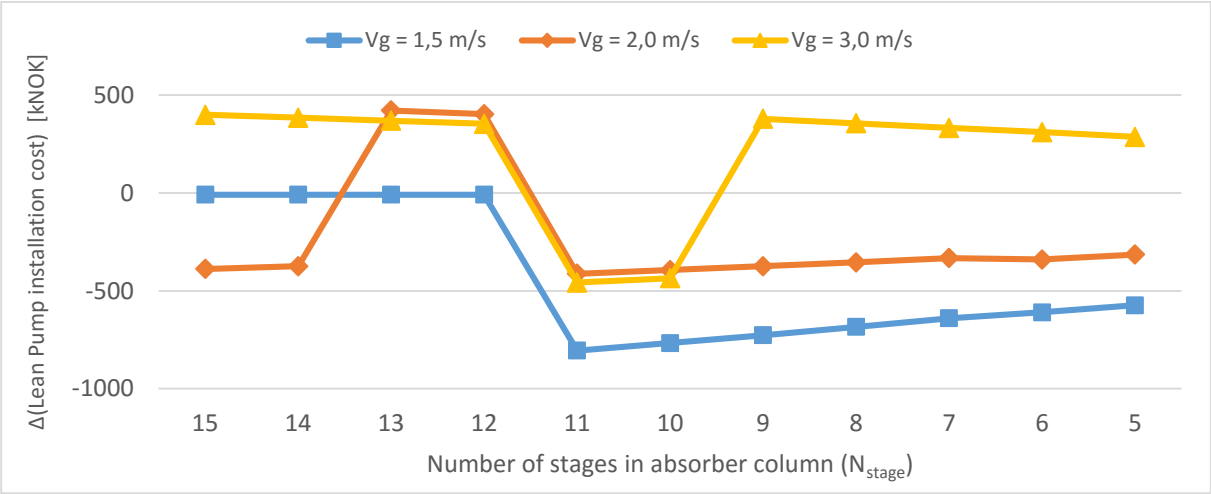

Figure 7-32 Δ(Lean Pump installation cost) due to variation of v_g in Alternative 3

Figure 7-32 shows the installation cost changes of Lean pump due to variation in v_g. Except a few fluctuations for between N_{stage} of 14 and 10, which are due to installation factor changes, the graphs display the similar trend as shown in Figure 7-11. Therefore, the same explanation given with Figure 7-11 may apply.

▪ **Net change of CAPEX**

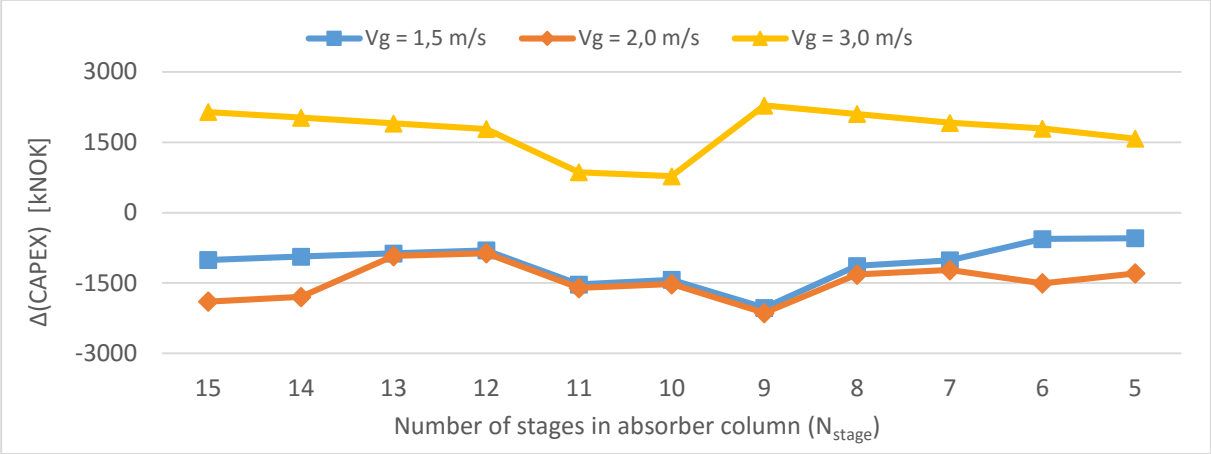

Figure 7-33 Δ(CAPEX) due to variation of v_g in Alternative 3

Combining the data in Figure 7-30, Figure 7-31 and Figure 7-32 together, the net changes of CAPEX can be obtained as shown in Figure 7-33. In contrast to Alternative 1 and 2 where the optimum v_g is close to 1,5 m/s, the overall trend in Figure 7-33 indicates that the v_g of 2,0 m/s yields the most reductions of CAPEX over the range of N_{stage}. Two main reasons for this result can be described as follows.

1. For the v_g of 1,5 m/s, the cost increase in packings is so high that the cost decreases in Flue gas fan and Lean Pump are not enough to make the 1,5 m/s the optimum gas velocity.
2. For the v_g of 2,0 m/s, the cost increase in packings is quite small, so the cost savings in Flue gas fan and Lean Pump make the 2,0 m/s more attractive gas velocity than 1,5 m/s in terms of reducing the CAPEX.

Detailed values corresponding to Figure 7-33 are summarized in Table 7-12.

Table 7-12 Δ(CAPEX) due to variation of v_g in Alternative 3 (unit: kNOK)

	N_{stage}										
v_g	15	14	13	12	11	10	9	8	7	6	5
3,0 m/s	2143	2024	1904	1782	862	775	2286	2103	1915	1791	1578
2,0 m/s	-1894	-1796	-922	-864	-1605	-1522	-2138	-1319	-1222	-1505	-1295
1,5 m/s	-1007	-937	-869	-802	-1531	-1430	-2028	-1133	-1015	-561	-544

7.4.2.2 Impact of v_g variation on operating cost change

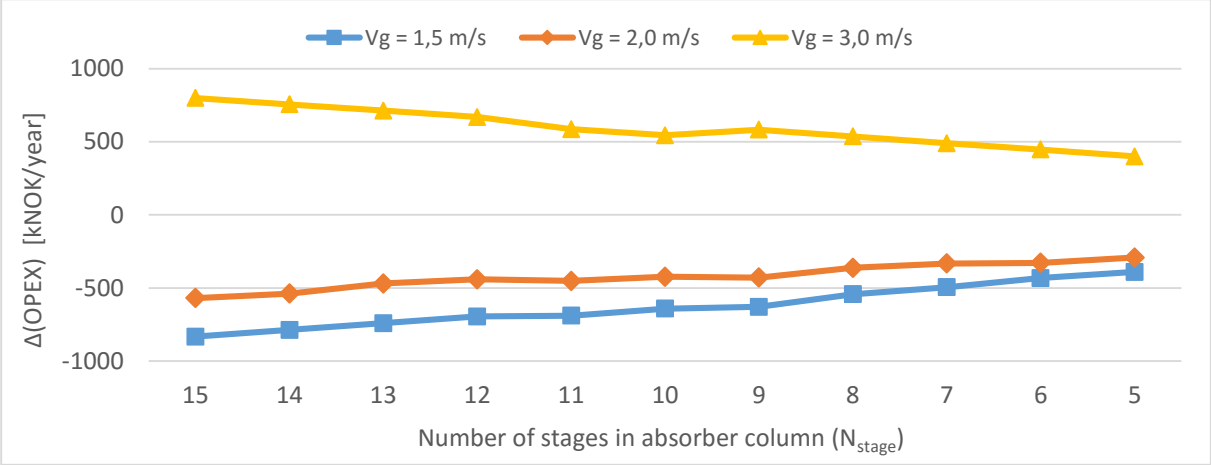

Figure 7-34 Δ(OPEX) due to variation of v_g in Alternative 3

Figure 7-34 shows the net changes in OPEX due to variation v_g. As previously seen in Figure 7-31 and Figure 7-32, a higher v_g leads to greater operating costs and vice versa. Therefore, the same explanations as given before may also apply for the trends in Figure 7-34. Detailed values corresponding to Figure 7-34 are summarized in Table 7-13.

Table 7-13 Δ(OPEX) due to variation of v_g in Alternative 3 (unit: kNOK/year)

	N_{stage}										
v_g	15	14	13	12	11	10	9	8	7	6	5
3,0 m/s	800	757	714	670	587	545	584	537	491	448	400
2,0 m/s	-569	-539	-469	-441	-453	-423	-429	-363	-333	-329	-292
1,5 m/s	-833	-787	-741	-695	-690	-642	-630	-543	-495	-432	-391

7.4.2.3 Impact of v_g variation on CO_2-capture cost change

For calculation of capture cost changes, the same procedures as performed in Chapter 7.2.2.3 may apply. The values of Δ(CAPEX), Δ (OPEX) and (CO_2-capture rate) in Equation 7-1 correspond to the figures in Table 7-12, Table 7-13 and Table 3-4 (third row; Alternative 3) respectively. Putting all values of the three tables into Equation 7-1, the overall calculation results of Δ(CO_2-capture cost) can be obtained as Table 7-14 below. For the same reasons as described before, the overall figures of Δ(CO_2-capture cost) show the same aspects as Table 7-13.

Table 7-14 Δ(capture cost) due to variation of v_g in Alternative 3 (unit: kNOK/tonne CO_2)

	N_{stage}										
v_g	15	14	13	12	11	10	9	8	7	6	5
3,0 m/s	0.004	0.004	0.004	0.004	0.003	0.003	0.003	0.003	0.003	0.003	0.003
2,0 m/s	-0.003	-0.003	-0.002	-0.002	-0.003	-0.002	-0.003	-0.002	-0.002	-0.002	-0.002
1,5 m/s	-0.004	-0.004	-0.004	-0.003	-0.004	-0.003	-0.004	-0.003	-0.003	-0.002	-0.002

By adding up the values in Table 7-14 to the original capture cost data (i.e. Figure 7-26), the overall capture costs obtained as Table 7-15, where the numbers are rounded to four decimal places. Figures in bold indicate the initial capture costs obtained before with the base velocity.

Table 7-15 Overall CO_2-capture cost in Alternative 3 (unit: kNOK/tonne CO_2)

	N_{stage}										
v_g	15	14	13	12	11	10	9	8	7	6	5
3,0 m/s	0.1050	0.1034	0.1016	0.1001	0.0989	0.0975	0.0980	0.0976	0.0971	0.1039	0.1105
2,5 m/s	**0.1007**	**0.0993**	**0.0978**	**0.0965**	**0.0960**	**0.0948**	**0.0945**	**0.0943**	**0.0941**	**0.1009**	**0.1076**
2,0 m/s	0.0975	0.0963	0.0954	0.0942	0.0934	0.0924	0.0918	0.0922	0.0921	0.0986	0.1055
1,5 m/s	0.0967	0.0956	0.0943	0.0932	0.0924	0.0914	0.0909	0.0914	0.0914	0.0985	0.1053

(Base case: 0,2360 kNOK/tonne CO_2)

Figure 7-35 gives a visual illustration of Table 7-15 depending on v_g and N_{stage}.

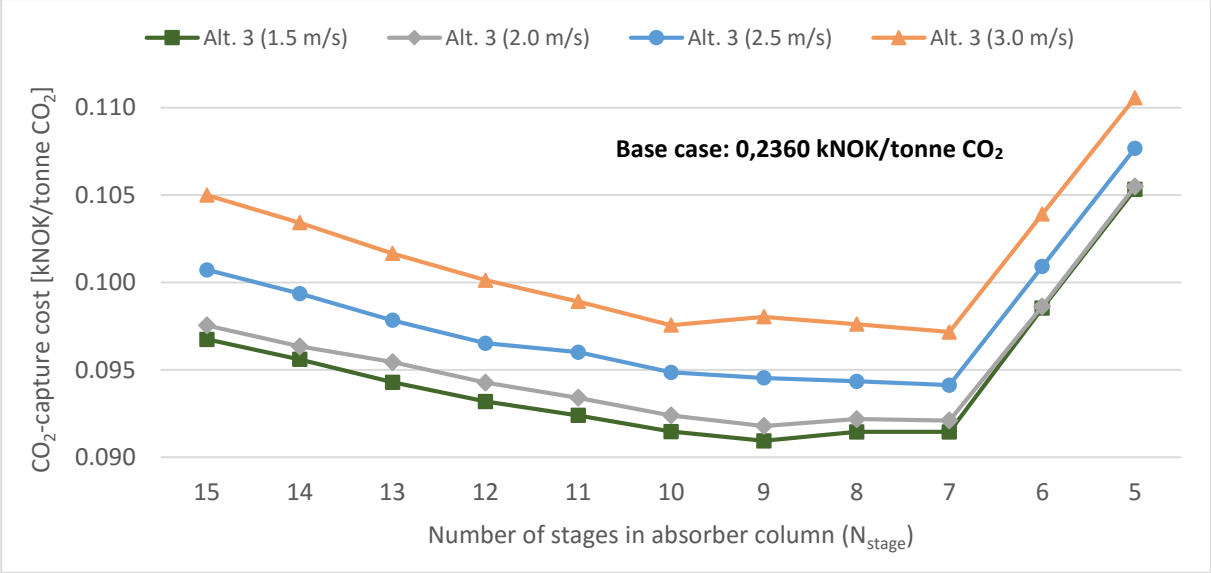

Figure 7-35 Overall CO_2-capture cost according to v_g and N_{stage} in Alternative 3

Referring to Table 7-15 and Figure 7-35, the following facts can be identified.

i) The lower the v_g is, the more optimized the capture cost becomes irrespective of N_{stage}. The optimum v_g is therefore determined to be 1,5 m/s.

ii) The optimum N_{stage} giving the minimum capture cost is seven when v_g is 2,0 m/s or less, whereas when the v_g is 2,5 m/s or 3,0 m/s the minimum capture cost is found at N_{stage} of nine. The overall trends in Figure 7-35, however, clearly indicate that the rebounding point (i.e. the point where the capture cost starts to rise rapidly) is N_{stage} of seven irrespective of v_g.

In elucidation of ii) described above, the discrepancy in the optimum N_{stage} between different v_g can be attributed to mutual interactions of CAPEX and OPEX fluctuations because the capture rate of Alternative 3 steadily decreases without any fluctuation, as seen in Figure 3-3. For reference of CAPEX and OPEX fluctuations along with N_{stage}, the overall comparison of CAPEX and OPEX is available in Appendix 11 and Appendix 12 respectively.

Although the overall capture cost data in Figure 7-35 show a clear tendency to rise sharply from N_{stage} of seven irrespective of v_g, the minimum capture cost is found at N_{stage} of nine when v_g is 1,5 m/s. Therefore, the initial capture cost obtained earlier as 0,0941 kNOK/tonne CO_2 is further optimized by switching to v_g of 1,5 m/s and N_{stage} of nine. The corresponding value is read off as 0,0909 kNOK/tonne CO_2 in Table 7-11.

Compared with the Alternative 2 as shown in Figure 7-23, it can be known that the minimum capture cost of Alternative 3 (i.e. 0,0909 kNOK/tonne CO_2) is even higher than Alternative 2 (i.e. 0,0871 kNOK/tonne CO_2).

7.5 Alternative 4

7.5.1 Impact analysis of N_{stage} on costs (v_g = 2,5 m/s)

7.5.1.1 Impact of N_{stage} on installation cost (v_g = 2,5 m/s)

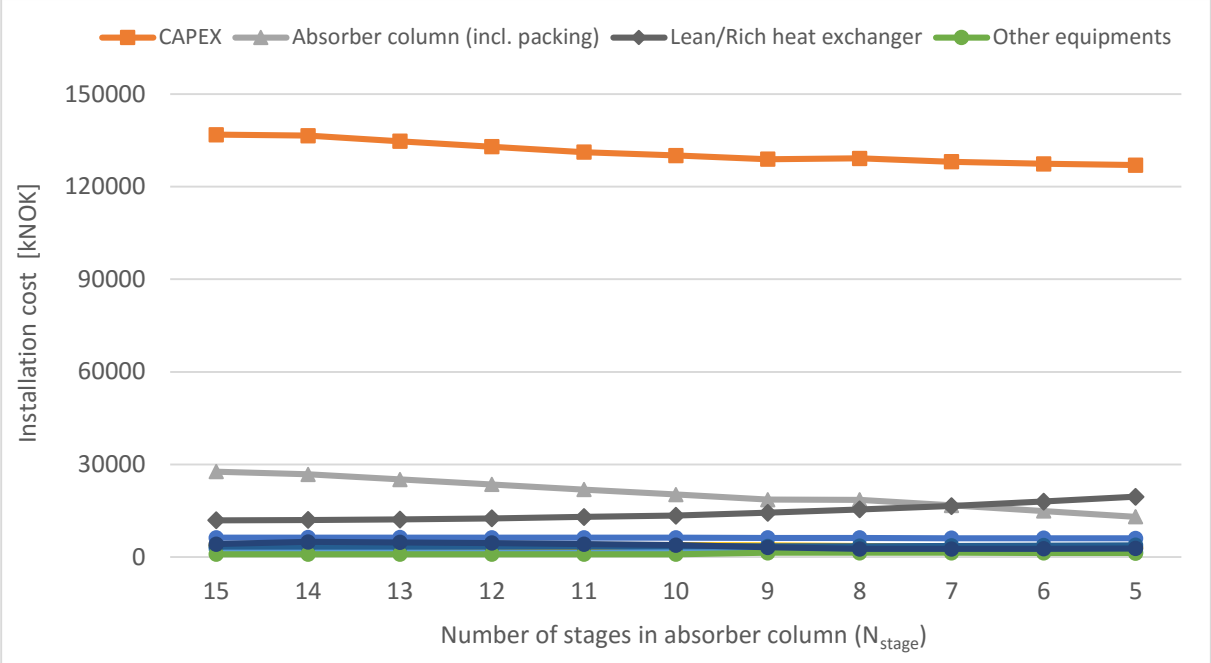

Figure 7-36 Installation cost versus N_{stage} in Alternative 4 (v_g = 2,5 m/s)

Figure 7-36 shows the installation cost changes for different equipments with decreasing N_{stage}. Although the absorber cost steadily declines with decreasing N_{stage}, a few differences from the three previous Alternatives are observed.

1. There exists a point where the absorber column cost becomes lower than L/R heat exchanger. This is because the flue gas rate in Alternative 4 is the minimum (i.e. 40 % of full flow), leading to the smallest size relative to other Alternatives.
2. Contrary to the previous Alternatives where the decrease in CAPEX is mainly attributed to absorber, some discrepancy is observed in Figure 7-36 between the changes of absorber cost and CAPEX. To put it concretely, the cost change of the absorber from N_{stage} of fifteen to five is around -15000 kNOK, whereas the CAPEX change over the corresponding range is -10000 kNOK. This is because the installation cost of Lean/Rich heat exchanger displays visible increases along with N_{stage}, weakening the dominance of the absorber cost over the CAPEX. Although the absorber cost may be saved by decreasing N_{stage}, a net reduction of CAPEX would not be of the same order of magnitude as that of absorber because the cost reductions in absorber will be partly offset by the cost increases of Lean/Rich heat exchanger.

For the other miscellaneous equipments exhibiting little visible change of the installation cost in Figure 7-36, an enlarged image is available in Appendix 27.

7.5.1.2 Impact of N_{stage} on operating cost (v_g = 2,5 m/s)

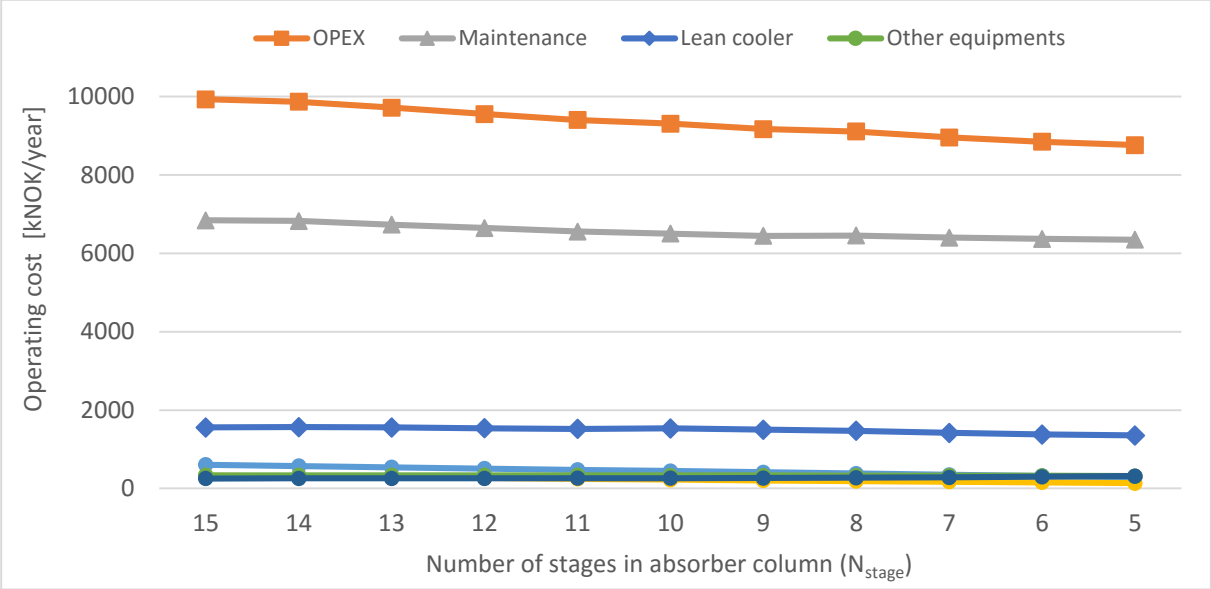

Figure 7-37 Operating cost versus N_{stage} in Alternative 4 (v_g = 2,5 m/s)

Figure 7-37 illustrates the operating cost changes for different equipment according to N_{stage}. The level of maintenance cost change is relatively marginal compared with that of the other Alternatives. This is because the CAPEX changes of Alternative 4 are relatively less significant than those of other Alternatives. As a result, the influence of maintenance cost on the OPEX becomes less dominant, while the operating cost reductions from other equipment are more reflected.

For other miscellaneous equipments displaying no visible operating cost changes in Figure 7-37, an enlarged image is available in Appendix 28.

7.5.1.3 Impact of N_{stage} on CO_2-capture cost (v_g = 2,5 m/s)

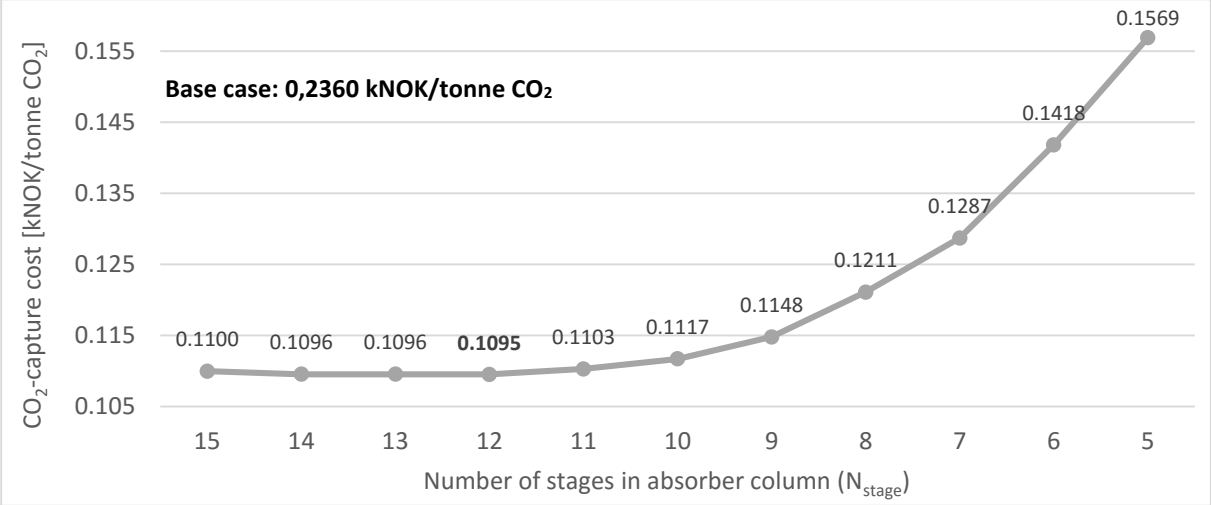

Figure 7-38 CO_2-capture cost versus N_{stage} in Alternative 4 (v_g = 2,5 m/s)

Figure 7-38 shows the changing aspects of capture cost along with N_{stage}. As seen in the previous Alternatives, the capture cost shows a tendency to decrease until N_{stage} reaches a certain point. Starting from N_{stage} of 12, however, the capture cost begins to rise dramatically until N_{stage} reaches five. The minimum capture cost is therefore found to be 0,1095 kNOK/tonne CO_2 at N_{stage} of 12, yet the degree of optimization is extremely marginal, i.e., 0,1100 – 0,1095 = 0,0005 kNOK/tonne CO_2. In other words, it can be said that Alternative 4 has little room for capture cost optimization over the entire range of N_{stage}. Furthermore, the overall capture costs in the figure are apparently much higher than those of any other Alternatives. Four main reasons for these trends can be described as follows.

1. CO_2-capture rate of Alternative 4 declines at a higher rate than any other Alternatives, particularly when N_{stage} is less than 9 more or less. (Figure 3-3)
2. Alternative 4 has the lowest flue gas rate (i.e. 40 %), and therefore its absorber diameter is also the smallest of all Alternatives. This in turn leads to the smallest size of packing beds, weakening the cost-reduction effect coming from the less number of stages in absorber column.
3. In addition, CAPEX savings by decreasing N_{stage} is partly compromised by the increasing trend of Lean/Rich heat exchanger installation cost, as shown in Figure 7-36. As a result, the degree of CAPEX reduction is not as high as expected, rendering the idea of reducing N_{stage} less attractive.
4. Smaller decreases of CAPEX along with N_{stage} also lead to less decreases of OPEX because the yearly maintenance cost, which accounts for a big part of OPEX, is directly linked with the CAPEX.

For the reasons mentioned above, it can be said that in the case of Alternative 4, making any reductions in N_{stage} is in a way meaningless with respect to the capture cost optimization.

Comparing the changing trends of CO_2-capture cost of the four Alternatives (i.e. Figure 7-8, Figure 7-17, Figure 7-26 and Figure 7-38), it can be deduced that as the flue gas rate is reduced, the rebounding point (i.e. the N_{stage} where the capture cost starts to rebound sharply) tends to appear earlier while decreasing N_{stage}. Table 7-16 summarizes the rebounding point observed in different Alternatives. Alternative 1 has no rebounding point within the defined range of N_{stage} (i.e. N_{stage} of 5 – 15), but judging from the table it can be inferred that the Alternative 1 might have a rebounding point at less N_{stage} than five.

Table 7-16 Comparison of rebounding point between Alternatives

Alternatives	Alt. 1	Alt. 2	Alt. 3	Alt. 4
Rebounding point	Not observed	$N_{stage} = 6$	$N_{stage} = 7$	$N_{stage} = 12$

7.5.2 Impact analysis of v_g variation on cost change

7.5.2.1 Impact of v_g variation on installation cost change

- **Installation cost change of absorber column (incl. packing)**

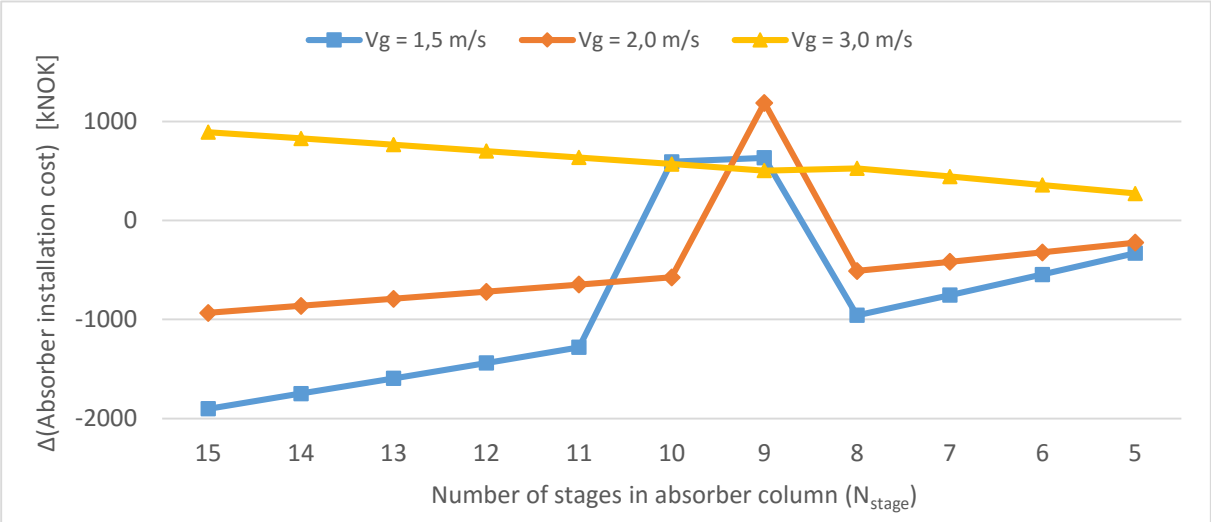

Figure 7-39 Δ(Absorber column installation cost) due to variation of v_g in Alternative 4

Figure 7-39 shows the installation cost changes of absorber column due to variation in v_g. Compared with Figure 7-9 and Figure 7-18, it can be seen that the respective position of the three graphs in Figure 7-39 is reversed. That is to say, the two lower velocities result in less expensive cost of absorber, whereas a higher velocity leads to a higher cost of absorber for all N_{stage}. The primary reason for this trend is that the installation cost of packings remains constant regardless of v_g. Figure 7-40 illustrates the installation cost changes of the packing due to variation in v_g.

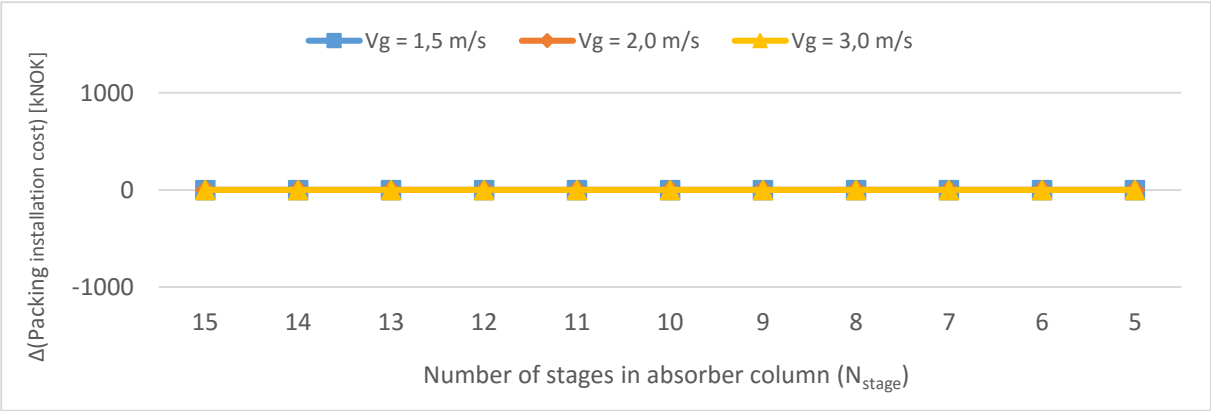

Figure 7-40 Δ(Absorber packing installation cost) due to variation of v_g in Alternative 4

As opposed to what was observed in previous Alternatives, no cost optimization regarding the packings is achieved irrespective of v_g and N_{stage}. This is because the liquid load (Q_L) in Alternative 4 exceeds 40 $m^3/(m^2 \cdot h)$ irrespective of v_g and N_{stage}, which is well demonstrated in Figure 7-41 below.

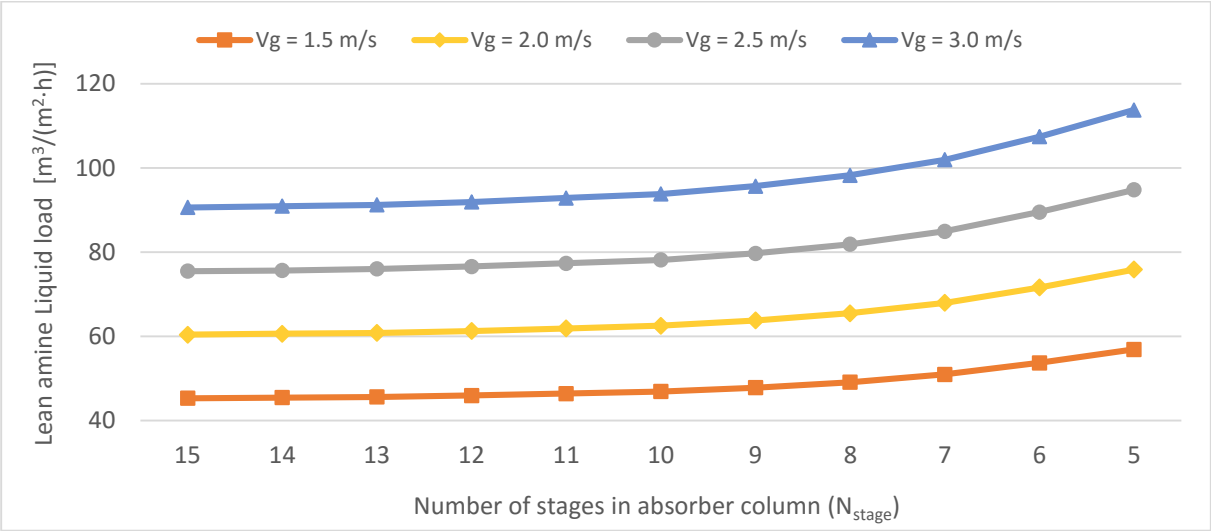

Figure 7-41 Lean amine liquid load (Q_L) according to v_g and N_{stage} in Alternative 4

Two main reasons for the trends in Figure 7-41 are:

1. Because the flue gas rate is the lowest (i.e. 40 % of full flow), Alternative 4 has the smallest absorber diameter of all Alternatives.
2. Alternative 4 has the highest Lean amine rate irrespective of N_{stage}. (Figure 3-5)

A combination of the two factors mentioned above causes the liquid load to become higher than 40 $m^3/(m^2 \cdot h)$ even at the lowest gas velocity (i.e. v_g = 1,5 m/s). Therefore, no change is made regarding both the packing volume and packing cost regardless of v_g and N_{stage}. Since the installation cost of absorber column is the sum of the two installation costs of column shell and packings, it can be said that the graphs in Figure 7-39 exactly reflect the cost changes of absorber shell only.

For the explanation of changing aspects in Figure 7-39, the same descriptions previously given in Chapter 7.2.2.1 may apply. Since there is no packing cost changes in Alternative 4, the cost-affecting factor i) only is involved in this case.

▪ **Installation cost change of Flue gas fan**

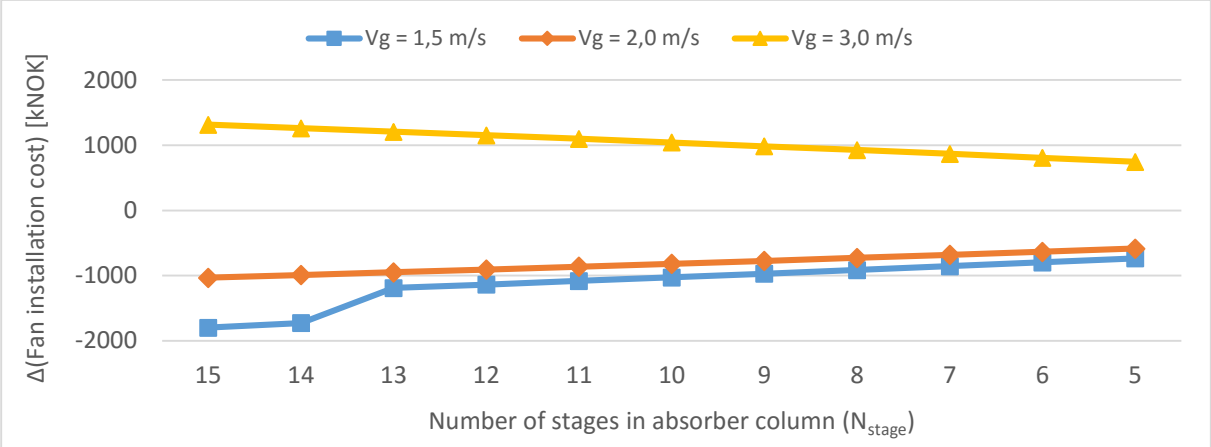

Figure 7-42 Δ(Flue gas fan installation cost) due to variation of v_g in Alternative 4

Figure 7-42 shows the installation cost changes of Flue gas fan cost due to variation in v_g. As expected, the two lower velocities than 2,5 m/s lead to reduced costs whereas a higher gas velocity makes the cost more expensive. Since the overall graphs in the figure show the same aspects as observed before, the same explanations previously given with Figure 7-10 may apply.

▪ **Installation cost change of Lean pump**

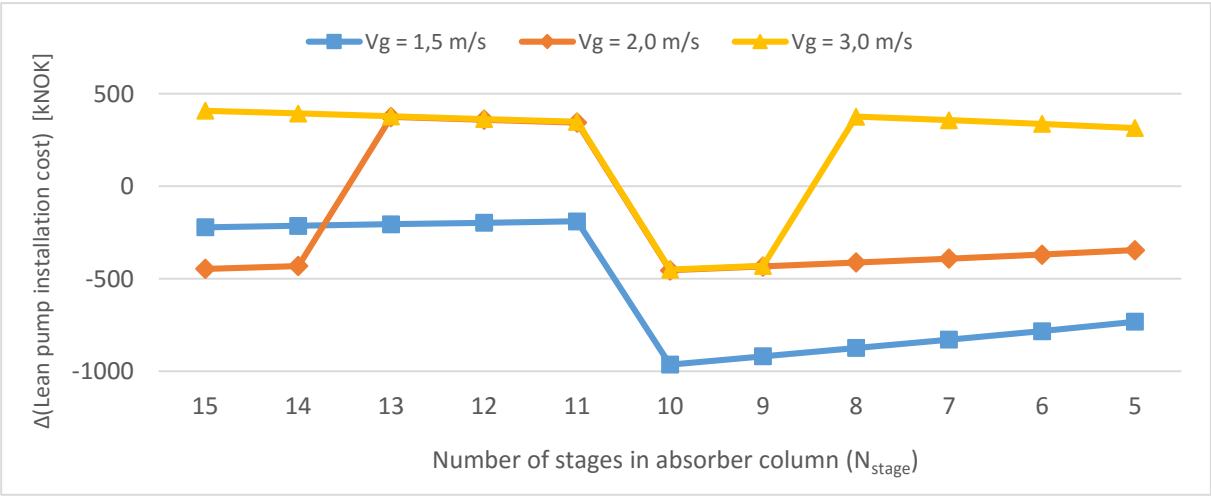

Figure 7-43 Δ(Lean pump installation cost) due to variation of v_g in Alternative 4

Figure 7-43 shows the installation cost changes of Flue gas fan cost due to variation in v_g. Except for some fluctuations, which are due to installation factor changes, the two gas velocities lower than 2,5 m/s lead to reduced cost whereas a higher gas velocity makes the cost more expensive. Overall, the graphs in the figure exhibit the same aspects as observed previously, so the same explanation given with Figure 7-11 may apply.

▪ **Net Change of CAPEX**

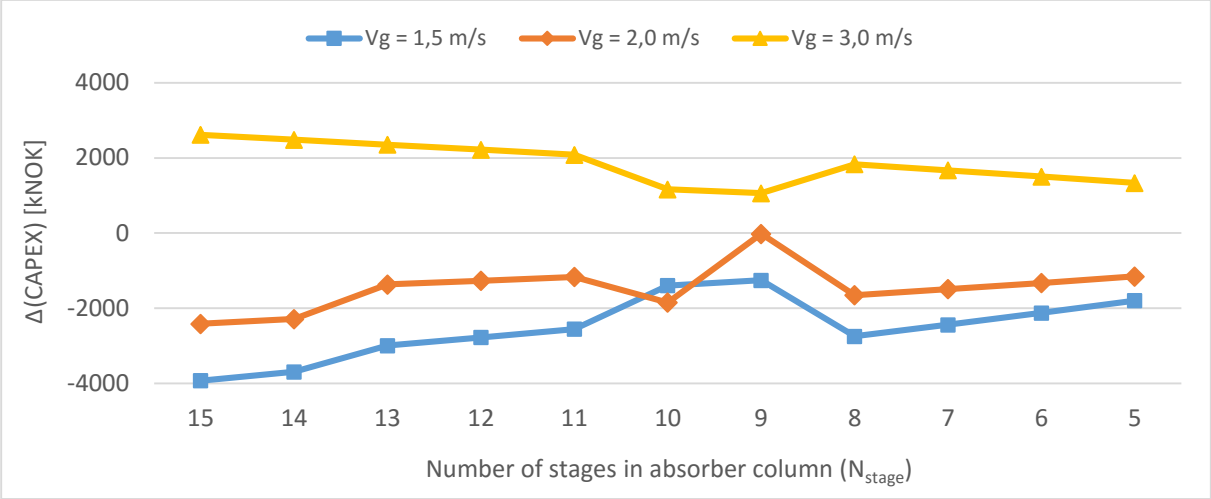

Figure 7-44 Δ(CAPEX) due to variation of v_g of Alternative 4

By adding up the data in Figure 7-39, Figure 7-43 and Figure 7-42 together, the net changes of CAPEX is obtained as shown in Figure 7-44. Except for a few fluctuations at N_{stage} of 10, the overall trend clearly indicates that a higher gas velocity always leads to more expensive cost and vice versa. Consequently, the v_g of 1,5 m/s yields the most reductions in CAPEX over the range of N_{stage}.

Detailed values corresponding to Figure 7-44 are summarized in Table 7-17.

Table 7-17 Δ(CAPEX) due to variation of v_g in Alternative 4 (unit: kNOK)

	N_{stage}										
v_g	15	14	13	12	11	10	9	8	7	6	5
3,0 m/s	616	583	551	518	485	413	382	395	361	327	293
2,0 m/s	-473	-448	-382	-358	-334	-349	-239	-302	-275	-248	-221
1,5 m/s	-793	-749	-681	-638	-594	-504	-465	-507	-460	-414	-365

7.5.2.2 Impact of N_{stage} on operating cost (v_g = 2,5 m/s)

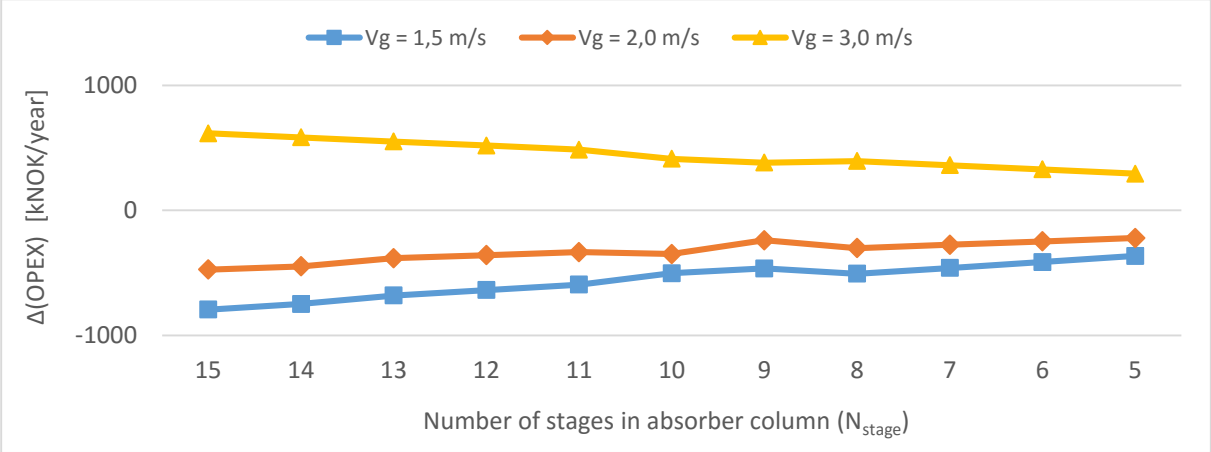

Figure 7-45 Δ(OPEX) due to variation of v_g in Alternative 4

Figure 7-45 shows the operating cost changes due to variation in v_g. As seen in Figure 7-43 and Figure 7-42, a higher v_g leads to greater operating costs and vice versa. Therefore, the same explanations given earlier may also apply for the trends in Figure 7-44. Detailed values corresponding to the figure are summarized in Table 7-18.

Table 7-18 Δ(OPEX) due to variation of v_g in Alternative 4 (unit: kNOK/year)

	N_{stage}										
v_g	15	14	13	12	11	10	9	8	7	6	5
3,0 m/s	616	583	551	518	485	413	382	395	361	327	293
2,0 m/s	-473	-448	-382	-358	-334	-349	-239	-302	-275	-248	-221
1,5 m/s	-793	-749	-681	-638	-594	-504	-465	-507	-460	-414	-365

7.5.2.3 Impact of v_g variation on CO_2-capture cost change

For calculation of capture cost changes, the same procedures as performed in Chapter 7.2.2.3 may apply. The values of Δ(CAPEX), Δ (OPEX) and (CO_2-capture rate) in Equation 7-1 correspond to the figures in Table 7-17, Table 7-18 and Table 3-4 (fourth row; Alternative 4) respectively. Putting all values of the three tables into Equation 7-1, the overall calculation results of Δ(CO_2-capture cost) can be obtained as Table 7-19. Due to the dominant influence of Δ(OPEX), the overall figures of Δ(CO_2-capture cost) show the same aspects as those of Δ(OPEX) (i.e. Table 7-18).

Table 7-19 Δ(capture cost) due to variation of v_g in Alternative 4 (unit: kNOK/tonne CO_2)

	N_{stage}										
v_g	15	14	13	12	11	10	9	8	7	6	5
3,0 m/s	0.004	0.004	0.004	0.004	0.004	0.003	0.003	0.003	0.003	0.003	0.003
2,0 m/s	-0.003	-0.003	-0.003	-0.002	-0.002	-0.003	-0.001	-0.003	-0.003	-0.003	-0.003
1,5 m/s	-0.006	-0.005	-0.005	-0.005	-0.004	-0.003	-0.003	-0.004	-0.004	-0.004	-0.004

By adding up the values in Table 7-19 to the original capture cost data (i.e. Figure 7-38), the overall capture cost according to v_g and N_{stage} are obtained as Table 7-20. The numbers are rounded to four decimal places. Figures in bold indicate the initial capture costs obtained previously with the base velocity.

Table 7-20 Overall CO_2-capture cost in Alternative 4 (unit: kNOK/tonne CO_2)

	N_{stage}										
v_g	15	14	13	12	11	10	9	8	7	6	5
3,0 m/s	0.1141	0.1135	0.1133	0.1131	0.1138	0.1144	0.1174	0.1243	0.1319	0.1450	0.1600
2,5 m/s	**0.1099**	**0.1095**	**0.1095**	**0.1095**	**0.1103**	**0.1117**	**0.1148**	**0.1211**	**0.1287**	**0.1418**	**0.1568**
2,0 m/s	0.1065	0.1063	0.1070	0.1071	0.1080	0.1089	0.1134	0.1184	0.1261	0.1392	0.1543
1,5 m/s	0.1043	0.1041	0.1047	0.1050	0.1060	0.1083	0.1116	0.1166	0.1244	0.1375	0.1527

(Base case: 0,2360 kNOK/tonne CO_2)

Figure 7-46 gives an visual illustration of Table 7-20 depending on v_g and N_{stage}.

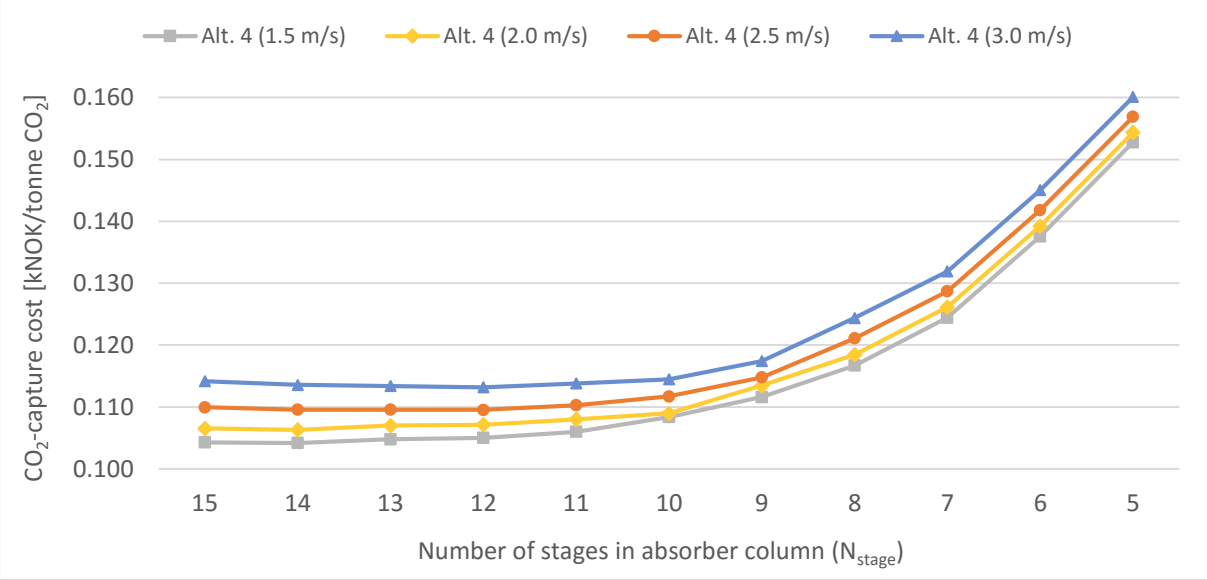

Figure 7-46 Overall CO_2-capture cost according to v_g and N_{stage} in Alternative 4

According to Figure 7-46, the following facts can be identified.

1. The lower the v_g is, the less the CO_2-capture cost becomes irrespective of N_{stage}.
2. Although the capture cost optimization is observed at several points, its degree of cost reduction is more or less insignificant, i.e., decreasing N_{stage} brings little visible improvement in capture cost regardless of v_g. The overall trends in the figure suggest that the capture cost displays no sensible changes despite decreasing N_{stage}.

As mentioned above, reducing N_{stage} does not seem to be quite beneficial to optimization in Alternative 4. Nevertheless, the initial capture cost obtained as 0,1095 kNOK/tonne CO_2 in Figure 7-38 can be effectively optimized by changing the gas velocity because it is clear that the two lower v_g than 2,5 m/s can lead to visible reductions in capture cost. The initial capture cost is therefore further reduced by switching to v_g of 1,5 m/s, while changing N_{stage} to 14. The corresponding value in Table 7-20 is 0,1041 kNOK/tonne CO_2, which is however even higher than the minimum capture cost previously obtained in Alternative 3 (i.e. 0,0909 kNOK/tonne CO_2).

After all, it can be said that the capture cost is best optimized in Alternative 1, whereas Alternative 4 is the least attractive in terms of process- and cost optimization. Table 7-21 summarizes the minimum capture cost obtained for each Alternative with the corresponding optimum parameters. It is apparent from the table that the more the flue gas rate is reduced, the higher the CO_2-capture cost becomes.

Table 7-21 Minimum CO_2-capture cost comparison between Alternatives and Base case

Item	Unit	Base case	Alt. 1	Alt. 2	Alt. 3	Alt. 4
v_g	[m/s]	1,5	1,5	1,5	1,5	1,5
N_{stage}	[-]	15	5	6	9	14
Reboiler power	[MW]	67,93	27,17	27,17	27,17	27,17
Capture cost	[kNOK/tCO_2]	0,2439	0,0858	0,0871	0,0909	0,1042

For further reference, overall comparison of CO_2-capture cost between the four Alternatives is visually represented in Appendix 6.

8 Uncertainty evaluation

This chapter evaluates several possible uncertainties which might have occurred during the process simulation, equipment dimensioning and cost estimation, etc.

8.1 Process simulation

Possible uncertainties regarding the simulation process may include the following:

1. Although the Murphree stage efficiencies are in practice affected by v_g, predetermined values (Appendix 3) were used. Since the stage efficiencies were not differentiated according to v_g in simulation environment, this might have caused some inaccuracies of MEA-CO_2 behaviors in absorber column.
2. The pressure drop across the absorber column is highly dependent on v_g and N_{stage}, yet the absorber column was configured to have a uniform pressure drop of 90 mbar throughout all simulation cases[13].
3. No pressure drop was specified to the Lean/Rich heat exchangers in HYSYS simulation.
4. Although the CO_2-absorption performance of MEA may be affected by heat or impurities like CO_2, O_2 and NO_x, the flue gas in simulation environment was set to contain H_2O, N_2 and CO_2 only. Also, no proprietary inhibitor in Lean amine stream was considered to avoid corrosion and allow for traditional construction materials (e.g. carbon steel). Therefore, neither the solvent degradation nor the MEA reclaimer unit was taken into account.
5. Absorber column unit in HYSYS simulation does not consider or reflect the inherent characteristics of a specific structured packing (e.g. Mellapak 250Y, 250X, etc.).
6. There was a couple of cases where a higher capture rate or efficiency is obtained with a lower number of stages, though the difference of which was not significant.

[13] The flue gas pressure in simulations is constant as 1,1 bar. Since the sweet gas out of the absorber column has the atmospheric pressure, it can be said that the pressure drop across the absorber column is 0,09 bar (i.e. ΔP = 1,1 bar − 1,01 bar = 0,09 bar = 90 mbar).

8.2 Equipment dimensioning

Possible uncertainties regarding the equipment dimensioning may include the following:

1. Though there will be liquid Lean amines flowing down through the packing, the dependence of pressure drops on liquid load (i.e. wet pressure drop) were not much considered owing to lack of experimental literature. For Mellapak 2X and Mellapak 250X, dry pressure drops data only were used. In the case of Mellapak 250Y, a constant liquid holdup of 0,09 was assumed despite the fact that the liquid load varies depending on N_{stage} and the column diameter. All of these assumptions would have definitely led to under-estimation of the practical pressure drops.
2. The effective interfacial areas of Mellapak 250Y and 250X were approximated by a normalized equation (Equation 4-4) instead of experimental data. Since the interfacial area affects the total packing volume as well as the absorber column height, the use of correlation might have led to errors more or less in absorber column dimensioning.
3. Although Equation 4-4 is only applicable to the structured packings having the geometric area of 250 m^2/m^3, the same equation was used for approximating the interfacial area of Mellapak 2X.
4. For all types of heat exchangers, the overall heat transfer coefficient (U) was respectively assumed. The value of U is in directly linked to the heat transfer area and, by extension, the installation cost. Therefore, any inaccuracy in assumptions of U might have led to some degree of error in heat transfer areas.
5. For Reboiler, Condenser and Waste heat boiler, the average temperature difference between the two fluids was calculated by LMTD method. LMTD formula, however, is generally not applicable to equipment involving the latent heat with phase change[55].
6. No fouling was assumed for all kinds of heat exchangers (i.e. Lean/Rich heat exchanger, Lean cooler, Condenser, Reboiler and Waste heat boiler).
7. Pressure drop across the Lean/Rich heat exchanger will vary depending on the operating conditions (e.g. Lean amine rate, fluid pressures, Reynold number etc.). However, the pressure drop across the Lean/Rich heat exchanger was assumed to be constant as 1 bar in equipment dimensioning.
8. Although the Murphree efficiency (η_m) in simulation environment is varied along the absorber column stage, a constant height per packing bed (i.e. 1 m/packing which is equivalent to η_m of 0,15), was assumed with the gas velocity of 2,5 m/s.

8.3 Cost estimation

Possible uncertainties regarding the cost estimation process may include the following:

1. In most of the installation cost calculations, several fluctuations were observed due to a sudden shift in installation factors. This might have made the overall trend of installation costs look less uniform.
2. The heat transfer area per heat exchanger unit was assumed to be 1000 m^2 for shell-and-tube type and 2000 m^2 for plate-and-frame type. This limitation might have given a different number of units for some pieces of equipment having similar duties. Different number of units, in turn, will lead to different total installation cost.
3. The power law was used out of range for some equipment (e.g. desorber column, Water pump and Flue gas fan). This might have brought out cost estimating error, particularly when the equipment capacity lies far from the reference size range.
4. Other miscellaneous costs such as labor cost, raw material (e.g. makeup amine) cost, land investment or office administration were not taken into consideration in detail.
5. Some limitations exist concerning cost indices. In particular, using the cost index for periods of more than 10 years is subject to reduced accuracy, at best ±10 %[76].
6. Instead of specifying the plant location, a location factor of 1 (i.e. Rotterdam) was assumed.

8.4 Feasibility of the optimum process parameter

Regarding the optimum process parameters determined in this study, some uncertainties may exist in terms of the applicability of these parameters. Two uncertainties to be considered are:

1. One major conclusion in this study is that the optimum process of partial-scale CO_2-capture is achieved when all the flue gases from cement kilns are routed into the absorber, with the number of absorber stages being five. However, the practicality of reducing the number of absorber stages as low as five was not sufficiently identified in a real-scale capture plant[14]. That is, the optimum process parameters (i.e. full flow of flue gas and five stages in absorber) were determined by theoretically considering

[14] In traditional post-combustion capture plants, the actual number of stages in absorber column typically ranges from 10 to 20 with commercial operating conditions[38, 45].

the aspect of capture cost only. In effect, there might be some limitations in decreasing the number of stages as low as five due to practical reasons (e.g. physical & chemical characteristic of packings, the gap between simulation environment and real operating conditions, etc.). The feasibility of applying the optimal process parameters mentioned above needs to be fully studied in a realistic way.

2. Although a lower gas velocity tends to reduce the capture cost, the three kinds of structured packings did not have the same optimum gas velocity (i.e. the gas velocity giving the minimum capture cost). While the Mellapak 250Y and 250X had the optimum v_g of 1,5 m/s, the Mellapak 2X had the optimum v_g of 2,0 m/s. This is partly because the pressure drop data used for Mellapak 2X were relatively too low compared to the other two packings. Since the pressure drops of Mellapak 2X are not significant, the lowest gas velocity (i.e. v_g = 1,5 m/s) does not necessarily lead to the minimum capture cost. That is, with the v_g of 1,5 m/s, the minor reductions of operating cost are more or less offset by other cost-increasing factors (e.g. increased absorber column diameter, increased volume of packing beds, etc.).

8.5 Project scope

Several essential process equipment (e.g. Direct contact cooler, Amine reclaimer, CO_2 compressor etc.) in a real-scale capture plant was not included in the project scope, and therefore some degree of under-estimation may have occurred in determining the capture cost. In particular, the facilities described below may be the major contributing factors to under-estimating the overall capture costs:

1. Scrubbing of the combustion exhaust gas from cement kilns were not addressed. The flue gases in practice need to be treated with a chain of chemical processes to remove the pollutants (e.g. NO_x, SO_x, particulate matters, etc.), which would otherwise react with amines and cause the solvent degradation[15]. To this end, gas purification technologies such as the selective catalytic reduction (SCR) for De-NO_x, flue gas desulphurization (FGD) scrubbers or the electrostatic precipitator (ESP) must be installed before the absorber column. Since the capital and operating costs of these

[15] The maximum content of NO_x and SO_x in the flue gases is limited to 20 and 10 ppmv, respectively[83].

pre-treatment equipments are expensive[16], the overall CO_2-capture costs determined in this study may have been under-estimated, especially for the cases where the flue gas inflow ratio is high (e.g. Alternative 1).

2. Flue gas transportation from cement kilns to the capture plant were not taken into consideration. Depending on the plant location and facility layout, transporting a large quantity of exhaust gases over the distances through pipelines can incur significant costs. This is because the pipeline transport involves expenditure including equipment construction, installation (e.g. compressor station), operation, maintenance as well as the specified material (e.g. stainless steel) costs to avoid corrosion. A higher flue gas rate, therefore, will result in greater transportation cost than the lower gas flow rates.

Consequenty, if the two factors mentioned above are considered, the process solution where all of the flue gas is routed into the absorber column (i.e. Alternative 1) might be less attractive than the other Alternatives where only part of the flue gas is let into the absorber column.

[16] For spray dry scrubbers in a coal-fired power station of smaller than 200 MW, typical SO_x-scrubbing costs range from 500 to 4.000 US$/tonne SO_2 (Cheremisinoff, 2016).

9 Conclusion

Through this study, the following conclusions could be reached.

▪ Operating CO_2-capture plants with steam is the most expensive alternative due to a high steam cost, with the capture cost reaching 236 NOK/tonne CO_2. However, the capture cost decreased to 101 NOK/tonne CO_2 by simply replacing the steam with waste heat.

▪ Reducing the number of absorber column stages turned out to be an effective way to reduce both the CAPEX and OPEX, mainly because of the expensive cost of absorber column.

▪ Despite the high CAPEX, letting all of the flue gas into the absorber column was found to be the most cost-efficient alternative because the capture rate was not only the highest but also it had little tendency to decline with the fewer number of absorber stages.

▪ Despite the lower CAPEX, letting part of the flue gas into the absorber column was less beneficial because the capture rate was not only lower but also declined noticeably with the fewer number of absorber stages.

▪ Assuming that 1 m/packing is equivalent to a Murphree efficiency of 0,15, the number of absorber stages giving the minimum capture cost was five when all the flue gases were routed into the absorber. When only part of the flue gas was led into the absorber, on the other hand, there were limitations in reducing the absorber stages to five due to a sharp decrease in CO_2-capture rate.

▪ For Mellapak 250Y and 250X, the optimal gas velocity was found to be as low as 1,5 m/s mainly due to reduced pressure drops. In the case of Mellapak 2X, the minimum capture cost was obtained with the gas velocity of 2,0 m/s.

▪ Mellapak 2X showed the minimum capture cost of the three structured packings, with its value being 85 NOK/CO_2. For Mellapak 250Y and 250X, they both showed the minimum capture cost of 86 NOK/CO_2. The capture cost differences between these packings are, however, not sufficiently significant to determine the most cost-effective packing.

▪ For Mellapak 250Y, increasing the packing cost by 1,5 times (i.e. 11200 \$/m^3) resulted in the minimum capture cost of 91 NOK/tonne CO_2. Increasing the cost twice (i.e. 15200 \$/m^3) yielded the minimum capture cost of 97 kNOK/tonne CO_2.

▪ The optimum process parameters (i.e. number of absorber stages, gas velocity and flue gas inflow ratio) giving the minimum capture cost were not much affected by the packing cost.

9.1 Suggestions for future work

To develop and elaborate the research work carried out in this study, this section presents several recommended research topics for future work. On the theoretical and practical side, the following pending problems may be considered:

1. Based on experimental data, developing rigid mathematical models of effective interfacial area for structured packings is necessary. Although there exist several models correlating the interfacial area versus liquid load, their applications are limited to only a few kinds of structured packings.
2. There is currently lack of experimental data on wet pressure drops of structured packings. To ensure reliability and accuracy of determining the optimum gas velocity, more experimental work on wet pressure drops of different packings with various operating conditions is needed.
3. Because each structured packing has different internal structures, in-depth studies ond solvent-gas behaviors (e.g. maldistribution, CO_2 mass transfer) through different structured packings with CFD simulations are recommended.
4. The likelihood of flooding for different structured packings was not encompassed in this study, so further studies on liquid loading, liquid holdup and the flooding are essential. As seen in Figure 7-28 and Figure 7-41, the liquid load substantially increases with the decreasing flue gas rate and N_{stage}. Therefore, it is likely that the flooding will occur in some of the process alternative cases of this study.
5. Some process equipment (e.g. Direct contact cooler, Amine reclaimer, CO_2 compressor etc.) were not considered in this study. Therefore, expanding the process simulation scope might be needed to obtain more realistic and practical capture costs.
6. This study set the Murphree efficiencies of the order of magnitude of 0,15 in all simulations without considering other operating conditions that might be influential. Therefore, to obtain more rigid simulation with enhanced reliability, estimating the Murphree efficiency with different operating conditions (e.g. liquid load, gas velocity, temperature, packing internal structure etc.) will be beneficial.

References

[1] Petty, GW (2004). A First Course in Atmospheric Radiation. Sundog Publishing. pp. 229–251. CO_2 absorbs and emits infrared radiation at wavelengths of 4.26 μm(asymmetric stretching vibrational mode) and 14.99 μm (bending vibrational mode).

[2] Etheridge, D., Steele, L., Langenfelds, R., Francey, R., Barnola, J. and Morgan, V. (1996). Natural and anthropogenic changes in atmospheric CO_2 over the last 1000 years from air in Antarctic ice and firn. Journal of Geophysical Research: Atmospheres, 101(D2), pp.4115-4128.

[3] Feely, R. (2004). Impact of Anthropogenic CO_2 on the $CaCO_3$ System in the Oceans. Science, 305(5682), pp.362-366.

[4] Team, E. (2016). ESRL Global Monitoring Division - Global Greenhouse Gas Reference Network. [online] Esrl.noaa.gov. Available at: http://www.esrl.noaa.gov/gmd/ccgg/trends/ [Accessed 12 Apr. 2016].

[5] Millero, F. (1995). Thermodynamics of the carbon dioxide system in the oceans. Geochimica et Cosmochimica Acta, 59(4), pp.661-677.

[6] Dlugokencky, E (5 February 2016). "Annual Mean Carbon Dioxide Data". Earth System Research Laboratory. National Oceanic & Atmospheric Administration. Retrieved12 February 2016.

[7] Makuch, K. and Pereira, R. (2012). Environmental and energy law. Chichester, West Sussex, U.K.: Wiley Blackwell.

[8] Bjerge, L. and Brevik, P. (2014). CO_2 Capture in the Cement Industry, Norcem CO_2 Capture Project (Norway). Energy Procedia, 63.

[9] Eia.gov. (2013). The cement industry is the most energy intensive of all manufacturing industries - Today in Energy - U.S. Energy Information Administration (EIA). [online] Available at: http://www.eia.gov/todayinenergy/detail.cfm?id=11911 [Accessed 12 Apr. 2016].

[10] Gale, J. and Kaya, Y. (2003). Greenhouse gas control technologies. Amsterdam: Pergamon.

[11] Davidovits, J. (2005). Geopolymer, green chemistry and sustainable development solutions. Saint-Quentin, France: Geopolymer Institute.

[12] L. A. Tokheim, "Kiln system modification for increased utilization of

alternative fuels at Norcem Brevik," Cement International, No. 4, 2006.

[13] N. Mahasenan, R. T. Dahowski, and C. L. Davidson, "The role of carbon dioxide capture and storage in reducing emissions from cement plants in North America," Pacific Northwest national laboratory, 902 battelle blvd, Richland, USA, 2005.

[14] Jilvero, H., Mathisen, A., Eldrup, N., Normann, F., Johnsson, F., Müller, G. and Melaaen, M. (2014). Techno-economic Analysis of Carbon Capture at an Aluminum Production Plant – Comparison of Post-combustion Capture Using MEA and Ammonia. Energy Procedia, 63, pp.6590-6601.

[15] B. Adina, M. Ondrej, and E. O. John, "CO_2 capture technologies for cement industry," Energy procedia, pp. 133-140, 2009.

[16] W. Shuangzhen and H. Xiaochun, "Sustainable Cement Production with improved energy efficiency and emerging CO_2 mitigation,"

[17] Hanle, L. J., Jayaraman, K. R., & Smith, J. S. (2004). CO_2 emissions profile of the US cement industry. Washington DC: Environmental Protection Agency.

[18] Torres-Carrasco, M., Rodríguez-Puertas, C., Alonso, M. and Puertas, F. (2015). Alkali activated slag cements using waste glass as alternative activators. Rheological behaviour. Boletín de la Sociedad Española de Cerámica y Vidrio, 54(2), pp.45-57.

[19] H. G. V. Oss, "US and world CEMENT production 2008 and 2009," USGS online survey, 2010.

[20] N. Mahasenan, S. Smith, and K. K. Humphreyys, "The cement industry and global climate change: current and potential future cement industry CO_2 emissions," in Proc. of the 6th International Conference on Greenhouse Gas Control Technologies, Kyoto, Japan, October 2002.

[21] Cement Technology Roadmap 2009, World Business Council for Sustainable Development (WBCSD) and International Energy Agency (IEA), December 2009.

[22] Metz, B., Davidson, O., Coninck, H. D., Loos, M., & Meyer, L. IPCC special report on carbon dioxide capture and storage. 2005. Working Group III. Intergovernmental Panel on Climate Change, Geneva (Switzerland).

[23] Globalccsinstitute.com. (2013). Capturing CO_2 from the Norwegian cement industry | Global Carbon Capture and Storage Institute. [online] Available at:

https://www.globalccsinstitute.com/insights/authors/dennisvanpuyvelde/2013/09/20/capturing-co2-norwegian-cement-industry [Accessed 12 Apr. 2016].

[24] Haugom, J. (2012). Norcem and HeidelbergCement Northern Europe.

[25] Udara, S. P. R., Kawan, D., Tokheim, L. A., & Melaaen, M. C. (2013). Model Development for CO_2 capture in the cement industry. International Journal of Modeling and Optimization, 3(6), 535.

[26] Energy.gov. (n.d.). Pre-Combustion Carbon Capture Research | Department of Energy. [online] Available at: http://energy.gov/fe/science-innovation/carbon-capture-and-storage-research/carbon-capture-rd/pre-combustion-carbon [Accessed 12 Apr. 2016].

[27] Globalccsinstitute.com. (n.d.). How CCS works - capture | Global Carbon Capture and Storage Institute. [online] Available at: https://www.globalccsinstitute.com/content/how-ccs-works-capture [Accessed 12 Apr. 2016].

[28] D'Alessandro, D., Smit, B. and Long, J. (2010). Carbon Dioxide Capture: Prospects for New Materials. Angewandte Chemie International Edition, 49(35), pp.6058-6082.

[29] Crf.sandia.gov. (2012). Coal Use and Carbon Capture Technologies | Combustion Research Facility. [online] Available at: http://crf.sandia.gov/coal-use-and-carbon-capture-technologies/ [Accessed 12 Apr. 2016].

[30] Chen, L., Yong, S. and Ghoniem, A. (2012). Oxy-fuel combustion of pulverized coal: Characterization, fundamentals, stabilization and CFD modeling. Progress in Energy and Combustion Science, 38(2), pp.156-214.

[31] Davidson, R. M., & Santos, S. O. (2010). Oxyfuel combustion of pulverised coal. London, UK: IEA Clean Coal Centre.

[32] Herzog, H., & Golomb, D. (2004). Carbon capture and storage from fossil fuel use. Encyclopedia of energy, 1, 1-11.

[33] Perrin, N., Dubettier, R., Lockwood, F., Court, P., Tranier, J. P., Bourhy-Weber, C., & Devaux, M. (2013). Oxycombustion for carbon capture on coal power plants and industrial processes: advantages, innovative solutions and key projects. Energy Procedia, 37, 1389-1404.

[34] Lenzen, M. (2010). Current State of Development of Electricity-Generating Technologies: A Literature Review. Energies, 3(3), pp.462-591.

[35] Yu, C. H., Huang, C. H., & Tan, C. S. (2012). A review of CO_2 capture by absorption and adsorption. Aerosol Air Qual. Res, 12(5), 745-769.

[36] Hassan, S. M. (2005). Techno-economic study of CO 2 capture process for cement plants.

[37] Øi, L. E. (2007, October). Aspen HYSYS simulation of CO_2 removal by amine absorption from a gas based power plant. In SIMS2007 Conference, Gøteborg, October (pp. 73-81).

[38] Øi, L. E. (2012). Removal of CO_2 from exhaust gas.

[39] O. Lassagne, L. Gosselin, M. Desilets, M. C. Iliuta, Chem. Eng. J. 2013, 230, 338.

[40] L. Raynal, P.-A. Bouillon, A. Gomez, P. Broutin, Chem. Eng. J. 2011, 171, 742.

[41] IEA Greenhouse Gas R&D Programme (IEA GHG), "CO_2 Capture in the Cement Industry", 2008/3, July 2008.

[42] Johnson, A. (1999). Invitation to organic chemistry. Sudbury, Mass.: Jones and Bartlett Publishers.

[43] Xie, H. B., Zhou, Y., Zhang, Y., & Johnson, J. K. (2010). Reaction mechanism of monoethanolamine with CO_2 in aqueous solution from molecular modeling. The Journal of Physical Chemistry A, 114(43), 11844-11852.

[44] Tcmda.com. (2010). Amine technology. [online] Available at: http://www.tcmda.com/en/Technology/Amine-technology/ [Accessed 15 Apr. 2016].

[45] Kallevik, O. B. (2010). Cost estimation of CO_2 removal in HYSYS.

[46] Svolsbru, C. B. (2013). CO_2 capture alternatives in cement plant.

[47] Chang, A., Pashikanti, K. and Liu, Y. (2012). Refinery engineering. Weinheim: Wiley-VCH.

[48] Smith, R. (2005). Chemical process design and integration. Chichester, West Sussex, England: Wiley.

[49] Górak, A. and Olujic, Z. (2014). Distillation: Equipment and Processes. San Diego, United States: Elsevier Science Publishing Co Inc.

[50] Rousseau, R. (1987). Handbook of separation process technology. New York: J. Wiley.

[51] Gorak, A. and Sorensen, E. (2014). Distillation: Fundamentals and Principles. Burlington: Elsevier Science.

[52] Røkke P.E., Barrio M., Kvamsdal H.M., Mejdell T., Haugen G., Nordbø Ø.

Kostnadsestimering av CO_2 håndtering, Report TRF6683. SINTEF, Trondheim. 2007.

[53] Lassauce, A., Alix, P., Raynal, L., Royon-Lebeaud, A., & Haroun, Y. (2014). Pressure Drop, Capacity and Mass Transfer Area Requirements for Post-Combustion Carbon Capture by Solvents. Oil & Gas Science and Technology–Revue d'IFP Energies nouvelles, 69(6), 1021-1034.

[54] Koch-glitsch.com. (2016). liquid_distributors. [online] Available at: http://www.koch-glitsch.com/masstransfer/pages/liquid_distributors.aspx [Accessed 27 Apr. 2016].

[55] Shah, R. and Sekulić, D. (2003). Fundamentals of heat exchanger design. Hoboken, NJ: John Wiley & Sons.

[56] Incropera, F., Incropera, F. and Incropera, F. (2013). Principles of heat and mass transfer. [Hoboken, N.J.]: Wiley.

[57] Knudsen, J. N., Jensen, J. N., Vilhelmsen, P. J., & Biede, O. (2007, September). First year operation experience with a 1 t/h CO_2 absorption pilot plant at Esbjerg coal-fired power plant. In Proceedings of European congress of chemical engineering (ECCE-6), Copenhagen (Vol. 16, p. 20).

[58] Aspentech.com. (2016). Oil and Gas Process Simulation Software – Process Optimization| Aspen HYSYS. [online] Available at: http://www.aspentech.com/products/aspen-hysys/ [Accessed 13 Apr. 2016].

[59] Arthur Kohl, R.N., Gas purification. 5 ed. 1997: Gulf publications.

[60] Distillation Design and Control Using Aspen Simulation. (2013). [s.l.]: John Wiley & Sons Inc.

[61] Smith, J. and Van Ness, H. (2001). Introduction to chemical engineering thermodynamics. 6th ed. New York: McGraw-Hill, p.260.

[62] Paneru, C. P. (2014). Optimum gas velocity and pressure drop in CO_2 absorption column.

[63] Tsai, R. E., Seibert, A. F., Eldridge, R. B., & Rochelle, G. T. (2011). A dimensionless model for predicting the mass-transfer area of structured packing. AIChE Journal, 57(5), 1173-1184.

[64] Zakeri, A., Einbu, A., Øi, L. and Svendsen, H. (2009). Liquid Hold-up and Pressure Drop in Mellapak 2X.

[65] Henrik Eldrup, N. (2016). Cost estimation.

[66] Lars, Ø. (2016). Equipment dimensioning.

[67] Amaratunga, P. D. M. (2015). Optimization of gas velocity, pressure drop and column diameter in CO_2 capture.

[68] B2bmetal.eu. (n.d.). IPE beams. European standard universal I beams (I section) with parallel flanges. Dimensions, specifications, accordance with former standard EU 19-57. [online] Available at: http://www.b2bmetal.eu/i-sections-ipe-specification [Accessed 15 Apr. 2016].

[69] Wermac.org. (n.d.). Dimensions of Steel Beams type HEM European standard NEN-EN 10025-1 and NEN-EN 10025-2. [online] Available at: http://www.wermac.org/steel/dim_hem.html [Accessed 15 Apr. 2016].

[70] Blaker E.A. Kostnadsestimering av CO_2-fjerning i Aspen HYSYS. Master thesis.

Telemark University College, Porsgrunn. 2008.

[71] A. A. Marcano, L. (2015). Design and evaluation of heat exchangers used in post-combustion CO_2 capture plants. MSc. Telemark University College.

[72] Ganapathy, V. (2002). Industrial boilers and heat recovery steam generators: design, applications, and calculations. CRC Press.

[73] Gerrard, A. (2000). Guide to capital cost estimating. Rugby, Warwickshire, U.K.: Institution of Chemical Engineers.

[74] Peters, M. and Timmerhaus, K. (1991). Plant design and economics for chemical engineers. 4th ed. New York: McGraw-Hill, pp.48~52.

[75] Eldrup N.H. Installation cost factors. Lecture material in course: FM3106 Project management and cost engineering. Telemark University College, Porsgrunn. 2015.

[76] Humphreys, K. and English, L. (2004). Project and cost engineers' handbook. 4th ed. Morgantown, W. Va.: AACE International.

[77] Newbold, P., Carlson, W. and Thorne, B. (2007). Statistics for business and economics. Upper Saddle River, N.J.: Pearson Prentice Hall.

[78] Sinnott, R. and Towler, G. (2009). Chemical Engineering Design. Burlington: Elsevier Science.

[79] Petley, G. J. (1997). A method for estimating the capital cost of chemical process plants: fuzzy matching (Doctoral dissertation, © Gary John Petley).

[80] Dimian, A., Bildea, C. and Kiss, A. (2014). Integrated design and simulation of chemical processes. 2nd ed. ELSEVIER.

[81] Lexicon.ft.com. (2014). Cash Flow Definition from Financial Times Lexicon. [online] Available at: http://lexicon.ft.com/Term?term=cash-flow [Accessed 14 Apr. 2016].

[82] Khatib, H. and Khatib, H. (2003). Economic evaluation of projects in the electricity supply industry. London: Institution of Electrical Engineers.

[83] Bosoaga, A., Masek, O., & Oakey, J. E. (2009). CO_2 capture technologies for cement industry. Energy Procedia, 1(1), 133-140.

[84] Chemengonline.com. (2016). Plant Cost Index - Chemical Engineering. [online] Available at: http://www.chemengonline.com/pci-home [Accessed 13 Apr. 2016].

[85] Usforex.com. (2016). Yearly Average Exchange Rates - US Forex Foreign Exchange. [online] Available at: http://www.usforex.com/forex-tools/historical-rate-tools/yearly-average-rates [Accessed 8 May 2016].

Appendices

University College of Southeast Norway

MASTER'S THESIS, COURSE CODE FMH606

Student:	**Kwangsu Park**		
Thesis title:	**Optimization of partial CO_2 capture**		
Signature:			
Number of pages:	**190**		
Keywords:	**CO_2 capture, Aspen HYSYS, process optimization, waste heat integration, cement plant, CO_2-capture cost, energy optimization**.		
Supervisor:	Lars Erik Øi	Sign.:	. . . . .
2nd supervisor:	Nils Henrik Eldrup	Sign.:	. . . . .
Censor:	<name>	Sign.:	. . . . .
External partner:	<name>	Sign.:	. . . . .
Availability:	<Open/Secret>		

Archive approval (supervisor signature)**:** Sign.: . . . . . .

Date : . . . . . .

Abstract:

The cement industry accounts for about 5 % of the global anthropogenic CO_2 emissions. Traditional post-combustion CO_2 capture with monoethanolamine absorption is highly energy-intensive, which in turn leads to expensive capture cost.

To optimize the capture cost in a cement plant, this study focused on optimizing the post-combustion CO_2 capture process with Aspen HYSYS using waste heat only. Impact analysis was carried out based on the three process parameters: flue gas inflow ratio into the absorber, number of stages in the absorber column and the superficial gas velocity.

Despite the high investment, routing all of the flue gas into the absorber was calculated to be the most effective alternative in terms of capture cost because it gave the highest CO_2-capture rate. The capture rate showed little decrease even with fewer absorber stages. With the assumption that 1 m/packing is equivalent to a Murphree efficiency of 0,15, the number of absorber stages giving the minimum capture cost was five.

On the other hand, routing only part of the flue gas into the absorber column consistently resulted in lower capture rate. There were also limitations in reducing the absorber column stages to five, largely due to a sharp decrease in CO_2-capture rate with fewer column stages.

The effect of the gas velocity on capture cost was also studied. For Mellapak 250Y and 250X, the optimal gas velocity was found to be as low as 1,5 m/s mainly due to reduced pressure drops. In the case of Mellapak 2X, the minimum capture cost was obtained with the gas velocity of 2,0 m/s.

Of the three structured packings, Mellapak 2X yielded the minimum capture cost, with the value being 85 NOK/tonne CO_2. For Mellapak 250Y and 250X, they both showed the minimum capture cost of 86 NOK/tonne CO_2. The capture cost differences between these packings are not significant to determine the most cost-effective packing.

Appendix 1: Project description

Telemark University College
Faculty of Technology

FMH606 Master's Thesis

Title: Optimization of partial CO_2 capture

TUC supervisor: Associate Professor Lars Erik Øi

Assistant supervisor: Nils Henrik Eldrup

Tasks:

The general aim is to develop further models in Aspen HYSYS for calculation, equipment dimensioning, cost estimation and cost optimization of CO_2 capture by atmospheric exhaust gas absorption into an amine solution. A special aim is to evaluate partial CO_2 capture.

1. Process description of CO_2 capture from an industrial source by absorption into an amine solution. One alternative is full capture and a second alternative is partly capture.
2. Aspen HYSYS simulations of CO_2 capture alternatives with absorption into an amine solution. Calculation of dependencies of different process alternatives. Energy optimization of different process alternatives.
3. Process equipment dimensioning and equipment cost estimation.
4. Evaluation of the most energy optimum and the most cost optimum process alternative, preferably using Aspen HYSYS.

Background:

The most promising method for capture of CO_2 from atmospheric exhaust is by the help of amine solutions. Cost estimates for CO_2 removal from gas based power plants have been made for Kårstø, Tjeldbergodden, Mongstad and Herøya. Master Projects from 2007 to 2015 at Telemark University College have included cost estimation in a spreadsheet connected to an Aspen HYSYS simulation. In a Master Thesis (Svolsbru, 2013), Aspen HYSYS simulations of CO_2 capture from a cement plant were performed. In a Master project, partial CO_2 capture from a cement plant was evaluated. These projects have used different tools for equipment cost estimation. Telemark University College has collaborated with different companies (Tel-Tek, Statoil, Aker Kværner, Norcem, Skagerak and Gassnova) which work with plans for CO_2 capture. Telemark University College is involved in a large project (Co2stCap) to evaluate partial CO_2 capture from industrial sources.

Student category: PT or EET

Adress: Kjølnes ring 56, NO-3918 Porsgrunn, Norway. **Phone:** 35 57 50 00. **Fax:** 35 55 75 47.

Practical arrangements:

The work will mainly be carried out at Telemark University College.

Signatures:

Supervisor (date and signature): 30/5-16

Student (date and signature): 30/5 2016 Kwangsu Park

Appendix 2: List of formulas

1. Absorber column diameter

$$D = \sqrt{\frac{4\dot{V}}{\pi \cdot v_g}}$$

where

D = absorber column diameter [m]
$\dot{V}$ = gas volume flow into absorber column [m^3/s]
v_g = superficial gas velocity [m/s]

2. Desorber column diameter

$$D = \sqrt{\frac{4\dot{V}}{\pi \cdot v_g}}$$

where

D = desorber column diameter [m]
$\dot{V}$ = Rich amine volume flow into desorber column [m^3/s]
v_g = superficial gas velocity [m/s]

3. Pump power [61]

$$P_p = \frac{\dot{V}(\Delta P)}{\eta_a} = \frac{\dot{V}(\rho g \Delta h)}{\eta_a} = \frac{\dot{m} g \Delta h}{\eta_a}$$

where

P_p = pump power [W]
$\dot{V}$ = fluid volume flow [m^3/s]
ΔP = pressure increase across pump [Pa]
ρ = fluid density [kg/m^3]
g = gravitational constant [m/s^2]
Δh = height difference [m]
η_a = adiabatic efficiency [-]

4. Log mean temperature difference for counterflow system [56]

$$\Delta T_{LMTD} = \frac{(T_{h,i} - T_{c,o}) - (T_{h,o} - T_{c,i})}{\ln\left[\frac{(T_{h,i} - T_{c,o})}{(T_{h,o} - T_{c,i})}\right]}$$

where

ΔT_{LMTD} = log mean temperature difference [°C]
$T_{h,i}$ = inlet temperature of hot fluid [°C]
$T_{h,o}$ = outlet temperature of hot fluid [°C]
$T_{c,i}$ = inlet temperature of cold fluid [°C]
$T_{c,o}$ = outlet temperature of cold fluid [°C]

For the Lean/Rich heat exchangers, the hot and cold fluid correspond to Lean and Rich amine stream, respectively.

5. Minimum approach temperature for counterflow system

i) When $C_h > C_c$ (i.e. $\Delta T_2 > \Delta T_1$)

$$\Delta T_{min} = \Delta T_1 = T_{h,i} - T_{c,o}$$

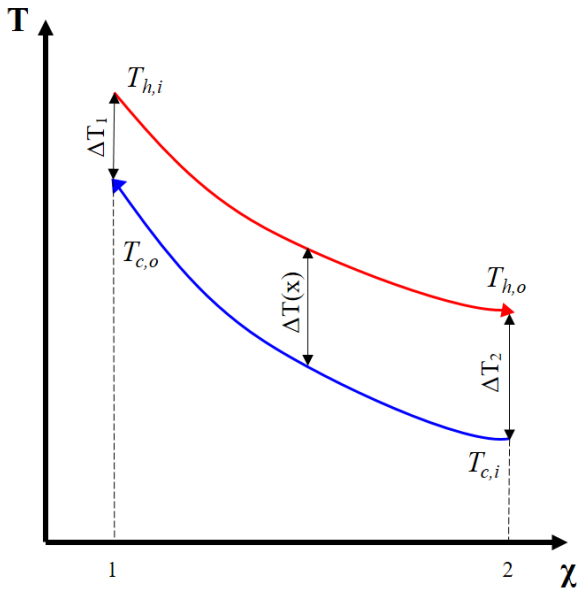

ii) When $C_h < C_c$ (i.e. $\Delta T_2 < \Delta T_1$)

$$\Delta T_{min} = \Delta T_2 = T_{h,o} - T_{c,i}$$

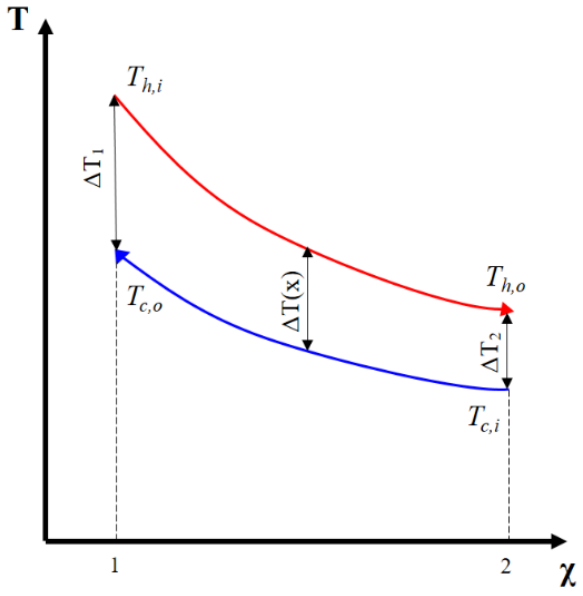

For the Lean/Rich heat exchangers, the heat capacity of Lean amine (hot stream) is higher than that of Rich amine (cold stream) (i.e. $C_h > C_c$). Therefore, ΔT_{min} corresponds to i).

6. Heat transfer area in heat exchanger

$$A = \frac{Q}{U \cdot \Delta T_{LMTD}}$$

where

A = heat transfer area [m^2]
Q = heat transfer rate [W]
U = overall heat transfer coefficient [$W/m^2 \cdot K$]
ΔT_{LMTD} = log mean temperature difference [℃]

7. Fluid mass flow in heat exchanger (without phase change) [56]

$$\dot{m} \approx \frac{Q}{\overline{C_p} \cdot \Delta T}$$

where

$\dot{m}$ = fluid mass flow [kg/s]
Q = heat transfer rate [kW]
$\overline{C_p}$ = average heat capacity of fluid [kJ/kg·°C]
ΔT = fluid temperature change across heat exchanger [°C]

8. Fluid mass flow in heat exchanger (with phase change)

$$\dot{m} \approx \frac{Q}{\overline{C_p} \cdot \Delta T + h_{fg}}$$

where

$\dot{m}$ = fluid mass flow [kg/s]
Q = heat transfer rate [W]
$\overline{C_p}$= average heat capacity of fluid [kJ/kg·°C]
ΔT = fluid temperature change across heat exchanger [°C]
h_{fg} = heat of vaporization (condensation)[1] [kJ/kg]

[1] $h_{fg} = h_g - h_f$ (h_g: specific enthalpy in saturated vapor phase, h_l: specific enthalpy in saturated liquid phase)

Appendix 3: Murphree efficiency in absorber [46]

	Number of stages in absorber column (N_{stage})										
	15	14	13	12	11	10	9	8	7	6	5
(Column top) 1	**0.210**	**0.210**	**0.210**	**0.210**	**0.210**	**0.210**	**0.210**	**0.210**	**0.210**	**0.210**	**0.210**
2	**0.210**	**0.210**	**0.210**	**0.210**	**0.210**	**0.210**	**0.210**	**0.210**	**0.210**	0.190	0.185
3	**0.210**	**0.210**	**0.210**	**0.210**	**0.210**	**0.210**	**0.210**	**0.210**	0.190	0.170	0.160
4	**0.210**	**0.210**	**0.210**	**0.210**	**0.210**	**0.210**	**0.210**	0.190	0.170	0.150	0.135
5	**0.210**	**0.210**	**0.210**	**0.210**	**0.210**	**0.210**	0.190	0.170	0.150	0.130	0.110
6	0.200	0.200	0.200	0.200	0.190	0.190	0.170	0.150	0.130	0.110	
7	0.190	0.190	0.190	0.185	0.170	0.170	0.150	0.130	0.110		
8	0.180	0.180	0.180	0.170	0.155	0.150	0.130	0.110			
9	0.170	0.170	0.170	0.155	0.140	0.130	0.110				
10	0.160	0.160	0.155	0.140	0.125	0.110					
11	0.150	0.150	0.140	0.125	0.110						
12	0.140	0.140	0.125	0.110							
13	0.130	0.125	0.110								
14	0.120	0.110									
(Column bottom) 15	0.110										

Appendix 4: Cost index & Currency exchange rate

Chemical Engineering Plant Cost Index (CEPCI) [48, 84]

Year	CEPCI	Cumulative inflation rate
2015 (yearly average)	556,8	–
2010 (yearly average)	550,8	$\frac{556,8}{550,8} = 101,09\ \%$
2010 (January)	532,9	$\frac{556,8}{532,9} = 104,48\ \%$
2000 (January)	391,1	$\frac{556,8}{391,1} = 142,37\ \%$

Currency exchange rate [85]

Year	Exchange rate
2015 (yearly average)	8,0674 [NOK/USD]
2010 (yearly average)	0.7549 [€/USD]

Appendix 5: Simulation parameter configuration

The following presents a series of procedures of configuring the simulation parameters (i.e. flue gas rate and N_{stage}) to derive a new process alternative from the base case.

i) Ignore (turn off) the recycler first[2].

ii) Depending on each Alternative, set the flue gas rate as the required value.

iii) Set the number of stages in absorber column as the required value.

iv) Adjust the Lean amine rate (into absorber column) such that the Reboiler duty becomes close to 27,17 MW.

v) Adjust the Rich amine temperature (before desorber column) to make ΔT_{min} of Lean/Rich heat exchanger close to 10,00 ℃. This often brings about perturbations in Reboiler duty.

vi) Repeat step iv) and v) alternatively until the Reboiler duty and ΔT_{min} of Lean/Rich heat exchanger are close to 27,17 MW and 10,00 ℃ respectively.

vii) Compare the mass flow of Lean amine (before absorber column) with that of Lean amine recycle stream (before recycler), and calculate the mass flow difference for H_2O and MEA. These mass flow differences indicate the loss of H_2O and MEA that occurred in the process loop.

viii) To achieve the mass balance for H_2O and MEA, compensate for H_2O and MEA losses by adding the respective mass flow difference obtained in step vii) to make-up streams.

ix) Turn on the recycler again and check if there is any change in the Reboiler duty, ΔT_{min}, as well as the mass fraction of all components in Lean amine flow (into absorber column).

x) A new process alternative is successfully made if no change is observed in step ix). If any change is observed after turning on the recycler, start again from step i).

[2] Ignoring the recycler indicates that the process loop is opened, i.e., the Lean amine stream is not circulated or recycled. This step reduces unexpected changes of the specified input parameters and thus facilitates the overall configuration procedures.

Appendix 6: CO_2-capture cost comparison

Mellapak 250Y (7600 $/m^3$)

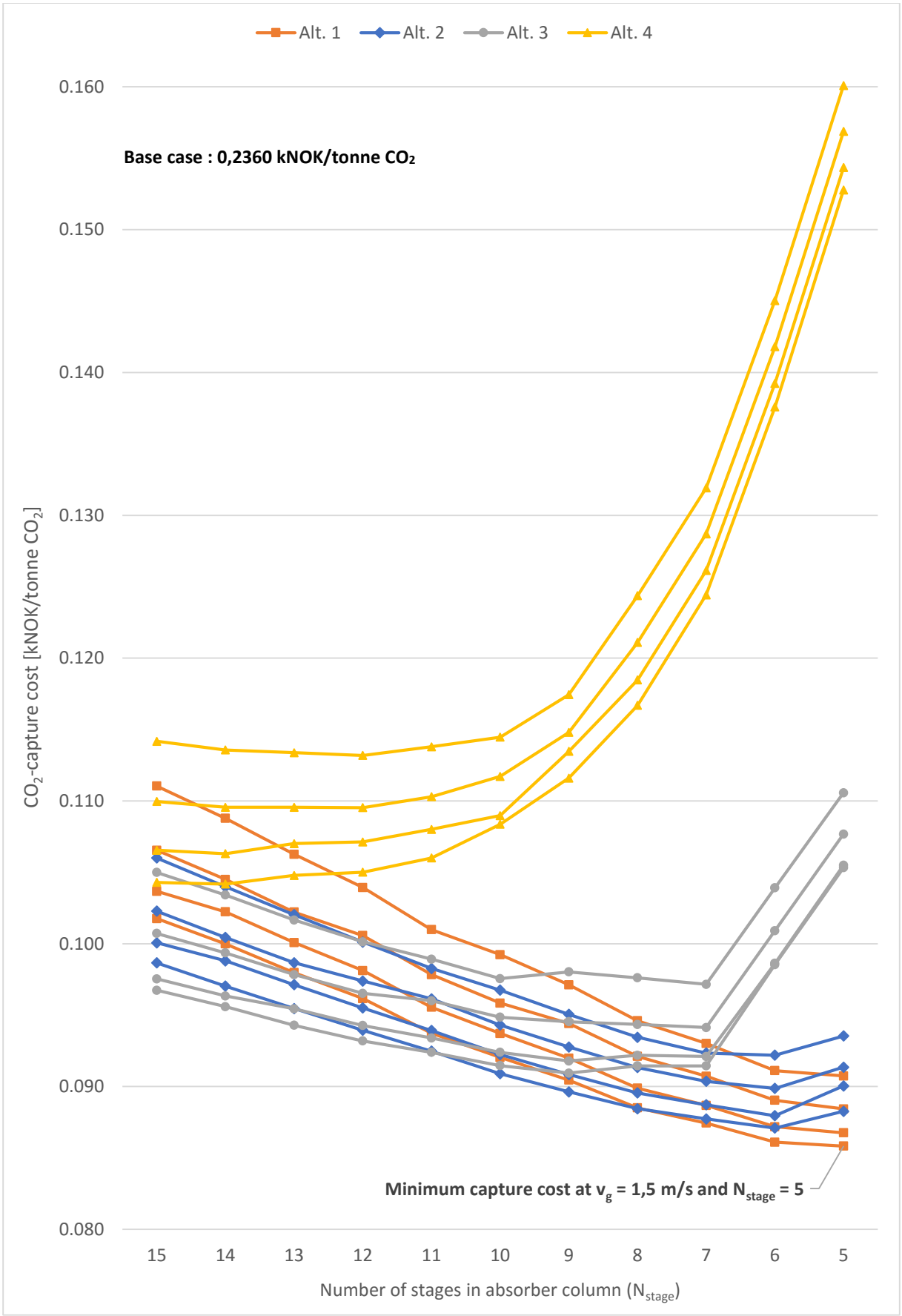

Appendix 7: CO_2-capture cost comparison

Mellapak 250Y (11200 $/m^3)

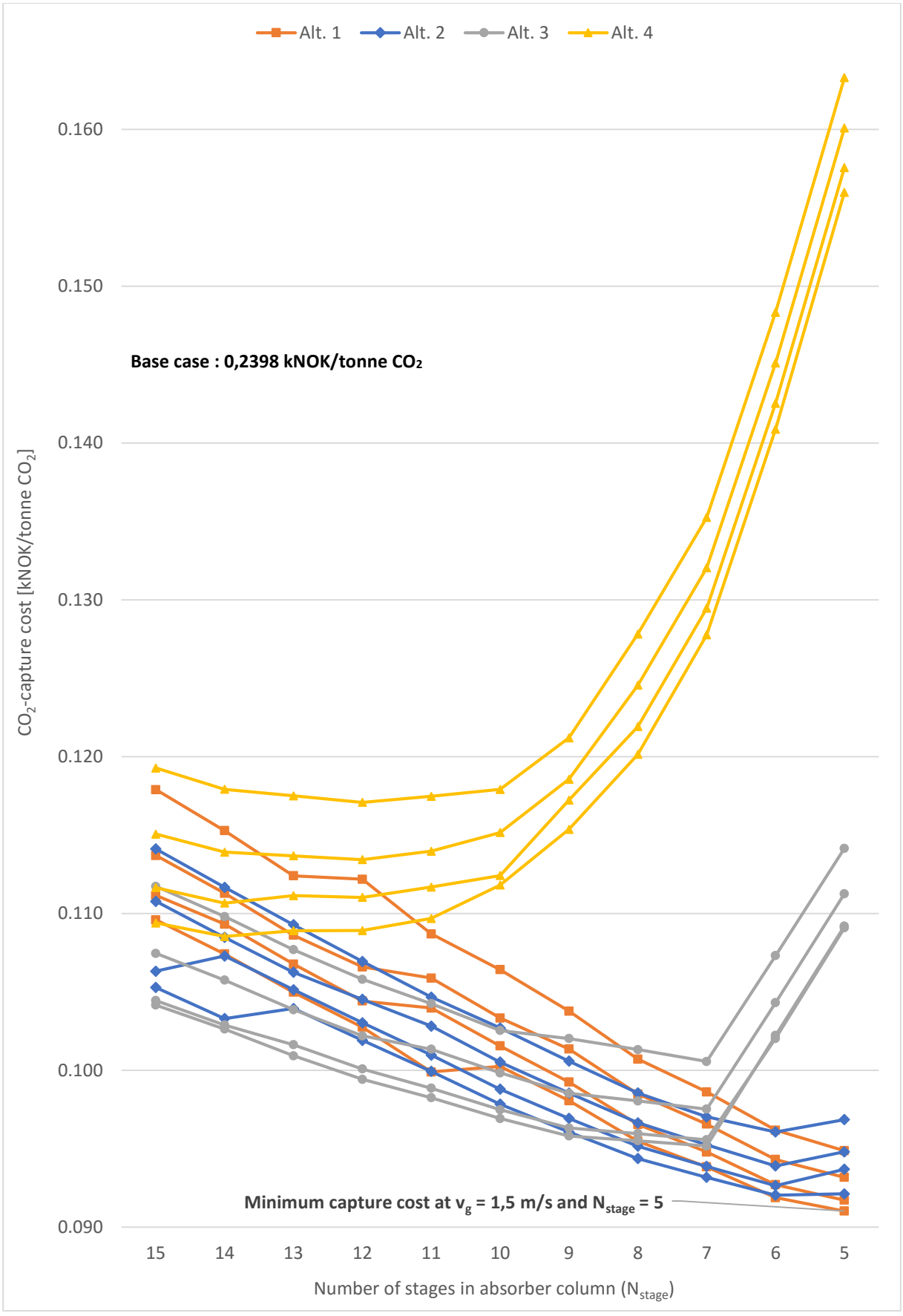

Appendix 8: CO_2-capture cost comparison

Mellapak 250Y (15200 $/m^3)

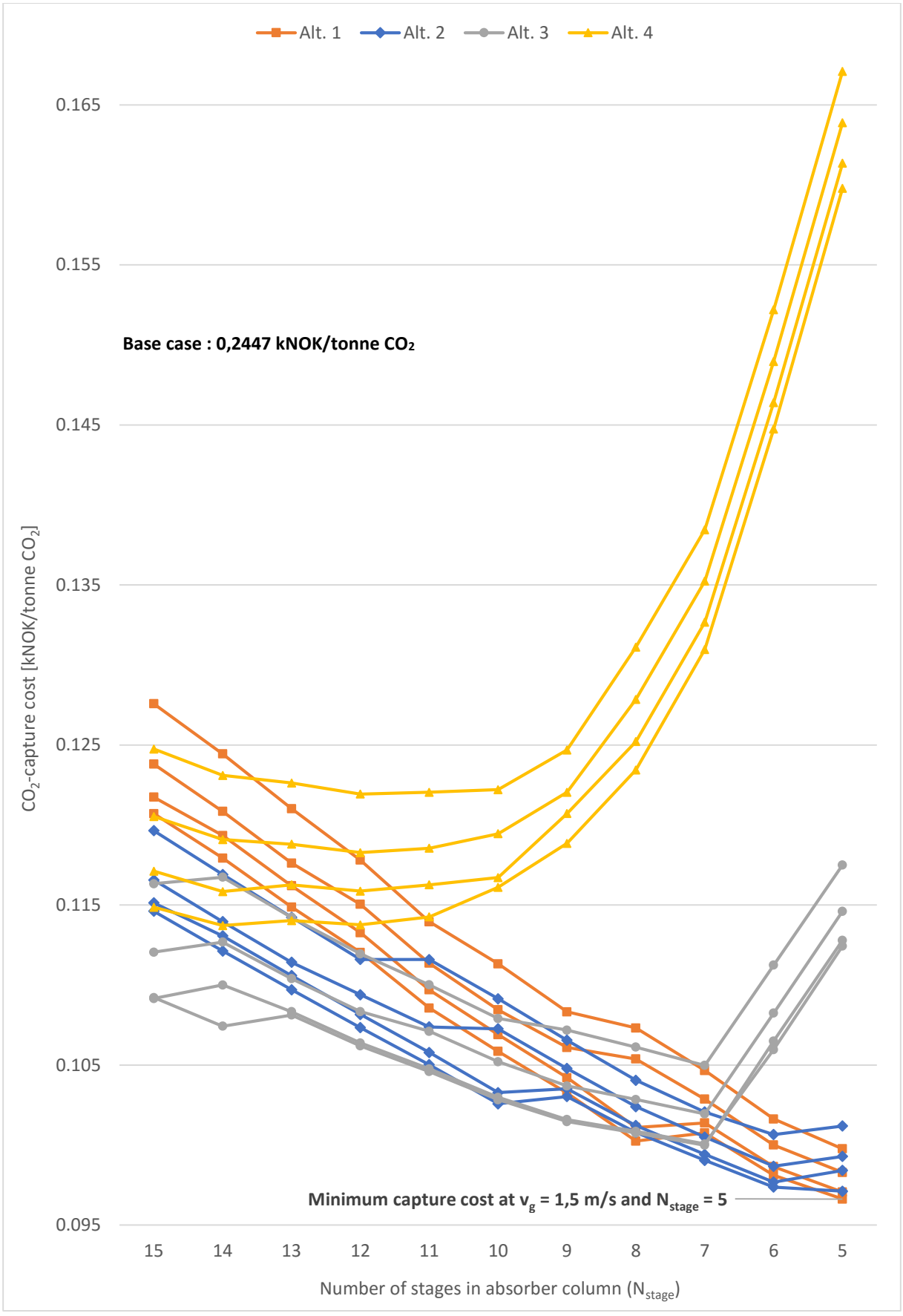

Appendix 9: CO_2-capture cost comparison

Mellapak 250X (7600 $/m^3)

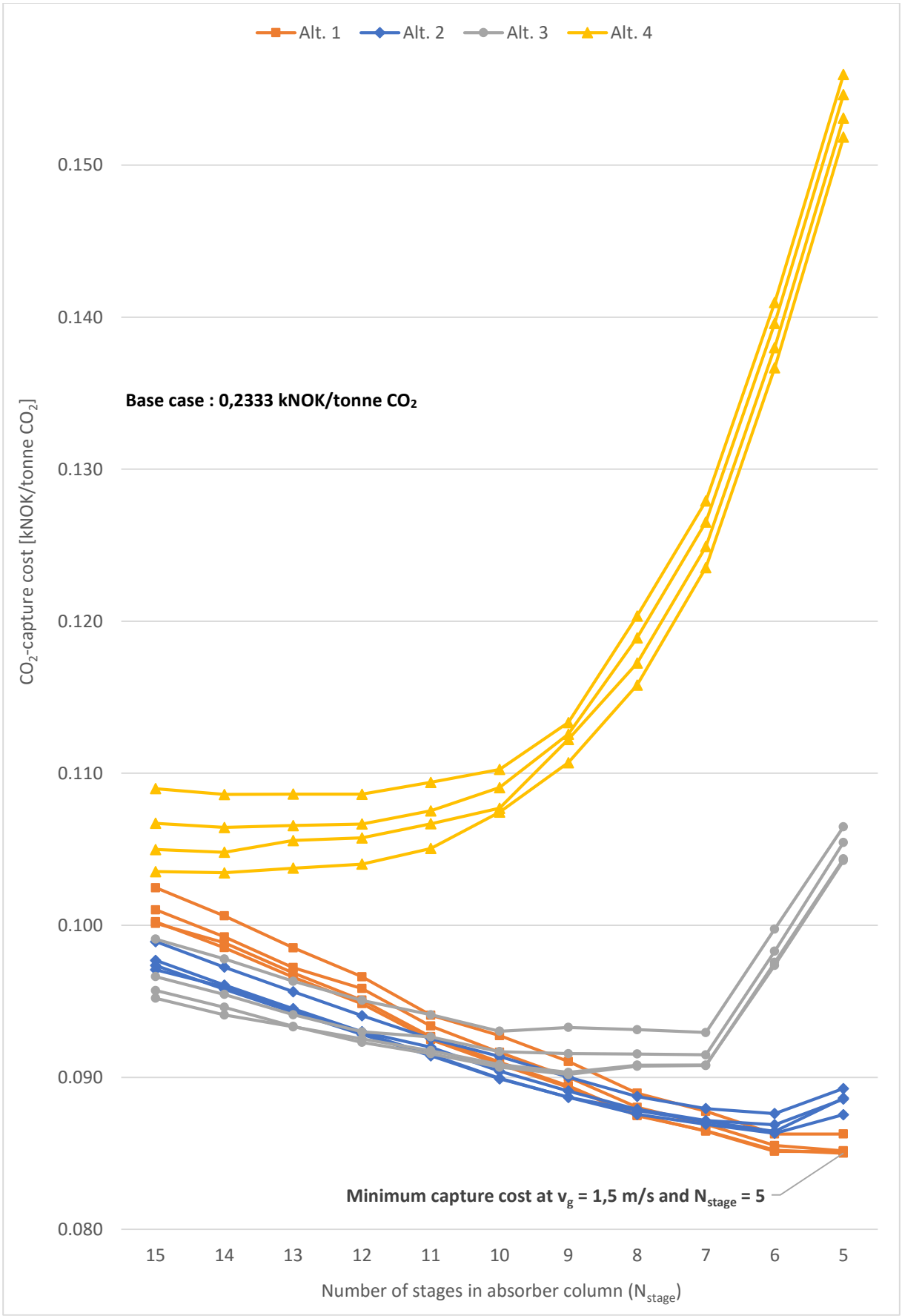

Appendix 10: CO_2-capture cost comparison

Mellapak 2X (7600 $/m^3)

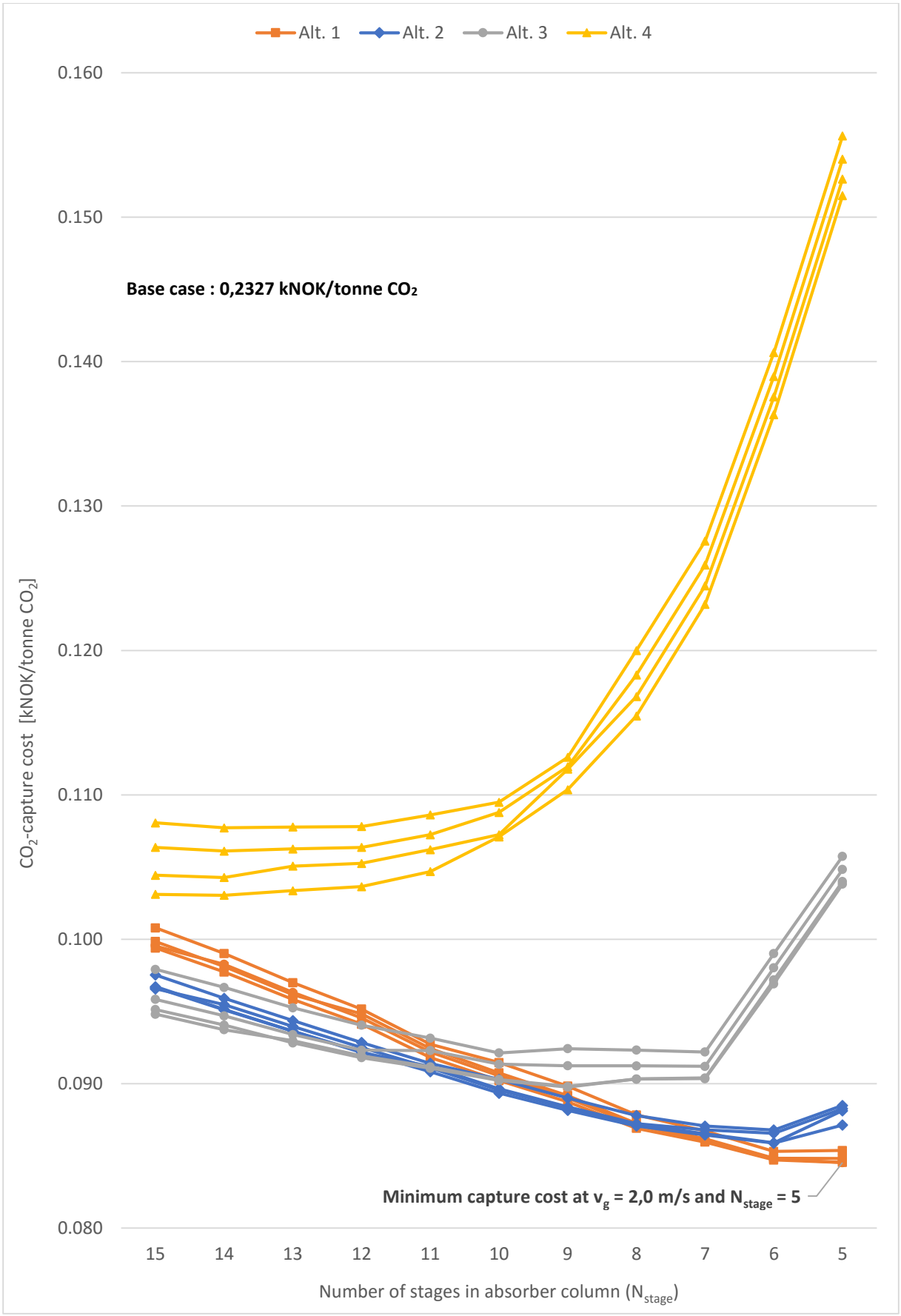

Appendix 11: Overall comparison of CAPEX

Mellapak 250Y (7600 $/m^3)

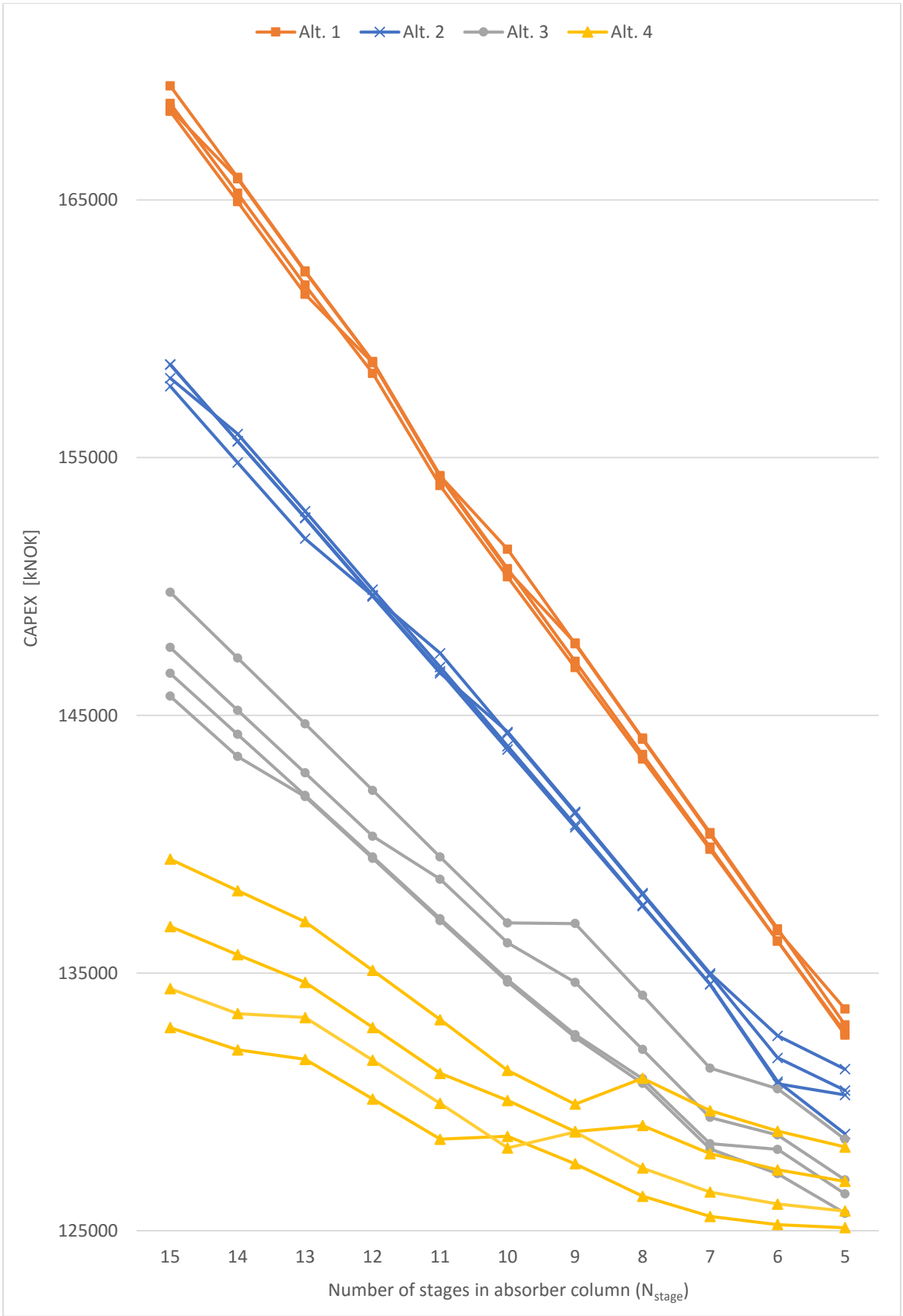

Appendix 12: Overall comparison of OPEX

Mellapak 250Y (7600 $/m^3)

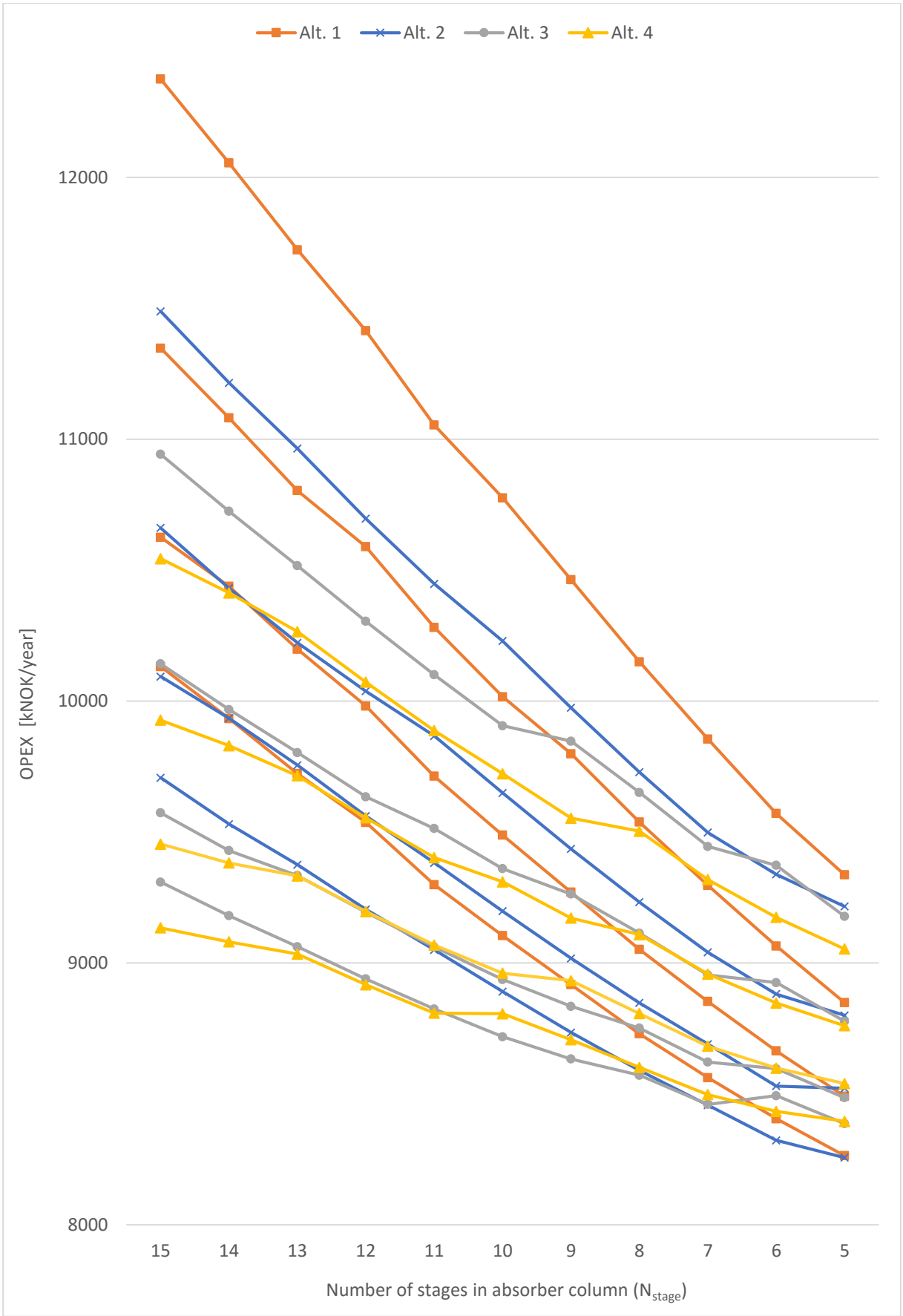

Appendix 13: CO_2-capture process illustration in Aspen HYSYS

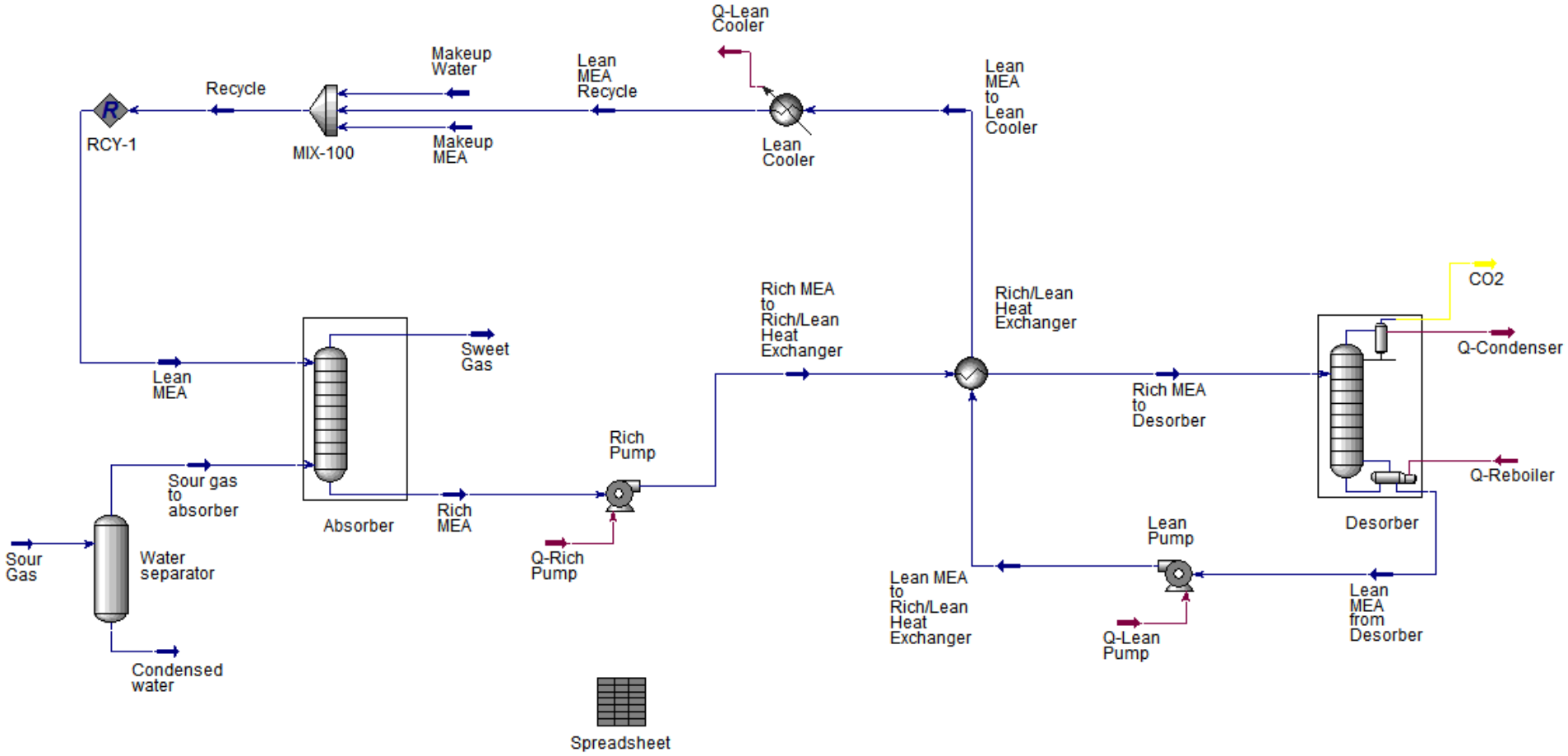

Appendix 14: Table of cost factors [75]

2013-2014	Fluid								Solid							
Cost of equipment in Carbon Steel (CS) (kNOK)	0-20	20-100	100-500	500-1000	1000-2000	2000-5000	5000-15000	>15000	0-20	20-100	100-500	500-1000	1000-2000	2000-5000	>5000
Equipment	1,00	1,00	1,00	1,00	1,00	1,00	1,00	1,00	1,00	1,00	1,00	1,00	1,00	1,00	1,00
Erection	0,70	0,37	0,20	0,14	0,11	0,09	0,08	0,06	1,55	0,82	0,48	0,34	0,28	0,20	0,17
Piping	2,80	1,51	0,88	0,65	0,51	0,38	0,32	0,23	0,57	0,31	0,17	0,13	0,10	0,08	0,07
Electric	0,81	0,56	0,38	0,32	0,27	0,22	0,20	0,14	1,37	0,86	0,57	0,44	0,37	0,31	0,26
Instrument	2,80	1,51	0,88	0,65	0,51	0,38	0,32	0,23	1,11	0,61	0,36	0,26	0,21	0,14	0,12
Civil work	0,43	0,28	0,20	0,16	0,13	0,11	0,10	0,07	0,99	0,59	0,38	0,29	0,23	0,19	0,16
Steel & concrete	1,41	0,92	0,62	0,50	0,43	0,34	0,31	0,22	1,97	1,22	0,80	0,62	0,52	0,41	0,37
Insulation	0,53	0,27	0,14	0,11	0,09	0,07	0,04	0,03	0,53	0,27	0,14	0,11	0,09	0,07	0,04
Direct Cost	**10,60**	**6,53**	**4,43**	**3,65**	**3,17**	**2,69**	**2,47**	**2,09**	**9,20**	**5,79**	**4,00**	**3,33**	**2,90**	**2,50**	**2,29**
Engineering Process	0,97	0,34	0,19	0,14	0,12	0,10	0,09	0,07	0,97	0,34	0,19	0,14	0,12	0,10	0,09
Engineering Mechanical	0,77	0,19	0,08	0,04	0,03	0,02	0,01	0,01	0,97	0,29	0,13	0,09	0,07	0,04	0,03
Engineering Piping	0,85	0,46	0,27	0,20	0,14	0,11	0,10	0,07	0,17	0,09	0,04	0,03	0,02	0,02	0,02
Engineering Electric	0,82	0,24	0,12	0,09	0,08	0,07	0,04	0,03	0,96	0,32	0,16	0,12	0,10	0,08	0,07
Engineering Instrument	1,46	0,57	0,28	0,20	0,16	0,11	0,10	0,07	0,95	0,28	0,12	0,09	0,07	0,04	0,03
Engineering Civil	0,31	0,09	0,03	0,02	0,02	0,01	0,01	0,01	0,39	0,13	0,07	0,04	0,03	0,02	0,02
Engineering Steel & Concrete	0,46	0,19	0,10	0,08	0,07	0,04	0,04	0,03	0,53	0,22	0,12	0,10	0,09	0,07	0,07
Engineering Insulation	0,21	0,07	0,02	0,01	0,01	0,01	0,01	0,01	0,21	0,07	0,02	0,01	0,01	0,01	0,01
Engineering Cost	**5,83**	**2,11**	**1,09**	**0,78**	**0,63**	**0,48**	**0,41**	**0,30**	**5,14**	**1,73**	**0,86**	**0,63**	**0,50**	**0,39**	**0,34**
Procurement	1,22	0,41	0,16	0,10	0,07	0,03	0,02	0,02	1,22	0,41	0,16	0,10	0,07	0,03	0,02
Project Control	0,29	0,11	0,04	0,03	0,03	0,02	0,02	0,02	0,26	0,09	0,04	0,03	0,02	0,02	0,01
Site Management	0,52	0,33	0,22	0,19	0,16	0,13	0,12	0,09	0,44	0,28	0,20	0,16	0,14	0,12	0,12
Project management	0,70	0,36	0,23	0,19	0,16	0,13	0,12	0,09	0,60	0,31	0,20	0,16	0,13	0,12	0,11
Administration Cost	**2,74**	**1,21**	**0,66**	**0,50**	**0,41**	**0,33**	**0,29**	**0,21**	**2,52**	**1,09**	**0,60**	**0,46**	**0,37**	**0,31**	**0,27**
Commissioning	0,57	0,26	0,13	0,08	0,08	0,04	0,04	0,03	0,49	0,23	0,12	0,09	0,07	0,04	0,03
Total Known Cost	**19,72**	**10,12**	**6,31**	**5,00**	**4,29**	**3,55**	**3,23**	**2,64**	**17,35**	**8,85**	**5,58**	**4,49**	**3,84**	**3,25**	**2,94**
Contingency	3,91	2,02	1,27	1,01	0,87	0,73	0,66	0,48	3,39	1,73	1,11	0,89	0,77	0,66	0,60
Total Cost	**23,63**	**12,13**	**7,57**	**6,02**	**5,16**	**4,28**	**3,89**	**3,11**	**20,73**	**10,59**	**6,69**	**5,38**	**4,60**	**3,90**	**3,54**

Material factors

When using other materials than CS, the factors for equipment and piping must be multiplied with the Material factor.

Material factors:
Stainless Steel (SS316) Welded: 1,75
Stainless Steel (SS316) Machined : 1,30
GRP: 1,00
Exotic: 2,50

Porsgrunn December 2013

Nils Henrik Eldrup

Appendix 15: Simulation specifications of Alternatives

Alternative 1

Simulation parameter		Unit	N_{stage}										
			15	14	13	12	11	10	9	8	7	6	5
Input Parameter	Flue gas rate	[kmol/h]	8974	8974	8974	8974	8974	8974	8974	8974	8974	8974	8974
	Lean amine rate (into absorber column)	[kg/h]	588300	588400	588100	589000	589500	589700	590800	591300	594000	595500	598000
	MEA content in Lean amine	[wt%]	28,8	28,8	28,8	28,8	28,8	28,8	28,8	28,8	28,8	28,8	28,8
	CO_2 content in Lean amine	[wt%]	5,5	5,5	5,5	5,5	5,5	5,5	5,5	5,5	5,5	5,5	5,5
	Rich temperature out of Lean/Rich HX	[°C]	101,8	101,9	101,9	101,9	102,0	102,1	102,2	102,3	102,6	102,7	103,2
Output Parameter	CO_2-capture efficiency	[-]	44,33	44,15	43,93	44,00	43,91	43,69	43,43	43,28	42,87	42,34	41,74
	Energy demand	[MJ/kg CO_2]	3,15	3,16	3,16	3,17	3,17	3,19	3,20	3,21	3,24	3,27	3,33
	Reboiler power	[MW]	27,17	27,17	27,17	27,17	27,17	27,17	27,17	27,17	27,17	27,17	27,17

Alternative 2

Simulation parameter		Unit	N_{stage}										
			15	14	13	12	11	10	9	8	7	6	5
Input Parameter	Flue gas rate	[kmol/h]	7179	7179	7179	7179	7179	7179	7179	7179	7179	7179	7179
	Lean amine rate (into absorber column)	[kg/h]	593000	593500	594000	594000	595500	595500	596300	596800	599600	604200	610000
	MEA content in Lean amine	[wt%]	28,9	28,9	28,9	28,9	28,9	28,9	28,9	28,9	28,9	28,9	28,9
	CO_2 content in Lean amine	[wt%]	5,5	5,5	5,5	5,5	5,5	5,5	5,5	5,5	5,5	5,5	5,5
	Rich temperature out of Lean/Rich HX	[°C]	102,5	102,5	102,6	102,6	102,7	102,8	102,9	103,0	103,3	103,7	104,3
Output Parameter	CO_2-capture efficiency	[-]	53,87	53,71	53,69	53,48	53,36	53,22	52,88	52,51	51,86	51,33	49,68
	Energy demand	[MJ/kg CO_2]	3,23	3,23	3,24	3,25	3,26	3,27	3,29	3,31	3,34	3,40	3,49
	Reboiler power	[MW]	27,17	27,17	27,17	27,17	27,17	27,17	27,17	27,17	27,17	27,17	27,17

Alternative 3

Simulation parameter		Unit	N_{stage}										
			15	14	13	12	11	10	9	8	7	6	5
Input Parameter	Lean amine rate (into absorber column)	[kmol/h]	5384	5384	5384	5384	5384	5384	5384	5384	5384	5384	5384
	MEA content in Lean amine	[kg/h]	601000	601100	601600	602400	603700	606000	608000	611100	614500	635600	660000
	CO_2 content in Lean amine	[wt%]	28,8	28,8	28,8	28,8	28,8	28,8	28,8	28,8	28,8	28,8	28,8
	Rich temperature out of Lean/Rich HX	[wt%]	5,4	5,4	5,4	5,4	5,4	5,4	5,4	5,4	5,4	5,4	5,4
	Lean amine rate (into absorber column)	[°C]	103,5	103,6	103,6	103,7	103,9	104,1	104,3	104,6	105,0	106,6	108,2
Output Parameter	CO_2-capture efficiency	[-]	69,59	69,43	69,41	68,96	68,4	68,14	67,23	66,43	65,29	60,73	56,13
	Energy demand	[MJ/kg CO_2]	3,37	3,38	3,38	3,40	3,42	3,44	3,49	3,53	3,58	3,86	4,18
	Reboiler power	[MW]	2,72	2,72	2,72	2,72	2,72	2,72	2,72	2,72	2,72	2,72	2,72

Alternative 4

Simulation parameter		Unit	N_{stage}										
			15	14	13	12	11	10	9	8	7	6	5
Input Parameter	Lean amine rate (into absorber column)	[kmol/h]	3590	3590	3590	3590	3590	3590	3590	3590	3590	3590	3590
	MEA content in Lean amine	[kg/h]	632700	633900	637000	641800	648300	655000	668000	686000	711800	750000	794500
	CO_2 content in Lean amine	[wt%]	28,8	28,8	28,8	28,8	28,8	28,8	28,8	28,8	28,8	28,8	28,8
	Rich temperature out of Lean/Rich HX	[wt%]	5,4	5,4	5,4	5,4	5,4	5,4	5,4	5,4	5,4	5,4	5,4
	Lean amine rate (into absorber column)	[°C]	106,7	106,8	107,0	107,3	107,7	108,1	108,8	109,4	109,4	109,5	109,5
Output Parameter	CO_2-capture efficiency	[-]	90,37	89,94	89,05	87,92	85,98	84,20	81,02	76,83	71,45	64,39	57,9
	Energy demand	[MJ/kg CO_2]	3,88	3,89	3,93	3,99	4,08	4,16	4,33	4,58	4,93	5,47	6,09
	Reboiler power	[MW]	2,72	2,72	2,72	2,72	2,72	2,72	2,72	2,72	2,72	2,72	2,72

Appendix 16: Dimensioning & Cost estimation (Flue gas fan)

Cost information

Base equipment cost (CS)	[USD]	12300	January 2000
Base capacity	[kW]	50	
Exponenential factor	[-]	0,76	
Cumulative inflation rate (CECPI)	[%]	142,37	= (556,8)/(391,1)
Currency exchange rate	[NOK/USD]	8,0674	2015 (yearly average)

Base case

	Item	Unit	Value	Note
A	Flue gas rate	[m^3/s]	50,86	obtained from HYSYS
B	Pressure drop per meter of packing bed ($\Delta P_{packing}$)	[mbar/m]	2,93	Mellapak 250Y
C	Height per packing bed ($h_{packing}$)	[m/packing]	1	1 m/packing assumed when $v_g = v_{g,b}$ = 2,5 m/s
D	Pressure drop per packing bed	[mbar/packing]	2,93	= B ∗ C
E	Total pressure drop across absorber column	[mbar]	55,67	= D ∗ (N_{stage} + 4), where N_{stage} = 15
F	Total pressure drop across absorber column	[kPa]	5,57	= E/10
G	Fan actual power	[kW]	377,5	= (A ∗ F)/0,75
H	Equipment cost (SS)	[kNOK]	853,6	= {[12300 ∗ (G/50)^0,76] ∗ 1,3} ∗ (142,37%) ∗ (8,0674/1000)
I	Installation factor (SS)	[-]	6,52	
J	Installation cost (SS)	[kNOK]	4278	= (H/1,3) ∗ I
K	Yearly operating cost	[kNOK/year]	1510	= G ∗ 4

Alternative 1 (v_g = 2,5 m/s)

Item		Unit	N_{stage}											Note
			15	14	13	12	11	10	9	8	7	6	5	
A	Flue gas rate	[m^3/s]	50,86	50,86	50,86	50,86	50,86	50,86	50,86	50,86	50,86	50,86	50,86	obtained from HYSYS
B	Pressure drop per meter of packing bed ($\Delta p_{packing}$)	[mbar/m]	2,93	2,93	2,93	2,93	2,93	2,93	2,93	2,93	2,93	2,93	2,93	Mellapak 250Y
C	Height per packing bed ($h_{packing}$)	[m/packing]	1	1	1	1	1	1	1	1	1	1	1	1 m/packing assumed when v_g = 2,5 m/s
D	Pressure drop per packing bed	[mbar/packing]	2,93	2,93	2,93	2,93	2,93	2,93	2,93	2,93	2,93	2,93	2,93	= B ∗ C
E	Total pressure drop across absorber column	[mbar]	55,67	52,74	49,81	46,88	43,95	41,02	38,09	35,16	32,23	29,3	26,37	= D ∗ (N_{stage} + 4)
F	Total pressure drop across absorber column	[kPa]	5,57	5,27	4,98	4,69	4,40	4,10	3,81	3,52	3,22	2,93	2,64	= E/10
G	Fan actual power	[kW]	377,5	357,7	337,8	317,9	298,0	278,2	258,3	238,4	218,6	198,7	178,8	= (A ∗ F)/0,75, where η = 0,75
H	Equipment cost (SS)	[kNOK]	853,6	819,2	784,4	749,1	713,2	676,8	639,7	602,0	563,5	524,1	483,8	= [12300 ∗ (G/50)^0,76] ∗ 1,3 ∗ 142,37% ∗ (8,0674/1000)
I	Installation factor (SS)	[-]	6,52	6,52	6,52	6,52	6,52	6,52	8,13	8,13	8,13	8,13	8,13	
J	Installation cost (SS)	[kNOK]	4278	4106	3931	3754	3574	3392	4003	3767	3526	3279	3027	= (H/1,3) ∗ I
K	Yearly operating cost	[kNOK/year]	1510	1431	1351	1272	1192	1113	1033	954	874	795	715	= G ∗ 4

Alternative 1 (v_g = 3,0 m/s)

Item		Unit	N_{stage}											Note
			15	14	13	12	11	10	9	8	7	6	5	
A	Flue gas rate	[m^3/s]	50,86	50,86	50,86	50,86	50,86	50,86	50,86	50,86	50,86	50,86	50,86	obtained from HYSYS
B	Pressure drop per meter of packing bed ($\Delta p_{packing}$)	[mbar/m]	4,14	4,14	4,14	4,14	4,14	4,14	4,14	4,14	4,14	4,14	4,14	Mellapak 250Y
C	Height per packing bed ($h_{packing}$)	[m/packing]	1,15	1,15	1,15	1,15	1,15	1,15	1,15	1,15	1,15	1,15	1,15	absorber column height, interfacial area changed
D	Pressure drop per packing bed	[mbar/packing]	4,75	4,75	4,75	4,75	4,74	4,74	4,74	4,74	4,74	4,74	4,74	= B ∗ C
E	Total pressure drop across absorber column	[mbar]	90,16	85,41	80,67	75,92	71,17	66,43	61,68	56,93	52,18	47,43	42,68	= D ∗ (N_{stage} + 4)
F	Total pressure drop across absorber column	[kPa]	9,02	8,54	8,07	7,59	7,12	6,64	6,17	5,69	5,22	4,74	4,27	= E/10
G	Fan actual power	[kW]	611,4	579,2	547,1	514,9	482,7	450,5	418,3	386,1	353,9	321,7	289,5	= (A ∗ F)/0,75, where η = 0,75
H	Equipment cost (SS)	[kNOK]	1231	1182	1132	1081	1029	976	923	868	813	756	698	= [12300 ∗ (G/50)^0,76] ∗ 1,3 ∗ 142,37% ∗ (8,0674/1000)
I	Installation factor (SS)	[-]	6,52	6,52	6,52	6,52	6,52	6,52	6,52	6,52	6,52	6,52	6,52	
J	Installation cost (SS)	[kNOK]	6171	5923	5671	5415	5156	4893	4625	4352	4073	3788	3496	= (H/1,3) ∗ I
K	Yearly operating cost	[kNOK/year]	2446	2317	2188	2059	1931	1802	1673	1544	1415	1287	1158	= G ∗ 4

Appendix 17: Dimensioning & Cost estimation (Absorber column)

Cost information on column shell

Base equipment cost (CS)	[USD]	65600	January 2000
Base capacity	[tonne]	8	
Exponential factor	[-]	0,89	
Cumulative inflation rate (CECPI)	[%]	142,37	= (556,8)/(391,1)
Currency exchange rate	[NOK/USD]	8,0674	2015 (yearly average)

Cost information on column packing

Base equipment cost (SS316)	[USD]	7600	January 2010
Base capacity	[m^3]	1	
Exponential factor	[-]	1	
Cumulative inflation rate (CECPI)	[%]	104,48	= (556,8)/(532,9)
Currency exchange rate	[NOK/USD]	8,0674	2015 (yearly average)

Base case & Alternative 1 (v_g = 2,5 m/s)

Item		Unit	Base case	Alternative 1											Note
				15	14	13	12	11	10	9	8	7	6	5	N_{stage}
A	Flue gas rate	[m^3/s]	50,85	50,85	50,85	50,85	50,85	50,85	50,85	50,85	50,85	50,85	50,85	50,85	obtained from HYSYS
B	Absorber column area	[m^2]	20,34	20,34	20,34	20,34	20,34	20,34	20,34	20,34	20,34	20,34	20,34	20,34	= A/v_g
C	Absorber inner diameter	[m]	5,09	5,09	5,09	5,09	5,09	5,09	5,09	5,09	5,09	5,09	5,09	5,09	= [(4/π) ∗ B]^0,5
D	Absorber outer diameter	[m]	5,11	5,11	5,11	5,11	5,11	5,11	5,11	5,11	5,11	5,11	5,11	5,11	= C + 0,02 (Thickness = 0,01 m)
E	Height per packing bed ($h_{packing}$)	[m/packing]	1	1	1	1	1	1	1	1	1	1	1	1	$h_{packing}$ = 1 m/packing at v_g of 2,5 m/s
F	Total packing height	[m]	15	15	14	13	12	11	10	9	8	7	6	5	= E ∗ N_{stage}
G	Total height of absorber column	[m]	45	45	42	39	36	33	30	27	24	21	18	15	= F ∗ 3
H	Volume of absorber column shell	[m^3]	7,21	7,21	6,73	6,25	5,77	5,29	4,81	4,33	3,84	3,36	2,88	2,40	= [(π/4) ∗ (D^2-C^2)] ∗ G
I	Weight of absorber column shell (CS)	[tonne]	56,6	56,6	52,8	49,0	45,3	41,5	37,7	34,0	30,2	26,4	22,6	18,9	(CS density) = 7850 kg/m^3
J	Equipment cost of absorber column shell (CS)	[kNOK]	4297	4297	4042	3784	3523	3261	2996	2728	2456	2181	1901	1616	[65600*(I/8)^0,89] ∗ (142,37%) ∗ (8,0674/1000)
K	Shell cost per unit volume (CS)	[kNOK/m^3]	596	596	601	606	611	617	623	631	639	648	659	673	= J/H
L	Liquid distributor shell volume	[m^3]	0,41	0,41	0,41	0,41	0,41	0,41	0,41	0,41	0,41	0,41	0,41	0,41	= A ∗ 0,01 ∗ 2
M	I-beam support volume	[m^2]	0,04	0,04	0,04	0,04	0,04	0,04	0,04	0,04	0,04	0,04	0,04	0,04	= (0,00201 ∗ C) ∗ 4
N	Total volume of liquid distributor	[m^3]	0,45	0,45	0,45	0,45	0,45	0,45	0,45	0,45	0,45	0,45	0,45	0,45	= L + M
O	Liquid distributor cost (SS)	[kNOK]	467	467	471	475	479	483	488	494	501	508	517	527	= (K ∗ N) ∗ 1,75
P	Shell equipment cost (incl. distributor)	[kNOK]	4765	4765	4512	4258	4002	3744	3484	3222	2957	2689	2418	2144	= J + O
Q	Installation factor (SS)	[-]	4,28	4,28	4,28	4,28	4,28	4,28	4,28	4,28	4,28	4,28	4,28	4,28	
R	Installation cost of absorber column shell (SS)	[kNOK]	20392	20392	19312	18225	17129	16025	14912	13788	12654	11508	10349	9175	= P ∗ Q
S	Total packing beds volume (incl. water wash)	[m^3]	345,8	345,8	325,4	305,1	284,8	264,4	244,1	223,7	203,4	183,1	162,7	142,4	= B ∗ (N_{stage} + 2)
T	Equipment cost of packing beds (CS)	[kNOK]	12658	12658	11913	11169	10424	9679	8935	8190	7446	6701	5957	5212	= [(S ∗ 7600) ∗ (104,48%) ∗ (8,0674/1000)]/1,75
U	Installation factor (SS)	[-]	2,87	2,87	2,87	2,87	2,87	2,87	2,87	2,87	2,87	2,87	2,87	2,87	
V	Installation cost of packing beds (SS)	[kNOK]	36328	36328	34191	32054	29917	27780	25643	23506	21369	19232	17095	14958	= T∗ U

Alternative 1 (continued)

	Item	Unit	N_{stage}											Note
			15	14	13	12	11	10	9	8	7	6	5	
①	Lean mass flow	[kg/h]	588800	588900	588600	589200	589500	589700	590800	591300	594000	595500	598000	obtained from HYSYS
②	Lean density	[kg/m^3]	1030,0	1030,0	1030,0	1030,0	1030,0	1030,0	1030,0	1030,0	1030,0	1030,0	1030,0	obtained from HYSYS
③	Lean volume flow	[m^3/h]	571,7	571,7	571,5	572,0	572,3	572,5	573,6	574,1	576,7	578,2	580,6	= ①/②
④	Lean liquid load	[m/h]	28,11	28,11	28,10	28,12	28,14	28,15	28,20	28,22	28,35	28,42	28,54	= ③/B
⑤	a_e/a_g	[-]	0,898	0,898	0,898	0,898	0,898	0,898	0,899	0,899	0,900	0,900	0,901	a_g = 250 m^2/m^3
⑥	Interfacial area (a_e)	[m^2/m^3]	224,4	224,5	224,4	224,5	224,5	224,5	224,6	224,7	224,9	225,0	225,3	= ⑤ ∗ 250
⑦	Total packing volume	[m^3]	345,8	325,4	305,1	284,8	264,4	244,1	223,7	203,4	183,1	162,7	142,4	= S
⑧	Total Interfacial area	[m^2]	77608,3	73046,0	68472,4	63922,9	59364,1	54802,0	50257,2	45697,4	41171,9	36619,1	32073,6	= ⑥ ∗ ⑦

Alternative 1 (v_g = 3,0 m/s)

	Item	Unit	N_{stage}											Note
			15	14	13	12	11	10	9	8	7	6	5	
A	Flue gas rate	[m^3/s]	50,85	50,85	50,85	50,85	50,85	50,85	50,85	50,85	50,85	50,85	50,85	constant within Alternative 1
B	Absorber area	[m^2]	16,95	16,95	16,95	16,95	16,95	16,95	16,95	16,95	16,95	16,95	16,95	= A/v_g
C	Lean amine volume flow	[m^3/h]	571,7	571,7	571,5	572,0	572,3	572,5	573,6	574,1	576,7	578,2	580,6	constant within Alternative 1
D	Lean amine liquid load	[m/h]	33,73	33,73	33,71	33,75	33,77	33,78	33,84	33,87	34,02	34,11	34,25	= C/B
E	a_e/a_g	[-]	0,940	0,940	0,940	0,940	0,940	0,940	0,941	0,941	0,942	0,943	0,944	
F	Effective interfacial area (a_e)	[m^2/m^3]	235,0	235,0	235,0	235,0	235,1	235,1	235,2	235,3	235,5	235,7	236,0	= E ∗ 250
G	Total effective area (previously obtained)	[m^2]	77608,3	73046,0	68472,4	63922,9	59364,1	54802,0	50257,2	45697,4	41171,9	36619,1	32073,6	Previously given with v_g of 2,5 m/s
H	New packing volume (incl. water wash)	[m^3]	330,3	310,8	291,4	272,0	252,5	233,1	213,7	194,2	174,8	155,4	135,9	= G/F
I	New packing height (incl. water wash)	[m]	19,5	18,3	17,2	16,0	14,9	13,8	12,6	11,5	10,3	9,2	8,0	= H/B
J	Height per packing bed (incl. water wash)	[m]	1,15	1,15	1,15	1,15	1,15	1,15	1,15	1,15	1,15	1,15	1,15	= $I/(N_{stage}+2) = \Delta h_{packing}$
K	Total height of absorber column	[m]	51,6	48,1	44,7	41,3	37,8	34,4	30,9	27,5	24,1	20,6	17,2	= (N_{stage} ∗ J) ∗ 3
L	Absorber shell volume	[m^3]	7,54	7,04	6,54	6,03	5,53	5,03	4,53	4,02	3,52	3,02	2,51	(Absorber ID) = (4*B/π)^0,5 and T = 0,01 m
M	Absorber shell weight	[tonne]	59,22	55,27	51,32	47,37	43,42	39,48	35,53	31,58	27,63	23,68	19,73	(CS density) = 7850 kg/m^3
N	Absorber shell cost (CS)	[kNOK]	4474,9	4208,4	3939,8	3668,8	3395,4	3119,2	2839,8	2557,2	2270,3	1979,1	1682,4	[65600 ∗ (M/8)^0,89]*142,37%*(8,0674/1000)
O	Absorber shell cost per unit volume	[$kNOK/m^3$]	593,2	597,7	602,6	607,9	613,8	620,3	627,5	635,7	645,1	656,1	669,4	= N/L
P	Liquid distributor shell volume	[m^3]	0,34	0,34	0,34	0,34	0,34	0,34	0,34	0,34	0,34	0,34	0,34	= B ∗ 0,01 ∗ 2
Q	I-beam support volume	[m^2]	0,04	0,04	0,04	0,04	0,04	0,04	0,04	0,04	0,04	0,04	0,04	= 0,00201 ∗ (Absorber ID) ∗ 4
R	Total volume of liquid distributor	[m^3]	0,38	0,38	0,38	0,38	0,38	0,38	0,38	0,38	0,38	0,38	0,38	= P + Q
S	Liquid distributor cost (SS)	[kNOK]	390,7	393,7	396,9	400,4	404,2	408,5	413,3	418,7	424,9	432,1	440,9	= (O ∗ R) ∗ 1,75
T	Absorber shell cost (incl. distributor)	[kNOK]	4866	4602	4337	4069	3800	3528	3253	2976	2695	2411	2123	= N + S
U	Absorber shell installation factor (SS)	[-]	4,28	4,28	4,28	4,28	4,28	4,28	4,28	4,28	4,28	4,28	4,28	
V	Absorber shell installation cost (SS)	[kNOK]	20825	19697	18561	17416	16262	15099	13923	12736	11535	10320	9088	= T ∗ U
W	Equipment cost of packing beds (CS)	[kNOK]	12090	11379	10668	9956	9245	8534	7822	7111	6399	5687	4976	= [(H ∗ 7600) ∗ 104,48% ∗ (8,0674/1000)]/1,75
X	Installation factor (SS)	[-]	2,87	2,87	2,87	2,87	2,87	2,87	2,87	2,87	2,87	2,87	3,02	
Y	Installation cost of packing beds (SS)	[kNOK]	34698	32657	30617	28574	26533	24492	22449	20408	18364	16322	15001	= W ∗ X

Appendix 18: Dimensioning & Cost estimation (Rich pump)

Cost information

Base equipment cost (CS)	[USD]	9840	January 2000
Base capacity	[kW]	4	
Exponential factor	[-]	0,55	
Cumulative Inflation rate (CECPI)	[%]	142,37	= (556,8)/(391,1)
Currency exchange rate	[NOK/USD]	8,0674	2015 (yearly average)

Base case

Item		Unit	Value	Note
A	Rich pump duty	[kW]	64,1	obtained from HYSYS
B	Rich amine mass flow	[kg/s]	457,0	obtained from HYSYS
C	Desorber column height	[m]	20	
D	Rich amine inlet height	[m]	16	= C ∗ 0,8
E	Gravitational constant	[kg·m/s^2]	9,81	
F	Adiabatic efficiency	[-]	0,75	
G	Additional duty required	[kW]	95,7	= (B ∗ D ∗ E)/(F ∗ 1000)
H	Rich pump actual duty	[kW]	159,8	= A + G
I	Equipment cost (SS)	[kNOK]	858,9	={I ∗ [(H/4)^0,55] ∗ (142,37%) ∗ 8,0674/1000} ∗ 1,3
J	Installation factor (SS)	[-]	6,52	
K	Installation cost (SS)	[kNOK]	5596	= (I/1,3) ∗ J
L	Yearly operating cost	[kNOK/year]	639,2	= H ∗ 4

Appendix 19: Dimensioning & Cost estimation (Lean/Rich heat exchanger)

Cost information

Base equipment cost (SS316)	[€]	57600	2010 (yearly average)
Base capacity	[m^2]	356	
Exponential factor	[-]	1	
Currency exchange rate	[USD/€]	1,325	2010 (yearly average)
Cumulative inflation rate (CECPI)	[%]	101,09	= (556,8)/(550,8)
Currency exchange rate	[NOK/USD]	8,0674	2015 (yearly average)

Base case

Item		Unit	Base case	Note
A	Heat transfer rate	[kW]	82452	obtained from HYSYS
B	LMTD	[°C]	11,58	obtained from HYSYS
C	Total heat transfer area	[m^2]	4748	= (A ∗ 1000)/(B ∗ 1500)
D	Number of units	[-]	3	Maximum area per unit: 2000 m^2 (plate-and-frame type)
E	Heat transfer area per unit	[m^2]	1583	= C/D
F	Equipment cost per unit (SS)	[kNOK]	2766	= [57600 ∗ (E/356)^1] ∗ (1,325) ∗ (101,09%) ∗ (8,0674/1000)
G	Installation factor (SS)	[-]	6,29	
H	Installation cost per unit	[kNOK]	9947	= (F/1,75) ∗ G
I	Total equipment cost (SS)	[kNOK]	8299	= D ∗ F
J	Total installation cost (SS)	[kNOK]	29840	= D ∗ H

Appendix 20: Dimensioning & Cost estimation (Desorber column)

Cost information on column shell

Base equipment cost (CS)	[USD]	65600	January 2000
Base capacity	[tonne]	8	
Exponential factor	[-]	0,89	
Cumulative inflation rate (CECPI)	[%]	142,37	= (556,8)/(391,1)
Currency exchange rate	[NOK/USD]	8,0674	2015 (yearly average)

Cost information on column packing

Base equipment cost (SS316)	[USD]	7600	January 2010
Base capacity	[m^3]	1	
Exponential factor	[-]	1	
Cumulative inflation rate (CECPI)	[%]	104,48	= (556,8)/(532,9)
Currency exchange rate	[NOK/USD]	8,0674	2015 (yearly average)

Base case & Alternative 1

	Item	Unit	Base case	Alternative 1											Note
				15	14	13	12	11	10	9	8	7	6	5	N_{stage}
A	Rich mass flow (vapor)	[kg/s]	2,86	2,98	2,94	2,99	2,92	2,94	2,90	2,85	2,82	2,73	2,67	2,49	obtained from HYSYS
B	Rich mass flow (liquid)	[kg/s]	454,18	164,29	164,33	164,31	164,53	164,70	164,82	165,23	165,50	166,42	167,08	168,47	
C	Rich density (vapor)	[kg/m^3]	2,14	2,32	2,32	2,32	2,32	2,32	2,31	2,31	2,31	2,30	2,29	2,27	
D	Rich density (liquid)	[kg/m^3]	1016,7	1022,9	1022,8	1022,9	1022,7	1022,7	1022,6	1022,4	1022,3	1022,0	1021,8	1021,3	
E	Rich volume flow (vapor)	[m^3/s]	1,34	1,28	1,27	1,29	1,26	1,27	1,25	1,23	1,22	1,19	1,16	1,09	= A/C
F	Rich volume flow (liquid)	[m^3/s]	0,45	0,16	0,16	0,16	0,16	0,16	0,16	0,16	0,16	0,16	0,16	0,16	= B/D
G	Total volume flow of Rich amine	[m^3/s]	1,78	1,44	1,43	1,45	1,42	1,43	1,41	1,39	1,38	1,35	1,33	1,26	= E + F
H	Desorber column area	[m^2]	1,78	1,44	1,43	1,45	1,42	1,43	1,41	1,39	1,38	1,35	1,33	1,26	v_g = 1,0m/s
I	Desorber inner diameter	[m]	1,51	1,36	1,35	1,36	1,35	1,35	1,34	1,33	1,33	1,31	1,30	1,27	
J	Desorber outer diameter	[m]	1,53	1,38	1,37	1,38	1,37	1,37	1,36	1,35	1,35	1,33	1,32	1,29	Shell thickness = 0,01 m
K	Number of stages in desorber column	[m]	10	10	10	10	10	10	10	10	10	10	10	10	1 m/packing assumed in desorber column
L	Total height of desorber column	[m]	20	20	20	20	20	20	20	20	20	20	20	20	= K ∗ 2
M	Volume of desorber column shell	[m^3]	0,95	0,86	0,85	0,86	0,85	0,85	0,85	0,84	0,84	0,83	0,82	0,80	= [(π/4) ∗ (J^2-I^2)] ∗ L
N	Weight of desorber column shell (CS)	[tonne]	7,48	6,74	6,70	6,75	6,68	6,70	6,67	6,62	6,60	6,52	6,46	6,30	(CS density) = 7850 kg/m^3
O	Equipment cost of column shell (CS)	[kNOK]	709,5	646,5	643,5	647,7	642,1	643,7	640,7	636,7	634,6	627,6	623,0	646,5	65600*(N/8)^0,89*142,37%*8,0674/1000
P	Column shell cost per unit volume (CS)	[kNOK/m^3]	744,8	753,4	753,9	753,3	754,1	753,8	754,3	754,9	755,2	756,2	756,9	753,4	= O/M
Q	Liquid distributor shell volume	[m^3]	0,036	0,029	0,029	0,029	0,028	0,029	0,028	0,028	0,028	0,027	0,027	0,025	= H ∗ 0,01 ∗ 2
R	I-beam support volume	[m^2]	0,012	0,011	0,011	0,011	0,011	0,011	0,011	0,011	0,011	0,011	0,010	0,010	= 0,00201 ∗ I ∗ 4
S	Total volume of liquid distributor	[m^3]	0,048	0,040	0,039	0,040	0,039	0,039	0,039	0,039	0,038	0,038	0,037	0,035	= Q + R
T	Liquid distributor cost (SS)	[kNOK]	62,2	52,4	52,0	52,6	51,8	52,0	51,6	51,0	50,7	49,7	49,0	47,0	= P ∗ S
U	Equipment cost of column (incl. distributor)	[kNOK]	771,8	698,9	695,5	700,3	693,9	695,7	692,3	687,6	685,3	677,3	672,0	655,7	= O + T
V	Column shell installation factor (SS)	[-]	6,02	6,02	6,02	6,02	6,02	6,02	6,02	6,02	6,02	6,02	6,02	6,02	
W	Column shell installation cost (SS)	[kNOK]	4646	4207	4187	4216	4177	4188	4168	4140	4126	4077	4045	3948	= U ∗ V
X	Total packing beds volume (incl. water wash)	[m^3]	21,38	17,32	17,14	17,39	17,06	17,15	16,97	16,73	16,61	16,20	15,93	15,12	= H ∗ (K+2)
Y	Equipment cost of packing beds (CS)	[kNOK]	782,7	634,0	627,4	636,7	624,4	627,9	621,3	612,4	608,0	592,9	583,1	553,3	= [(X*7600)*104,48%]*(8,0674/1000)]/1,75
Z	Installation factor (SS)	[-]	3,65	3,65	3,65	3,65	3,65	3,65	3,65	3,65	3,65	3,65	3,65	3,65	
α	Installation cost of packing beds (SS)	[kNOK]	2855	2313	2288	2322	2278	2290	2266	2234	2218	2163	2127	2018	= Y ∗ Z

Appendix 21: Dimensioning & Cost estimation (Condenser)

Cost information

Base equipment cost (SS316)	[€]	223200	2010 (yearly average)
Base capacity	[m^2]	995,7	
Exponential factor	[-]	0,68	
Currency exchange rate	[USD/€]	1,325	2010 (yearly average)
Cumulative inflation rate (CECPI)	[%]	101,09	= (556,8)/(550,8)
Currency exchange rate	[NOK/USD]	8,0674	2015 (yearly average)

Base case

Item		Unit	Value	Note
A	Condenser duty	[kW]	9141	obtained from HYSYS
B	Vapor temperature into condenser	[°C]	103,4	
C	Vapor temperature out of condenser	[°C]	96,6	
D	LMTD	[°C]	6,26	Cooling water specification : T_{in} = 8 °C, T_{out} = 23 °C
E	Total heat transfer area	[m^2]	54,1	= (A ∗ 1000)/(D ∗ 2000)
F	Number of units	[-]	1	Maximum area per unit: 1000 m^2 (Shell-and-tube type)
G	Heat exchanger area per unit	[m^2]	54,1	= E/F
H	Equipment cost per unit (SS)	[kNOK]	333	= 223200 ∗ (1,325) ∗ [(E/995,7)^0,68] ∗ (101,09%) ∗ (8,0674/1000)
I	Installation factor (SS)	[-]	8,98	
J	Installation cost per unit (SS)	[kNOK]	1708	= (F/1,75) ∗ G
K	Total equipment cost (SS)	[kNOK]	333	= D ∗ F
L	Total installation cost (SS)	[kNOK]	8,98	= D ∗ H
M	Yearly operating cost	[kNOK/year]	838,8	= A ∗ 0,09177

Appendix 22: Dimensioning & Cost estimation (Reboiler)

Cost information

Base equipment cost (SS316)	[€]	223200	2010 (yearly average)
Base capacity	[m^2]	995,7	
Exponential factor	[-]	0,68	
Currency exchange rate	[USD/€]	1,325	2010 (yearly average)
Cumulative inflation rate (CECPI)	[%]	101,09	= (556,8)/(550,8)
Currency exchange rate	[NOK/USD]	8,0674	2015 (yearly average)

Base case & Alternatives

Item		Unit	Base case	Alternatives	Note
A	Reboiler duty	[kW]	67930	27172	obtained from HYSYS
B	Lean amine temperature into reboiler	[°C]	116,4	116,4	
C	Lean amine temperature out of reboiler	[°C]	120	120	
D	Superheated steam temperature into reboiler	[°C]	130	130	
E	Saturated water temperature out of reboiler	[°C]	120	120	
F	LMTD	[°C]	6,26	6,26	((D-C)-(E-B))/LN((D-C)/(E-B)), where LN indicates natural logarithms
G	Heat exchanger area	[m^2]	4337,5	1735,0	= (A ∗ 1000)/(2500 ∗ F)
H	Number of units	[-]	5	2	Maximum area per unit: 1000 m^2 (Shell-and-tube type)
I	Heat exchanger area per unit	[m^2]	867,5	867,5	= G/H
J	Equipment cost per unit (SS)	[kNOK]	2196	2195,5	= 223200 ∗ (1,325) ∗ [(E/995,7)^0,68] ∗ (101,09%) ∗ (8,0674/1000)
K	Installation factor (SS)	[-]	6,29	6,29	
L	Installation cost per unit	[kNOK]	7895	7895	= (J/1,75) ∗ K
M	Total equipment cost (SS)	[kNOK]	10978	4391	= J ∗ H
N	Total installation cost (SS)	[kNOK]	39473	15789	= L ∗ H
O	Yearly operating cost	[kNOK/year]	87981	–	= A ∗ 1,295 (for Base case)

Appendix 23: Dimensioning & Cost estimation (Lean pump)

Cost information

Base equipment cost (CS)	[USD]	9840	January 2000
Base capacity	[kW]	4	
Exponential factor	[-]	0,55	
Cumulative Inflation rate (CECPI)	[%]	142,37	= (556,8)/(391,1)
Currency exchange rate	[NOK/USD]	8,0674	2015 (yearly average)

Base case

Item		Unit	Value	Note
A	Lean pump duty	[kW]	117,0	obtained from HYSYS
B	Lean amine mass flow across pump	[kg/s]	433,6	obtained from HYSYS
C	Absorber column height	[m]	45	= $N_{stage} * 3 = 15 * 3$
D	Rich amine inlet height at Absorber column	[m]	36	= C * 0,8
E	Gravitational constant	[kg·m/s^2]	9,81	
F	Adiabatic efficiency	[-]	0,75	
G	Additional power due to Δh	[kW]	204,2	= (B * E * D)/(F * 1000)
H	Lean pump actual duty	[kW]	204,2	= A + H = H (Duty in HYSYS ignored)
I	Equipment cost (SS)	[kNOK]	1277,8	={I * [(H/4)^0,55] * (142,37%) * 8,0674/1000} * 1,3
J	Installation factor (SS)	[-]	6,52	
K	Installation cost (SS)	[kNOK]	6403,8	= (I/1,3) * J
L	Yearly operating cost	[kNOK/year]	816,8	= A * 4

Appendix 24: Dimensioning & Cost estimation (Lean cooler)

Cost information

Base equipment cost (SS316)	[€]	223200	2010 (yearly average)
Base capacity	[m^2]	995,7	
Exponential factor	[-]	0,68	
Currency exchange rate	[USD/€]	1,325	2010 (yearly average)
Cumulative inflation rate (CECPI)	[%]	101,09	= (556,8)/(550,8)
Currency exchange rate	[NOK/USD]	8,0674	2015 (yearly average)

Base case

	Item	Unit	Base case	Note
A	Lean cooler duty	[kW]	42677	obtained from HYSYS
B	Lean amine temperature into cooler	[°C]	71,37	
C	Lean amine temperature out of cooler	[°C]	45,00	
D	LMTD	[°C]	42,43	Cooling water : T_{in} = 8 °C, T_{out} = 23 °C
E	Total heat transfer area	[m^2]	1257,2	= (A ∗ 1000)/(800 ∗ D)
F	Number of units	[-]	2	Maximum area per unit : 1000 m^2
G	Heat transfer area per unit	[m^2]	628,6	= E/F
H	Equipment cost per unit (SS)	[kNOK]	1764	= 223200 ∗ (1,325) ∗ [(E/995,7)^0,68] ∗ (101,09%) ∗ (8,0674/1000)
I	Installation factor (SS)	[-]	6,29	
J	Installation cost per unit (SS)	[kNOK]	6342	= (H/1,75) ∗ I
K	Total equipment cost (SS)	[kNOK]	3527	= F ∗ H
L	Total installation cost (SS)	[kNOK]	12683	= F ∗ J
M	Yearly operating cost	[kNOK/year]	3916,3	= A ∗ 0,09177

Appendix 25: Dimensioning & Cost estimation (Waste heat boiler)

Cost information

Base equipment cost (SS316)	[€]	223200	2010 (yearly average)
Base capacity	[m^2]	995,7	
Exponential factor	[-]	0,68	
Currency exchange rate	[USD/€]	1,325	2010 (yearly average)
Cumulative inflation rate (CECPI)	[%]	101,09	= (556,8)/(550,8)
Currency exchange rate	[NOK/USD]	8,0674	2015 (yearly average)

Alternatives

	Item	Unit		Note
A	Waste heat boiler duty	[kW]	27172	Same as Reboiler duty
B	Flue gas temperature into boiler	[°C]	300	
C	Flue gas temperature out of boiler	[°C]	150	
D	Saturated water temperature into boiler	[°C]	120	(Boiler operating pressure) = 2 bar
E	Superheated steam temperature out of boiler	[°C]	130	
F	LMTD	[°C]	80,71	
G	Overall heat transfer coefficient (U)	[$W/m^2 \cdot K$]	50	
H	Total heat transfer area	[m^2]	6733,2	= (A ∗ 1000)/(F ∗ G)
I	Number of units	[-]	7	Maximum area per unit: 1000 m^2 (Shell-and-tube type)
J	Heat transfer area per unit	[m^2]	961,9	= H/I
K	Equipment cost per unit (SS)	[kNOK]	2355	= 223200 ∗ (1,325) ∗ [(J/995,7)^0,68] ∗ (101,09%) ∗ (8,0674/1000)
L	Installation factor (SS)	[-]	6,29	
M	Installation cost per unit (SS)	[kNOK]	8469	= (K/1,75) ∗ L
N	Total equipment cost (SS)	[kNOK]	16487	= I ∗ K
O	Total installation cost (SS)	[kNOK]	59282	= I ∗ M

Appendix 26: Dimensioning & Cost estimation (Water pump)

Cost information

Base equipment cost (CS)	[USD]	9840	January 2000
Base capacity	[kW]	4	
Exponential factor	[-]	0,55	
Cumulative Inflation rate (CECPI)	[%]	142,37	= (556,8)/(391,1)
Currency exchange rate	[NOK/USD]	8,0674	2015 (yearly average)

Alternatives

Item		Unit	Value	Note
A	Reboiler power	[kW]	27172	
B	Superheated steam temperature into reboiler	[°C]	130	(Reboiler pressure) = 2 bar
C	Saturated water temperature out of reboiler	[°C]	120	
D	Heat capacity of superheated steam	[kJ/K]	2,149	Average value between 120 °C and 130 °C at P = 2 bar
E	Heat of condensation of saturated steam	[kJ/kg]	2201,6	at P = 2 bar and T ≈ 120 °C
F	Saturated water mass flow out of reboiler	[kg/s]	12,22	= A/[E+(B—C) ∗ D]
G	Saturated water density	[kg/m3]	942,94	P = 2 bar
H	Saturated water volume flow out of reboiler	[m3/s]	0,013	= F/G
I	Pressure increase across Water pump	[kPa]	100	
J	Adiabatic efficiency	[-]	0,75	
K	Water pump duty	[kW]	1,73	= (H ∗ I)/J
L	Equipment cost (SS)	[kNOK]	92,6	= {9840 ∗ [(K/4)^0,55] ∗ (142,37%) ∗ (8,0674/1000)} ∗ 1,3
M	Installation factor (SS)	[-]	12,88	
N	Installation cost (SS)	[kNOK]	918	= (L/1,3) ∗ M

Appendix 27: Installation cost details (v_g = 2,5 m/s)

Alternative 1

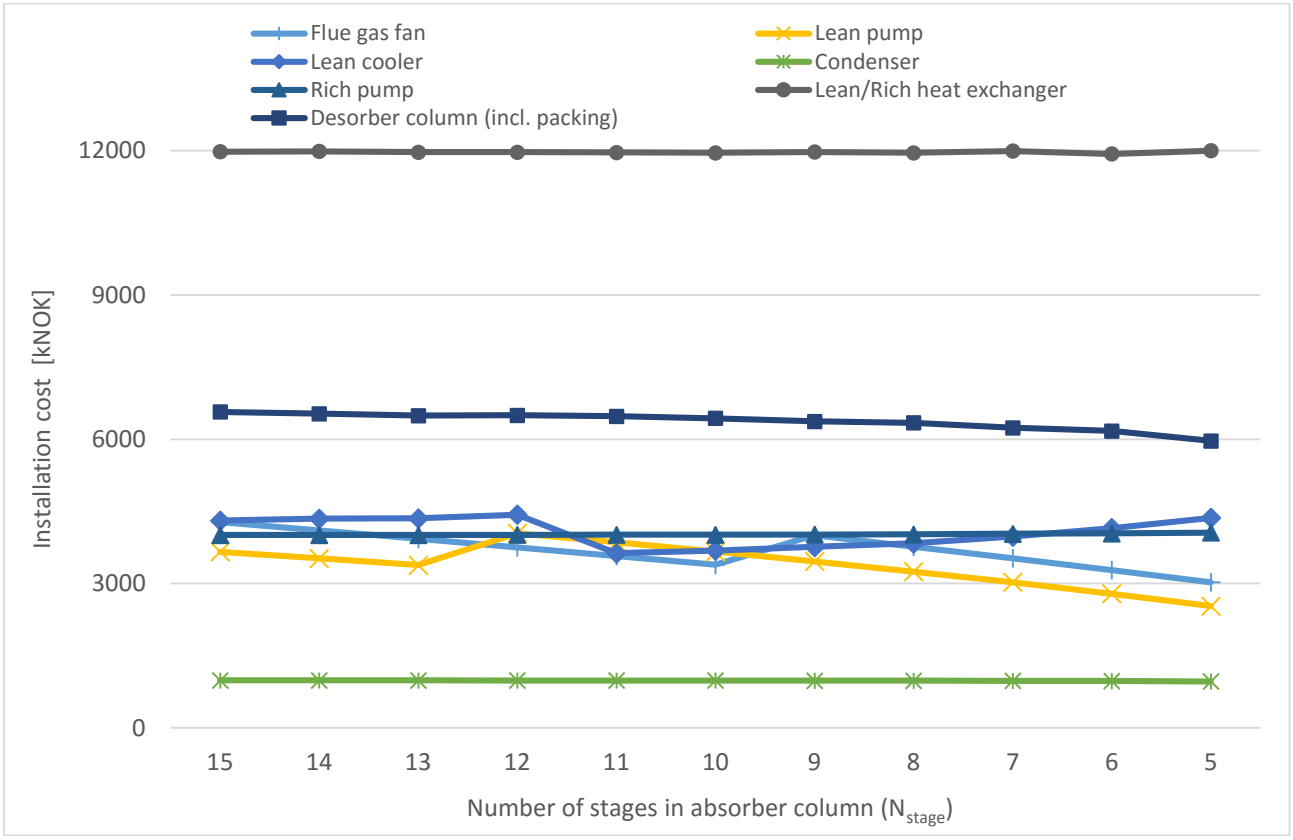

Alternative 2

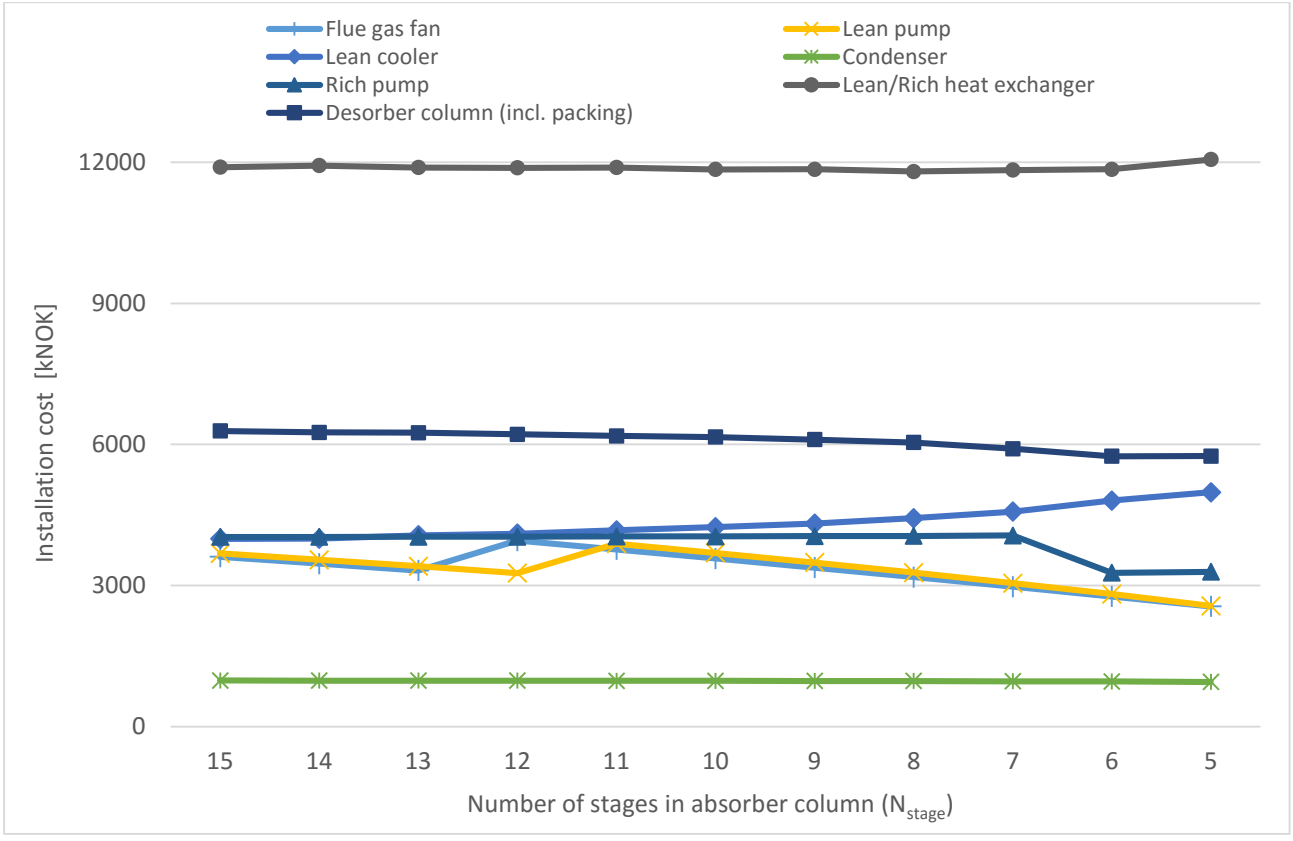

Alternative 3

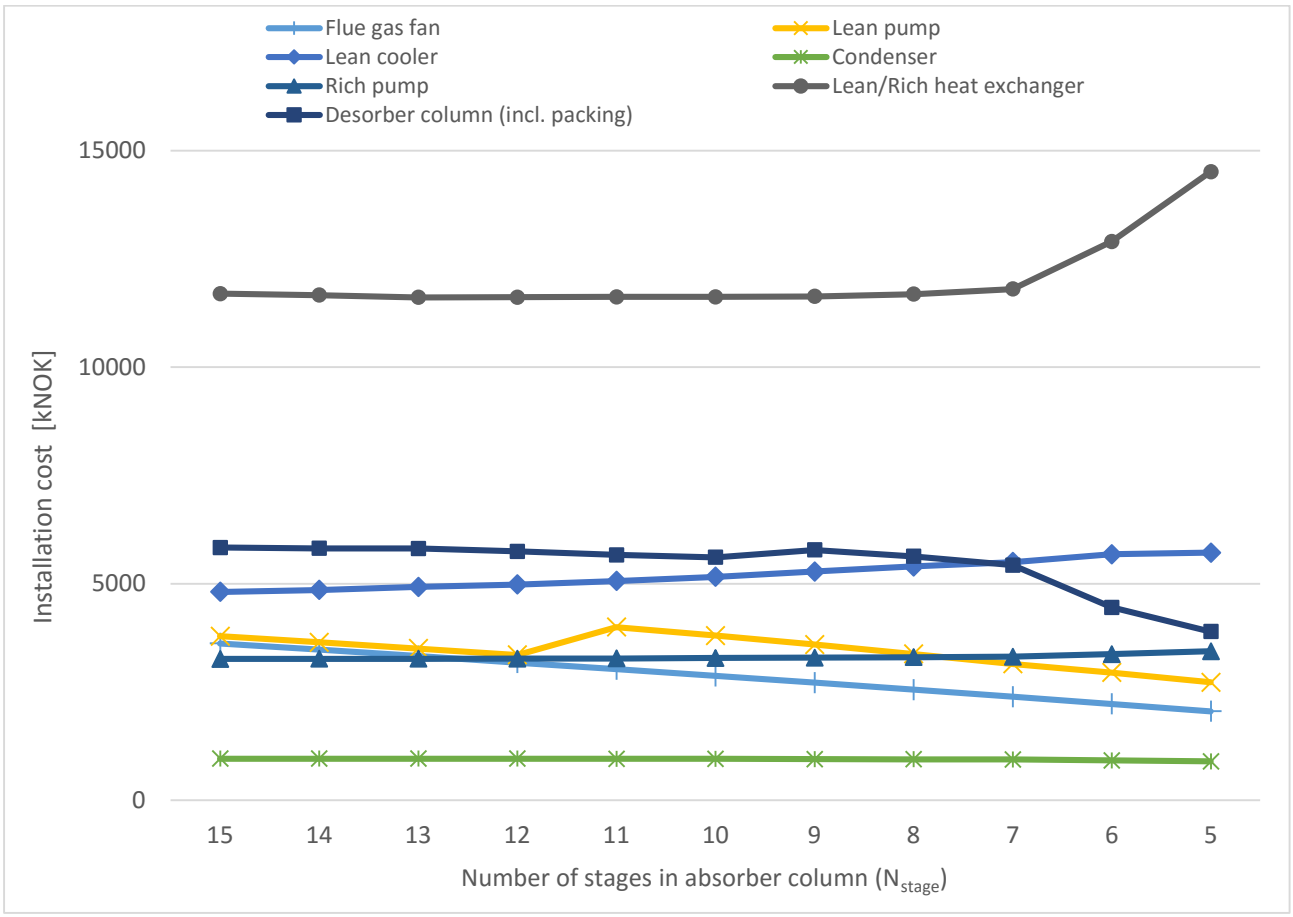

Alternative 4

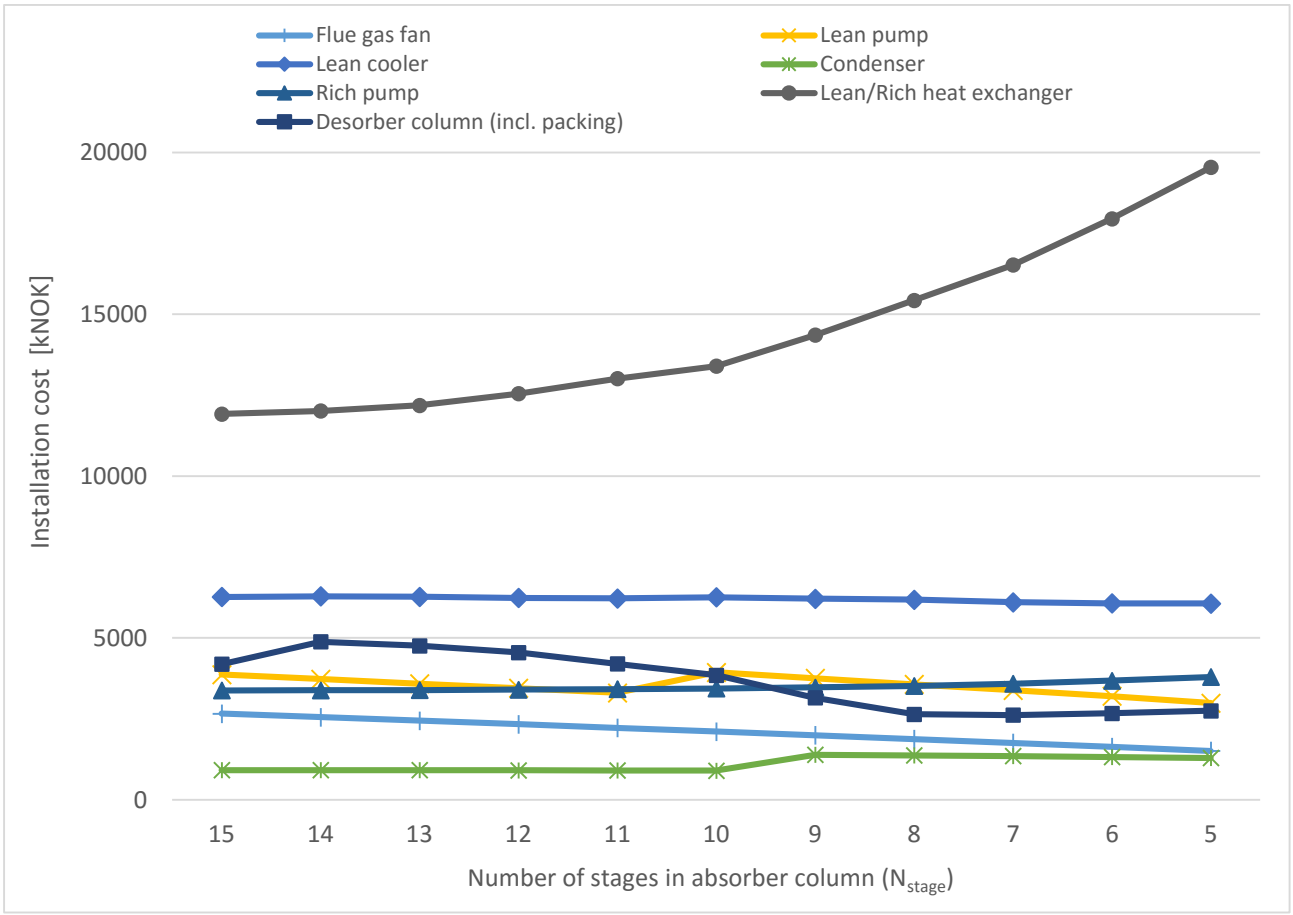

Appendix 28: Operating cost details (v_g = 2,5 m/s)

Alternative 1

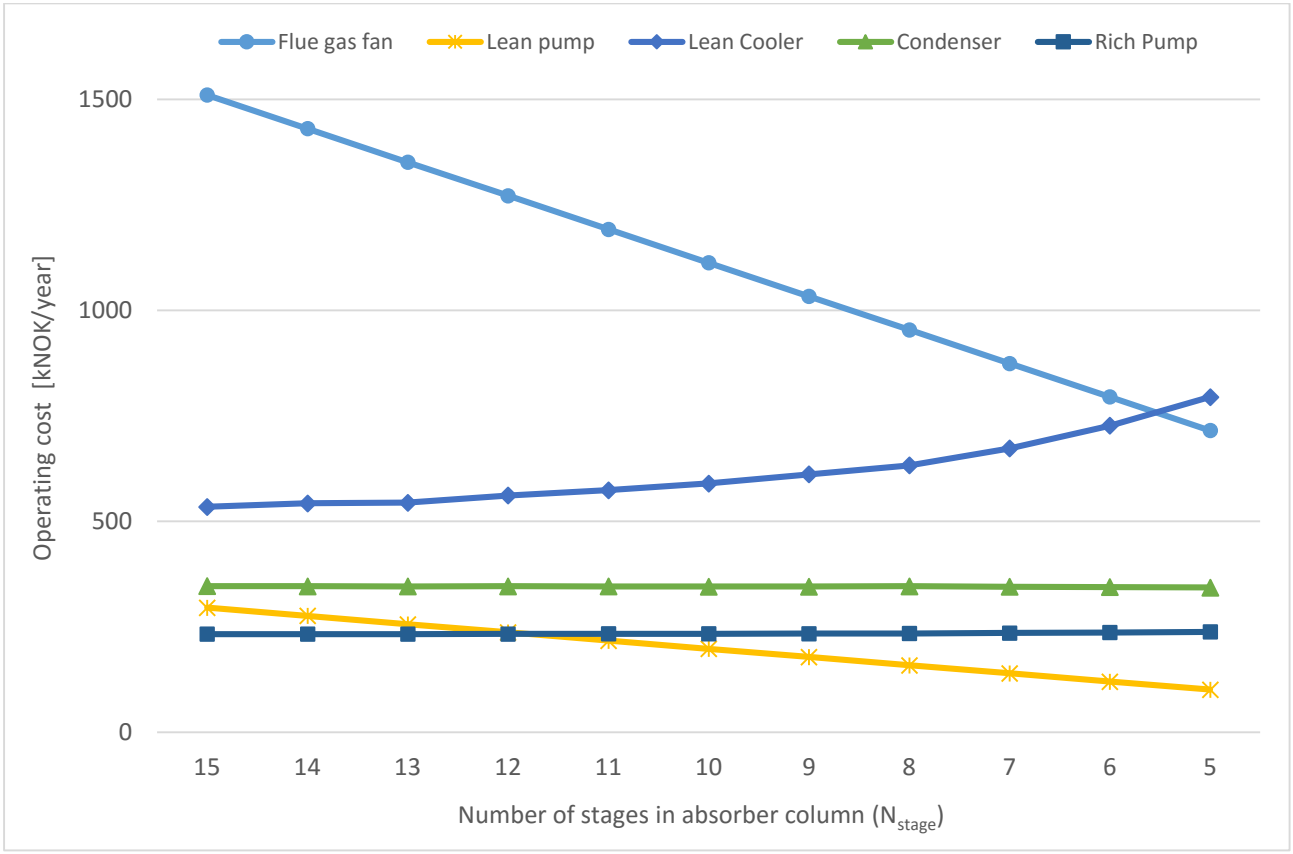

Alternative 2

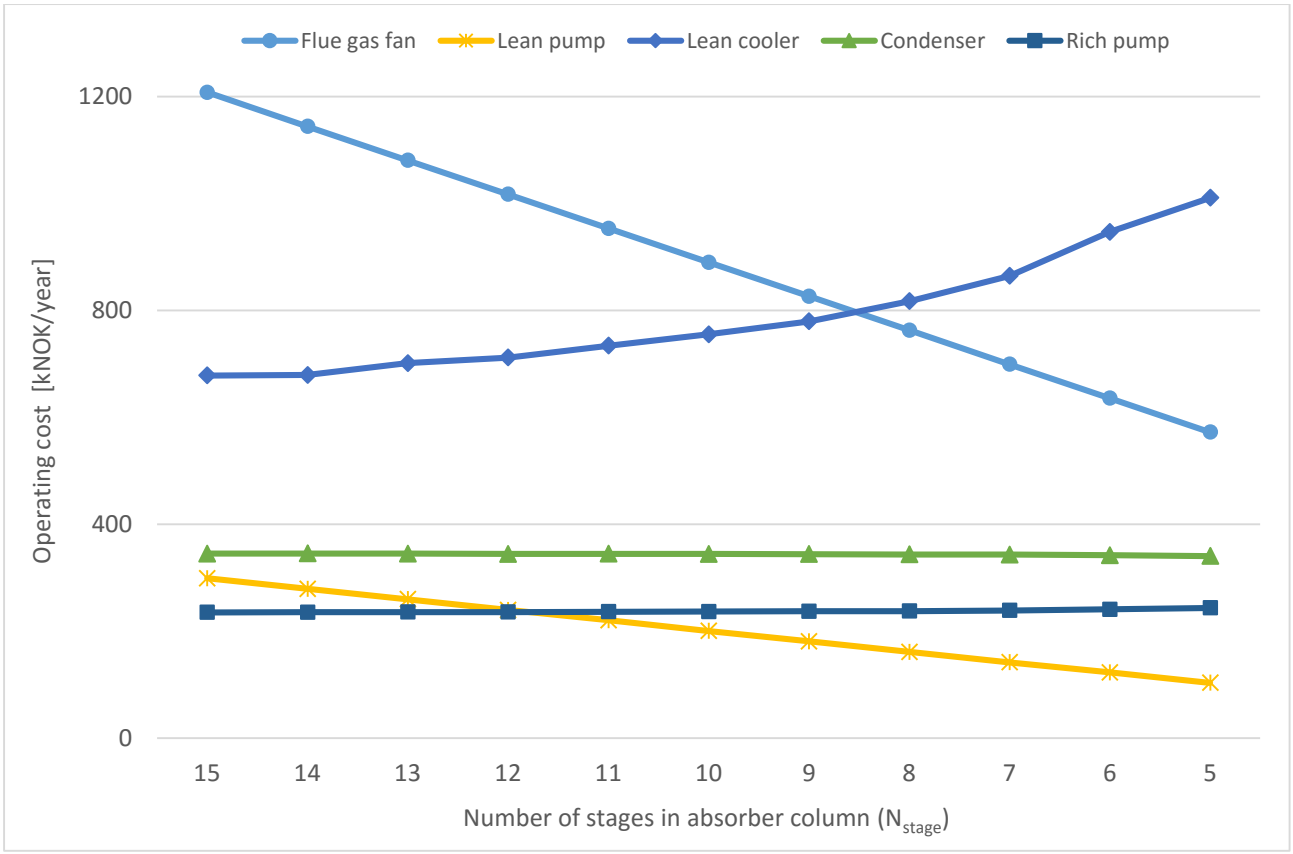

Alternative 3

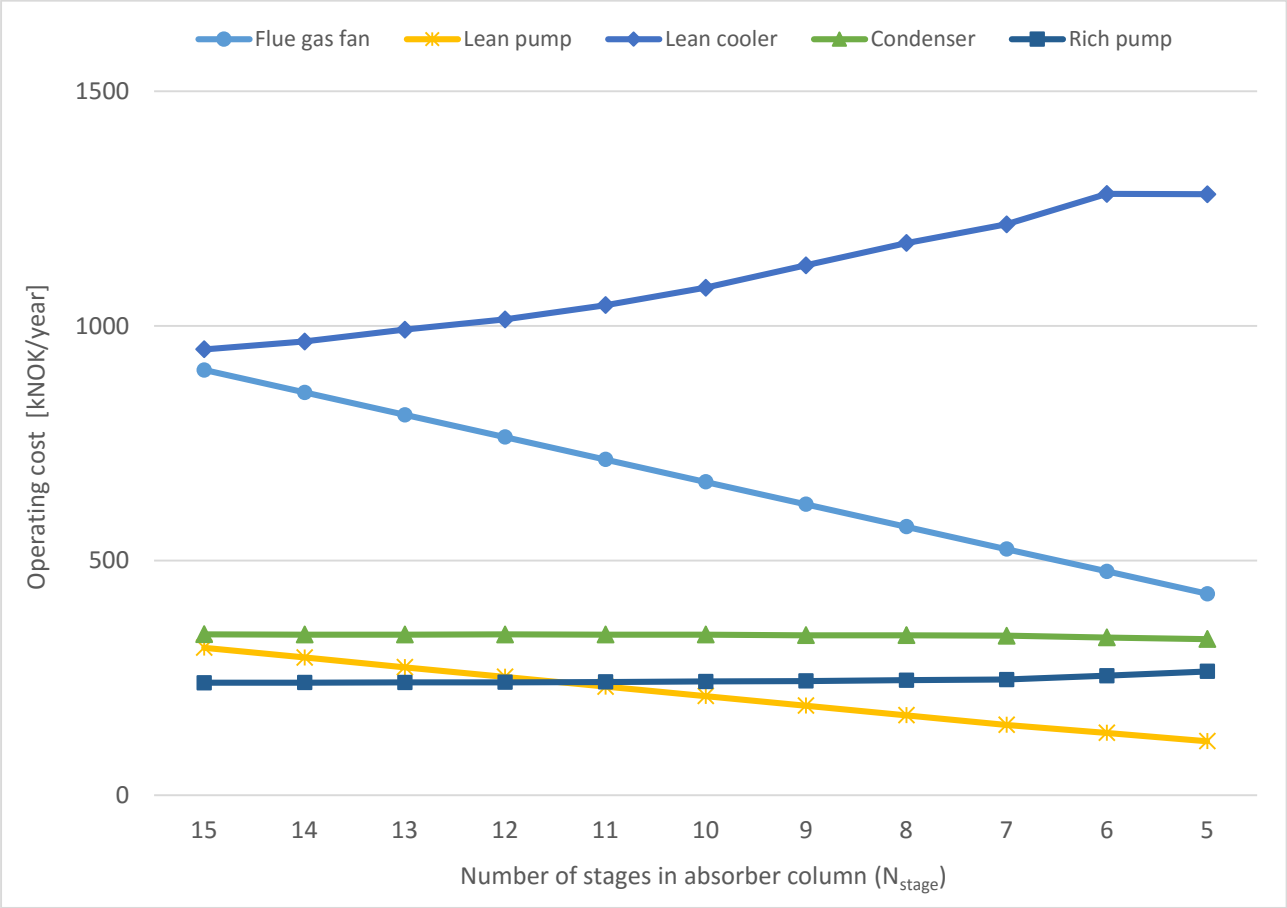

Alternative 4

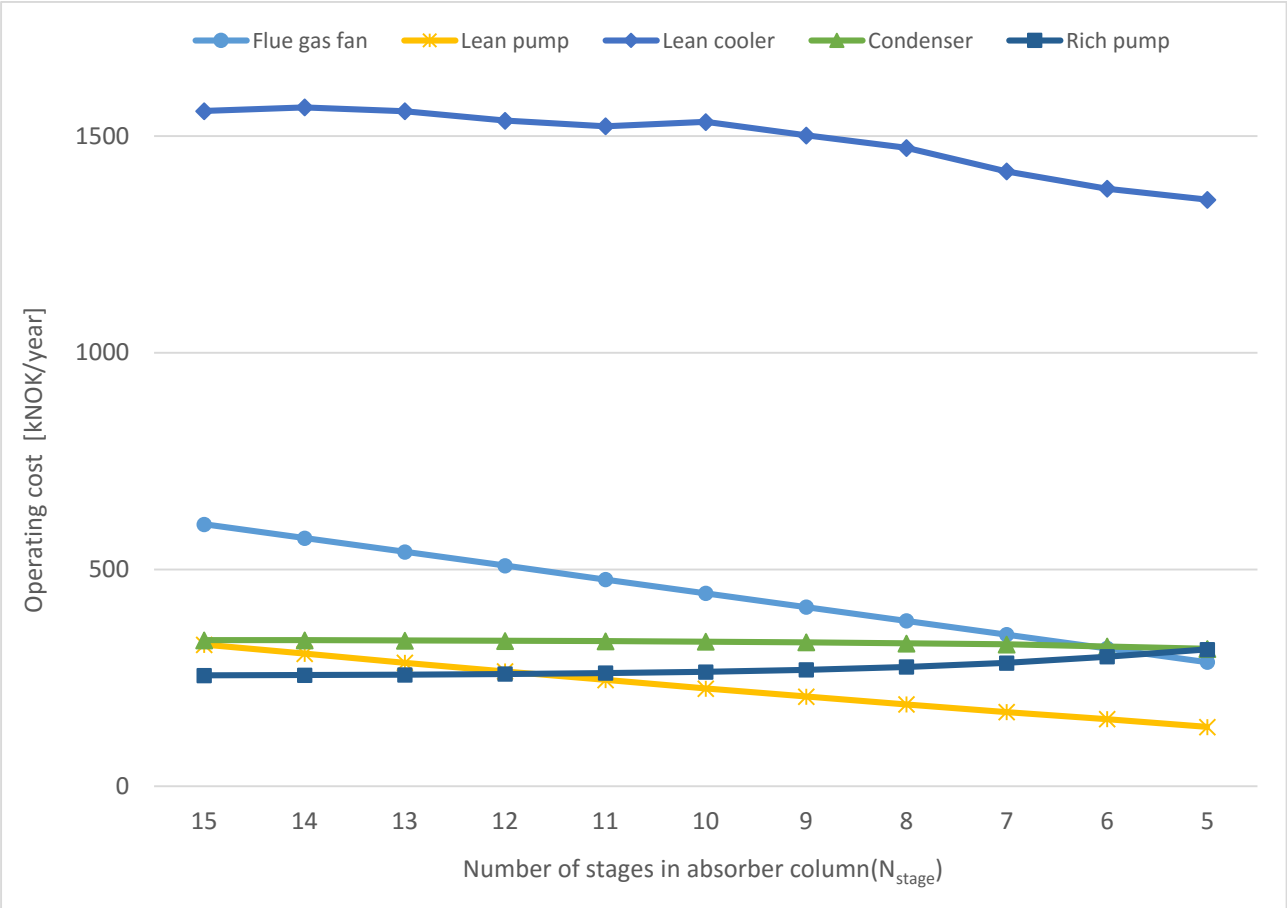

Appendix 29: CO_2-capture rate

Alternative 1

Item		Unit	Base case	N_{stage}											Note
				15	14	13	12	11	10	9	8	7	6	5	
A	CO_2 mass flow out of condenser	[kg/h]	62836,0	31050,5	30961,1	30920,6	30863,2	30824,7	30696,4	30539,4	30497,6	30176,7	29956,4	29381,9	obtained from HYSYS
B	Uptime	[h/year]	8000	8000	8000	8000	8000	8000	8000	8000	8000	8000	8000	8000	
C	CO_2-capture rate	[tonne/year]	**502688**	**248404**	**247688**	**247365**	**246906**	**246597**	**245571**	**244315**	**243981**	**241413**	**239651**	**235055**	= (A/1000) ∗ B

Alternative 2

Item		Unit	N_{stage}											Note
			15	14	13	12	11	10	9	8	7	6	5	
A	CO_2 mass flow out of condenser	[kg/h]	30335,6	30274,5	30219,3	30122,2	30031,6	29958,8	29791,3	29595,7	29259,8	28796,3	28062,2	obtained from HYSYS
B	Uptime	[h/year]	8000	8000	8000	8000	8000	8000	8000	8000	8000	8000	8000	
C	CO_2-capture rate	[tonne/year]	**242685**	**242196**	**241754**	**240977**	**240253**	**239671**	**238330**	**236766**	**234079**	**230370**	**224498**	= (A/1000) ∗ B

Alternative 3

Item		Unit	N_{stage}											Note
			15	14	13	12	11	10	9	8	7	6	5	
A	CO_2 mass flow out of condenser	[kg/h]	29034,4	28936,1	28898,5	28787,4	28588,6	28442,8	28228,0	27777,4	27316,0	25368,9	23421,7	obtained from HYSYS
B	Uptime	[h/year]	8000	8000	8000	8000	8000	8000	8000	8000	8000	8000	8000	
C	CO_2-capture rate	[tonne/year]	**232275**	**231489**	**231188**	**230299**	**228709**	**227543**	**225824**	**222219**	**218528**	**202951**	**187374**	= (A/1000) ∗ B

Alternative 4

Item		Unit	N_{stage}											Note
			15	14	13	12	11	10	9	8	7	6	5	
A	CO_2 mass flow out of condenser	[kg/h]	25244,5	25115,8	24875,1	24517,7	23994,6	23480,5	22581,6	21362,5	19859,4	17876,5	16058,0	obtained from HYSYS
B	Uptime	[h/year]	8000	8000	8000	8000	8000	8000	8000	8000	8000	8000	8000	
C	CO_2-capture rate	[tonne/year]	**201956**	**200927**	**199001**	**196141**	**191957**	**187844**	**180653**	**170900**	**158875**	**143012**	**128464**	= (A/1000) ∗ B

Appendix 30: Correlation table of equipment cost [73]

Table 2.1 Typical equipment capacity delivered capital cost correlations.

Equipment	Material of construction	Capacity measure	Base size Q_B	Base cost C_B ($)	Size range	Cost exponent M
Agitated reactor	CS	Volume (m^3)	1	1.15×10^4	1–50	0.45
Pressure vessel	SS	Mass (t)	6	9.84×10^4	6–100	0.82
Distillation column (Empty shell)	CS	Mass (t)	8	6.56×10^4	8–300	0.89
Sieve trays (10 trays)	CS	Column diameter (m)	0.5	6.56×10^3	0.5–4.0	0.91
Valve trays (10 trays)	CS	Column diameter (m)	0.5	1.80×10^4	0.5–4.0	0.97
Structured packing (5 m height)	SS (low grade)	Column diameter (m)	0.5	1.80×10^4	0.5–4.0	1.70
Scrubber (Including random packing)	SS (low grade)	Volume (m^3)	0.1	4.92×10^3	0.1–20	0.53
Cyclone	CS	Diameter (m)	0.4	1.64×10^3	0.4–3.0	1.20
Vacuum filter	CS	Filter area (m^2)	10	8.36×10^4	10–25	0.49
Dryer	SS (low grade)	Evaporation rate (kg $H_2O \cdot h^{-1}$)	700	2.30×10^5	700–3000	0.65
Shell-and-tube heat exchanger	CS	Heat transfer area (m^2)	80	3.28×10^4	80–4000	0.68
Air-cooled heat exchanger	CS	Plain tube heat transfer area (m^2)	200	1.56×10^5	200–2000	0.89
Centrifugal pump (Small, including motor)	SS (high grade)	Power (kW)	1	1.97×10^3	1–10	0.35
Centrifugal pump (Large, including motor)	CS	Power (kW)	4	9.84×10^3	4–700	0.55
Compressor (Including motor)		Power (kW)	250	9.84×10^4	250–10,000	0.46
Fan (Including motor)	CS	Power (kW)	50	1.23×10^4	50–200	0.76
Vacuum pump (Including motor)	CS	Power (kW)	10	1.10×10^4	10–45	0.44
Electric motor		Power (kW)	10	1.48×10^3	10–150	0.85
Storage tank (Small atmospheric)	SS (low grade)	Volume (m^3)	0.1	3.28×10^3	0.1–20	0.57
Storage tank (Large atmospheric)	CS	Volume (m^3)	5	1.15×10^4	5–200	0.53
Silo	CS	Volume (m^3)	60	1.72×10^4	60–150	0.70
Package steam boiler (Fire-tube boiler)	CS	Steam generation ($kg \cdot h^{-1}$)	50,000	4.64×10^5	50,000–350,000	0.96
Field erected steam boiler (Water-tube boiler)	CS	Steam generation ($kg \cdot h^{-1}$)	20,000	3.28×10^5	10,000–800,000	0.81
Cooling tower (Forced draft)		Water flowrate ($m^3 \cdot h^{-1}$)	10	4.43×10^3	10–40	0.63

CS = carbon steel; SS (low grade) = low-grade stainless steel, for example, type 304; SS (high grade) = high-grade stainless steel, for example, type 316

Appendix 31: CO_2-capture cost derivation

Item	Unit	Year number					
		0	1	2	3	...	25
CAPEX	[kNOK]	A					
OPEX	[kNOK/year]		B	B	B	...	B
CO_2-capture rate	[tCO_2/year]		C	C	C	...	C
CO_2-capture cost	[kNOK/tCO_2]		D	D	D	...	D
Yearly income	[kNOK/year]		$C * D$	$C * D$	$C * D$	...	$C * D$
Cash flow	[KNOK/year]	$-A$	$C * D - B$	$C * D - B$	$C * D - B$	...	$C * D - B$
Discount factor	[-]	1,00	0,93	0,87	0,80	...	0,16
NPV	[kNOK]	$-A$	$0{,}93 * (C * D - B)$	$0{,}87 * (C * D - B)$	$0{,}80 * (C * D - B)$	...	$0{,}16 * (C * D - B)$
Accumulated NPV	[kNOK]	$-A$	$-A + 0{,}93 * (C * D - B)$	$-A + (0{,}93 + 0{,}87) * (C * D - B)$	$-A + (0{,}93 + 0{,}87 + 0{,}80) * (C * D - B)$	...	$-A + (0{,}93 + 0{,}87 + 0{,}80 + \cdots + 0{,}16) * (C * D - B)$

The CO_2-capture cost is determined by equating the accumulated NPV in year 25 with zero as below.

$$-A + (0{,}93 + 0{,}87 + 0{,}80 + \cdots + 0{,}16) * (C * D - B) = 0$$

Rearranging the equation with regard to D gives

$$D = \frac{\frac{A}{(0{,}93 + 0{,}87 + 0{,}80 + \cdots + 0{,}16)} + B}{C} = \frac{\frac{A}{11{,}15} + B}{C}$$

where

A = CAPEX [kNOK]
B = OPEX [kNOK/year]
C = CO_2-capture rate [tonne CO_2/year]
D = CO-capture cost [kNOK/tonne CO_2]

Appendix 32: Base cost data of SHTE [65]

ITEM REPORT

Processing Date : Thu Mar 03 01:32:04 PM 2016
Version : Aspen In-Plant Cost Estimator 19.0.0(Build 2556)

Project : Optimization of partial CO_2 capture
Scenario : Shell-and-tube type heat exchanger

Shell-and-tube heat exchanger (STHE)

Item Code: DHE U TUBE
Internal Name : DHE U TUBE STHE

Design Data

Parameter	Value	Units
Item type	U TUBE	
Number of identical items	1	
GENERAL DESIGN DATA		
TEMA type	BEU	
Heat exchanger design option	STAND	
Heat exchanger design+cost tool	ECON	
Heat transfer area	995.700	M2
Number of shells	1	
Number of tube passes	2	
Number of shell passes	1	
Vendor grade	HIGH	
SHELL DATA		
Shell material	SS316	
Shell diameter	1300.000	MM
Shell length	9.1000	M
Shell design gauge pressure	500.000	KPAG
Shell design temperature	120.000	DEG C
Shell operating temperature	120.000	DEG C
Shell corrosion allowance	0.0	MM
Shell wall thickness	7.0000	MM
ASA rating Shell side	150	CLASS

Number of baffles	18	
Shell fabrication type	PLATE	
Expansion joint	NO	
TUBE DATA		
Tube material	316LW	
Number of tubes per shell	694	
Tube outside diameter	25.000	MM
Tube length extended	18.000	M
Tube design gauge pressure	500.000	KPAG
Tube design temperature	120.000	DEG C
Tube operating temperature	120.000	DEG C
Tube corrosion allowance	0.0	MM
Tube wall thickness	1.2000	MM
Tube gauge	18	BWG
Tube pitch symbol	TRIANGULAR	
Tube pitch	32.000	MM
Tube seal type	SEALW	
TUBE SHEET DATA		
Tube sheet material	316L	
Tube sheet thickness	65.000	MM
Tube sheet corrosion allowance	0.0	MM
Channel material	316L	
TUBE SIDE HEAD DATA		
Head material Tube side	316L	
ASA rating Tube side	150	CLASS
Head thickness Tube side	7.0000	MM
SHELL SIDE HEAD DATA		
Head material Shell side	SS316	
ASA rating Shell side	150	CLASS
Head thickness Shell side	7.0000	MM
WEIGHT DATA		
Shell	2100	KG
Tubes	9500	KG
Heads	240	KG
Internals and baffles	1500	KG
Nozzles	330	KG
Flanges	470	KG
Base ring and lugs	32	KG
Tube sheet	420	KG
Saddles	210	KG

Fittings and miscellaneous	100	KG
Total weight	14900	KG
VENDOR COST DATA		
Material cost	152490	EURO
Shop labor cost	17818	EURO
Shop overhead cost	17946	EURO
Office overhead cost	16943	EURO
Profit	18003	EURO
Total cost	223200	EURO
Cost per unit weight	14.980	EUR/KG
Cost per unit area	224.164	EUR/M2

Summary Costs

Item	Material(EUR)	Manpower(EUR)	Manhours
Equipment&Setting	223200.	3353.	63
Piping	0.	0.	0
Civil	0.	0.	0
Structural Steel	0.	0.	0
Instrumentation	0.	0.	0
Electrical	0.	0.	0
Insulation	0.	0.	0
Paint	0.	0.	0
Subtotal	**223200**	**3353**	**63**

Total material and manpower cost = EUR 226600.

Appendix 33: Base cost data of PHE [65]

ITEM REPORT

Processing Date : Thu Mar 03 01:35:03 PM 2016
Version : Aspen In-Plant Cost Estimator 19.0.0(Build 2556)

Project : Optimization of partial CO_2 capture
Scenario : Plate-and-frame type heat exchanger

Plate heat exchanger (PHE)

Item Code: DHE PLAT FRAM
Internal Name : DHE PLAT FRAM PHE

Design Data

Parameter	Value	Units
Item type	PLAT FRAM	
Number of identical items	1	
EQUIPMENT DESIGN DATA		
Plate material	SS316	
Heat transfer area	356.000	M2
Number of plates	315	
Design gauge pressure	500.000	KPAG
Design temperature	120.000	DEG C
WEIGHT DATA		
Shell	4900	KG
Total weight	4900	KG
VENDOR COST DATA		
Total cost	57600	EURO
Cost per unit weight	11.755	EUR/KG

Summary Costs

Item	Material(EUR)	Manpower(EUR)	Manhours
Equipment&Setting	57600.	4613.	86
Piping	0.	0.	0

Civil	0.	0.	0
Structural Steel	0.	0.	0
Instrumentation	0.	0.	0
Electrical	0.	0.	0
Insulation	0.	0.	0
Paint	0.	0.	0
Subtotal	**57600**	**4613**	**86**

Total material and manpower cost = EUR 62200.